Stability and Bifurcation Analysis of Some Real Life Problems

A Thesis submitted to the

BABASAHEB BHIMRAO AMBEDKAR UNIVERSITY

(A CENTRAL UNIVERSITY)

LUCKNOW

for the award of the Degree of

DOCTOR OF PHILOSOPHY

in Applied Mathematics

Under the supervision of

Prof. B.S. Bhadauria

By

Manoj Kumar Singh

DEPARTMENT OF APPLIED MATHEMATICS

SCHOOL FOR PHYSICAL SCIENCES

BABASAHEB BHIMRAO AMBEDKAR UNIVERSITY

LUCKNOW - 226025

INDIA

Enrollment No. 383/13 **Year 2017**

Dedicated to

my family members for

their interest in my higher studies

DECLARATION

I, Manoj Kumar Singh, hereby declare that the work embodied in this Ph.D. thesis entitled as **"Stability and Bifurcation Analysis of Some Real Life Problems"** is my own work carried out by me under the supervision of Prof. B.S. Bhadauria, Department of Applied Mathematics, Babasaheb Bhimrao Ambedkar University (A Central University) Lucknow, India. The information presented in this Ph.D. thesis has not been submitted for the award of any degree, diploma, associateship of any University or Institution. I declare that I have faithfully acknowledged, given credit to and referred to the research workers whenever their works have been cited in the text and the body of the thesis. I further declare that I have not willful lifted up some others work, para, text, data, results, etc. reported in the journals, books, magazines, reports, dissertations, thesis, etc., or available at websites and included them in this thesis and cited my own work.

Date: 12/06/2017

Manoj Kumar Singh

(Research Scholar)

BABASAHEB
BHIMRAO
AMBEDKAR
UNIVERSITY

LUCKNOW

प्रज्ञा शील करुणा
ESTABLISHED 1996

बाबासाहेब भीमराव अम्बेडकर विश्वविद्यालय
(केन्द्रीय विश्वविद्यालय)
विद्या विहार, रायबरेली रोड, लखनऊ - 226025

Babasaheb Bhimrao Ambedkar University
(A Central University)
Vidya Vihar, Raebareli Road, Lucknow-226025

Letter No. : 19/DAM/BBAU
Date : 12/06/2017

CERTIFICATE

This is to certify that the thesis titled **"Stability and Bifurcation Analysis of Some Real Life Problems"** submitted by **Mr. Manoj Kumar Singh** is an original research work and has not been previously submitted in part or full for the award of any other degree or diploma to this or any other university.

The thesis submitted to the Babasaheb Bhimrao Ambedkar University, Lucknow satisfies all the requirements as stipulated in the Doctor of Philosophy (Ph.D.) regulations −1999 as amended in 2010 and it is fit for submission and evaluation for the award of the degree of Doctor of Philosophy of the university.

Date: 12/06/2017

Dr. B.S. Bhadauria
(Supervisor)
Dr. B. S. Bhadauria
Professor of Mathematics
Department of Applied Mathematics
B.B. Ambedkar University, Lucknow

Dr. B.S. Bhadauria 12/06/2017
(Head of the Department)
Professor B. S. Bhadauria
Head
Department of Applied Mathematics
B.B. Ambedkar University, Lucknow

Acknowledgements

On the occasion of submission of my Ph.D. thesis, first of all it is my pious obligation to express from the inner most core of the heart my indebtedness to Almighty God without His blessing this work would not have seen the light of the day.

I express my sincere thanks and gratitude to my eminent Supervisor, Prof. B.S. Bhadauria for providing me the opportunity to undergo this Project work and also for his able guidance, encouragement and moral support during the journey of my research work. Without his continuous motivation, cooperation, assistance and moral support this work would not have been possible. I am extremely grateful to him for his masterly guidance, valuable suggestions. His devotion to duty will remain an ideal to me in future, and his creative criticism proved to be a boon in the study.

I am also thankful to Dr. B.K. Singh, Assistant Professor of the Department from the bottom of my heart for his kind cooperation and encouragement during period of my study.

I express my deepest thanks to all my dear friends Ajay, Vineet, Promod for making my stay in the campus a pleasant one with lively discussions and all supports.

I thank all the staff members, Mr. Rakesh and Mr. Vinay Kumar Sahu of the Department for their cooperation and help during the course of my Project work.

I am also thankful to my wife, Mrs. Reena and my dear younger ones, Aditya and Antriksh whose smiling faces have always been source of inspiration even in time of distress moments.

Last but not the least, I express my heartiest gratitude to my dear parents who, nourished and taught me the first lesson in life, nurtured me from the very beginning, and motivated me for higher studies and brought me up to the position of submission of this Project work, despite great difficulties.

At the end I extend my thanks to all those who helped me directly or indirectly for successful completion of this Project work.

Manoj Kumar Singh

Contents

List of Figures **v**

1 Introduction **1**

1.1 Dynamical System 1

1.2 Stability Analysis 3

1.3 Bifurcation Analysis 6

1.3.1 Saddle-node Bifurcation 7

1.3.2 Transcritical Bifurcation 8

1.3.3 Pitchfork Bifurcation 9

1.3.4 Hopf Bifurcation 10

1.3.5 Bogdanov-Takens Bifurcation 11

1.3.6 Homoclinic Bifurcation 14

1.4 Predator-prey Dynamical System 15

1.4.1 Per Capita Prey Growth Function 15

1.4.2 Functional Response 17

1.4.3 Predator Growth Function 20

1.5 Some Predator-prey Models 21

1.5.1 Lotka-Volterra Predator-prey Model 21

1.5.2 Rosenzweig-MacArthur Predator-prey Model 24

1.5.3 Leslie-Gower Predator-prey Model 24

1.5.4 Holling-Tanner Predator-prey Model 26

1.5.5 Modified Leslie-Gower Predator-prey Model 26

1.6 Allee Effect 28

1.7 Harvesting Functions . . . 33
1.8 Additional Food . . . 35
1.9 Dynamical Complexity of Convective Motion in Porous Medium . . . 36

2 Leslie-Gower Predator-prey Model with Nonlinear Harvesting 38

2.1 Introduction . . . 38
2.2 Model with Nonlinear Predator Harvesting . . . 40
2.2.1 Model Equations . . . 40
2.2.2 Equilibria and their Stability . . . 41
2.2.3 Bifurcation Analysis . . . 47
2.2.4 Numerical Simulations . . . 54
2.2.5 Results and Discussion . . . 61
2.3 Model with nonlinear prey harvesting . . . 64
2.3.1 Model Equations . . . 64
2.3.2 Bogdanov-Takens Bifurcation: Normal Form . . . 65
2.3.3 Numerical Simulations . . . 72
2.3.4 Results and Discussion . . . 76

3 Ratio-dependent Holling-Tanner Predator-prey Model with Nonlinear Prey Harvesting 77

3.1 Introduction . . . 77
3.2 Model Equations . . . 79
3.3 Equilibria and their Stability . . . 82
3.4 Bifurcation Analysis . . . 92
3.4.1 Hopf Bifurcation . . . 92
3.4.2 Saddle-node Bifurcation . . . 93
3.4.3 Bogdanov-Takens bifurcation . . . 95
3.5 Numerical Simulations . . . 100
3.6 Results and Discussion . . . 104

4 Modified Leslie-Gower Predator-prey Model with Weak Allee Effect *II* 105

4.1 Introduction . . . 105

4.2 Model Equations . . . 106

4.3 Equilibria and their Stability . . . 108

4.3.1 Model with no Allee Effect . . . 108

4.3.2 Model with Allee Effect . . . 110

4.4 Bifurcation Analysis . . . 113

4.4.1 Model with no Allee Effect . . . 114

4.4.2 Model with Allee Effect . . . 115

4.5 Numerical Simulations . . . 121

4.6 Results and Discussion . . . 130

5 Modified Leslie-Gower Predator-prey Model with Double Allee Effect 132

5.1 Introduction . . . 132

5.2 Model Equations . . . 133

5.3 Equilibria and their Stability . . . 136

5.3.1 Strong Allee Effect . . . 136

5.3.2 Weak Allee Effect . . . 140

5.4 Bifurcation Analysis . . . 141

5.4.1 Strong Allee Effect . . . 142

5.4.2 Weak Allee Effect . . . 146

5.5 Numerical Simulations . . . 147

5.6 Results and Discussion . . . 156

6 Predator-prey Model with Allee Effect and Additional Food for the Predators 158

6.1 Introduction . . . 158

6.2 Model Equations . . . 160

6.3 Equilibria and their Stability . . . 161

6.4 Bifurcation Analysis . . . 166

6.4.1 Hopf Bifurcation . . . 166

6.4.2 Transcritical Bifurcation 167
6.4.3 Saddle-node Bifurcation 168
6.4.4 Bogdanov-Takens Bifurcation 169
6.5 Numerical Simulations 174
6.6 Results and Discussion 179

7 Stability Analysis under Internal Heating and Gravity Modulation Effects 182

7.1 Introduction 182
7.2 Mathematical Formulation 184
7.3 Basic State 186
7.4 Analysis of Periodic Solution 187
7.5 Bifurcation Analysis 191
7.5.1 Hopf Bifurcation 192
7.5.2 Pitchfork bifurcation 192
7.6 Results and Discussion 193
7.7 Conclusions 195

Bibliography 202

List of Publications 218

List of Figures

1.1 Graphs of logistic, $\theta-$logistic, Gompertz and Smith types per capita negative density-dependent prey growth rate functions. 16

1.2 Graphs of Holling Type I, II, III and IV functional responses. 18

1.3 Phase portrait for Lotka-Volterra predator-prey mode (1.5.1) 23

1.4 *Phase portrait for model* (1.5.5). *The red curve is the predator nullcline and purple curve is prey nullcline. (a) The unique interior equilibrium point is stable for low K. (b) The unique interior equilibrium point is unstable for large K and a stable limit cycle appears around the point.* 24

1.5 *Phase portrait for model* (1.5.6). *The red curve is predator nullcline and purple curve is prey nullcline. The unique interior equilibrium point is globally stable.* 25

1.6 *Phase portrait for model* (1.5.7). *The red curve is predator nullcline and purple curve is prey nullcline. (a) The unique interior equilibrium point is globally stable. (b) The unique interior equilibrium point is unstable and a stable limit cycle arises around the equilibrium point. (c) The unique interior equilibrium point is stable and two limit cycle arises around the unique interior equilibrium point.* 27

1.7 *The relationships between the per capita single population growth rate and population size for negative density dependence, strong, weak and special weak Allee effects.* 30

1.8 *Per-capita growth rate of a single population in the presence of no Allee effect, single Allee effect $(x - m)$, single $\frac{r}{x+n}$ and double Allee effects. (a) Strong Allee effect $(m > 0)$. (b) Weak Allee effect $(m < 0)$. (c) affect of n.* . 32

2.1 *This diagram shows the number and location of the positive interior equilibrium points of the system* (2.2.3). *The green, red and black color curves are the predator nullclines for different values of* h *and the straight line is the prey nullcline* ***(a)*** $h > c$, *for black color parabola* $h > \overline{h}$, *for red color parabola* $h = \overline{h}$ *and for green color parabola* $h < \overline{h}$ ***(b)*** $h = c$ ***(c)*** $h < c$. . . . 42

2.2 *Phase portrait for system* (2.2.3). *For figure (a) and (b)* $\beta = 0.1, c = 0.01, h = 0.5$ ***(a)*** $\rho = 0.75$ *the interior equilibrium point* $E_2 = (0.210806, 0.789194)$ *is an asymptotically stable, axial equilibrium point* $e = (1, 0)$ *is asymptotically stable and interior equilibrium point* $E_1 = (0.435558, 0.564442)$ *is a saddle point.* ***(b)*** $\rho = 0.9$ *the point* E_2 *is unstable,* e *is asymptotically stable and* E_1 *is a saddle.* ***(c)*** $\beta = 0.1, c = 0.01, h = 0.01, \rho = 0.9$ *the interior equilibrium point* $E_4 = (0.091818, 0.908182)$ *is an asymptotically stable, axial equilibrium point* $e = (1, 0)$ *is saddle.* ***(d)*** $\beta = 0.1, c = 0.01, h = 0.005, \rho = 0.9$ *The interior equilibrium point* $E_5 = (0.0913611, 0.908639)$ *is an asymptotically stable, axial equilibrium point* $e = (1, 0)$ *is saddle.* ***(e)*** *when no interior equilibrium exist, the origin is always a saddle.* 55

2.3 ***(a)*** $\beta = 0.1, c = 0.01, h = 0.5, \rho^* = 0.865973, \rho = 0.854$ *an unstable limit cycle arises around the interior equilibrium point* E_2. ***(b)*** $\beta = 0.02, c = 0.1, h = 0.8, \rho^* = 0.173169, \rho = 0.175$ *a stable limit cycle arises around the interior equilibrium point* E_2. 56

2.4 $\beta = 0.5, c = 0.1, \overline{h} = 0.33341, \rho = 0.4$. *The system* (2.2.3) *has a double interior equilibrium point* E_3. ***(a)*** *The point* E_3 *is stable from above of the saperatrix curve and a saddle frow below.* ***(b),(c)*** *Saddle-node bifurcation diagram.* 57

2.5 $\beta = 0.12, c = 0.1, h_0 = 0.583001, \rho_0 = 0.781849$ ***(a)*** *BT Bifurcation diagram in the $\lambda_1\lambda_2$ plane.* ***(b)*** *The equilibrium point E_3 is a cusp when $(\lambda_1, \lambda_2) = (0, 0)$.* ***(c)*** *No interior equilibrium point exist when $(\lambda_1, \lambda_2) = (0.04, 0.001)$ lies in the region I.* ***(d)*** *An unstable focus when $(\lambda_1, \lambda_2) = (0.03, -0.001)$ lies in the region II.* ***(e)*** *An unstable limit cycle when $(\lambda_1, \lambda_2) = (0.03, -0.002)$ lies in the region III.* ***(f)*** *A stable focus when $(\lambda_1, \lambda_2) = (0.03, -0.004)$ lies in the region IV.* 63

2.6 **(a)** Bifurcation diagram for attracting B-T bifurcation. The red trajectory is homoclinic bifurcation curve and black trajectory is the hopf bifurcation curve. **(b)** A cusp of codimension 2 when $(\lambda_1, \lambda_2) = (0, 0)$. **(c)** No interior equilibrium point exist when $(\lambda_1, \lambda_2) = (0.0002, -0.001)$ lies in the first region. **(d)** An unstable focus when $(\lambda_1, \lambda_2) = (-0.0001, -0.001)$ lies in the region II. **(e)** A stable homoclinic loop rises when $(\lambda_1, \lambda_2) = (-0.000568, -0.001)$ lies on the homoclinic bifurcation curve. **(f)** A stable limit cycle when $(\lambda_1, \lambda_2) = (-0.001, -0.001)$ lies in the region III. **(g)** A stable focus when $(\lambda_1, \lambda_2) = (-0.002, -0.001)$ lies in the region IV. 73

2.7 **(a)** Bifurcation diagram for repelling B-T bifurcation. The blue trajectory is homoclinic bifurcation curve and violet trajectory is the hopf bifurcation curve. **(b)** No interior equilibrium point exist when $(\lambda_1, \lambda_2) = (0.003, 0.08)$ lies in the region I. **(c)** An unstable focus when $(\lambda_1, \lambda_2) = (-0.0005, -0.04)$ lies in the region II. **(d)** An unstable limit cycle when $(\lambda_1, \lambda_2) = (-0.0006, -0.04)$ lies in the region III. **(e)** An unstable Homoclinic loop when $(\lambda_1, \lambda_2) = (-0.00106893, -0.04)$ lies on the homoclinc bifurcation curve. **(f)** A stsble focus when $(\lambda_1, \lambda_2) = (-0.002, -0.04)$ lies in the region IV. 75

3.1 These diagrams shows the number of interior equilibrium points of the system (3.2.2), when the parameter h varies through critical value $h^{[SN]}$ and all other parameters are fixed. $\alpha = 0.6$, $\beta = 0.5$, $c = 0.1$, $\rho = 0.6$ $(a)h = 0.16$ $(b)h = 0.2025$ $(c)h = 0.21$. 85

3.2 The phase portrait diagram of the system (3.2.2). (a) $\alpha = 0.6,\ \beta = 0.3,\ h = 0.2,\ c = 0.02,\ \rho = 0.2$ satisfies the conditions of the theorem 3.3.4 (a). It shows that E_0 is globally stable. (b) $\alpha = 0.4,\ \beta = 0.3,\ h = 0.12,\ \rho = 0.2,\ c = 0.13$ satisfies the conditions of the theorem 3.3.4 (b).The equilibrium points E_0 and E_2^* are locally asymptotically stable points. (c) $\alpha = 0.7,\ \beta = 0.4,\ c = 0.1,\ \rho = 0.1,\ h = 0.096$ satisfies the conditions of the theorem 3.3.4 (c). It shows that E_0 and E_2^* are locally asymptotically stable. The red trajectory is a separatrix. 88

3.3 (a) The blue curve is Saddle-node bifurcation curve, red curve is Hopf bifurcation curve and green curve is Homoclinic bifurcation curve. (b) When $\lambda_1 = \lambda_2 = 0$, the unique equilibrium point $\overline{E}$ is a cusp of codimention 2. (c) When $\lambda_1 = 0.001, \lambda_2 = 0.001$ lies in the region I, then the system (3.2.2) has no interior equilibrium point and the origin is globally asymptotically stable. (d) When $\lambda_1 = -0.001, \lambda_2 = -0.1$ lies in the region II, the system (3.2.2) has two interior equilibrium point. One point is unstable and other is a saddle point. (e) When $\lambda_1 = -0.001, \lambda_2 = -0.09$ lies in the region III, the system (3.2.2) has two interior equilibrium point. One point is enclosed by an unstable limit cycle and other is a saddle point. (d) When $\lambda_1 = -0.001, \lambda_2 = -0.07$ lies in the region IV, the system (3.2.2) has two interior equilibrium point. One point is asymptotically stable and other is a saddle point. $\alpha = 0.9,\ \beta = 0.5,\ h = 0.16,\ c = 0.1,\ \rho = 0.4$. 101

3.4 The phase portrait diagram of the system (3.2.2) E_1^* is always a saddle point. $\alpha = 0.9,\ \beta = 0.7,\ h = 0.1,\ c = 0.01$. (a) $\rho = 0.18071$, an unstable limit cycle bifurcates around the interior point E_2^* (b) $\rho = 0.2$, E_2^* is a stable point. (c) $\rho = 0.15$, E_2^* is an unstable point. (d) $\rho = 0.2117091$, Homoclinic loop is created around the interior point E_2^*. 102

3.5 The phase portrait diagram of the system (3.2.2) for $\alpha = 0.6,\ \beta = 0.5,\ c = 0.1,\ \rho = 0.6$. The red trajectories are the separatrix. (a) $h = 0.16, E_0$ and E_2^* are two locally asymptotically stable points and E_1^* is a saddle point. (b) $h = 0.202499$, the point $\overline{E}$ is stable from right side of the separatrix and unstable from left side of the separatrix. (c) and (d) are the Saddle-node bifurcation diagrams. 103

3.6 The phase portrait diagram of the system (3.2.2) for $\alpha = 0.7,\ \beta = 0.6,\ c = 0.5,\ h = 0.36875$, the red trajectory is the separatrix. (a) $\rho = 0.14597$, a stable limit cycle is created around the unique interior equilibrium point. (b) $\rho = 0.2$, the unique interior point is stable. 103

4.1 $\alpha = 0.4,\ m = 0.2,\ \delta = 0.5,\ \beta = 0.0$. System (4.2.4) has a unique interior equilibrium points $e_3 = (0.2, 0.8)$, one trivial equilibrium point $e_0 = (0, 0)$ and two axial equilibrium points $e_1 = (1, 0)$ and $e_2 = (0.0.4)$. (a) $\rho = 0.16$, point e_3 is unstable (b) $\rho = 0.2$. System (4.2.4) undergoes to a supcritical hopf bifurcation at the point e_3 and an stable limit cycle arises around this point (c) $\rho = 0.22$, point e_3 is asymptotically stable (d) $\delta = 0.35,\ \rho = 0.22$. System (4.2.4) has no interior equilibrium point and prey free equilibrium point e_2 is asymptotically stable. 122

4.2 $\alpha = 0.3,\ m = 0.01,\ \delta = 0.4, \beta = 0.00625$. System (4.2.4) has unique interior equilibrium point $E_4 = (0.125, 0.3375)$ (a) Saddle-node bifurcation diagram (b) $\rho = 0.6$ unique interior equilibrium points E_4 of system (4.2.4) is a repelling saddle-node point (c) $\beta = 0.98$ unique interior equilibrium points E_4 of system (4.2.4) is an attracting saddle-node point 123

4.3 $\alpha = 0.3, \quad m = 0.01, \quad \delta = 0.4, \quad \beta = 0.006$. System (4.2.4) has two interior equilibrium points $E_2 = (0.15, 0.4), E_3 = (0.1, 0.275)$, one unstable trivial equilibrium point $E_0 = (0, 0)$ and one saddle axial equilibrium point $E_1 = (1, 0)$. The green curve is prey isocline and the purple line is the predator isocline. (a) $\rho = 0.5$, point E_2 is unstable and point E_3 is saddle (b) $\rho = 0.746875$, System (4.2.4) undergoes to a subcritical Hopf bifurcation at the point E_2 and an unstable limit cycle arises around this point, point E_3 is saddle (c) $\rho = 0.763715$, System (4.2.4) undergoes to a Homoclinic bifurcation at the point E_2 and an unstable loop (red loop) arises around this point and point E_3 is saddle (d) $\beta = 0.77$, point E_2 is asymptotically stable and point E_3 is saddle. 125

4.4 $\alpha = 0.3, \quad m = 0.01, \quad \delta = 0.4, \beta = 0.00625, \quad \rho = 0.810185$. (a) Bifurcation diagram of system (4.2.4); blue line is the Saddle-node bifrcation curve, green curve is the Hopf bifurcation curve and red curve is the Homoclinic bifurcation curve (b) $\lambda_1 = 0, \quad \lambda_2 = 0$. The unique interior equilibrium point E_4 is a cusp of of codimension 2. (c) $\lambda_2 = -0.1, \quad \lambda_1 = 0.0005$ lies in region I. No interior equilibrium point exist. (d) $\lambda_2 = -0.1, \quad \lambda_1 = -0.0002$ lies in in region II. The system (4.2.4) has two interior equilibrium points $E_2 = (0.147361, 0.393402)$ and $E_3 = (0.102639, 0.281598)$. Point E_2 is unstable and Point E_3 is saddle (e) $\lambda_2 = -0.1, \quad \lambda_1 = -0.0007$ lies in region III. The system (4.2.4) has two interior equilibrium points $E_2 = (0.166833, 0.442083)$ and $E_3 = (0.083167, 0.232917)$. Point E_2 is surrounded by an unstable limit cycle and Point E_3 is saddle. (f) $\lambda_2 = -0.1, \quad \lambda_1 = -0.002$ lies in region IV. The system (4.2.4) has two interior equilibrium points $E_2 = (0.195711, 0.514277)$ and $E_3 = (0.0542893, 0.160723)$. Point E_2 is asymptotically stable and Point E_3 is saddle. 129

5.1 Strong Allee effect: $\beta = 0.4, \gamma = 0.1, \xi = 0.1, \rho = 0.2$. (a) This diagram shows how the number of interior equilibrium points changes with θ. All parabola are the prey nullcline for different values of θ and line is predator nullcline. For solid parabola $\theta = 0.05$ for dashed parabola $\theta = 0.225$ and for dotted parabola $\theta = 0.5$. (b) Phase portrait diagram of system (5.2.2) for $\theta = 0.225$. The dotted trajectories are the separatrix. (c) and (d) are the bifurcation diagram of the system (5.2.2). The upper curve stands for the stable equilibrium and the lower curve stands for unstable equilibrium. . . . 148

5.2 Strong Allee effect: $\beta = 0.4, \gamma = 0.1, \xi = 0.1, \theta = 0.2$. (a) $\rho = 0.2$ two interior equilibrium points exist. E_1^* is asymptotically stable and E_2^* is saddle. (b) $\rho = 0.009722$ an unstable limit cycle bifurcates through Hopf bifurcation around E_1^* (c) $\rho = 0.0166067444209415$ The diagram shows that the limit cycle collides with the saddle point E_2^* to give a Homoclinic loop. (d) $\rho = 0.008$ E_1^* is unstable point. The Dotted trajectories are the stable and unstable manifolds. 149

5.3 Strong Allee effect: $\beta = 0.3, \theta = 0.1, \gamma = 0.2$. (a) Bifurcation diagram of system (5.2.2) in $\xi\rho$ space (b) $\xi = 0.17335, \rho = 0.12793$ phase portrait diagram of the system (5.2.2). (c) $\xi = 0.175, \rho = 0.05$ lie in region I. No interior equilibrium point exist. The equilibrium point E_γ is globally stable. (d) $\xi = 0.170, \rho = 0.1$ lie in in region II. Two interior equilibrium points exist.(e) $\xi = 0.169, \rho = 0.0634$ lie in in region III. Two interior equilibrium points exist. (f) $\xi = 0.172, \rho = 0.05$ lie in in region IV. Two interior equilibrium points exist. 152

5.4 Weak Allee effect: $\beta = -0.05, \gamma = 0.3, \xi = 0.4, \theta = 0.3$. (a) $\rho = 0.3$ two interior equilibrium points exist. e_1^* is asymptotically stable and e_2^* is saddle. (b) $\rho = 0.134615$ an unstable limit cycle bifurcates through Hopf bifurcation around e_1^* (c) $\rho = 0.14681$. The diagram shows that the limit cycle collides with the saddle point e_2^* to give a Homoclinic loop.(d) $\rho = 0.12$, the point e_1^* is unstable point. The Dotted trajectories are the stable and unstable manifolds. 153

5.5 Weak Allee effect: $\beta = -0.25, \gamma = 0.3, \xi = 0.5, \theta = 0.45$. (a) $\rho = 0.3$ only one interior equilibrium point e_* exists, which is asymptotically stable. (b) $\rho = 0.0910797$ a stable limit cycle bifurcates through Hopf bifurcation around e_* 154

5.6 Weak Allee effect: $\beta = -0.225, \gamma = 0.3, \xi = 0.4, \theta = 0.45$. (a) $\rho = 0.5$ only one interior equilibrium point e exists, which is asymptotically stable. (b) $\rho = 0.13482$ a stable limit cycle bifurcates through Hopf bifurcation around e. 154

5.7 Weak Allee effect: $\beta = -0.2, \gamma = 0.3, \xi = 0.5, \theta = 0.45$. (a) Bifurcation diagram of system (5.2.2) (b) $\xi = 0.4, \rho = 0.16$ phase portrait diagram of the system (5.2.2). (c) $\xi = 0.45, \rho = 0.10$ lie in region I. No interior equilibrium point exist. The equilibrium point E_γ is globally stable. (d) $\xi = 0.36, \rho = 0.20$ lie in in region II. Two interior equilibrium points exist.(e) $\xi = 0.3, \rho = 0.2$ lies in region III. Only one interior equilibrium points exist which is globally stable. (f) $\xi = 0.38, \rho = 0.110355$ lie in region IV (region between red and blue curve). Two interior equilibrium points exist. (g) $\xi = 0.38, \rho = 0.05$ lie in region V. Two interior equilibrium points exist. 155

6.1 $\gamma = 10,\ \alpha = 1,\ \beta = 0.5,\ \xi = 1.5,\ \delta = 0.4$ (a) $\theta = 0.3$. System (6.2.4) has two interior equilibrium points $E_1^* = (4.81386, 3.79307), E_2^* = (7.68614, 2.35693)$. The point E_1^* is stable and E_2^* is saddle. (b) $\theta = \theta^{[hf]} = 0.2160448$. System (6.2.4) has two interior equilibrium points $E_1^* = (8.57824, 1.57506), E_2^* = (3.92176, 3.9033)$. A stable limit cycle arises through Hopf bifurcation around E_1^*, E_2^* is a saddle point. (c) $\theta = \theta^{[SN]} = 0.3515625$. System (6.2.4) has a unique interior equilibrium points $E_4 = (6.25, 3.28125)$ which is a saddle-node point. The red color trajectories are unstable manifold, the orange color trajectories are the stable manifold, the green color curve the prey nullcline and purple color curve is the predator nullcline. (d) Saddle-node bifurcation diagram. Upper curve stands for unstable equilibria and lower curve stands for stable equilibria. 175

6.2 $\gamma = 10,\ \alpha = 2,\ \beta = 0.5,\ \xi = 1.5,\ \delta = 0.18$ (a) $\theta = 2$. System (6.2.4) has two interior equilibrium points $E_1^* = (1.18206, 4.56951), E_2^* = (8.72419, 1.62336)$. The point E_1^* is unstable and E_2^* is saddle. (b) $\theta = 4.31764$. System (6.2.4) has two interior equilibrium points $E_1^* = (3.86489, 4.8252), E_2^* = (6.04136, 3.97502)$. A stable limit cycle arises through Hopf bifurcation around E_1^*, point E_2^* is saddle. (c) $\theta = 4.45$. System (6.2.4) has two interior equilibrium points $E_1^* = (4.29003, 4.73358), E_2^* = (5.61622, 4.21554)$. The point E_1^* is stable and E_2^* is saddle. (d) $\theta = 4.1$. System (6.2.4) has two interior equilibrium points $E_1^* = (3.40121, 4.8839), E_2^* = (6.50504, 3.67147)$. A stable Homoclinic loop is emerging through Hopf bifurcation around E_1^*. (e) $\theta = 4.528168$. System (6.2.4) has a unique interior equilibrium points $E_4 = (4.95313, 4.51853)$ which is a saddle-node point. The red color trajectories are unstable manifold, the orange color trajectories are the stable manifold, the green color curve the prey nullcline and purple color curve is the predator nullcline. (f) Saddle-node bifurcation diagram. Upper curve stands for unstable equilibria and lower curve stands for stable equilibria. . . 176

6.3 (a) Bifurcation diagram for the system (6.2.4). The blue curve is Saddle-node bifurcation curve, red curve is the Hopf bifurcation curve and green curve is the Homoclinic bifurcation curve. (b) $\lambda_1 = \lambda_2 = 0$ The unique interior equilibrium point E_4 is a cusp of codimension 2 (c) System (6.2.4) has no interior equilibrium point, whenever $(\lambda_1, \lambda_2) = (0.029, -0.1)$ lies in region I (d) System (6.2.4) has two interior equilibrium points, whenever $(\lambda_1, \lambda_2) = (0.02861, -0.1)$ lies in region II, in which one is a saddle and other is stable focus (e) System (6.2.4) has two interior equilibrium points whenever $(\lambda_1, \lambda_2) = (0.02791, -0.1)$ lies in region III, a stable limit cycle enclosing an interior point and the other interior point is a saddle. (f) System (6.2.4) has two interior equilibrium points, whenever $(\lambda_1, \lambda_2) = (0.02161, -0.1)$ lies in region IV, in which one is a saddle and other is unstable focus. 180

7.1 Physical configuration of the problem. 185

7.2 Hopf bifurcation diagram for parameter values $\lambda_2 = 0.1, \Omega = 1, \delta = 0.02, R_i = 0.4$ (a) $\lambda_1 = 0.5$ (b) $\lambda_1 = 0.14336936$ (c) Supercritical Hopf bifurcation in the phase parameter (x, y, α) space (d) Paraboloid surface formed by α family of limit cycles. 196
7.3 The point A is stable while the origin is unstable. $\lambda_1 = 0.5, \lambda_2 = 0.1, \Omega = 2, \delta = 0.02, R_i = 1$ 197
7.4 Supercritical Pitchfork Bifurcation. $\lambda_1 = 0.5, \lambda_2 = 0.1, \Omega = 2, \delta = 0.02, R_i = 1, s = \pi/3$ 197
7.5 Effect of Ri on Nu For fixed values of the other parameters. 197
7.6 Effect of λ_1 on Nu For fixed values of the other parameters. 198
7.7 Effect of λ_2 on Nu For fixed values of the other parameters. 198
7.8 Effect of δ on Nu For fixed values of the other parameters. 198
7.9 Effect of Ω on Nu For fixed values of the other parameters. 199
7.10 Comparison between internal and non-internal heating system. 199
7.11 Stremlines at (a) $s = 0.0$, (b) $s = 0.13$, (c) $s = 0.16$, (d) $s = 0.2$, (e) $s = 0.3$, (f) $s = 0.43$. 200
7.12 Isotherms at (a) $s = 0.0$, (b) $s = 0.13$, (c) $s = 0.16$, (d) $s = 0.2$, (e) $s = 0.3$, (f) $s = 0.43$. 201
7.13 Phase portrait diagram for $A(s)$ and s, shows that $A(s)$ is stable when s increases. 201

Chapter 1

Introduction

This chapter introduces some basic terminology, definitions, lemmas, theorems, models and methods required to comprehend the following chapters.

1.1 Dynamical System

The initial value problems governed by nonlinear ordinary or partial differential equations, or by difference equations are being used frequently to model many natural, physical and social phenomena. Generally, an initial value problem governed by a system of n ordinary or partial differential equations, or by difference equations is referred as "dynamical system" of dimension n, and determines the time behaviour of evolutionary process. For example, motion of celestial bodies, interactions between predators and their preys, spreading of diseases, fluid turbulance, price fluctuations of markets and stock market etc. The theory of dynamical systems was originated with the work of Henri Poincare (1854-1912), which was concerned with the stability and evolution of the solar system. A dynamical system gives a functional description of the mathematical model. In the last few decades, the theory of dynamical system has been a matter of great importance in many areas, like engineering, ecology, economics, biology, mathematics, etc.

Suppose $U \subset \mathbb{R}^n$ and $V \subset \mathbb{R}^m$ are the open sets, then initial value problems

$$\frac{dX}{dt} = F(X, t; \mu), \qquad X(t_0) = X_0, \tag{1.1.1}$$

and

$$X \mapsto G(X;\mu), \qquad X(t_0) = X_0, \tag{1.1.2}$$

where $X \in U$ is a state vector, $F(X,t;\mu)$ is a smooth function, $t \in I \subseteq \mathbb{R}$ is the independent variable and is often referred to "time", $\mu \in V$ is the parameter and G is a smooth map, are termed as the dynamical systems. The system (1.1.1) is called a continuous-time dynamical system and the system (1.1.2) is called a discrete-time dynamical system. If F does not depend explicitly on t, the system (1.1.1) is called an autonomous system. If F depends explicitly on t, the system (1.1.1) is called a non-autonomous system.

A continuously differentiable function $X(t), X : I \to \mathbb{R}^n$ is called a solution of the system (1.1.1) on an interval $I \subset \mathbb{R}$, if $X(t)$ satisfies the system (1.1.1). The solution $X(t)$ of the system (1.1.1) gives the past ($t < t_0$) and future ($t > t_0$) evolutions of the system. It may be represented by directed curves called trajectories on $\mathbb{R}^n$ plane formed by dependent variables of the system (1.1.1) which is known as phase plane of the system. The phase portrait of system (1.1.1) is a picture (in $\mathbb{R}^n$) of a collection of all qualitatively different trajectories of the system. The phase portrait consists of a number of information about the dynamical behavior of the system such as, number and nature of equilibrium points.

Consider two autonomous dynamical systems

$$\frac{dX}{dt} = F_1(X), \quad X \in \mathbb{R}^n \tag{1.1.3}$$

and

$$\frac{dX}{dt} = F_2(X), \quad X \in \mathbb{R}^n \tag{1.1.4}$$

The system (1.1.3) is said to be topologically equivalent to the system (1.1.4) in a neighbourhood of origin, if there exists a homeomorphism $H : U \to V$, where $U \subset \mathbb{R}^n$ and $V \subset \mathbb{R}^n$ are two open sets containing the origin, such that the trajectories of system (1.1.3) in U are mapped onto the trajectories of system (1.1.4) in V and preserving the direction of time.

In this thesis, emphasis has been given on the qualitative analysis of some real life problems, which can be formulated as two dimensional continuous-time autonomous dy-

namical systems (one prey one predator system) and a weakly nonlinear thermal instability problems reduced to a complex Ginzburg-Landau (one and two dimensional) equation.

1.2 Stability Analysis

It is well known that analytical solutions of nonlinear differential equations (dynamical systems) are impossible to obtain except for some special forms. Hence, different mathematical tools are required in order to study these systems. Stability analysis of the dynamical system is one of the aspect to study the system. Stability of dynamical system is usually analyzed near some special points called equilibrium points. Stability of a dynamical system means that a small change in the system at some instant gives only a small change in its behavior at all future time i.e. it determines whether the system settle down to equilibrium or keeps repeating in cycles.

Various methods have been introduced to study the stability of nonlinear dynamical systems; for example, Lyapunov method, Poincare method, Lagrange method, Lyapunov indirect method, etc. In this thesis Lyapunov indirect method (Linearization method) has been applied, in which the system has been linearized at the equilibrium points.

Consider an n dimensional autonomous nonlinear dynamical system

$$\frac{dX}{dt} = F(X(t)), \qquad X(t) \in \mathbb{R}^n, \tag{1.2.1}$$

with the initial condition $X(0) = X_0$.

i) An equilibrium point of the system (1.2.1) is a point $X^* \in \mathbb{R}^n$ such that

$$F(X^*) = 0, \tag{1.2.2}$$

i.e., a solution that is initialized at X^* will remain unchanged for all future time. The terms equilibrium solution, fixed point, stationary point, rest point, singularity, critical point and steady state are using as synonym of equilibrium point.

ii) The equilibrium point X^* is said to be locally stable (Lyapunov stable) if for given

$\epsilon > 0$, there exist a $\delta > 0$ depends on ϵ, such that, if $|X_0 - X^*| < \delta$ (where $|\cdot|$ is a norm on R^n), then $|X(t) - X^*| < \epsilon$, for all $t \geq 0$. That is, the equilibrium point X^* will be locally stable if solutions starting from small neighbourhood of the point remains in the neighbourhood of the point for all future times.

iii) A locally stable equilibrium point X^* is said to be locally asymptotically stable, if the positive constant δ can be chosen such that, if $|X_0 - X^*| < \delta$, then $\lim_{t\to\infty} |X(t) - X^*| = 0$. That is, the point X^* will be asymptotically stable if solutions starting from small neighbourhood of the point converge to the point as $t \to \infty$.

iv) An equilibrium point X^* is said to be globally asymptotically stable, if $\lim_{t\to\infty} |X(t) - X^*| = 0$, for all $X_0 \in \mathbb{R}^n$. That is, if X^* is asymptotically stable for any initialization.

v) An equilibrium point which is not stable is known as unstable.

Linearization Method

To investigate the stability of the equilibrium point X^* one must understand the nature of solutions in the neighbourhood of the point X^*. Shift the equilibrium point X^* of the system (1.2.1) to the origin by means of transformation $Y = X - X^*$. Then, by Taylor series expansion and equilibrium equation (1.2.2), the system (1.2.1) in a neighborhood of the origin can be written as

$$\frac{dY}{dt} = DF(X^*)Y + \frac{1}{2}D^2F(X^*)(Y,Y) + \cdots \tag{1.2.3}$$

Assuming that the quadratic and higher order terms are small, then

$$\frac{dY}{dt} \approx DF(X^*)Y. \tag{1.2.4}$$

This is known as the linearized system for the nonlinear system (1.2.1) in a neighborhood of the equilibrium point X^*. The matrix $J_{X^*} = DF(X^*)$ is called the Jacobian matrix of the system (1.2.1) at the equilibrium point X^*.

An equilibrium point X^* is known as hyperbolic equilibrium point of the system (1.2.1) if none of the eigenvalues of the matrix J_{X^*} have zero real part. The nonlinear

system near the hyperbolic equilibrium point has the similar local behaviour that of the associated linearized system (Hartman-Grobman theorem J. Guckenheimer and P. Holmes 1983) and is determined by the signs of the real parts of the eigenvalues of the matrix $DF(X^*)$.

Theorem 1.2.1. *If X^* is a hyperbolic equilibrium point of the system* (1.2.1) *such that all of the eigenvalues of $DF(X^*)$ have strictly negative real parts, then the equilibrium X^* is locally asymptotically stable.*

The Routh-Hurwitz criterion provides necessary and sufficient condition for a polynomial equation to have all the roots with negative real part.

Theorem 1.2.2 (Routh-Hurwitz Test (Wiggins 2003))**.** *All of the roots of the polynomial equation*

$$a_0 z^n + a_1 z^{n-1} + \cdots + a_{n-1} z + a_n = 0, \qquad a_i \in \mathbb{R}, \quad a_0 \neq 0$$

have real parts strictly less than zero if and only if all $n+1$ elements in the first column of the Routh table

$$\begin{array}{ccccc} a_0 & a_2 & a_4 & a_6 & \cdots \\ a_1 & a_3 & a_5 & a_7 & \cdots \\ r_{3,1} & r_{3,2} & r_{3,3} & r_{3,4} & \cdots \\ r_{4,1} & r_{4,2} & r_{4,3} & r_{4,4} & \cdots \\ \vdots & \vdots & \vdots & \vdots & \vdots \\ r_{n+1,1} & r_{n+1,2} & r_{n+1,3} & r_{n+1,4} & \cdots \end{array}$$

where

$(r_{i,1}\ r_{i,2}\ \cdots) \equiv (r_{i-2,2}\ r_{i-2,3}\ \cdots) - \frac{r_{i-2,1}}{r_{i-1,1}}(r_{i-1,2}\ r_{i-1,3}\ \cdots)$, $i > 2$, *are nonzero and have the same sign.*

The linearized technique can only provide local information of the system and it is interesting to find the condition under which local stability implies the global stability.

Dulac's Criteria

A solution $X(t)$ of the autonomous system (1.2.1) through the point X_0 is called a periodic solution if there exist a real number $\tau > 0$ such that

$$X(t+\tau, X_0) = X(t, X_0), \qquad \forall t \in \mathbb{R}.$$

The least value of τ is known as the period of the solution. In the phase plane, periodic solutions appear as closed orbit (or cycle or periodic orbit). An isolated periodic solution (cycle) of an autonomous system is called a limit cycle, which can only occur in nonlinear systems. If all neighbouring trajectories are attracted by the limit cycle, it is called a stable limit cycle. If all neighbouring trajectories are repelled by the limit cycle, it is called an unstable limit cycle. If neighbouring trajectories of one side are attracted and other side are repelled by the limit cycle, it is called a semistable limit cycle.

Theorem 1.2.3 (Dulac's Criteria (Perko 1996))**.** *Consider the planar system*

$$\frac{dX}{dt} = F(X) \tag{1.2.5}$$

with $F = (f_1, f_2)^T$ *and* $X = (x, y)^T \in \mathbb{R}^2$. *Let* $F \in C^1(E)$ *where* E *is a simply connected region in* $\mathbb{R}^2$. *If there exists a function* $B \in C^1(E)$ *such that* $\nabla.(BF)$ *is not identically zero and does not change sign in* E, *then* (1.2.5) *has no closed orbit lying entirely in* E.

1.3 Bifurcation Analysis

The qualitative behavior of a dynamical system may depends upon the parameters involved because it is often found that the qualitative behavior of the system remains unchanged for certain ranges of the parameter(s) and for certain range of parameter(s) a sudden change occur, such as, equilibria appear, disappear, change of stability of the equilibrium point(s), change in the nature of trajectories, etc. These changes are known as "bifurcation" and the associated parameter(s) is (are) known as bifurcation parameter(s). The parameter value at which bifurcation occur is known as bifurcation value of the parameter and the point at

which the bifurcation occurs is called the bifurcation point. The qualitative changes occur at the equilibrium point due to change in parameter(s) are known as local bifurcations. Transcritical bifurcation, Saddle-node bifurcation, Pitchfork bifurcation, Hopf bifurcation and Bogdano-Taken bifurcations are the example of local bifurcation. If larger invariant sets, such as periodic orbits, collide with each other, or with equilibria of the system are known as global bifurcations. The Homoclinic bifurcation (limit cycle collides with a saddle point) and Heteroclinic bifurcation (limit cycle collides with two or more saddle points) are the example of global bifurcation. Bifurcation associated with a single parameter are known as codimension 1 bifurcation, such as, Transcritical bifurcation, Saddle-node bifurcation, Pitchfork bifurcation etc. Bifurcations associated with two parameters are known as codimension 2 bifurcation, such as, Bogdanov-Takens bifurcation. The diagram of the parameter values versus the fixed points of the system is called bifurcation diagram.

1.3.1 Saddle-node Bifurcation

If the number of equilibrium points of a dynamical system remains unchanged for a certain range of a parameter and for a certain range of the parameter two equilibrium points disappear in which one of the two equilibria is stable and the other is unstable, before they disappear, this change in the qualitative behavior of the system is known as Saddle-node bifurcation. The Sotomayor's theorem analytically shows the occurrence of Saddle-node bifurcation.

Theorem 1.3.1 (Sotomayor (Perko 1996))**.** *Let us consider a system*

$$\frac{dX}{dt} = F(X, \mu), \quad X \in \mathbb{R}^n, \quad \mu \in \mathbb{R}. \tag{1.3.1}$$

Suppose that $F(X^*, \mu^*) = 0$ *and that the* $n \times n$ *Jacobian matrix* $J_{(X^*,\mu^*)} = DF(X^*, \mu^*)$ *has a simple eigenvalue* $\lambda = 0$ *with eigenvector* V *and that* J^T *has an eigenvector* W *corresponding to the eigenvalue* $\lambda = 0$*. Furthermore, suppose that* J *has* k *eigenvalues with negative real part and* $(n-k-1)$ *eigenvalues with positive real part and that the following conditions are*

satisfied

$$W^T F_\mu(X^*, \mu^*) \neq 0, \quad \text{and} \quad W^T[D^2F(X^*, \mu^*)(V, V)] \neq 0, \tag{1.3.2}$$

then there is a smooth curve of equilibrium points of (1.3.1) *in* $\mathbb{R}^n \times \mathbb{R}$ *passing through* (X^*, μ^*) *and tangent to the hyperplane* $\mathbb{R}^n \times \{\mu^*\}$. *Depending on the signs of the expressions in* (1.3.2)*, there are no equilibrium points of* (1.3.1) *near* X^* *when* $\mu > \mu^*$ *(or when* $\mu < \mu^*$*). The two equilibrium points of* (1.3.1) *near* X^* *are hyperbolic and have stable manifolds of dimension* k *and* $k+1$ *respectively; i.e., the system* (1.3.1) *experiences a saddle-node bifurcation at the equilibrium point* X^* *as the parameter* μ *passes through the bifurcation value* $\mu = \mu^*$.

For a one dimensional system, the expressions in (1.3.2) reduce to

$$\frac{\partial F}{\partial \mu}(X^*, \mu^*) \neq 0, \quad \text{and} \quad \frac{\partial^2 F}{\partial X^2}(X^*, \mu^*) \neq 0, \text{respectively.}$$

For a two dimensional system with $F = (F_1, F_2)^T$ and $X = (x, y)^T$

$$F_\mu(X^*, \mu^*) = \begin{bmatrix} \frac{\partial F_1}{\partial \mu} \\ \\ \frac{\partial F_2}{\partial \mu} \end{bmatrix}, \quad D^2F(X^*, \mu^*)(V, V) = \begin{bmatrix} V_1^2 \frac{\partial^2 F_1}{\partial x^2} + 2V_1V_2 \frac{\partial^2 F_1}{\partial x \partial y} + V_2^2 \frac{\partial^2 F_1}{\partial y^2} \\ \\ V_1^2 \frac{\partial^2 F_2}{\partial x^2} + 2V_1V_2 \frac{\partial^2 F_2}{\partial x \partial y} + V_2^2 \frac{\partial^2 F_2}{\partial y^2} \end{bmatrix}_{(X^*, \mu^*)}.$$

1.3.2 Transcritical Bifurcation

If for a certain range of a parameter there are two equilibria, one stable and other unstable and for a certain range of the parameter the two equilibria exchange their stability, i.e., the unstable equilibrium becomes stable and the stable one becomes unstable, this change in the qualitative behavior of the system is known as Transcritical bifurcation. The Sotomayor's theorem analytically shows the occurrence of Transcritical bifurcation, if the expressions in (1.3.2) are changed to

$$W^T F_\mu(X^*, \mu^*) = 0, \quad W^T[DF_\mu(X^*, \mu^*)V] \neq 0, \quad \text{and} \quad W^T[D^2F(X^*, \mu^*)(V, V)] \neq 0. \tag{1.3.3}$$

For a one dimensional system, the expressions in (1.3.3) reduce to

$$\frac{\partial F}{\partial \mu}(X^*, \mu^*) = 0, \quad \frac{\partial^2 F}{\partial x \partial \mu}(X^*, \mu^*) \neq 0 \quad \text{and} \quad \frac{\partial^2 F}{\partial X^2}(X^*, \mu^*) \neq 0, \text{respectively.}$$

For a two dimensional system

$$DF_\mu(X^*, \mu^*)V = \begin{bmatrix} V_1 \frac{\partial^2 F_1}{\partial x \partial \mu} + V_2 \frac{\partial^2 F_1}{\partial y \partial \mu} \\ \\ V_1 \frac{\partial^2 F_2}{\partial x \partial \mu} + V_2 \frac{\partial^2 F_2}{\partial y \partial \mu} \end{bmatrix}_{(X^*, \mu^*)}.$$

1.3.3 Pitchfork Bifurcation

If equilibrium points of a dynamical system, which has symmetry between left and right directions, appear for a certain range of a parameter and for a certain range of the parameter it disappear in symmetrical pair, this change in the qualitative behavior of the system is known as Pitchfork bifurcation. The Sotomayor's theorem analytically shows the occurrence of Pitchfork bifurcation, if the expressions in (1.3.2) are changed to

$$W^T F_\mu(X^*, \mu^*) = 0, \quad W^T[DF_\mu(X^*, \mu^*)V] \neq 0, \quad W^T[D^2F(X^*, \mu^*)(V, V)] = 0, \quad \text{and}$$

$$W^T[D^3F(X^*, \mu^*)(V, V, V)] \neq 0. \tag{1.3.4}$$

For a one dimensional system the expressions in (1.3.4) reduces to

$$\frac{\partial F}{\partial \mu}(X^*, \mu^*) = 0, \ \frac{\partial^2 F}{\partial x \partial \mu}(X^*, \mu^*) \neq 0, \ \frac{\partial^2 F}{\partial X^2}(X^*, \mu^*) = 0 \text{ and } \frac{\partial^3 F}{\partial X^3}(X^*, \mu^*) \neq 0, \text{respectively.}$$

For a two dimensional system

$$D^3F(X^*, \mu^*)(V, V, V) = \begin{bmatrix} V_1^3 \frac{\partial^3 F_1}{\partial x^3} + 3V_1^2 V_2 \frac{\partial^3 F_1}{\partial x^2 \partial y} + 3V_1 V_2^2 \frac{\partial^3 F_1}{\partial x \partial y^2} + V_2^3 \frac{\partial^3 F_1}{\partial y^3} \\ \\ V_1^3 \frac{\partial^3 F_2}{\partial x^3} + 3V_1^2 V_2 \frac{\partial^3 F_2}{\partial x^2 \partial y} + 3V_1 V_2^2 \frac{\partial^3 F_2}{\partial x \partial y^2} + V_2^3 \frac{\partial^3 F_1}{\partial y^3} \end{bmatrix}_{(X^*, \mu^*)}.$$

1.3.4 Hopf Bifurcation

If for a certain range of a parameter of a dynamical system, there is a stable equilibrium point and for a certain range of the parameter equilibrium points losses its stability and gives birth to a limit cycle and vice versa, this change in the qualitative behavior of the system is known as Hopf bifurcation. The Hopf bifurcation for a system occurs, when a pair of a complex conjugate eigenvalues of the Jacobian matrix at an equilibrium point becomes purely imaginary. Thus, a Hopf bifurcation can only occur in two dimensional or higher dimensional systems. There are two types of Hopf bifurcations; Supercritical and Subcritical. Supercritical Hopf bifurcation occurs, when stable limit cycles arises around an unstable equilibrium point, while Subcritical Hopf bifurcation occurs, when unstable limit cycles arises around a stable equilibrium point.

Theorem 1.3.2 (Hopf (Guckenheimer and Holmes 1983))**.** *Suppose that the system* (1.3.1) *has an equilibrium at* (X^*, μ^*) *at which following properties are satisfied:*

$H_1 : J_{(X^*,\mu^*)} = DF(X^*, \mu^*)$ *has a simple pair of purely imaginary eigenvalues and no other eigenvalues with zero real parts.*

Then H_1 *implies that there is a smooth curve of equilibrium points* $(X(\mu), \mu)$ *with* $X(\mu^*) = X^*$*. The eigenvalues* $\lambda(\mu), \overline{\lambda}(\mu)$ *of* $DF(X(\mu), \mu^*)$ *which are imaginary at* $\mu = \mu^*$ *vary smoothly with* μ*. If, moreover,*

$H_2 : \frac{d}{d\mu}(Re\lambda(\mu))|_{\mu=\mu^*} \neq 0,$

is satisfied, then there exists a unique branch of periodic solution of the system (1.3.1) *near* (X^*, μ^*)*.*

Theorem 1.3.2 shows the existence of a unique periodic solution of the system but it does not says about the stability of the periodic solution (limit cycle). To investigate the stability of this periodic solution, one can rely on the sign of the first Lyapunov number (Perko 1996).

Consider a Planar system

$$\begin{cases} \frac{dx}{dt} = ax + by + p(x, y), \\ \frac{dy}{dt} = cx + dy + q(x, y), \end{cases} \tag{1.3.5}$$

with $\Delta = ad - bc > 0, \quad a + d = 0$ and

$$p(x, y) = \sum_{i+j\geq 2} a_{ij} x^i y^j, \quad q(x, y) = \sum_{i+j\geq 2} b_{ij} x^i y^j. \tag{1.3.6}$$

The first Lyapunov number σ is given by the formula

$$\begin{aligned} \sigma = -\frac{3\pi}{2b\Delta^{3/2}} \{ & \big[ac(a_{11}^2 + a_{11}b_{02} + a_{02}b_{11}) + ab(b_{11}^2 + a_{20}b_{11} + a_{11}b_{02}) + \\ & c^2(a_{11}a_{02} + 2a_{02}b_{02}) - 2ac(b_{02}^2 - a_{20}a_{02}) - 2ab(a_{20}^2 - b_{20}b_{02}) - \\ & b^2(2a_{20}b_{20} + b_{11}b_{20}) + (bc - 2a^2)(b_{11}b_{02} - a_{11}a_{20})\big] - \\ & (a^2 + bc)[3(cb_{03} - ba_{30}) + 2a(a_{21} + b_{12}) + (ca_{12} - bb_{21})]\big\} . \end{aligned} \tag{1.3.7}$$

If $\sigma \neq 0$, then a Hopf bifurcation occurs at the origin of the planar analytic system (1.3.5) at the bifurcation value given by $a + d = 0$; in particular, if $\sigma < 0$, then a unique stable limit cycle bifurcates from the origin of (1.3.5) as $(a + d)$ increases from zero and if $\sigma > 0$, then a unique unstable limit cycle bifurcates from the origin of (1.3.5) as $(a + d)$ decreases from zero (Perko 1996).

The technique to calculate the first Lyapunov number for a three dimensional and higher dimensional system is given in (Hassard et al. 1981).

1.3.5 Bogdanov-Takens Bifurcation

The occurrence of codimension 1 bifurcations has been discussed so far, now the occurrence of codimension 2 bifurcations such as Bogdanov-Takens bifurcation will be discussed. This codimension 2 bifurcation occurs at a point lying on the saddle-node bifurcation, whenever Jacobian matrix of the system at the point has a zero eigenvalue of (algebraic) mulitplicity 2. The BT bifurcation point in the parameter space is the intersection point of the Saddle-node bifurcation curve and the Hopf bifurcation curve. In this thesis, the procedure given in Xiao and Ruan (1999) has been used to obtain the normal form of Bogdanov-Takens bifurcation.

Consider a two dimensional autonomous system

$$\begin{cases} \frac{dx}{dt} = f(x, y, \lambda), \\ \frac{dy}{dt} = g(x, y, \lambda). \end{cases} \tag{1.3.8}$$

Suppose system (1.3.8) is C^∞ smooth with respect to the variables x, y and λ and $(x, y) = (x^*, y^*)$ is an equilibrium point at which the Jacobian matrix of the system (1.3.8) has a zero eigenvalue of mulitplicity two at $\lambda = \lambda^*$ but the Jacobian matrix is not a zero matrix.

Consider the transformation $x_1 = x - x^*, \quad x_2 = y - y^*$, then the system (1.3.8) reduces to

$$\begin{bmatrix} \frac{dx_1}{dt} \\ \\ \frac{dx_2}{dt} \end{bmatrix} = Lx + \begin{bmatrix} \langle P_1 x, x\rangle \\ \\ \langle Q_1 x, x\rangle \end{bmatrix} + O(|x|^3), \tag{1.3.9}$$

where $\langle \cdot, \cdot \rangle$ is a cartesian product in $\mathbb{R}^2$, $\quad O(|x|^3)$ is C^∞ in all variable, at least the third order with respect to $x = (x_1, x_2)^T$ and the matrices L, P_1 and Q_1 are defined as follows

$$L = \begin{bmatrix} \frac{\partial f}{\partial x} & \frac{\partial f}{\partial y} \\ \\ \frac{\partial g}{\partial x} & \frac{\partial g}{\partial y} \end{bmatrix}_{(x^*, y^*, \lambda^*)} \triangleq \begin{bmatrix} a & b \\ \\ c & d \end{bmatrix},$$

$$P_1 = \begin{bmatrix} \frac{\partial^2 f}{\partial x^2} & \frac{\partial^2 f}{\partial x \partial y} \\ \\ \frac{\partial^2 f}{\partial x \partial y} & \frac{\partial^2 f}{\partial y^2} \end{bmatrix}_{(x^*, y^*, \lambda^*)} \triangleq \begin{bmatrix} p_{11} & p_{12} \\ \\ p_{21} & p_{22} \end{bmatrix},$$

$$Q_1 = \begin{bmatrix} \frac{\partial^2 g}{\partial x^2} & \frac{\partial^2 g}{\partial x y} \\ \\ \frac{\partial^2 g}{\partial x y} & \frac{\partial^2 g}{\partial y^2} \end{bmatrix}_{(x^*, y^*, \lambda^*)} \triangleq \begin{bmatrix} q_{11} & q_{12} \\ \\ q_{21} & q_{22} \end{bmatrix}.$$

The above assumptions conclude that the matrix L is similar to the Jordan matrix

$$\begin{bmatrix} 0 & 1 \\ 0 & 0 \end{bmatrix}.$$

Therefore $b^2 + c^2 \neq 0$. Considering $b \neq 0$ and $y = Mx$, then the system (1.3.9) reduces to

$$\begin{bmatrix} \frac{dy_1}{dt} \\ \\ \frac{dy_2}{dt} \end{bmatrix} = MLM^{-1} \begin{bmatrix} y_1 \\ \\ y_2 \end{bmatrix} + M \begin{bmatrix} \langle (M^{-1})^T P_1 M^{-1} y, y \rangle \\ \\ \langle (M^{-1})^T Q_1 M^{-1} y, y \rangle \end{bmatrix} + O(|y|^3), \tag{1.3.10}$$

where $M = \begin{bmatrix} 1 & 0 \\ a & b \end{bmatrix}$ $\left(\text{if } b = 0 \text{ and } c \neq 0, \text{then set } \begin{bmatrix} 0 & 1 \\ c & -d \end{bmatrix} \right)$.

In the abstract form

$$\frac{dy}{dt} = Ay + h^2(y) + O(|y|^3), \tag{1.3.11}$$

where $A = \begin{bmatrix} 0 & 1 \\ bc - ad & a + d \end{bmatrix} \equiv \begin{bmatrix} 0 & 1 \\ 0 & 0 \end{bmatrix}$.

and

$$h^2(y) = \begin{bmatrix} \left(p_{11} - \frac{2a}{b} p_{12} + \frac{a^2}{b^2} p_{22}\right) y_1^2 + \left(\frac{2}{b} p_{12} - \frac{2a}{b^2} p_{22}\right) y_1 y_2 + \frac{1}{b^2} p_{22} y_2^2 \\ \\ d_1 y_1^2 + \overline{d}_1 y_1 y_2 + \left(\frac{a}{b^2} p_{22} + \frac{1}{b} q_{22}\right) y_2^2 \end{bmatrix}.$$

with

$$d_1 = a p_{11} - \frac{2a^2}{b} p_{12} + \frac{a^3}{b^2} p_{22} + b q_{11} - 2a q_{12} + \frac{a^2}{b} q_{22}$$

and

$$\overline{d}_1 = \frac{2a}{b} p_{12} - \frac{2a^2}{b^2} p_{22} + 2 q_{12} - \frac{2a}{b} q_{22}.$$

By the theory of normal forms, there exists a C^∞ change of variables in the vicinity of $(0, 0)$, such that the system (1.3.11) can be written as

$$\begin{bmatrix} \frac{dz_1}{dt} \\ \\ \frac{dz_2}{dt} \end{bmatrix} = A \begin{bmatrix} z_1 \\ \\ z_2 \end{bmatrix} + \begin{bmatrix} 0 \\ \\ d_1 z_1^2 + d_2 z_1 z_2 \end{bmatrix} + O(|z|^3), \tag{1.3.12}$$

where $d_2 = 2q_{12} + 2p_{11} - \frac{2a}{b}(p_{12} + p_{22})$.

If $d_1 d_2 \neq 0$ (nondegeneracy condition), the point (x^*, y^*) of the system (1.3.8) is a cusp of codimension 2.

Lemma 1.3.1. *If $d_1 d_2 \neq 0$, then in a small neighborhood of (x^*, y^*, λ^*), system (1.3.8) is C^∞ equivalent to*

$$\begin{cases} \frac{dx_1}{dt} = x_2 + \phi_1(x, \lambda), \\ \frac{dx_2}{dt} = d_1 x_1^2 + d_2 x_1 x_2 + \phi_2(x, \lambda), \end{cases} \tag{1.3.13}$$

where $\lambda = (\lambda_1, \lambda_2) \in \mathbb{R}^2, \phi_1, \phi_2 \in C^\infty(\mathbb{R}^2 \times \mathbb{R}^2, \mathbb{R}^2)$ and $\phi_1(x, \lambda^*), \phi_2(x, \lambda^*)$ are power series in (x_1, x_2) of powers $x_1^i x_2^j$ satisfying $i + j \geq 3$.

Lemma 1.3.2. *In a small neighborhood of $(0, 0, \lambda^*)$, system (1.3.13) is C^∞ equivalent to*

$$\begin{cases} \frac{dy_1}{dt} = y_2, \\ \frac{dy_2}{dt} = \phi_1(\lambda) + \phi_2(\lambda) y_1 + y_1^2 + y_2(\psi(\lambda) + \Phi(y_1, \lambda)) + y_2^2 \Psi(y, \lambda), \end{cases} \tag{1.3.14}$$

where $\Phi, \Psi \in C^\infty$ and $\Phi(y_1, \lambda^*) = \frac{d_2}{\sqrt{d_1}} y_1 \neq 0, \Psi(y, \lambda^*) = 0, \phi_1(\lambda^*) = \phi_2(\lambda^*) = \psi(\lambda^*) = 0$.

Theorem 1.3.3. *If the matrix*

$$\left[\begin{array}{cc} \frac{\partial(\phi_1(\lambda) - \frac{1}{4}\phi_2^2(\lambda))}{\partial \lambda_1} & \frac{\partial(\phi_1(\lambda) - \frac{1}{4}\phi_2^2(\lambda))}{\partial \lambda_2} \\ \\ \frac{\partial(\psi(\lambda) - \frac{d_2}{2\sqrt{d_1}}\phi_2(\lambda))}{\partial \lambda_1} & \frac{\partial(\psi(\lambda) - \frac{d_2}{2\sqrt{d_1}}\phi_2(\lambda))}{\partial \lambda_2} \end{array} \right]_{\lambda^*}$$

is nonsingular, bifurcation parameters can be chosen such that system (1.3.8) undergoes the Bogdanov-Takens bifurcation.

For more equivalent forms of Bogdanov-Takens bifurcation, one can refer Kuznetsov (2004) and Peng and Jiang (2011).

1.3.6 Homoclinic Bifurcation

An orbit that is asymptotic to the same equilibrium point as $t \to \pm\infty$ is known as Homoclinic orbit.

If there is a saddle point and a limit cycle for a certain range of a parameter of a dynamical system and for certain range of the parameter the limit cycle disappear but the

limit cycle collide with the saddle point and a Homoclinic orbit arises, before it disappear or vice versa. This change in the qualitative behavior of the system is known as Homoclinic bifurcation. This bifurcation is a global bifurcation.

1.4 Predator-prey Dynamical System

Species interact to each other in harmony in the ecosystem. These interactions may be in forms like competition, predation, parasitism and mutualism. These interactions are the base block of the ecosystem. In two species interaction, if the growth rate of one population decreases and others increases, then the populations are in a predator-prey situation. The predator-prey interactions are very interesting and have a great impact on the ecosystem. Lotka (1925) and Volterra (1926) independently formulated a two species continuous time predator-prey model which is known as Lotka-Volterra predator-prey model. This is the simplest predator-prey model, ignored many real life phenomenon. Later on Gause (1934) and May (1976) formulated predator-prey models based on laboratory experiment data.

Generally, a predator-prey system is formulated as

$$\begin{cases} \frac{dx}{dt} = xg(\cdot) - yp(\cdot), \\ \frac{dy}{dt} = yQ(\cdot), \end{cases} \tag{1.4.1}$$

with the initial conditions $x(0) > 0, y(0) > 0$, where $x(t)$ and $y(t)$ are prey and predator densities at time t, $g(\cdot)$ is the per capita growth rate of the prey species in the absence of predators, $p(\cdot)$ is the functional response of the predator to the prey and $Q(\cdot)$ is known as the predator growth function.

1.4.1 Per Capita Prey Growth Function

The per capita prey growth rate function $g(\cdot)$ is a continuous and differentiable function. It is the following two types

(*a*) *Density independent:* $g(\cdot) = r$, where $r > 0$ is constant and called intrinsic growth rate of the prey species.

(*b*) *Density-dependent:* $g(\cdot) = g(x, K)$, where K is the environmental carrying capacity of the prey. The density-dependent growth function $g(x, K)$ satisfies the following basic assumptions $g(K, K) = 0$, $g(0, K) > 0$, $\lim_{K\to\infty} g(0, K) < \infty$, $g_x(x, K) < 0$, $g_K(x, K) \geq 0$, $\lim_{K\to\infty} g_x(x, K) = 0$ and $g_{xK}(x, K) > 0$ for any $x > 0$. The following are the types of Density-dependent growth function.

(*i*) *Negative density-dependent:* In negative density dependent per capita growth rate is a decreasing function of population abundance. For example, logistic growth function $g(x, K) = r\left(1 - \frac{x}{K}\right)$, θ-logistic growth function $g(x, K) = r\left(1 - \left(\frac{x}{K}\right)^{\theta}\right)$, where θ parameter is the curvature of the relationship; whenever $\theta < 1$ the relationship is concave and whenever $\theta > 1$ the relationship is convex (Ayala et al. 1973), Gompertz growth function $g(x, K) = r \ln\left(\frac{K}{x}\right)$ (Gompertz 1825), Smith growth function $\frac{r(K-x)}{K+ax}$ (Smith 1963).

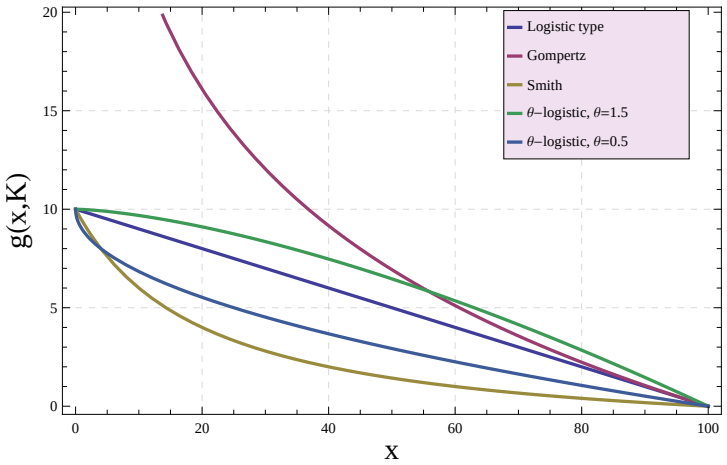

Figure 1.1: Graphs of logistic, $\theta-$logistic, Gompertz and Smith types per capita negative density-dependent prey growth rate functions.

(*ii*) Positive density-dependent: In positive density dependent per capita growth rate is a increasing function. For example, prey growth in the presence of Allee effect.

If the density dependent growth rate function $g(x, K)$ is non-negative and decreasing for $x \in (0, K)$, the system (1.4.1) is called compensation model and if it is increasing for small x, the model (1.4.1) is called depensation system. The logistic growth rate is very common in predator-prey model.

1.4.2 Functional Response

Functional response or consumption rate function $p(\cdot) \in C^1$ is described as the rate by which prey are consumed by individual predator (Solomon 1949). It depends on many factors, for example, prey escape ability, the various prey densities, the efficiency with which predators can search out and kill the prey, the handling time etc. Functional response can be divided into following two types

(i) **Prey-dependent Functional Response**

Functional response that depends on prey density only ($p(\cdot) = p(x)$) is the simplest functional response and known as prey dependent functional response. The functional responses satisfying the hypothesis (Hale and Somolinos 1983) $p(0) = 0,\ p_x(x) > 0, \forall x \geq 0$ and $\lim_{x\to\infty} p(x) = n < \infty$ are called monotonic prey dependent functional responses. Holling type I, Holling type II and Holling type III functional responses are the examples of monotonic functional response and the Holling type IV functional response is the example of the non-monotonic functional response.

Holling type I functional response is based on the principle of mass action, i.e., $p(x) = mx, m > 0$ is the maximum consumption rate of predator. It occurs whenever predator encounter on prey at random (searching strategy), for example passive predators like spiders. It leads to some conceptual shortcomings as the abundant food supply causes the increase in the equilibrium density of predator, but not in that of prey. It will finally lead to destabilizing the positive equilibrium.

Holling type II functional response is an asymptotic (cytoid) curve that is nonlinear as well as bounded. It is proposed by Michaelis and Menten (1913) as $p(x) = \frac{mx}{a+x}$, where $m > 0$ is the maximum consumption rate of predator and $a > 0$ is the half-saturation constant, for "nonlearning" predators or when given only one type of prey for which to search. Whenever prey densities are low, $p(x)$ approximates the Holling type I, i.e., predation rate is proportional to prey density. Whenever prey densities are high, then $p(x) = m$, i.e., predation rate levels off. Holling type II functional response has been shown to model the behavior of arthropod predators

(Hassel and May 1973).

Holling type III functional response is a sigmoid curve proposed by Holling (1959), when the predator learns over time how better to catch the prey and becomes increasingly motivated by the increasing density of a particular prey species and begins to feed on it selectively, or if at very low prey densities the return for the predator is lower than the energy expended for foraging. The mathematical form of Holling type III functional response is $p(x) = \frac{mx^2}{a+x^2}$, where $m > 0$ is the maximum consumption rate of predator and $a > 0$ is constant. This is non-linear and bounded function such that at low prey densities it becomes quadratic in prey density, and at high prey densities it becomes constant. Ecologically, the number of prey attacked per predator increases at an increasing rate at low prey densities, whereas at a decreasing rate at higher densities until it levels off. The Holling type III form appears to model the behaviour of vertebrate predators (DeAngelis 1992).

Sokol and Howell (1980) proposed a non-monotonic functional response (Holling type IV functional response) $p(x) = \frac{mx}{a+x^2}$, where $m > 0$ is the maximum consumption rate of predator and $a > 0$ is half-saturation constant in the absence of any inhibitory effect. The Holling type IV functional response form appears to model predator-prey system if antipredator behaviour exists, for example, group defence.

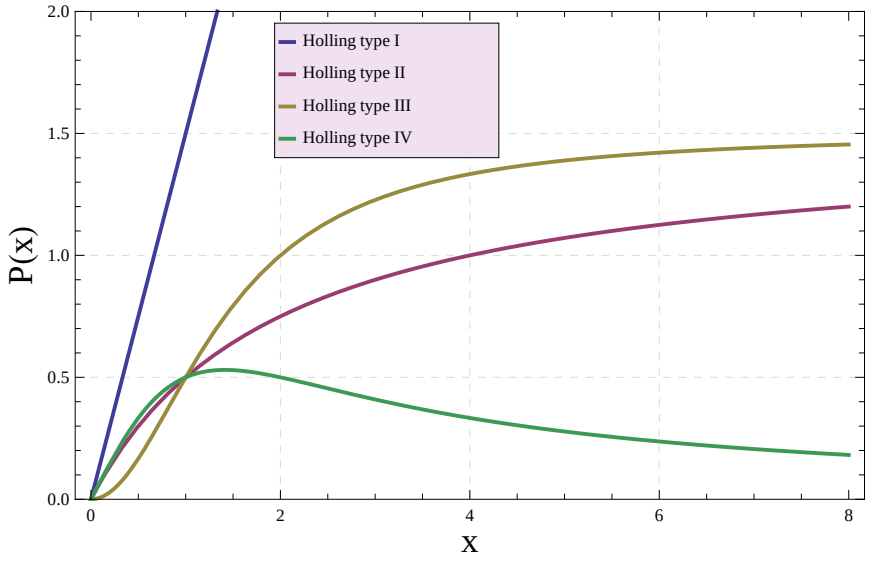

Figure 1.2: Graphs of Holling Type I, II, III and IV functional responses.

(*ii*) **Predator-dependent Functional Response**

When the number of predators haltingly changes (relative to prey change), there is a regular contest among the predators and the per capita rate of predation does not depend upon prey density alone rather it ought to depend on the densities of both prey and predator. For example, when predators have to search for food and consequently have to share or compete for food (Arditi and Ginzburg 1989; Arditi et al. 1991; and Gutierrez 1992). This type of functional response is called predator density-dependent functional response ($p(\cdot) = p(x, y)$). Some very common predator-dependent functional responses are Beddington-DeAngelis type and Crowley-Martin type.

A special type of predator dependent functional is proposed by Arditi and Ginzburg (1989) known as ratio-dependent functional response. They argued that the prey dependent functional response describes the consumption rate of predators on a very short behavioral time scale (minutes or hours) as compared to the growth of population which is on the longer time scale (days or months). They further suggested that functional response should be considered on the slow time scale of population dynamics for consistency, and presented the functional response as the ratio of prey to predator abundance i.e. $p(\cdot) = p(\frac{x}{y})$. This functional response has been criticised by Abrams (1994) and Sarnelle and Wilson (2008), but numerous field and laboratory experiments were performed which strongly offered strong evidence that in many real-world conditions ratio-dependent functional response is more realistic (Arditi and Ginzburg 1989; Arditi et al. 1991; Arditi and Ginzburg 1991; Berezovskaya et al. 2001; Arditi and Ginzburg 2012). The ratio dependent form of Holling type I, II and III functional responses are $p(\frac{x}{y}) = \frac{mx}{y}$, $p(\frac{x}{y}) = \frac{mx}{ay+x}$ and $p(\frac{x}{y}) = \frac{mx^2}{ay^2+x^2}$, respectively. The form $p(\frac{x}{y}) = \frac{mx}{ay+x}$ has been used extensively by the researchers Kuang and Beretta (1998); Xiao and Ruan (2001); Jost et al. (1999) and many more.

The prey-dependent predator-prey model exhibits the "paradox of enrichment" and also the so-called "biological control paradox" while the ratio-dependent does

not exhibit these (Hsu et al. 2001a, 2001b). It allows mutual extinction as possible outcome of predator-prey interaction (Kuang and Bertta 1998; Jost et al. 1999). Arino et al. (2004) gives the biological relevance of the prey-dependent and the ratio-dependent predator-prey models.

1.4.3 Predator Growth Function

In predator-prey literature two types of predator growth function have been commonly used. First is based on the assumption that predator's rate of increase is proportional to the amount of food ingested. The mathematical form of this function is,

$$Q(\cdot) = q(\cdot) - \delta, \tag{1.4.2}$$

where $\delta > 0$ is a constant and represents the per capita predator's death rate and $q(\cdot)$ is known as numerical response and describes how predators convert the consumed prey into the growth of predators. In most classical predator-prey models numerical response is assumed proportional to the functional response, i.e., $q(\cdot) = ep(\cdot)$ (Freedman 1980), so

$$Q(\cdot) = ep(\cdot) - \delta, \tag{1.4.3}$$

where e is the conversion efficiency of predators which consumed prey into their growth ($0 < e < 1$). A number of literature is available for such type of predator growth function. For example, Lotka-Volterra (1926), Seo and DeAngelis (2011) for Holling type-I; Bazykin (1998), Freedman (1980), Kuang and Freedman (1988) for Holling type-II; Lamontagne, Coutu and Rousseau (2008) for generalized Holling type-III; Huang and Xiao (2004) for Holling type-IV; Hwang(2003, 2004) for Beddington-DeAngelis functional and Arditi and Ginzburg (1989), Kuang and Bertta, (1998), Jost et al. (1999) for ratio-dependent functional response.

Other is based on the assumption that the predator growth function is of logistic form, where environmental carrying capacity of predator is proportional to the number of prey, that is, predator growth function is function of the ratio of predators and their prey

(Leslie 1948; Leslie and Gower 1960). The mathematical form of this function is

$$Q(\cdot) = Q(x, y) = s\Big(1 - \frac{y}{nx}\Big), \tag{1.4.4}$$

where parameter s is the intrinsic growth rates of predator and the parameter n is a measure of the food quality that the prey provides for conversion into predator births. A rich literature is available for such type of predator growth function. For example, Leslie and Gower (1960) for Holling type-I; Leslie (1948), Holling (1965), Tanner (1975) for Holling type-II; Jicai Huang et al. (2013) for Holling type-III; Li and Xiao (2007) for Holling type-IV; Liang and Pan (2007) for ratio-dependent functional response.

1.5 Some Predator-prey Models

The ODE system (1.4.1) offered a large variety of predator-prey system depends on the choices of prey growth function, functional response and predator growth functions (May 2001). In this section some basic predator-prey models with a brief outcome which are the base of this thesis are discussed.

1.5.1 Lotka-Volterra Predator-prey Model

The Lotka-Volterra predator-prey model is obtained by taking density independent prey growth rate, Holling type I functional response and (1.4.3) type predator growth function. Thus the system of first order differential equations (Volterra 1926)

$$\begin{cases} \frac{dx}{dt} = rx - mxy, \\ \frac{dy}{dt} = emxy - \delta y, \end{cases} \tag{1.5.1}$$

represents the Lotka-Volterra predator-prey interaction model, where the variables x, y and parameters r, m, e and δ have same meaning as defined earlier. The model (1.5.1) has two equilibrium points; $(0, 0)$ and $\Big(\frac{\delta}{em}, \frac{r}{m}\Big)$.

On linearizing the system (1.5.1) in the neighbourhood of the point $(0,0)$, one gets

$$\begin{cases} \frac{dx}{dt} = rx, \\ \frac{dy}{dt} = -\delta y. \end{cases} \tag{1.5.2}$$

The solution of the system (1.5.2) is $x(t) = x_0 e^{rt},\ y(t) = y_0 e^{-\delta t}$. It implies that in the neighbourhood of the origin the density of prey increases exponentially while density of predator decreases exponentially, that is, origin is unstable. This type of point is known as saddle point. Suppose $u = x - \frac{\delta}{em},\ v = y - \frac{r}{m}$, then the system (1.5.1) reduces to

$$\begin{cases} \frac{du}{dt} = -m(\frac{\delta}{em}v + uv), \\ \frac{dv}{dt} = em(\frac{r}{m}u + uv). \end{cases} \tag{1.5.3}$$

On linearizing the system (1.5.3) in the neighbourhood of the point $\left(\frac{\delta}{em}, \frac{r}{m}\right)$, it will become

$$\begin{cases} \frac{du}{dt} = -\frac{\delta}{e}v, \\ \frac{dv}{dt} = eru. \end{cases} \tag{1.5.4}$$

Eliminating t from the system (1.5.4), one gets

$$\frac{du}{dv} = -\frac{\delta v}{e^2 ru}.$$

On integrating, one gets

$$e^2 ru^2 + \delta v^2 = c^2,$$

where c^2 is integrating constant. In terms of x and y, above equation can be written as

$$e^2 r\Big(x - \frac{\delta}{em}\Big)^2 + \delta\Big(y - \frac{r}{m}\Big)^2 = c^2.$$

It represents a family of ellipses with center at $(\frac{\delta}{em}, \frac{r}{m})$.

In order to study the global stability of the unique interior equilibrium point, define a scalar function

$$V(u,v) = \int_0^u \frac{emt}{t + \frac{\delta}{em}}dt + \int_0^v \frac{mt}{t + \frac{r}{m}}dt.$$

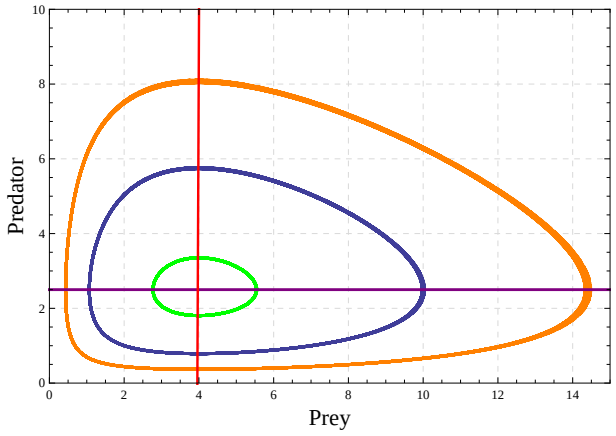

Figure 1.3: Phase portrait for Lotka-Volterra predator-prey mode (1.5.1)

It is clear that, $V(u,v) > 0$ and $V(0,0) = 0$. Now

$$\dot{V}(u,v) = \frac{emu\dot{u}}{u + \frac{\delta}{em}} + \frac{mv\dot{v}}{v + \frac{r}{m}} = emu(-mv) + mv(emu) = 0.$$

Thus, the equilibrium point $\left(\frac{\delta}{em}, \frac{r}{m}\right)$ is stable but not asymptotically stable. Therefore, point $\left(\frac{\delta}{em}, \frac{r}{m}\right)$ is a centre. Since the solutions are closed orbits about the equilibrium point, they must be periodic.

The Jacobian matrix of the system (1.5.1) at the equilibrium point $\left(\frac{\delta}{em}, \frac{r}{m}\right)$ is

$$\begin{bmatrix} 0 & -\frac{\delta}{e} \\ re & 0 \end{bmatrix}.$$

Thus, the eigenvalues of the above Jacobian matrix are purely imaginary which are given by $\lambda_{1,2} = \pm\iota\sqrt{r\delta}$. Therefore, the perturbations to prey and predator populations are linear combinations of $\exp(\sqrt{r\delta}t)$ and $\exp(-\sqrt{r\delta}t)$, that is, linear combinations of $cos(\sqrt{r\delta}t)$ and $sin(\sqrt{r\delta}t)$ with the coefficients depending upon the initial disturbances. Hence, one obtains neutral stability with perturbation leading to undamped pure oscillations with frequency $\sqrt{r\delta}$ and period $\frac{2\pi}{\sqrt{r\delta}}$. The amplitudes depend on the initial values only (Figure 1.3).

1.5.2 Rosenzweig-MacArthur Predator-prey Model

The model (1.4.1) is called Rosenzweig-MacArthur predator-prey model, when per capita prey growth rate is logistic type, functional response is Holling type II and predator growth function is (1.4.3) type, i.e., the system of two first order differential equations (Rosenzweig and MacArthur 1963)

$$\begin{cases} \frac{dx}{dt} = rx(1-\frac{x}{K}) - \frac{mxy}{x+a}, \\ \frac{dy}{dt} = \frac{emxy}{x+a} - \delta y, \end{cases} \tag{1.5.5}$$

represents Rosenzweig-MacArthur predator-prey model. The variables x, y and parameters r, K, m, e, a and δ have same meaning as defined earlier. This system reproduces the so-called paradox of enrichment: If the parameter K is small, the coexistence point (when it exists) is stable (Figure 1.4(a)). If K is large, the system (1.5.5) undergoes to Hopf bifurcation. The coexistence point becomes unstable and a stable periodic orbit appears around the unstable point(Figure. 1.4(b)) (Edelstein-Keshe, 1988).

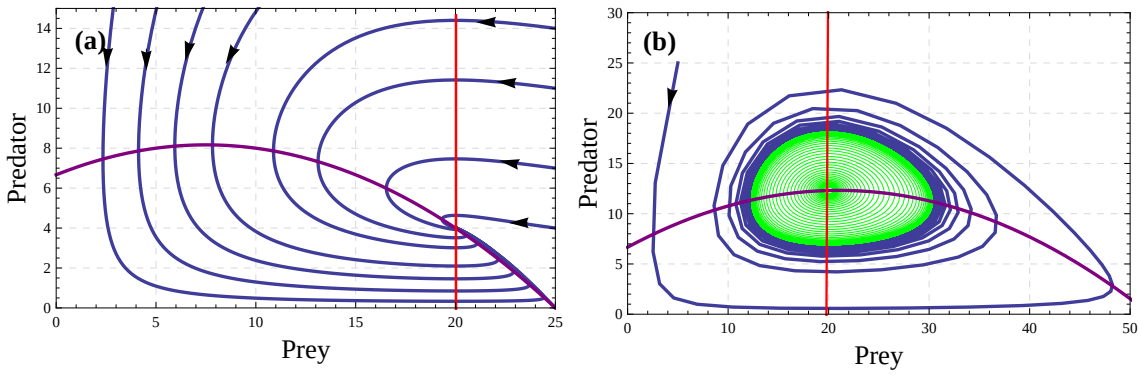

Figure 1.4: *Phase portrait for model* (1.5.5). *The red curve is the predator nullcline and purple curve is prey nullcline. (a) The unique interior equilibrium point is stable for low K. (b) The unique interior equilibrium point is unstable for large K and a stable limit cycle appears around the point.*

1.5.3 Leslie-Gower Predator-prey Model

The Leslie-Gower predator-prey model is based on the assumption that reduction in a predator population has a reciprocal relationship with per capita availability of its favourite food. This interesting formulation for the predator dynamics has attracted much attention and studied by Leslie and Gower (1960); Pielou (1969); Hsu and Hwang (1998); Mena-Lorca

(2007). The model (1.4.1) represents Leslie-Gower predator-prey model, if per capita prey growth is logistic type, functional response is Holling type I and predator growth function is (1.4.4) type (Mena-Lorca, 2007)

$$\begin{cases} \frac{dx}{dt} = rx(1-\frac{x}{K}) - mxy, \\ \frac{dy}{dt} = sy(1-\frac{y}{nx}), \end{cases} \tag{1.5.6}$$

with initial conditions $x(0) > 0, y(0) > 0$. The parameters r, K, m, s and n have same meaning as discussed earlier. The term nx is the carrying capacity of the predator and the term $\frac{y}{nx}$ is known as Leslie-Gower term which measures the loss in the predator population due to rarity of its favorite food.

The model (1.5.6) has two equilibrium points; (i) axial equilibrium point $(K, 0)$, and (ii) positive interior equilibrium point $(x^*, y^*) = \left(\frac{rK}{r+mnK}, \frac{rnK}{r+mnK}\right)$. It is clear that, the quantity of predators at the equilibrium depends directly on the quantity of prey at equilibrium multiplied by the food quality that the prey offers. The axial equilibrium point $(K, 0)$ is a saddle point while the positive interior equilibrium point is globally asymptotically stable (Figure 1.5). Mena-Lorca (2007) conclude that, if the food (prey) is of good quality $(n \to \infty)$, more predator can survive and require less quantity of prey. Moreover, if it is of bad quality, less predators will survive.

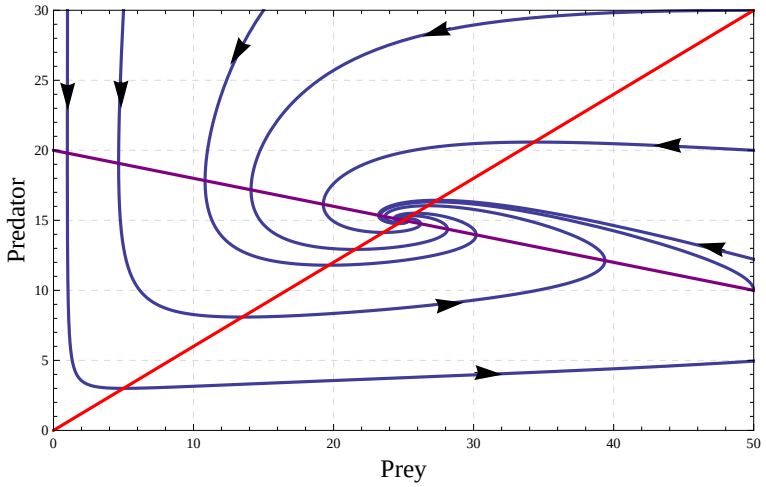

Figure 1.5: *Phase portrait for model* (1.5.6). *The red curve is predator nullcline and purple curve is prey nullcline. The unique interior equilibrium point is globally stable.*

1.5.4 Holling-Tanner Predator-prey Model

If Holling type II functional response is taken into the model (1.5.6), this new model is known as Holling-Tanner predator-prey model (Holling 1965; Tanner 1975; May 2001)

$$\begin{cases} \frac{dx}{dt} = rx(1-\frac{x}{K}) - \frac{mx}{x+a}y, \\ \frac{dy}{dt} = sy(1-\frac{y}{nx}), \end{cases} \tag{1.5.7}$$

with initial conditions $x(0) > 0, y(0) > 0$. The model (1.5.7), apart from the axial equilibrium point $(K, 0)$, has a unique positive interior equilibrium point whose abscissa is the positive root of the quadratic equation $rx^2 - (rK - ra - Kmn)x - raK = 0$ and ordinate is $y = nx$. Hsu and Hwang (1995) discussed the local stability of the positive equilibrium point of the system and derived the parametric conditions under which local stability of the unique positive equilibrium point implies global stability (Figure. 1.6(a)). Further, they showed that the system has a unique limit cycle when the unique positive equilibrium point becomes unstable (Figure 1.6(b)). Saez and Gonzalez-Olivares (1999) described the bifurcation diagram of limit cycle and showed that local stability and global stability of the unique positive equilibrium are not equivalent for system. Gasull et al. (1997) also showed that the asymptotic stability of the unique positive equilibrium does not imply the global stability by means of the Poincare-Lyapunov constants in case a weak focus occurs. They constructed an example with two limit cycles in which the innermost being unstable and the outermost being stable (Figure 1.6(c)).

1.5.5 Modified Leslie-Gower Predator-prey Model

One of the main demerits of the model (1.5.7) is that, at low density of prey, predator population can not switch to alternative prey since its growth will be limited by the fact that its most favorite food, the prey, is absent or is in short supply. This demerit is resolved by adding a positive additional constant in the denominator of the last term of the predator growth function. This new model is known as modified Leslie-Gower predator-prey model

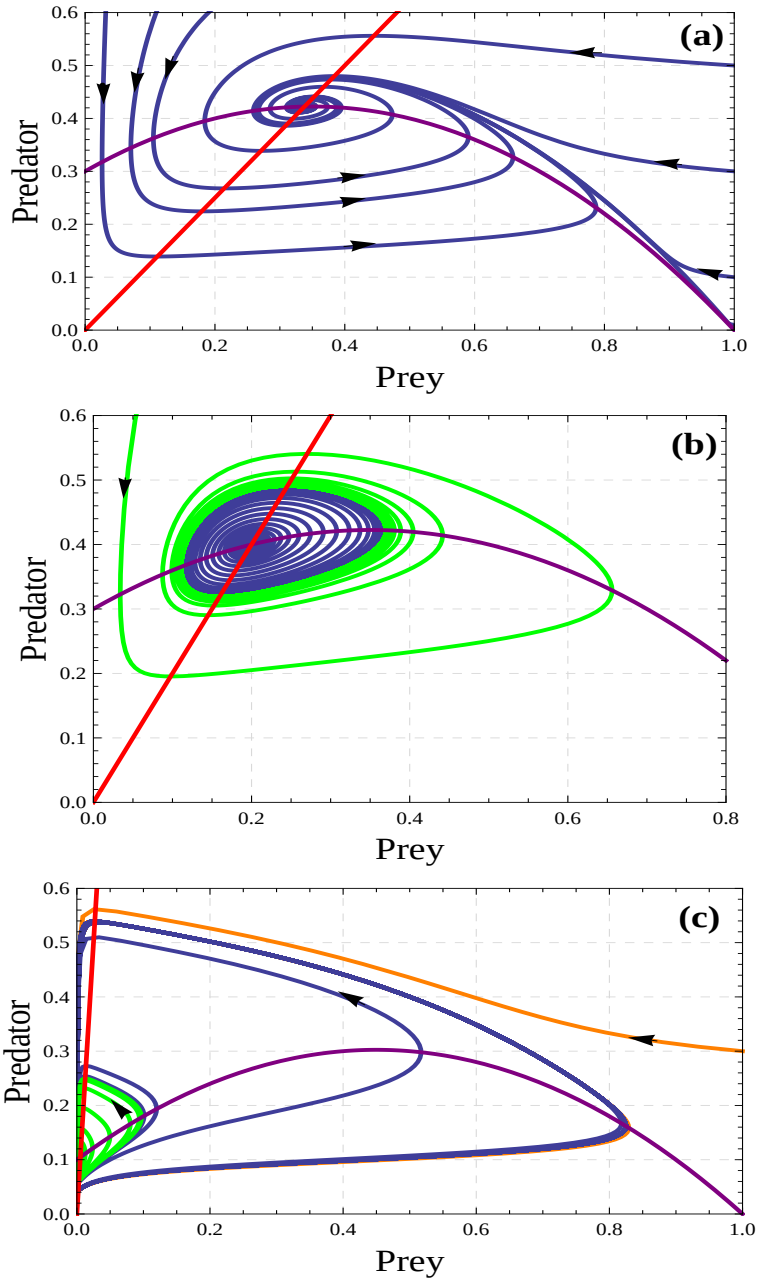

Figure 1.6: *Phase portrait for model* (1.5.7). *The red curve is predator nullcline and purple curve is prey nullcline. (a) The unique interior equilibrium point is globally stable. (b) The unique interior equilibrium point is unstable and a stable limit cycle arises around the equilibrium point. (c) The unique interior equilibrium point is stable and two limit cycle arises around the unique interior equilibrium point.*

(Aziz-Alaoui and Daher Okiye 2003)

$$\begin{cases} \frac{dx}{dt} = rx(1-\frac{x}{K}) - \frac{mx}{x+a}y, \\ \frac{dy}{dt} = sy(1-\frac{ny}{x+a_1}), \end{cases} \tag{1.5.8}$$

with initial conditions $x(0) > 0, y(0) > 0$, where a and a_1 measures the extent to which the environment provides protection to prey and predator respectively. Aziz-Alaoui and Okiye (2003) studied the boundedness of solutions and global stability of the positive equilibrium of the model. Du et al. (2009) obtained the sufficient criteria for the permanence of model and studied the globally asymptotic stability of solutions. Zhu and Wang (2011) obtained some sufficient conditions for the existence and global attractivity of positive periodic solutions of the model. The long time behavior as well as persistent condition for the model has been established with stochastic perturbation under the assumption $a = a_1$ by Ji et al. (2009, 2011).

With the advancement of the ecological knowledge due to theoretical, empirical, and observational research, more elements are recognized as essential to the phenomenon of predation. Some of them which has been the key feature of this thesis are given below.

1.6 Allee Effect

Warder Clyde Allee, an American ecologist in 1930s by means of experimental observational data concluded that the evolution of social structures was not only driven by competition, but that cooperation was another, if not the most, fundamental principle in animal species (Allee 1931). The dynamical consequences of this importance of animal aggregations directly led to what Odum called in 1953 "the Allee principle", now known as the Allee effect (Odum 1953). Allee effect is a positive relationship between any component of individual fitness and either numbers or density of conspecifics (Courchamp et al. 1999, Page no. 02). The Allee effect, also named as negative competition effect (Wang et al., 1999) in population dynamics or depensation (Dennis 1989; Clark 1990; Lierman 2001) in fisheries sciences, caused by a wide range of biological phenomena (Table 1 in Berec 2007 or Table

2.1 in Courchamp et al. 2008), difficulties in finding mates is one of the main cause.

Within the Allee effect domain, a most important distinction is made between component and demographic Allee effects (Stephens et al. 1999). Component Allee effect refers to a positive relationship between any measurable component of individual fitness and population size or density, for example juvenile survival or litter size. Whereas, demographic Allee effect refers to a positive relationship between total individual fitness, usually quantified by the per capita population growth rate, and population size or density (Berec et al. 2007). A demographic Allee effect is classified in the context of the nature of density dependence at low population densities into strong Allee effect and weak Allee effect (Deredec and Courchamp 2003). Strong Allee effect can induce a critical density below which per capita growth rate is negative and extinction tends to occur, and above which the per capita growth rate is positive and the population increases (density enhances) on average yielding convergence to the carrying capacity. Whereas weak Allee effect may result in reduced, but still positive, growth rate as population size or density decreases (Groom 1998).

In last some decades, Allee effect has been attracting much attention due to its strong potential impact on population dynamics (Berec et al. 2007; Courchamp et al. 2008; Owen and Lewis 2001; Petrovskii et al. 2002; Shi and Shivaji 2006; Wang and Kot 2001). It is widely observed that the Allee effect may increase the extinction risk of low-density populations (Dennis 1989; Lande 1987). Allee effects are mostly considered as single mechanisms of positive density dependence (Kang and Yakubu 2011; Gonzlez-Olivares et al. 2011; Sen et al. 2012; Gao and Li 2013). In predator-prey system either prey or predator or both predator and prey may be subject to the Allee effect. Whenever prey species subject to Allee effect, two different types of Allee effects may exhibit due to different mechanisms, namely Allee effect I and Allee effect II. Allee effect, that increases the intrinsic death rate or decrease the intrinsic birth rate of the prey population, causing the per capita growth rate of the prey to be decreased at low population density (Dennis, 1989; Reinhardt and Kohler, 2002) is known as Allee effect I. Allee effect I may occur due to several mechanisms, like, social thermoregulation, reduction of inbreeding, and genetic drift, etc. Allee effect II occur due to anti-predator defense, for example, anti-predator vigilance and aggression

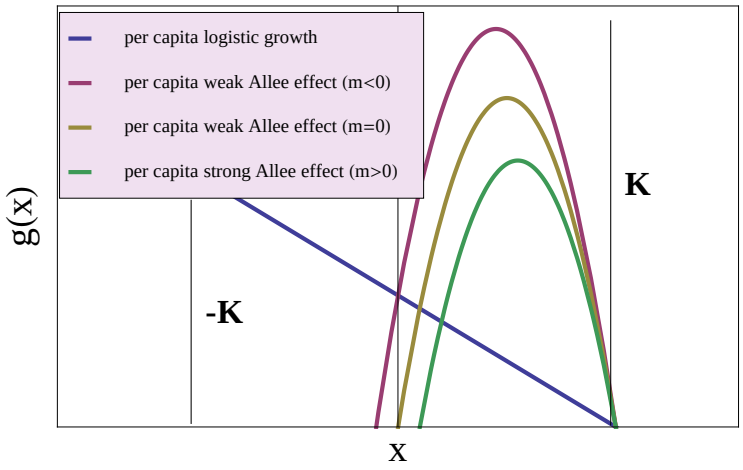

Figure 1.7: *The relationships between the per capita single population growth rate and population size for negative density dependence, strong, weak and special weak Allee effects.*

(Dennis 1989; Cote and Gross 1993). In mathematical terms, Allee effect I is expressed modifying the natural prey's per capita growth function, while Allee effect II is expressed modifying the functional response (Zhou et al. 2005). In predator-prey models Allee effect I may be of two forms; Multiplicative Allee effect and Additive Allee effect.

The per capita growth function of a single population affected by multiplicative Allee effect is given by (Lewis and Kareiva 1993; Owen and Lewis 2001)

$$g(\cdot) = g(x) = r\Big(1 - \frac{x}{K}\Big)(x - m), \tag{1.6.1}$$

The term $(x-m)$ is due to multiplicative Allee effect, where $-K < m << K$. The function $g(x)$ grows as the population size increases from $x \geq 0$ until it attains a maximum value and then, it decreases for larger population size to zero. If $m > 0$, Eq. (1.6.1) represents the strong Allee effect and the parameter m is a prey survival threshold; Notice, if $0 < x < m$, the per capita growth rate is negative, hence population experiences extinction. If $m \leq 0$, Eq. (1.6.1) represents the weak Allee effect, no threshold value exist. The difference between per capita logistic growth and population growth affected by strong, weak and special weak Allee effects has been shown in Figure 1.7.

Recent ecological research has suggested two or more Allee effects can generate mechanisms acting simultaneously on a single population (Table 1 in Berec 2007 or Table

2.1 in Courchamp et al. 2008); the combined impact of these phenomena has been called multiple Allee effect (Berec et al. 2007). The per capita growth function of a single population affected by multiplicative double Allee effect is given by

$$g(\cdot) = g(x) = \frac{r}{x+n}\Big(1 - \frac{x}{K}\Big)(x-m), \tag{1.6.2}$$

where $n > 0$ is known as auxiliary parameter satisfying $m > -n$. In Eq. (1.6.2), there are two independent Allee effects, affecting the same population growth; the factor $(x-m)$ represents the Allee effect which has been discussed in Eq. (1.6.1) and the factor $\frac{r}{x+n}$ represents the other Allee effect affecting the intrinsic growth rate of the species caused due to some external difficulties. Auxiliary parameter n affects the overall shape of the per-capita growth curve, as n increases, the curve becomes increasingly flatter and reaches lower maximum values (Boukal et al., 2007) (Figure 1.8(c)). The difference between per capita logistic growth and population growth affected by single and double for strong Allee effect has been shown in Figure 1.8(a) and for weak Allee effects has been shown in Figure 1.8(b).

The per capita growth function of a single population affected by additive Allee effect is given by (Dennis, 1989; Stephens and Sutherland 1999)

$$g(\cdot) = g(x) = r\Big(1 - \frac{x}{K} - \frac{m}{x+b}\Big), \tag{1.6.3}$$

the term $\frac{m}{x+b}$ is due to additive Allee effect. The parameters $m > 0$ and $0 < b < K$ are Allee effect constants, where b is the population size at which fitness is half of its maximum value and the constant m will allow the severity of the Allee effect to be modeled.

The Allee effect II modifies the functional response of the predator-prey model (1.4.1) as (Zhou et al. 2005)

$$p(\cdot)\Big(1 + \frac{A}{x}\Big), \tag{1.6.4}$$

where $A > 0$ is a constant for Allee effect II. The bigger A is, the stronger Allee effect II of the prey. Notice that the functional response term will be two times at $A = x$.

The Allee effect in predator species has been studied very less. The predator growth

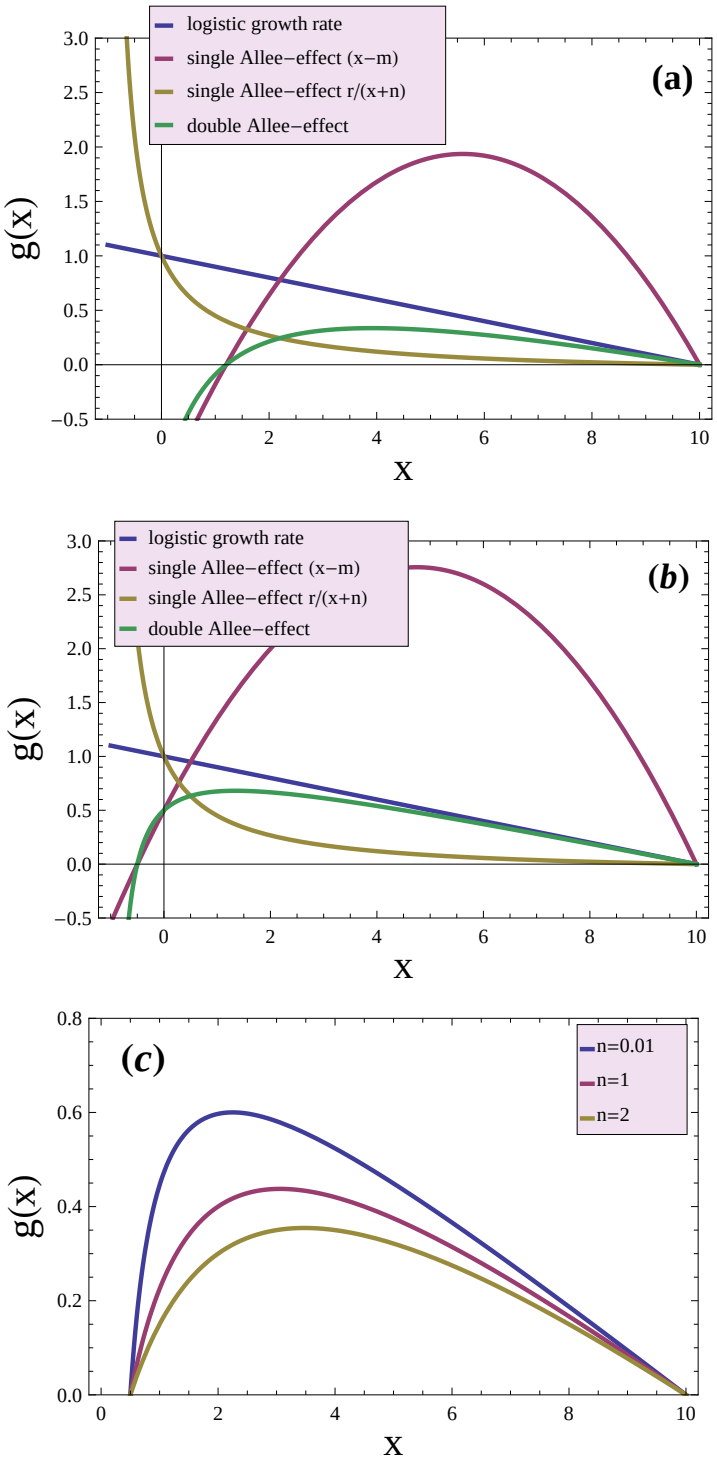

Figure 1.8: *Per-capita growth rate of a single population in the presence of no Allee effect, single Allee effect* $(x - m)$*, single* $\frac{r}{x+n}$ *and double Allee effects. (a) Strong Allee effect* $(m > 0)$*. (b) Weak Allee effect* $(m < 0)$*. (c) affect of* n*.*

function affected by Allee effect is given below

i) When the predator-prey model is Gauss type, the predator growth function is given by (Lai et al. 2010)

$$Q(\cdot) = ep(\cdot)\frac{y}{y+B} - d. \tag{1.6.5}$$

The term $\frac{y}{y+B}$ is for the Allee effect and parameter $B > 0$ is the Allee effect constant. The bigger the B is, the stronger such effect will be, and the slower the per capita growth rate of the predator population.

ii) When the predator-prey model is Leslie-Gower type, the predator growth function is given by (Feng and Kang 2015)

$$Q(\cdot) = Q(x, y) = r\Big(\frac{y}{y+B} - \frac{y}{nx}\Big). \tag{1.6.6}$$

The term $\frac{y}{y+B}$ is for the Allee effect as discussed above.

1.7 Harvesting Functions

The growing population demand for more resources/foods and energy has led to increase exploitation of several biological resources. The exploitation of biological resources and the harvesting of populations are commonly practiced in fishery, forestry, and wildlife management. Harvesting generally has a strong influence on the dynamic evaluation of a population subjected to it. The severity of the influence, which depends on the nature of the applied harvesting strategy, may range from rapid depletion to complete preservation of a population.

The harvested predator-prey models are very important because it attracts the interest of the commercial harvesting industry as well as scientific communities including biology, ecology, and economics, especially because of concerns such as profit, overexploitation, and extinction of a species being harvested. The inter-specific competition between two species is sometime considered as quadratic harvesting and has been proposed by Gause (1935), but he did not study the effect of harvesting. Clark (1976) discussed the problem of

combined or non-selective harvesting of two ecologically independent and logistically growing fish species. The problem of harvesting of a single species in a two-species ecologically competing population model has been discussed in Clark (1990).

The harvested single species model is given by

$$\frac{dx}{dt} = F(x) - H(x, E), \tag{1.7.1}$$

where H is the harvesting function and E is the effort applied to harvest the species. In general, three types of harvesting function have been studied in the literature (Das et al. 2009a; Gupta et al. 2013; Srinivasu 2001).

i) Constant harvesting

$$H(x, E) = C,$$

where C is a suitable constant.

ii) Proportionate harvesting

$$H(x, E) = qEx,$$

the catch is proportional to the stock as well as effort. q is the catchability coefficient.

iii) Nonlinear harvesting

$$H(x, E) = \frac{qEx}{m_1E + m_2x},$$

where m_1, m_2 are suitable positive constants. Nonlinear harvesting is more realistic and exhibit saturation effects with respect to both, the stock abundance and the effort level (Gupta 2015). Notice that

$$\lim_{E\to\infty} H(x, E) = \frac{qx}{m_1}, \qquad \lim_{x\to\infty} H(x, E) = \frac{qE}{m_2}.$$

Moreover, the constant m_1 is proportional to the ratio of the stock-level to the harvesting rate (catch-rate) at higher levels of effort and the constant m_2 is proportional to the ratio of the effort-level to the harvesting rate (catch-rate) at higher stock-levels.

1.8 Additional Food

In most of the classical predator-prey models it is assumed that the predator feed only its favorite prey, but it is not realistic because most of the predators are generalist rather than specialists. For these types of predator species, alternative food needs to be assumed to develop a realistic predator-prey model. The predator-prey models with alternative prey has applications in biological control, species conservation, bio-remediation, resource management etc. Theoretical studies Baalen et al. (2001); Holt (1994); Lawton (1994) and Rijn et al. (2002) conclude that presence of additional food to predators enhances the predator density and also their effect on target prey, thereby helping to decrease the density of target prey. The reduction of prey density due to presence of alternative food for predators is termed as apparent competition (Holt 1977). However, empirical studies Lawton (1994); Murdoch et al. (1985) and Wootton (1994) indicate that provision of additional food to predators need not always increase target predation, so there is an apparent conflict between theory and observations.

To resolve the conflict between theory and observations Srinivasu (2007) modeled a predator-prey system with the assumption that the additional food is uniformly distributed in the habitat and the number of encounters per predator with the additional food is proportional to the density of the additional food. They observed that additional food serves as a biological control agent with which both prey as well as predators can be controlled. Moreover, the nutritive value and the quantity of the additional food play crucial role in the controllability of the predator-prey system. The authors Srinivasu (2007); Srinivasu and Prasad (2010) and Stiefs et al. (2010) concluded that provision of additional food of high nutritive value could increase target predation and reduce the prey density. Whereas additional food with low nutritive value could release the prey from predation pressure and decrease predator density.

1.9 Dynamical Complexity of Convective Motion in Porous Medium

Convection

Convection is a phenomenon in which heat transfer occurs via macroscopic motion of the fluid from a hot to a cool region. In convection, there are two types of mechanisms. Energy transfer due to random molecular motion (diffusion); in this case energy is transferred by the bulk, or macroscopic motion of the fluid and another is transformed due to temperature gradient. Boiling of water is a very common example of convective heat transfer.

Porous medium

By porous medium, we mean that a material consisting of a solid matrix (either rigid or it undergoes to small deformation) with an interconnected void (fluid motion is possible). Beach sand, rye bread, wood and human lung are some examples of natural porous medium.

Internal heating

There are many practically important situations, where the porous material offers its own source of heat. This gives a different way in which a convective flow can be set up through the local heat generation within the porous media. Such a situation can occur through radioactive decay or through, in the present perspective, a relatively weak exothermic reaction which can take place within the porous material. To be more specific, internal heat is the main source of energy for celestial bodies caused by nuclear fusion and decaying of radioactive materials, which keeps the celestial objects warm and active. It is due to the internal heating of the earth that there exists a thermal gradient between the interior and exterior of the earth's crust, saturated by multicomponents fluids, which helps convective flow, thereby transferring the thermal energy towards the surface of the earth. Therefore, the role of internal heat generation becomes very important in several applications that include geophysics, reactor safety analyses, metal waste form development for spent nuclear fuel, fire and combustion studies, and storage of radioactive materials. However, there are relatively very few studies available in which the effect of internal heating on convective flow has been investigated.

Viscoelastic fluid

The fluid that obey the Newton's law is known as Newtonian fluid and the fluid that does not obey the Newton's law is known as non-Newtonian fluid or Viscoelastic fluid.

Modulation

The gravity modulation of the system leads to the variable coefficients in the governing equations of thermal instability and involves the vertical time periodic vibrations of the system. Gravity modulation is known as g-jitter in literature.

Mathematical model under the Boussinesq approximation is given by

$$\begin{cases} \rho_0 \frac{\partial \overrightarrow{q}}{\partial t} = - \bigtriangledown p + \rho g - \frac{\mu}{K} \overrightarrow{q}, \\ \\ \frac{\partial T}{\partial t} + (\vec{q}.\nabla)T = \kappa_T \nabla^2 T, \end{cases} \tag{1.9.1}$$

subject to

$$\nabla.\vec{q} = 0, \tag{1.9.2}$$

and

$$\rho = \rho_0[1 - \alpha_T(T - T_0)], \tag{1.9.3}$$

where ρ_0 is the density of fluid at the basic state, $\vec{q}$ is the velocity of fluid, p is the reduced pressure, g is the acceleration due to gravity, μ is the dynamic viscoelastic, K is the permeability, T is the temperature, κ_T is the effective thermal diffusivity, α_T is the coefficient of thermal expansion and $\nabla^2 = \frac{\partial^2}{\partial x^2} + \frac{\partial^2}{\partial y^2} + \frac{\partial^2}{\partial z^2}$.

The first equation of the system (1.9.1) is known as momentum equation while the second equation is known as energy equation. The equation (1.9.2) is the equation of continuity and the equation (1.9.3) is the density equation at the basic state.

The above system has been reduced to Ginzburg-Landau equation through the perturbation method. The Ginzburg-Landau equation (Bernoulli equation) and obtaining its analytical solution is difficult due to its non-autonomous nature. Therefore, it has been solved numerically.

Chapter 2

Leslie-Gower Predator-prey Model with Nonlinear Harvesting

2.1 Introduction

Marine life is a renewable natural resources that provides not only food to a large population of humans but also involved in the regulation of the Earth's ecosystem. The growing human needs for more food and more energy have led to increased exploitation of these resources which affects the Earth's ecosystem. Thus, it is imperative to design harvesting strategies which aim at maximizing economic gains giving due consideration to the ecological health of the concerned Earth's ecological system. A number of literature is available in which the influence of harvesting strategies on the predator-prey model has been examined. For example, the influence of constant rate harvesting Brauer and Soudack (1979); Xiao and Ruan (1999); Xiao and Jennings (2005); Xiao et al. (2006), the influence of proportionate harvesting Xiao and Cao (2009); Christopher et al. (2015) and the influence of nonlinear harvesting (Holling type II) Das et al. (2009); Gupta et al. (2012); Gupta and Chandra

First part of this chapter is based on the research article: Qualitative analysis of a Leslie-Gower predator-prey system with nonlinear harvesting in predator, International Journal of Engineering Mathematics. Volume 2016, Article ID 2741891, 15 pages (Hindawi).
Second part of this chapter is based on the research article: Bogdanov-Takens bifurcations for a predator-prey system with nonlinear harvesting in prey, Communicated.

(2013); Upadhyay et al. (2014); Gupta et al. (2015). In Chapter 1, it has been discussed that nonlinear harvesting is more realistic and exhibit saturation effects.

A number of researchers studied the dynamical behaviour of Leslie-Gower predator-prey model in the presence of harvesting. For example, May et al. (1979) proposed a Leslie-Gower predator-prey model in which two different constant-yield harvesting on both prey and predator species have been considered and this model was studied by Beddington and Cooke (1982). Beddington and May (1980) proposed and studied Leslie-Gower predator-prey model, when both the prey and predators were harvested with constant-effort. Beddington and Cooke (1982) studied a Leslie-Gower predator-prey model in which the preys are harvested at a constant-yield rate and predators are harvested with constant-effort rate. Zhu and Lan (2010) studied a Leslie-Gower predator-prey model with constant-yield prey harvesting. Gong and Huang (2014) studied the Bogdanov-Takens bifurcation for the model and shown that for different parameter values the model has a limit cycle or a homoclinic loop. Gupta et al. (2012) discussed the bifurcation of a Leslie-Gower prey-predator model in the presence of nonlinear prey harvesting. Huang et. al (2013) studied the effect of constant yield predator harvesting on the dynamics of a Leslie-Gower type model and shown that the model has Bogdanov-Taken (BT) singularity of codimension 3 or a weak focus of multiplicity two for some parameter values. They have shown that as the parameters changes, the model exhibits saddle node bifurcation, repelling and attracting BT bifurcations, supercritical, subcritical and degenerate Hopf bifurcations.

This chapter is divided into (i) dynamical behaviour of Leslie-Gower predator-prey model in the presence of nonlinear predator harvesting, and (ii) Bogdanov-Takens bifurcation for Leslie-Gower predator-prey model in the presence of nonlinear prey harvesting.

2.2 Model with Nonlinear Predator Harvesting

2.2.1 Model Equations

Consider Leslie-Gower predator-prey model (1.5.6) with nonlinear predator harvesting

$$\begin{cases} \frac{dX}{dT} = r\Big(1 - \frac{X}{K}\Big)X - mXY, \\ \frac{dY}{dT} = s(1 - \frac{Y}{nX})Y - \frac{qEY}{m_1E + m_2Y}, \quad (X, Y) \neq (0, 0), \end{cases} \tag{2.2.1}$$

with initial conditions $X(0) > 0, Y(0) > 0$, where $X \equiv X(T)$ and $Y \equiv Y(T)$ are the prey density and predator density at time T respectively. The parameters r, s, K, m, n, q and E are positive and represent the intrinsic growth rate of prey, intrinsic growth rate of predator, carrying capacity of prey in the absence of predator, maximal predator per capita consumption rate, measure of the food quality that the prey provides for conversion into predator births, catchability coefficient and effort applied to harvest the individuals respectively and m_1, m_2 are suitable positive constants. In section (1.5.3), the model (2.2.1) without harvesting has been discussed in brief.

The model (2.2.1) is not well defined at $(0, 0)$. In order to define the system (2.2.1) at $(0, 0)$, it has been modified as given in Freedman and Waltman (1984). The system (2.2.1) reduces to

$$\begin{cases} \frac{dX}{dT} = r\Big(1 - \frac{X}{K}\Big)X - mXY, \\ \frac{dY}{dT} = s(1 - \frac{Y}{nX})Y - \frac{qEY}{m_1E + m_2Y}, \quad (X, Y) \neq (0, 0), \\ \frac{dY}{dT} = 0, \quad (X, Y) = (0, 0), \end{cases} \tag{2.2.2}$$

with initial conditions $X(0) > 0, Y(0) > 0$. For nondimensionalizing the system (2.2.2), consider the following substitutions:

$$X = Kx, \quad mY = ry, \quad rT = t.$$

The system (2.2.2) reduces to

$$\begin{cases} \frac{dx}{dt} = x(1-x-y), \\ \frac{dy}{dt} = \rho y(1-\frac{\beta y}{x}-\frac{h}{c+y}), \quad (x,y) \neq (0,0), \\ \frac{dy}{dt} = 0, \quad (x,y) = (0,0), \end{cases} \tag{2.2.3}$$

with the initial conditions $x(0) > 0, y(0) > 0$, where $\rho = \frac{s}{r}$, $\beta = \frac{r}{mnK}$, $h = \frac{qEm}{srm_2}$, $c = \frac{m_1 mE}{m_2 r}$.

For the existence of the biological meaning of the variables in model, the system (2.2.3) is studied in the closed first quadrant, $\mathbb{R}^2_+$, in $xy-$ plane defined by $\mathbb{R}^2_+ = \{(x,y) \in \mathbb{R}^2 : x \geq 0, y \geq 0\}$.

2.2.2 Equilibria and their Stability

The equilibrium points of the system (2.2.3) are the nonnegative real solutions of the system $\frac{dx}{dt} = \frac{dy}{dt} = 0$. It is obvious that the system (2.2.3) has the trivial equilibrium point $E_0 = (0,0)$, the axial equilibrium point $e = (1,0)$, and the abscissa of the positive interior equilibrium points are the roots of the quadratic equation

$$(1+\beta)x^2 - (1+2\beta+c+\beta c-h)x + \beta(1+c) = 0, \tag{2.2.4}$$

and the ordinance of the positive interior equilibrium points are given by $y_{1,2} = 1 - x_{1,2}$, $0 \leq x_{1,2} \leq 1$. The quadratic equation (2.2.4) has two positive roots $x_1 = \frac{1+2\beta+c+\beta c-h+\sqrt{(1+c+\beta c-h)^2-4\beta h}}{2(1+\beta)}$ and $x_2 = \frac{1+2\beta+c+\beta c-h-\sqrt{(1+c+\beta c-h)^2-4\beta h}}{2(1+\beta)}$, whenever $h < 1 + 2\beta + c + \beta c - 2\sqrt{\beta(1+c+\beta+\beta c)} = \overline{h}$(say), a double positive root $x_3 = \frac{1+2\beta+c+\beta c-h}{2(1+\beta)}$, whenever $h = \overline{h}$ and no positive root, whenever $h > \overline{h}$. The number and location of the equilibrium points of the system (2.2.3) lying in the set Ω are given in the following lemma.

Lemma 2.2.1. *The system* (2.2.3) *has*

(a) four equilibrium points; trivial equilibrium point $E_0 = (0,0)$, axial equilibrium point $e = (1,0)$ and two interior equilibrium points $E_1 = (x_1, y_1)$ and $E_2 = (x_2, y_2)$, whenever $0 < c < h < \overline{h}$,

where $x_1 = \frac{1+2\beta+c+\beta c-h+\sqrt{(1+c+\beta c-h)^2-4\beta h}}{2(1+\beta)}$, $y_1 = \frac{1+h-c-\beta c-\sqrt{(1+c+\beta c-h)^2-4\beta h}}{2(1+\beta)}$, $x_2 = \frac{1+2\beta+c+\beta c-h-\sqrt{(1+c+\beta c-h)^2-4\beta h}}{2(1+\beta)}$, $y_2 = \frac{1+h-c-\beta c+\sqrt{(1+c+\beta c-h)^2-4\beta h}}{2(1+\beta)}$ *and* $\overline{h} = 1+2\beta+c+\beta c-2\sqrt{\beta(1+c+\beta+\beta c)}$.

(b) *three equilibrium points; trivial equilibrium point* $E_0 = (0,0)$*, axial equilibrium point* $e = (1,0)$ *and a double interior equilibrium points* $E_3 = (x_3, y_3)$*, whenever* $c < h = \overline{h}$*, where* $x_3 = \sqrt{\frac{\beta(1+c)}{1+\beta}}$ *and* $y_3 = 1 - \sqrt{\frac{\beta(1+c)}{1+\beta}}$.

(c) *three equilibrium points; trivial equilibrium point* $E_0 = (0,0)$*, axial equilibrium point* $e = (1,0)$ *and an interior equilibrium points* $E_4 = (x_4, y_4)$*, whenever* $c = h$ *and* $\beta c < 1$*, where* $x_4 = \frac{\beta(1+c)}{(1+\beta)}$ *and* $y_4 = \frac{1-\beta c}{(1+\beta)}$.

(d) *three equilibrium points; trivial equilibrium point* $E_0 = (0,0)$*, axial equilibrium point* $e = (1,0)$ *and an interior equilibrium points* $E_5 = (x_5, y_5)$*, whenever* $h < c$ *where* $x_5 = \frac{1+2\beta+c+\beta c-h-\sqrt{(1+c+\beta c-h)^2-4\beta h}}{2(1+\beta)}$ *and* $y_5 = \frac{1+h-c-\beta c+\sqrt{(1+c+\beta c-h)^2-4\beta h}}{2(1+\beta)}$.

(e) *two equilibrium points; trivial equilibrium point* $E_0 = (0,0)$ *and axial equilibrium point* $e = (1,0)$ *whenever* $\overline{h} < h$ *and* $c < h$.

The number and location of interior equilibrium points have been depicted in Figure 2.1.

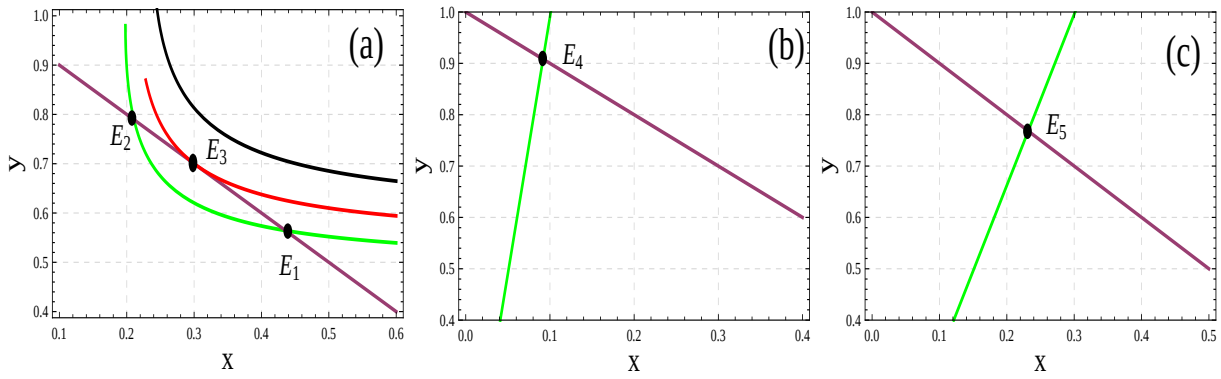

Figure 2.1: *This diagram shows the number and location of the positive interior equilibrium points of the system* (2.2.3)*. The green, red and black color curves are the predator nullclines for different values of* h *and the straight line is the prey nullcline* ***(a)*** $h > c$*, for black color parabola* $h > \overline{h}$*, for red color parabola* $h = \overline{h}$ *and for green color parabola* $h < \overline{h}$ ***(b)*** $h = c$ ***(c)*** $h < c$.

Now, the stability of the equilibrium points has been discussed. The Jacobian matrix of the system (2.2.3) at the equilibrium point E_0 cannot be calculated as the term $\frac{y}{x}$ is not define at $(0,0)$. The blow-up technique (Jost et al. 1999) has been applied to analyze the stability at the equilibrium point E_0. Let $x = x, \quad y = xv$, then the system (2.2.3) reduces to

$$\begin{cases} \frac{dx}{dt} = x(1-x-xv), \\ \frac{dv}{dt} = v\Big(\rho - 1 + x - \rho\beta v + xv - \frac{h\rho}{c+xv}\Big). \end{cases} \tag{2.2.5}$$

The system (2.2.5) has two equilibrium points $\overline{E}_0 = (0,0)$ and $\overline{E}_1 = \Big(0, \frac{1}{\rho\beta}\big(\rho - 1 - \frac{h\rho}{c}\big)\Big)$, whenever $\rho - 1 - \frac{h\rho}{c} > 0$. The Jacobian matrix of the system (2.2.5) at the equilibrium point $\overline{E}_0$ is

$$J_{\overline{E}_0} = \begin{bmatrix} 1 & 0 \\ 0 & \rho - 1 - \frac{h\rho}{c} \end{bmatrix}.$$

Thus the equilibrium point $\overline{E}_0$ of the system (2.2.5) is an unstable point as $\rho - 1 - \frac{h\rho}{c} > 0$. The Jacobian matrix of the system (2.2.5) at the equilibrium point $\overline{E}_1$ is

$$J_{\overline{E}_1} = \begin{bmatrix} 1 & 0 \\ \frac{1}{\rho\beta}\big(\rho - 1 - \frac{h\rho}{c}\big)\Big(1 + \frac{1}{\rho\beta}\big(\rho - 1 - \frac{h\rho}{c\beta}\big) + \frac{h}{\beta c^2}\big(\rho - 1 - \frac{h\rho}{c}\big)\Big) & -(\rho - 1 - \frac{h\rho}{c}) \end{bmatrix}.$$

Thus the equilibrium point $\overline{E}_1$ of the system (2.2.5) is always saddle as $\rho - 1 - \frac{h\rho}{c} > 0$. The above discussions can be concluded as follows

Theorem 2.2.2. *The trivial equilibrium point E_0 of the system* (2.2.3) *is a saddle point.*

The Jacobian matrix of the system (2.2.3) at the equilibrium point e is

$$J_e = \begin{bmatrix} -1 & -1 \\ 0 & \rho\Big(1 - \frac{h}{c}\Big) \end{bmatrix}.$$

The Jacobian matrix of the system (2.2.3) at the positive interior equilibrium point E is

$$J_E = \begin{bmatrix} -x & -x \\ \frac{\rho\beta y^2}{x^2} & \frac{\rho y}{x}\Big(\frac{x - 2\beta y - \beta c}{c+y}\Big) \end{bmatrix}.$$

The determinant of the above Jacobian matrix is $\det(J_E) = \frac{\rho y}{x(c+y)}(\beta(1+c) - (1+\beta)x^2)$ and the trace is $tr(J_E) = \frac{\rho y}{x}\left(\frac{x-2\beta y-\beta c}{c+y}\right) - x$.

Theorem 2.2.3. *(a) The equilibrium point e is asymptotically stable, whenever $c < h$ and a saddle, whenever $h < c$.*

(b) The equilibrium point E_1, if exists, is always a saddle point.

(c) The equilibrium point E_2, if exists, is asymptotically stable, whenever $\frac{\rho y_2}{x_2}\left(\frac{x_2-2\beta y_2-\beta c}{c+y_2}\right) - x_2 < 0$ and is unstable, whenever $\frac{\rho y_2}{x_2}\left(\frac{x_2-2\beta y_2-\beta c}{c+y_2}\right) - x_2 > 0$.

(d) The equilibrium point E_3, if exists, is a degenerate singular point.

(e) The equilibrium point E_4, if exists, is always asymptotically stable.

(f) The equilibrium point E_5, if exists, is asymptotically stable, whenever $\frac{\rho y_5}{x_5}\left(\frac{x_5-2\beta y_5-\beta c}{c+y_5}\right) - x_5 < 0$ and is unstable, whenever $\frac{\rho y_5}{x_5}\left(\frac{x_5-2\beta y_5-\beta c}{c+y_5}\right) - x_5 > 0$.

Proof. (a) The eigenvalues of the Jacobian matrix J_e are -1 and $\rho(1-\frac{h}{c})$, so the equilibrium point e is asymptotically stable, whenever $c < h$ and a saddle whenever $h < c$.

(b) The determinant $\det(J_{E_1}) < 0$, so the interior equilibrium point E_1 is a saddle point.

(c) The determinant $\det(J_{E_2}) > 0$ and $tr(J_{E_2}) = \frac{\rho y_2}{x_2}\left(\frac{x_2-2\beta y_2-\beta c}{c+y_2}\right) - x_2$, so the interior equilibrium point E_2 is asymptotically stable whenever $\frac{\rho y_2}{x_2}\left(\frac{x_2-2\beta y_2-\beta c}{c+y_2}\right) - x_2 < 0$ and unstable, whenever $\frac{\rho y_2}{x_2}\left(\frac{x_2-2\beta y_2-\beta c}{c+y_2}\right) - x_2 > 0$.

(d) The determinant $\det(J_{E_3}) = 0$, so the interior equilibrium point E_3 is a degenerate singular point.

(e) The determinant $\det(J_{E_4}) > 0$ as $\beta c < 1$ and $tr(J_{E_4}) < 0$ always, so the interior equilibrium point E_4 is always asymptotically stable.

(f) The determinant $\det(J_{E_5}) > 0$ and $tr(J_{E_5}) = \frac{\rho y_5}{x_5}\left(\frac{x_5-2\beta y_5-\beta c}{c+y_5}\right) - x_5$, so the interior equilibrium point E_5 is asymptotically stable, whenever $\frac{\rho y_5}{x_5}\left(\frac{x_5-2\beta y_5-\beta c}{c+y_5}\right) - x_5 < 0$ and unstable, whenever $\frac{\rho y_5}{x_5}\left(\frac{x_5-2\beta y_5-\beta c}{c+y_5}\right) - x_5 > 0$.

■

From Lemma 2.2.1 if $h = c$, the system (2.2.3) has unique interior equilibrium point E_4 and if $h < c$, the system (2.2.3) has unique interior equilibrium point E_5. In Theorem 2.2.3, it is proved that these interior equilibrium points are always asymptotically stable. Below, it has been shown that these equilibrium points are globally asymptotically stable.

Theorem 2.2.4. *The equilibrium points E_4 and E_5, if exists, are globally asymptotically stable.*

Proof. From Lemma 2.2.1, the system (2.2.3) has one trivial equilibrium point E_0, one axial equilibrium point e and one interior equilibrium point E_4, whenever $h = c$. Further, it has one trivial equilibrium point E_0, one axial equilibrium point e and one interior equilibrium point E_5, whenever $h < c$. Also from Theorem 2.2.3, the trivial equilibrium point E_0 is always a saddle point, axial equilibrium point e is a saddle point, whenever $h \leq c$ and the interior equilibrium points E_4 and E_5 are asymptotically stable. Define a function,

$$L(x, y) = \frac{\partial}{\partial x}(M(x, y)f(x, y)) + \frac{\partial}{\partial y}(M(x, y)g(x, y)),$$

where $f(x, y) = x(1 - x - y)$, $g(x, y) = \rho y(1 - \frac{\beta y}{x} - \frac{h}{c+y})$ and $M(x, y) = \frac{1}{xy^2}$.
After simplification, one can obtain, $L(x, y) = -\frac{1}{y^2}\left(1 + \frac{y^2+(c-h)(c+2y)}{x(c+y)^2}\right) < 0$ as $h = c$ or $h < c$. Thus, by using the Dulac's criterion (Perko 1996), system (2.2.3) will not have any non-trivial periodic orbit in Ω. Note that y-axis and x-axis are the stable manifolds of the trivial and the axial equilibrium points respectively. Using this in conjunction with the Poincare-Bendixson theorem (Perko 1996) gives that the interior equilibrium point E_4 and E_5 will be globally stable. ∎

In Theorem 2.2.3, it is shown that the equilibrium point E_3 is a degenerate singular point. Next, the properties of this equilibrium point has been studied.

Theorem 2.2.5. *The equilibrium point E_3, if exists, is*

(a) a saddle-node, whenever $\frac{\rho y_3}{x_3}(\frac{x_3-2\beta y_3-\beta c}{c+y_3}) - x_3 \neq 0$.

(b) a cusp of codimension 2, whenever $\frac{\rho y_3}{x_3}(\frac{x_3-2\beta y_3-\beta c}{c+y_3}) - x_3 = 0$.

Proof. First, equilibrium point $E_3 = (x_3, y_3)$ has been shifted to the origin by means of transformation $u_1 = x - x_3, v_1 = y - y_3$. The system (2.2.3) reduces into the form

$$\begin{cases} \frac{du_1}{dt} = -x_3u_1 - x_3v_1 - u_1^2 - u_1v_1, \\ \frac{dv_1}{dt} = \frac{\rho\beta y_3^2}{x_3^2}u_1 + \frac{\rho y_3}{x_3}(\frac{x_3-2\beta y_3-\beta c}{c+y_3})v_1 - \eta_1u_1^2 + \eta_2u_1v_1 + \eta_3v_1^2 + O(|(u_1, v_1)|^3), \end{cases} \tag{2.2.6}$$

where

$$\eta_1 = \frac{\rho\beta y_3^2}{x_3^3}, \quad \eta_2 = \frac{2\rho\beta y_3}{x_3^2}, \quad \eta_3 = \rho\left(\frac{ch}{(c+y_3)^3} - \frac{\beta}{x_3}\right).$$

If $\frac{\rho y_3}{x_3}(\frac{x_3-2\beta y_3-\beta c}{c+y_3}) - x_3 \neq 0$, the point E_3 is a saddle-point. Consider $\frac{\rho y_3}{x_3}(\frac{x_3-2\beta y_3-\beta c}{c+y_3}) - x_3 = 0$, that is, $tr(J_{E_3}) = 0$. Both eigenvalues of the Jacobian matrix J_{E_3} are zero and system (2.2.6) reduces to

$$\begin{cases} \frac{du_1}{dt} = -x_3u_1 - x_3v_1 - u_1^2 - u_1v_1, \\ \frac{dv_1}{dt} = \frac{\rho\beta y_3^2}{x_3^2}u_1 + x_3v_1 - \eta_1u_1^2 + \eta_2u_1v_1 + \eta_3v_1^2 + O(|(u_1, v_1)|^3). \end{cases} \tag{2.2.7}$$

Consider affine transformation $u_2 = u_1,\ v_2 = -x_3u_1 - x_3v_1$, system (2.2.7) reduces to

$$\begin{cases} \frac{du_2}{dt} = v_2 + \frac{1}{x_3}u_2v_2, \\ \frac{dv_2}{dt} = \eta_4u_2^2 + \eta_5u_2v_2 - \eta_6v_2^2 + O(|(u_2, v_2)|^3), \end{cases} \tag{2.2.8}$$

where

$$\eta_4 = x_3(\eta_1 + \eta_2 - \eta_3), \quad \eta_5 = \eta_2 - 2\eta_3 - 1, \quad \eta_6 = \frac{\eta_3}{x_3}.$$

Consider the C^∞ change of coordinates in the small vicinity of $(0, 0)$:

$$u_3 = u_2, \quad v_3 = v_2 + \eta_6u_2v_2.$$

Then, the system (2.2.8) reduces to

$$\begin{cases} \frac{du_3}{dt} = v_3 + (\frac{1}{x_3} - \eta_6)u_3v_3 + \tilde{O}(|(u_3, v_3)|^3), \\ \frac{dv_3}{dt} = \eta_4u_3^2 + \eta_5u_3v_3 + O(|(u_3, v_3)|^3). \end{cases} \tag{2.2.9}$$

Let the C^∞ change of coordinates in the small neighbourhood of $(0,0)$:

$$u_4 = u_3 - \frac{1}{2}\Big(\frac{1}{x_3} - \eta_6\Big)u_3^2, \quad v_4 = v_3.$$

The system (2.2.9) reduces to

$$\begin{cases} \frac{du_4}{dt} = v_4 + \tilde{O}(|(u_4, v_4)|^3) \\ \frac{dv_4}{dt} = \eta_4 u_4^2 + \eta_5 u_4 v_4 + O(|(u_4, v_4)|^3). \end{cases} \tag{2.2.10}$$

Choose the final C^∞ change of coordinates in the small neighbourhood of $(0,0)$:

$$u = u_4, \quad v = v_4 + \tilde{O}(|(u_4, v_4)|^3).$$

The system (2.2.10) reduces to

$$\begin{cases} \frac{du}{dt} = v, \\ \frac{dv}{dt} = \eta_4 u + \eta_5 uv + O(|(u, v)|^3). \end{cases} \tag{2.2.11}$$

If $\eta_4\eta_5 = x_3\rho\Big(\frac{\beta y_3^2}{x_3^3} + \frac{2\beta y_3}{x_3^2} - \frac{hc}{(c+y_3)^3} + \frac{\beta}{x_3}\Big)\Big(\frac{2\rho\beta y_3}{x_3^2} - \frac{2\rho hc}{(c+y_3)^3} + \frac{2\beta\rho}{x_3} - 1\Big) \neq 0$ (non-degeneracy condition), the origin $(0,0)$ of system (2.2.11) is a cusp of codimension 2, that is, the interior equilibrium point E_3 of the system (2.2.3) is a cusp of codimension 2. ■

2.2.3 Bifurcation Analysis

Hopf Bifurcation

In Theorem 2.2.3, it is shown that the interior equilibrium point E_2 is stable, whenever $\frac{\rho y_2}{x_2}(\frac{x_2 - 2\beta y_2 - \beta c}{c+y_2}) - x_2 < 0$ and unstable, whenever $\frac{\rho y_2}{x_2}(\frac{x_2 - 2\beta y_2 - \beta c}{c+y_2}) - x_2 > 0$. Now, consider the parametric condition $\frac{\rho y_2}{x_2}(\frac{x_2 - 2\beta y_2 - \beta c}{c+y_2}) - x_2 = 0$. In this parametric condition the equilibrium point E_2 is a weak focus or a center. Hence, the system (2.2.3) may enters to a Hopf bifurcation at the point E_2. The parameter ρ has been considered as the Hopf bifurcation parameter and the parametric conditions under which the stability of E_2 will change and system (2.2.3) exhibits Hopf bifurcations has been obtained.

Theorem 2.2.6. *The system* (2.2.3) *undergoes a Hopf bifurcation with respect to parameter* ρ *around the equilibrium point* E_2*, if exists, whenever* $\frac{\rho y_2}{x_2}(\frac{x_2-2\beta y_2-\beta c}{c+y_2}) - x_2 = 0$*. Moreover,*

(a) The equilibrium point E_2 *is a weak focus of multiplicity* 1*, if the parameter set* (ρ, β, h, c) *is in* H_{sup} *or* H_{sub} *and is stable and unstable according as* (ρ, β, h, c) *is in* H_{sup} *or* H_{sub}*.*

(b) The system (2.2.3) *has, at least one unstable limit cycle, whenever* (ρ, β, h, c) *is in* $H_{sub}, 0 < \rho < \rho^*$ *and* $|\rho - \rho^*| << 1$*, and at least one stable limit cycle, whenever* (ρ, β, h, c) *is in* $H_{sup}, \rho > \rho^*$ *and* $|\rho - \rho^*| << 1$*.*

Proof. A critical magnitude of the bifurcation parameter $\rho = \rho^* = \frac{x_2^2(c+y_2)}{y_2(1-\beta c-(1+2\beta)y_2)}$, exists as $1 - \beta c - (1 + 2\beta)y_2 \neq 0$ such that, at $\rho = \rho^*$, $tr(J_E) = 0$ and $\det(J_E) > 0$. In order to ensure the existence of a Hopf bifurcation, the transversality condition $\frac{d}{d\rho}(tr(J_E))|_{\rho=\rho^*} \neq 0$ (Perko 1996) must hold. On computing one gets $\frac{d}{d\rho}(tr(J_E))|_{\rho=\rho^*} = \frac{y_2}{x_2}(\frac{x_2-\beta y_2}{c+y_2} - \beta) \neq 0$ as $1 - \beta c - (1 + 2\beta)y_2 \neq 0$. Hence, the transversality condition for a Hopf bifurcation is satisfied. To determine the direction of Hopf bifurcation and stability of E_2, the first Lyapunov coefficient of the system (2.2.3) at the equilibrium point E_2 has been computed below.

Let $x = u - x_2,\ y = v - y_2$, then the equilibrium point E_2 is shifted to the origin $(0, 0)$ and the system (2.2.3) can be rewritten as

$$\begin{cases} \dfrac{du}{dt} = a_{10}u + a_{01}v + a_{20}u^2 + a_{11}uv + a_{02}v^2 + a_{30}u^3 + a_{21}u^2v + \\ \qquad a_{12}uv^2 + a_{03}v^3, \\ \dfrac{dv}{dt} = b_{10}u + b_{01}v + b_{20}u^2 + b_{11}uv + b_{02}v^2 + b_{30}u^3 + b_{21}u^2v + \\ \qquad b_{12}uv^2 + b_{03}v^3 + P(u, v), \end{cases} \tag{2.2.12}$$

where $a_{10} = -x_2,\ \ a_{01} = -x_2,\ \ a_{20} = -1,\ \ a_{11} = -1,\ \ a_{02} = 0,\ \ a_{30} = 0\ \ a_{21} = 0,\ \ a_{12} = 0,\ \ a_{03} = 0,\ \ b_{10} = \frac{\rho\beta y_2^2}{x_2^2},\ \ b_{01} = \frac{\rho y_2}{x_2}(\frac{x_2-\beta y_2}{c+y_2} - \beta),\ \ b_{20} = -\frac{\rho\beta y_3^2}{x_3^3},\ \ b_{11} = \frac{2\rho\beta y_2}{x_2^2},\ \ b_{02} = \rho\left(\frac{ch}{(c+y_2)^3} - \frac{\beta}{x_2}\right),\ \ b_{30} = \frac{\rho\beta y_2^2}{x_2^4}\ \ a_{21} = -\frac{2\rho\beta y_2}{x_2^3},\ \ b_{12} = \frac{\rho\beta}{x^2},\ \ b_{03} = \frac{\rho y_2 h}{(c+y_2)^4} - \frac{\beta h}{(c+y_2)^3}$, and $P(u, v) = \sum_{i+j=4}^{\infty} b_{ij}u^iv^j$.

The first Lyapunov number σ (defined in equation 1.3.7) at the origin of the system (2.2.12) is

$$\begin{aligned}\sigma = -\frac{3\pi}{2a_{01}\Delta^{3/2}}\Big\{\big[&a_{10}b_{10}(a_{11}^2+a_{11}b_{02}+a_{02}b_{11})+a_{10}a_{01}(b_{11}^2+a_{20}b_{11}+a_{11}b_{02})\\&+b_{10}^2(a_{11}a_{02}+2a_{02}b_{02})-2a_{10}b_{10}(b_{02}^2-a_{20}a_{02})-2a_{10}a_{01}(a_{20}^2-b_{20}b_{02})\\&-a_{01}^2(2a_{20}b_{20}+b_{11}b_{20})+(a_{01}b_{10}-2a_{10}^2)(b_{11}b_{02}-a_{11}a_{20})\big]\\&-(a_{10}^2+a_{01}b_{10})[3(b_{10}b_{03}-a_{01}a_{30})+2a_{10}(a_{21}+b_{12})+(b_{10}a_{12}-a_{01}b_{21})]\Big\},\end{aligned}$$

where $\Delta = \frac{\rho y_2}{(c+y_2)}\sqrt{(1+c+\beta c-h)^2-4\beta h}$.

If $\sigma \neq 0$, then the origin of (2.2.12) is a weak focus of multiplicity 1: also origin is stable, when $\sigma < 0$ and unstable, when $\sigma > 0$. Hence, in parameter space (ρ, β, h, c), there exist surfaces $H_{sub} = \{(\rho,\beta,h,c) : \sigma > 0, 0 < c < h < \overline{h}, \frac{\rho y_2}{x_2}(\frac{x_2-\beta y_2}{c+y_2} - \beta) - x_2 = 0\}$ and $H_{sup} = \{(\rho,\beta,h,c) : \sigma < 0, 0 < c < h < \overline{h}, \frac{\rho y_2}{x_2}(\frac{x_2-\beta y_2}{c+y_2} - \beta) - x_2 = 0\}$, called subcritical and supercritical hopf bifurcation surface respectively, such that if the parameter set (ρ, β, h, c) lies on the surface H_{sub}, the equilibrium point E_2 of system (2.2.3) is a weak focus of multiplicity 1 and is unstable, and if the parameter set (ρ, β, h, c) lies on the surface H_{sup} the equilibrium point E_2 of system (2.2.3) is a weak focus of multiplicity 1 and is stable.

From above discussion, the equilibrium point E_2 of system (2.2.3) is a weak focus of multiplicity 1 and is unstable, if (ρ, β, h, c) is in H_{sub}. Also from Theorem 2.2.3, the equilibrium point E_2 is stable, whenever $\frac{\rho y_2}{x_2}(\frac{x_2-\beta y_2}{c+y_2} - \beta) - x_2 < 0$, that is, $\rho < \rho^*$ and is unstable, whenever $\frac{\rho y_2}{x_2}(\frac{x_2-\beta y_2}{c+y_2} - \beta) - x_2 > 0$, that is, $\rho > \rho^*$. Thus, the equilibrium point E_2 generates an unstable limit cycle as the bifurcation parameter ρ passes through the bifurcation value $\rho = \rho^*$. From one side of the surface H_{sub} to the other side, system (2.2.3) can undergo to a subcritical Hopf bifurcation. An unstable limit cycle arises in the small neighborhood of the equilibrium point E_2, whenever (ρ, β, h, c) is in $H_{sub}, 0 < \rho < \rho^*$ and $|\rho - \rho^*| << 1$. Similarly, a stable limit cycle arises in the small neighborhood of the equilibrium point E_2, whenever (ρ, β, h, c) is in $H_{sup}, \rho > \rho^*$ and $|\rho - \rho^*| << 1$. ■

Saddle-node Bifurcation

In Subsection 2.2.2, it is shown that the system (2.2.3) admits the double point E_3, whenever $h = \overline{h}$. In Theorem 2.2.5, it is shown that the point E_3 is a saddle-node, whenever $\frac{\rho y_3}{x_3}\left(\frac{x_3-2\beta y_3-\beta c}{c+y_3}\right) - x_3 \neq 0$. Now, it is shown that the system (2.2.3) experiences a saddle-node bifurcation of codimension 1 around the equilibrium point E_3 at the threshold value of the bifurcation parameter $h = \overline{h}$ by means of the Sotomayor's theorem (Perko 1996).

Theorem 2.2.7. *The System* (2.2.3) *undergoes a saddle-node bifurcation with respect to the parameter h around the equilibrium point E_3, whenever $h = \overline{h} = 1 + 2\beta + c + \beta c - 2\sqrt{\beta(1 + c + \beta + \beta c)}$ and $\frac{\rho y_3}{x_3}\left(\frac{x_3-2\beta y_3-\beta c}{c+y_3}\right) - x_3 \neq 0$.*

Proof. It has been shown that if $h = \overline{h} = 1 + 2\beta + c + \beta c - 2\sqrt{\beta(1 + c + \beta + \beta c)}$ and $\frac{\rho y_3}{x_3}\left(\frac{x_3-2\beta y_3-\beta c}{c+y_3}\right) - x_3 \neq 0$, one eigenvalue of the Jacobian matrix J_{E_3} is zero and other has nonzero real part. Suppose V and W are the eigenvectors corresponding to the zero eigenvalues of the Jacobian matrix J_{E_3} and transpose matrix $J_{E_3}^T$ respectively, then $V = \begin{bmatrix} 1 & -1 \end{bmatrix}^T, W = \begin{bmatrix} \frac{\rho\beta y_3^2}{x_3^3} & 1 \end{bmatrix}^T$.

Now $f_h(E_3, \overline{h}) = \begin{bmatrix} 0 \\ \frac{\rho y_3}{c+y3} \end{bmatrix}, D^2(f(E_3, \overline{h}))(V, V) = \begin{bmatrix} 0 \\ -\frac{2\rho\beta y_3^2}{x_3^3} - \frac{4\rho\beta y_3}{x_3^2} + 2\rho\left(-\frac{\beta}{x} + \frac{\overline{h}c}{(c+y_3)^3}\right) \end{bmatrix}$.

Therefore, $W^T f_h(E_3, \overline{h}) = \frac{\rho y_3}{c+y3} > 0$ and $W^T[D^2(f(E_3, \overline{h}))(V, V)] = -2\rho\left(\frac{\beta}{x_3^3} - \frac{\overline{h}c}{(c+y_3)^3}\right)$. Since $\frac{\overline{h}}{(c+y_3)^2} = \frac{\beta}{x^2}$ so, $W^T[D^2(f(E_3, \overline{h}))(V, V)] = -\frac{\rho\beta(1+c)y_3}{x_3^3(c+y_3)} < 0$. Thus Sotomayor's theorem confirms that the system (2.2.3) experiences a saddle-node bifurcation of codimension 1 around interior equilibrium point E_3. This means that, there are no equilibrium points for $h > \overline{h}$, while there are two co-existence equilibrium points E_1 and E_2 for $h > \overline{h}$, one of which is saddle point and the other is a stable node. ∎

Bogdanov-Taken bifurcation

In Theorem (2.2.5), it has been proved that the interior equilibrium point E_3 is a cusp of codimension 2, whenever $\frac{\rho y_3}{x_3}\left(\frac{x_3-2\beta y_3-\beta c}{c+y_3}\right) - x_3 = 0$ and $\eta_4\eta_5 \neq 0$, which implies that there may exist the Bogdanov-Takens bifurcation in system (2.2.3). The parameters h and ρ are taken as the bifurcation parameters as they are important from Biological point of view

and by means of a series of transformations as given in Xiao and Ruan (1999), normal form has been derived.

Theorem 2.2.8. *The system* (2.2.3) *undergoes to a Bogdanov-Takens bifurcation with respect to the bifurcation parameters h and ρ around the double equilibrium point E_3, if* $c < h = \overline{h}$, $\frac{\rho y_3}{x_3}\Big(\frac{x_3-2\beta y_3-\beta c}{c+y_3}\Big) - x_3 = 0$ *and* $\eta_4\eta_5 \neq 0$.

Proof. It is considered that the parameters h and ρ vary in a small neighbourhood of the BT-point (h_0, ρ_0). Let $(h_0 + \lambda_1, \rho_0 + \lambda_2)$ be a point of this neighbourhood, where λ_1, λ_2 are small. The system (2.2.3) reduces to

$$\begin{cases} \frac{dx}{dt} = x(1-x-y), \\ \frac{dy}{dt} = (\rho_0+\lambda_1)\Big(1 - \frac{\beta y}{x} - \frac{h_0+\lambda_2}{c+y}\Big)y. \end{cases} \tag{2.2.13}$$

Translating the equilibrium point E_3 into the origin by using the transformation $u_1 = x - x_3,\ u_2 = y - y_3$ and then using the Taylor's series expansion, the system (2.2.13) reduces to

$$\begin{cases} \frac{du_1}{dt} = -x_3u_1 - x_3u_2 - u_1^2 - u_1u_2, \\ \frac{du_2}{dt} = \alpha_0 + \alpha_1u_1 + \alpha_2u_2 + \alpha_3u_1^2 + \alpha_4u_1u_2 + \alpha_5u_2^2 + R_1(u_1,u_2), \end{cases} \tag{2.2.14}$$

where $\alpha_0 = -\frac{(\rho_0+\lambda_1)\lambda_2 y_3}{c+y_3}$, $\alpha_1 = \frac{\beta(\rho_0+\lambda_1)y_3^2}{x_3^2}$, $\alpha_2 = -(\rho_0+\lambda_1)\Big(\frac{\beta y_3}{x_3} + \frac{c\lambda_2 - h_0y_3}{(c+y_3)^2}\Big)$, $\alpha_3 = -\frac{\beta(\rho_0+\lambda_1)y_3^2}{x_3^3}$, $\alpha_4 = \frac{2\beta(\rho_0+\lambda_1)y_3}{x_3^2}$, $\alpha_5 = (\rho_0+\lambda_1)\Big(-\frac{\beta}{x_3} + \frac{c(h_0+\lambda_2)}{(c+y_3)^3}\Big)$ and $R_1(u_1,u_2)$ is a power series in (u_1,u_2) with powers $u_1^iu_2^j$ satisfying $i+j \geq 3$.

Making the affine transformation $v_1 = u_1,\ v_2 = -x_3u_1 - x_3u_2$, then the system (2.2.14) reduces to

$$\begin{cases} \frac{dv_1}{dt} = v_2 + \frac{1}{x_3}v_1v_2, \\ \frac{dv_2}{dt} = \beta_0 + \beta_1v_1 + \beta_2v_2 + \beta_3v_1^2 + \beta_4v_1v_2 + \beta_5v_2^2 + R_2(v_1,v_2), \end{cases} \tag{2.2.15}$$

where $\beta_0 = -\alpha_0x_3,\ \beta_1 = x_3(\alpha_2-\alpha_1),\ \beta_2 = \alpha_2 - x_3,\ \beta_3 = x_3(\alpha_4-\alpha_5-\alpha_3),\ \beta_4 = \alpha_4 - 2\alpha_5 - 1,\ \beta_5 = -\frac{\alpha_5}{x_3}$ and $R_2(v_1,v_2)$ is a power series in (v_1,v_2) with powers $v_1^iv_2^j$ satisfying $i+j \geq 3$.

Consider the C^∞ change of coordinates in the small neighbourhood of $(0,0)$:

$$w_1 = v_1 - \frac{1}{2x_3}v_1^2, \quad w_2 = v_2 - \beta_5 v_1 v_2,$$

the system (2.2.15) reduces to

$$\begin{cases} \frac{dw_1}{dt} = w_2 + R_3(w_1, w_2), \\ \frac{dw_2}{dt} = \gamma_0 + \gamma_1 w_1 + \gamma_2 w_2 + \gamma_3 w_1^2 + \gamma_4 w_1 w_2 + R_4(w_1, w_2), \end{cases} \tag{2.2.16}$$

where $\gamma_0 = \beta_0,\ \gamma_1 = \beta_1 - \beta_0\beta_5,\ \gamma_2 = \beta_2,\ \gamma_3 = \frac{\beta_1 - \beta_0\beta_5}{2x_3} + \beta_3 - \beta_1\beta_5,\ \gamma_4 = \beta_4,\ R_3(w_1, w_2)$ and $R_4(w_1, w_2)$ are the power series in (w_1, w_2) with powers $w_1^i w_2^j$ satisfying $i + j \geq 3$.

Consider the C^∞ change of coordinates in the small neighbourhood of $(0,0)$:

$$z_1 = w_1,\ z_2 = w_2 + R_3(w_1, w_2),$$

the system (2.2.16) reduces to

$$\begin{cases} \frac{dz_1}{dt} = z_2, \\ \frac{dz_2}{dt} = \gamma_0 + \gamma_1 z_1 + \gamma_3 z_1^2 + F_1(z_1) + \gamma_2 z_2 + \gamma_4 z_1 z_2 + z_2 F_2(z_1) + z_2^2 F_3(z_1, z_2), \end{cases} \tag{2.2.17}$$

where F_1, F_2 and F_3 are the power series in z_1 and (z_1, z_2) with powers $z_1^{k_1}, z_2^{k_2}$ and $z_1^i z_2^j$ satisfying $k_1 \geq 3, k_2 \geq 2$ and $i + j \geq 1$, respectively.

Applying the Malgrange Preparation theorem (Chow and Hale 1983), one gets

$$\gamma_0 + \gamma_1 z_1 + \gamma_3 z_1^2 + F_1(z_1) = \Big(z_1^2 + \frac{\gamma_1}{\gamma_3} z_1 + \frac{\gamma_0}{\gamma_3}\Big) B(z_1, \lambda),$$

where $B(0, \lambda) = \gamma_3$ and B is a power series in z_1 whose coefficients depend on parameters (λ_1, λ_2).

The sign of γ_3 is tedious to determine. So, by means of numerical computation it is found that $\gamma_3 > 0$ as $\lambda_1, \lambda_2 \to 0$. Consider the transformation

$$X_1 = z_1,\ X_2 = \frac{z_2}{\sqrt{\gamma_3}},\ dT = \sqrt{\gamma_3}dt,$$

the system (2.2.17) reduces to

$$\begin{cases} \frac{dX_1}{dT} = X_2, \\ \frac{dX_2}{dT} = \frac{\gamma_0}{\gamma_3} + \frac{\gamma_1}{\gamma_3}X_1 + X_1^2 + \frac{\gamma_2}{\sqrt{\gamma_3}}X_2 + \frac{\gamma_4}{\sqrt{\gamma_3}}X_1X_2 + S_1(X_1, X_2, \lambda), \end{cases} \tag{2.2.18}$$

where $S_1(X_1, X_2, 0)$ is a power series in (X_1, X_2) with powers $X_1^i X_2^j$ satisfying $i+j \geq 3$ and $j \geq 2$.

Applying the parameter dependent affine transformation $Y_1 = X_1 + \frac{\gamma_1}{2\gamma_3},\ Y_2 = X_2$ in the system (2.2.18), then it will become

$$\begin{cases} \frac{dY_1}{dT} = Y_2, \\ \frac{dY_2}{dT} = \frac{\gamma_0}{\gamma_3} - \frac{\gamma_1^2}{4\gamma_3^2} + \frac{1}{\sqrt{\gamma_3}}\Big(\gamma_2 - \frac{\gamma_1\gamma_4}{2\gamma_3}\Big)Y_2 + Y_1^2 + \frac{\gamma_4}{\sqrt{\gamma_3}}Y_1Y_2 + S_2(Y_1, Y_2, \lambda), \end{cases} \tag{2.2.19}$$

where $S_2(Y_1, Y_2, 0)$ is a power series in (Y_1, Y_2) with powers $Y_1^i Y_2^j$ satisfying $i + j \geq 3$ and $j \geq 2$.

By means of C^∞ transformation

$$X = \frac{\gamma_4^2}{\gamma_3}Y_1,\ Y = \frac{\gamma_4^3}{(\gamma_3)^{\frac{3}{2}}}Y_2, dT = \frac{\sqrt{\gamma_3}}{\gamma_4}d\tau,$$

the system (2.2.19) reduces to

$$\begin{cases} \frac{dX}{d\tau} = Y, \\ \frac{dY}{d\tau} = \frac{\gamma_0\gamma_4^4}{\gamma_3^3} - \frac{\gamma_1^2\gamma_4^4}{4\gamma_3^4} + \Big(\frac{\gamma_2\gamma_4}{\gamma_3} - \frac{\gamma_4^2\gamma_1}{2(\gamma_3)^2}\Big)Y + X^2 + XY + S_3(X, Y, \lambda), \end{cases} \tag{2.2.20}$$

where $S_3(X, Y, 0)$ is a power series in (X, Y) with powers $X^i Y^j$ satisfying $i + j \geq 3$ and $j \geq 2$.

The above system is topologically equivalent to the normal form of the Bogdanov-Takens bifurcation which is given by

$$\begin{cases} \frac{dx}{dt} = y, \\ \frac{dy}{dt} = \mu_1(\lambda_1, \lambda_2) + \mu_2(\lambda_1, \lambda_2)y + x^2 + xy. \end{cases} \tag{2.2.21}$$

The system undergoes a Bogdanov-Takens bifurcation if $J\left(\frac{\mu_1,\mu_2}{\lambda_1,\lambda_2}\right)_{(\lambda_1=0,\lambda_2=0)} \neq 0$. When the system (2.2.3) undergoes Bogdanov-Takens bifurcation at $\lambda_1 = \lambda_2 = 0$, three bifurcation curves in $\lambda_1\lambda_2$ plane through the BT point are given by,

1. Saddle-node bifurcation curve: $SN = \{(\lambda_1, \lambda_2) : \mu_1(\lambda_1, \lambda_2) = 0, \mu_2(\lambda_1, \lambda_2) \neq 0\}$.
2. Hopf bifurcation curve: $H = \{(\lambda_1, \lambda_2) : \mu_2(\lambda_1, \lambda_2) = \sqrt{-\mu_1(\lambda_1, \lambda_2)}, \mu_1(\lambda_1, \lambda_2) < 0\}$.
3. Homoclinic bifurcation curve:

$$HL = \{(\lambda_1, \lambda_2) : \mu_2(\lambda_1, \lambda_2) = \tfrac{5}{7}\sqrt{-\mu_1(\lambda_1, \lambda_2)}, \mu_1(\lambda_1, \lambda_2) < 0\}.$$

■

2.2.4 Numerical Simulations

In this section, numerical simulations have been performed to support our analytical findings.

(1) $\beta = 0.1, c = 0.01, h = 0.5$. The system (2.2.3) has two interior equilibrium points $E_1 = (0.435558, 0.564442)$ and $E_2 = (0.210806, 0.789194)$, trivial equilibrium point $E_0 = (0, 0)$ and an axial equilibrium point $e = (1, 0)$. If $\rho = 0.75$, the interior equilibrium point E_2 is asymptotically stable (Figure 2.2(a)) and if $\rho = 0.9$, the interior equilibrium point E_2 is unstable (Figure 2.2(b)). The axial equilibrium point e is an asymptotically stable point and the interior equilibrium point E_1 is always a saddle point. If $h = 0.01, \rho = 0.9$, the system (2.2.3) has only one positive interior equilibrium point $E_4 = (0.091818, 0.908182)$ which is globally asymptotically stable (Figure 2.2(c)). If $h = 0.05, \rho = 0.9$, the system (2.2.3) has only one positive interior equilibrium point $E_5 = (0.0913611, 0.908639)$ which is also globally asymptotically stable (Figure 2.2(d)). If $\beta = 0.1, c = 0.01, \overline{h} = 0.544367 < h = 0.6$, the system (2.2.3) has no positive interior equilibrium point and the phase portrait diagram is shown in Figure 2.2(e). The trivial equilibrium point is always a saddle point.

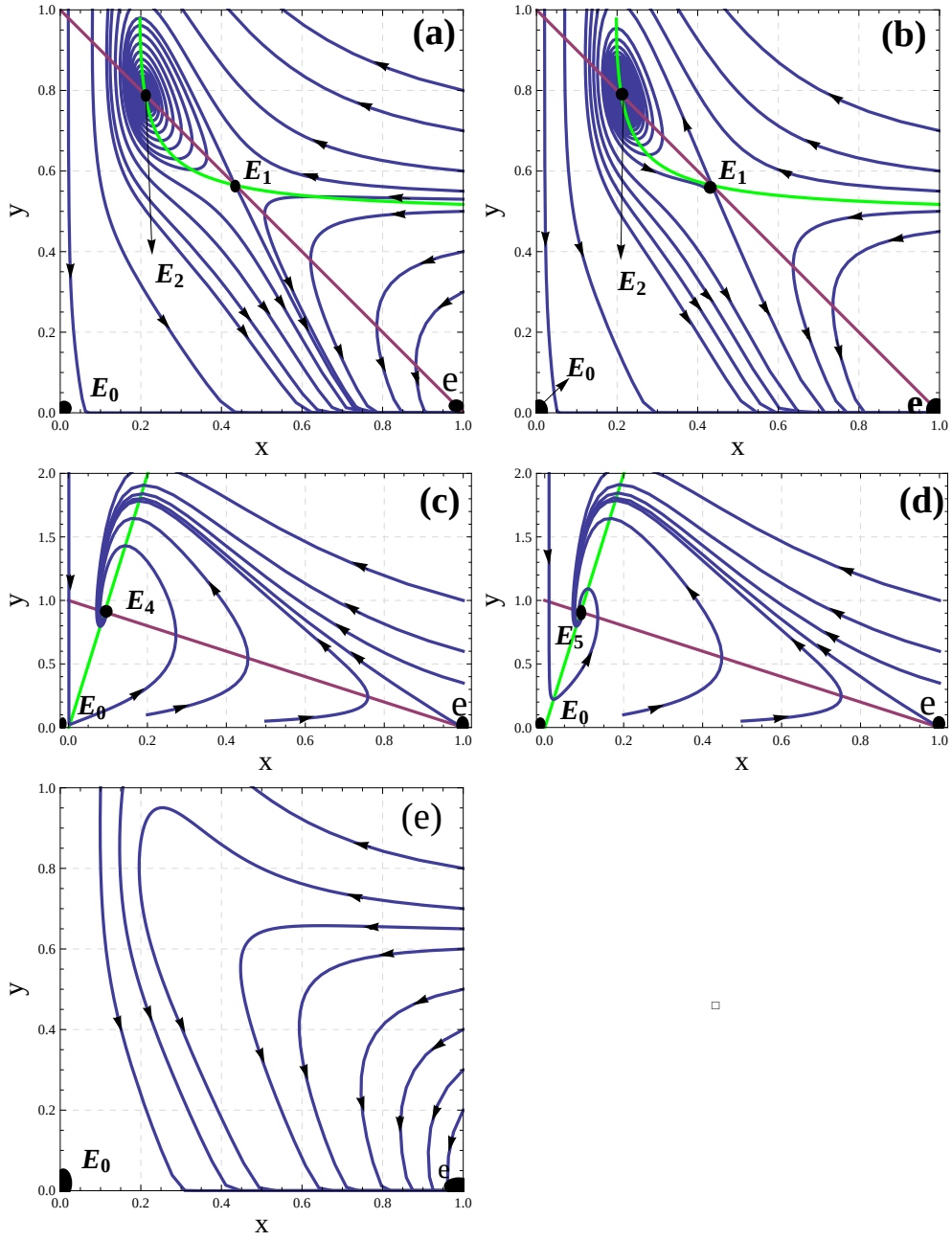

Figure 2.2: *Phase portrait for system* (2.2.3). *For figure (a) and (b)* $\beta = 0.1, c = 0.01, h = 0.5$ ***(a)*** $\rho = 0.75$ *the interior equilibrium point* $E_2 = (0.210806, 0.789194)$ *is an asymptotically stable, axial equilibrium point* $e = (1, 0)$ *is asymptotically stable and interior equilibrium point* $E_1 = (0.435558, 0.564442)$ *is a saddle point.* ***(b)*** $\rho = 0.9$ *the point* E_2 *is unstable,* e *is asymptotically stable and* E_1 *is a saddle.* ***(c)*** $\beta = 0.1, c = 0.01, h = 0.01, \rho = 0.9$ *the interior equilibrium point* $E_4 = (0.091818, 0.908182)$ *is an asymptotically stable, axial equilibrium point* $e = (1, 0)$ *is saddle.* ***(d)*** $\beta = 0.1, c = 0.01, h = 0.005, \rho = 0.9$ *The interior equilibrium point* $E_5 = (0.0913611, 0.908639)$ *is an asymptotically stable, axial equilibrium point* $e = (1, 0)$ *is saddle.* ***(e)*** *when no interior equilibrium exist, the origin is always a saddle.*

(2) $\beta = 0.1, c = 0.01, h = 0.5$, then $\rho^* = 0.865973$. The system (2.2.3) undergoes to hopf bifurcation and the first Lyapunov coefficient $\sigma = 214.922 > 0$, so an unstable limit cycle arises around the equilibrium point $E_2 = (0.210806, 0.789194)$. Take $\rho = 0.854$ (Figure 2.3(a)). $\beta = 0.02, c = 0.1, h = 0.8$, then $\rho^* = 0.173169$. The system (2.2.3) undergoes to hopf bifurcation and the first Lyapunov coefficient $\sigma = -762.219 < 0$, so a stable limit cycle arises around the equilibrium point $E_2 = (0.0867959, 0.913204)$. Take $\rho = 0.175$ (Figure 2.3(b)).

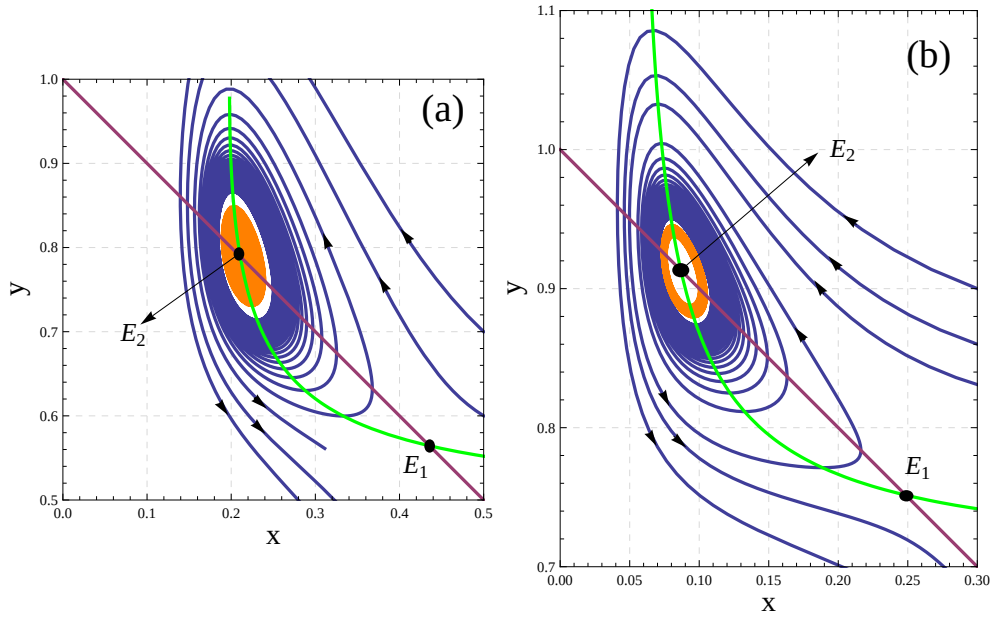

Figure 2.3: ***(a)*** $\beta = 0.1, c = 0.01, h = 0.5, \rho^* = 0.865973, \rho = 0.854$ *an unstable limit cycle arises around the interior equilibrium point* E_2. ***(b)*** $\beta = 0.02, c = 0.1, h = 0.8, \rho^* = 0.173169, \rho = 0.175$ *a stable limit cycle arises around the interior equilibrium point* E_2.

(3) $\beta = 0.5, c = 0.1, \rho = 0.4, \overline{h} = 0.33341$. The system (2.2.3) has a double interior equilibrium point $\overline{E} = (0.60553, 0.39447)$, which is a saddle-node point. The phase portrait diagram is shown in Figure 2.4(a) and the saddle-node bifurcation is shown in Figures 2.4(b) and 2.4(c).

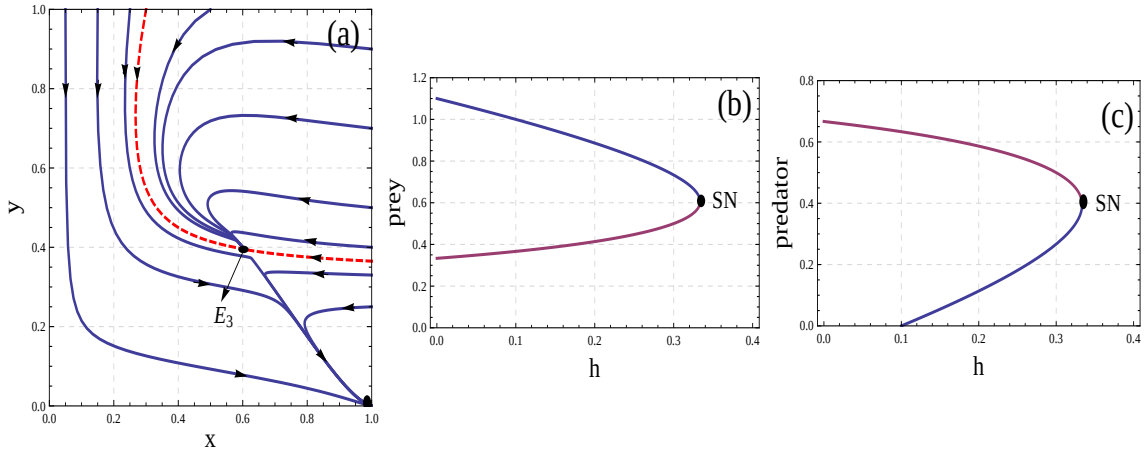

Figure 2.4: $\beta = 0.5, c = 0.1, \overline{h} = 0.33341, \rho = 0.4$. *The system* (2.2.3) *has a double interior equilibrium point* E_3. ***(a)*** *The point* E_3 *is stable from above of the saperatrix curve and a saddle frow below.* ***(b),(c)*** *Saddle-node bifurcation diagram.*

(4) $\beta = 0.12, c = 0.1$, then one can obtain $h_0 = 0.583001, \rho_0 = 0.781849$. Thus, the system (2.2.3) is

$$\begin{cases} \frac{dx}{dt} = x(1-x-y), \\ \frac{dy}{dt} = (0.781849+\lambda_1)(1-\frac{0.12y}{x}-\frac{(0.583001+\lambda_2)}{0.1+y})y. \end{cases} \tag{2.2.22}$$

The system (2.2.22) has a unique positive interior equilibrium point $E_3 = (0.343303, 0.656697)$.

Translating the equilibrium point E_3 into the origin by using the transformation $u_1 = x - 0.343303,\ u_2 = y - 0.656697$ and by the Taylor's series expansion, the system (2.2.22) reduces to

$$\begin{cases} \frac{du_1}{dt} = -0.343303u_1 - 0.343303u_2 - u_1^2 - u_1u_2, \\ \frac{du_2}{dt} = \alpha_0(\lambda) + \alpha_1(\lambda)u_1 + \alpha_2(\lambda)u_2 + \alpha_3(\lambda)u_1^2 + \alpha_4(\lambda)u_1u_2 \\ \qquad + \alpha_5(\lambda)u_2^2 + R_1(u_1,u_2), \end{cases} \tag{2.2.23}$$

where $\alpha_0(\lambda) = -0.678525\lambda_2 - 0.867847\lambda_1\lambda_2,\ \alpha_1(\lambda) = 0.343303 + 0.439092\lambda_1,\ \alpha_2(\lambda) = 0.343303 + 0.439092\lambda_1 - 0.136546\lambda_2 - 0.174645\lambda_1\lambda_2,\ \alpha_3(\lambda) = -1 - 1.27902\lambda_1,\ \alpha_4(\lambda) = 1.04555 + 1.33727\lambda_1,\ \alpha_5(\lambda) = -0.168089 - 0.214989\lambda_1 + 0.18045\lambda_2 + 0.230799\lambda_1\lambda_2$ and $R_1(u_1,u_2)$ is a power series in (u_1,u_2) with powers $u_1^iu_2^j$ satisfying $i+j \geq 3$.

Making the affine transformation $v_1 = u_1,\ v_2 = -0.343303u_1 - 0.343303u_2$, the system (2.2.23) reduces to

$$\begin{cases} \frac{dv_1}{dt} = v_2 + \frac{1}{0.343303}v_1v_2, \\ \frac{dv_2}{dt} = \beta_0(\lambda) + \beta_1(\lambda)v_1 + \beta_2(\lambda)v_2 + \beta_3(\lambda)v_1^2 + \beta_4(\lambda)v_1v_2 \\ \qquad + \beta_5(\lambda)v_2^2 + R_2(v_1,v_2), \end{cases} \tag{2.2.24}$$

where $\beta_0(\lambda) = 0.23294\lambda_2 + 0.297935\lambda_1\lambda_2,\quad \beta_1(\lambda) = -0.0468767\lambda_2 - 0.0599562\lambda_1\lambda_2,\ \beta_2(\lambda) = 0.439092\lambda_1 - 0.136546\lambda_2 - 0.174645\lambda_1\lambda_2,\quad \beta_3(\lambda) = 0.759948 + 0.971988\lambda_1 - 0.0619491\lambda_2 - 0.0792341\lambda_1\lambda_2,\quad \beta_4(\lambda) = 0.381724 + 1.76725\lambda_1 - 0.3609\lambda_2 -$

$0.461599\lambda_1\lambda_2, \quad \beta_5(\lambda) = 0.489622 + 0.626236\lambda_1 - 0.525629\lambda_2 - 0.67229\lambda_1\lambda_2.$

Performing the C^∞ change of coordinates $w_1 = v_1 - \frac{1}{2x_3}v_1^2, \quad w_2 = v_2 - \beta_5 v_1 v_2$ and $z_1 = w_1, \ z_2 = w_2 + R_3(w_1, w_2)$ in the small neighbourhood of $(0,0)$, the system (2.2.24) reduces to

$$\begin{cases} \dfrac{dz_1}{dt} = z_2, \\ \dfrac{dz_2}{dt} = \gamma_0(\lambda) + \gamma_1(\lambda)z_1 + \gamma_3(\lambda)z_1^2 + F_1(z_1) + \gamma_2(\lambda)z_2 + \gamma_4(\lambda)z_1z_2 + \\ \qquad z_2F_2(z_1) + z_2^2F_3(z_1, z_2), \end{cases} \tag{2.2.25}$$

where $\gamma_0(\lambda) = 0.23294\lambda_2 + 0.297935\lambda_1\lambda_2, \gamma_1(\lambda) = -0.160929\lambda_2 - 0.351707\lambda_1\lambda_2 - 0.186578\lambda_1^2\lambda_2 + 0.12244\lambda_2^2 + 0.313206\lambda_2\lambda_2^2 + 0.200298\lambda_1^2\lambda_2^2, \gamma_2(\lambda) = 0.439092\lambda_1 - 0.136546\lambda_2 - 0.174645\lambda_1\lambda_2, \gamma_3(\lambda) = 0.759948 + 0.971988\lambda_1 - 0.273381\lambda_2 - 0.532762\lambda_1\lambda_2 - 0.234192\lambda_1^2\lambda_2 + 0.153687\lambda_2^2 + 0.393136\lambda_1\lambda_2^2 + 0.251414\lambda_1^2\lambda_2^2, \gamma_4(\lambda) = 0.381724 + 1.76725\lambda_1 - 0.3609\lambda_2 - 0.461599\lambda_1\lambda_2$ and F_1, F_2 and F_3 are the power series in z_1 and (z_1, z_2) with powers $z_1^{k_1}, z_2^{k_2}$ and $z_1^i z_2^j$ satisfying $k_1 \geq 3, k_2 \geq 2$ and $i + j \geq 1$, respectively.

Applying the Malgrange Preparation theorem, one gets

$$\gamma_0 + \gamma_1 z_1 + \gamma_3 z_1^2 + F_1(z_1) = \Big(z_1^2 + \frac{\gamma_1}{\gamma_3}z_1 + \frac{\gamma_0}{\gamma_3}\Big)B(z_1, \lambda),$$

where $B(0, \lambda) = \gamma_3$ and B is a power series in z_1 whose coefficients depend on parameters (λ_1, λ_2).

on computing, $\gamma_3 = 0.759948 > 0$ as $\lambda_1, \lambda_2 \to 0$. consider the transformation

$$X_1 = z_1, \ X_2 = \frac{z_2}{\sqrt{\gamma_3}}, \ dT = \sqrt{\gamma_3}dt,$$

the system (2.2.25) reduces to

$$\begin{cases} \frac{dX_1}{dT} = X_2, \\ \frac{dX_2}{dT} = \frac{\gamma_0}{\gamma_3} + \frac{\gamma_1}{\gamma_3}X_1 + X_1^2 + \frac{\gamma_2}{\sqrt{\gamma_3}}X_2 + \frac{\gamma_4}{\sqrt{\gamma_3}}X_1X_2 + S_1(X_1, X_2, \lambda), \end{cases} \tag{2.2.26}$$

where $S_1(X_1, X_2, 0)$ is a power series in (X_1, X_2) with powers $X_1^i X_2^j$ satisfying $i+j \geq 3$ and $j \geq 2$.

Applying the parameter dependent affine transformation $Y_1 = X_1 + \frac{\gamma_1}{2\gamma_3},\ Y_2 = X_2$ in the system (2.2.26), one gets

$$\begin{cases} \frac{dY_1}{dT} = Y_2, \\ \frac{dY_2}{dT} = \frac{\gamma_0}{\gamma_3} - \frac{\gamma_1^2}{4\gamma_3^2} + \frac{1}{\sqrt{\gamma_3}}\Big(\gamma_2 - \frac{\gamma_1\gamma_4}{2\gamma_3}\Big)Y_2 + Y_2^2 + \frac{\gamma_4}{\sqrt{\gamma_3}}Y_1Y_2 + S_2(Y_1, Y_2, \lambda), \end{cases} \tag{2.2.27}$$

where $S_2(Y_1, Y_2, 0)$ is a power series in (Y_1, Y_2) with powers $Y_1^i Y_2^j$ satisfying $i + j \geq 3$ and $j \geq 2$.

Consider the C^∞ transformation

$$X = \frac{\gamma_4^2}{\gamma_3}Y_1,\ Y = \frac{\gamma_4^3}{(\gamma_3)^{\frac{3}{2}}}Y_2, dT = \frac{\sqrt{\gamma_3}}{\gamma_4}d\tau.$$

Then, the system (2.2.27) reduces to

$$\begin{cases} \frac{dX}{d\tau} = Y, \\ \frac{dY}{d\tau} = \mu_1 + \mu_2 Y + X^2 + XY + S_3(X, Y, \lambda), \end{cases} \tag{2.2.28}$$

where $\mu_1 = \frac{\gamma_0\gamma_4^4}{\gamma_3^3} - \frac{\gamma_1^2\gamma_4^4}{4\gamma_3^4}, \mu_2 = \left(\frac{\gamma_2\gamma_4}{\gamma_3} - \frac{\gamma_4^2\gamma_1}{2(\gamma_3)^2}\right)$ and $S_3(X, Y, 0)$ is a power series in (X, Y) with powers X^iY^j satisfying $i + j \geq 3$ and $j \geq 2$. Also $J\Big(\frac{\mu_1,\mu_2}{\lambda_1,\lambda_2}\Big)_{(\lambda_1=0,\lambda_2=0)} = -0.154391$. Thus, the system (2.2.22) undergoes to Bogdanov-Taken bifurcation.

The local representations of the bifurcation curves:

(a) $SN = \{(\lambda_1, \lambda_2) : \mu_1(\lambda_1, \lambda_2) = 0, \mu_2(\lambda_1, \lambda_2) \neq 0\}$.

(b) $H = \{(\lambda_1, \lambda_2) : \mu_2(\lambda_1, \lambda_2) = \sqrt{-\mu_1(\lambda_1, \lambda_2)}, \mu_1(\lambda_1, \lambda_2) < 0\}$.

(c) $HL = \{(\lambda_1, \lambda_2) : \mu_2(\lambda_1, \lambda_2) = \frac{5}{7}\sqrt{-\mu_1(\lambda_1, \lambda_2)}, \mu_1(\lambda_1, \lambda_2) < 0\}$.

These bifurcation curves are sketched in a small neighborhood of the origin in the $\lambda_1\lambda_2$ plane (Figure 2.5(a)). The bifurcation curves divide the parameter plane into four parts: I, II, III, and IV. The saddle-node bifurcation curve (SN) is the horizontal

axis i.e. $\lambda_2 = 0$ axis and the homoclinic bifurcation curve (HL) and hopf bifurcation curve (H) lies in the fourth quadrant. When $(\lambda_1, \lambda_2) = (0, 0)$, then the system (2.2.3) has a unique interior equilibrium point which is a cusp of codimension 2 (Figure 2.5(b)). When the parameters λ_1 and λ_2 varies and lie in the region I, then the system (2.2.3) has no interior equilibrium point and all the solution trajectories goes to the axial equilibrium point, that is, the axial equilibrium point is globally stable (Figure 2.5(c)). Hence, in this case, the predator will go to extinct and prey will approach to the carrying capacity. When the parameters λ_1 and λ_2 pass the SN bifurcation curve and lie in the region II, the cusp of codimension 2 break into a hyperbolic saddle and an unstable focus (Figure 2.5(d)). When the parameters λ_1 and λ_2 lie in the region III, the cusp of codimension 2 breaks into a stable focus and a hyperbolic saddle. The change of stability of the focus yields an unstable limit cycle (Figure 2.5(e)). Further, when the parameters λ_1 and λ_2 lie in the region IV, the cusp of codimension 2 breaks into a saddle point and a stable focus (Figure 2.5(f)). Hence, an open set of initial population densities exists for which both predator and prey approach to a stable steady state.

2.2.5 Results and Discussion

In this section, a Leslie-Gower predator-prey model has been analyzed in the presence of nonlinear predator harvesting. It is shown that the system has at most four equilibrium points in $\mathbb{R}^2_+$, in which the trivial equilibrium point and the axial equilibrium point always exist, while the positive interior equilibrium point changes from two to zero. The qualitative properties of solutions in the vicinity of $(0, 0)$ has been studied by using a blow up technique, and it is found that the origin will never be stable; ecologically speaking, the two species cannot go to extinction together. The axial equilibrium point is either asymptotically stable or globally stable or a saddle depends on the parametric conditions. Thus, ecologically speaking, the prey species never goes to extinction, whatever be the choice of initial population density. If two interior equilibrium points exist, then one is always a saddle point while the other is either asymptotically stable or unstable or the system

undergoes a Hopf bifurcation around this point, that is, for certain parametric domain the system exhibits a bistability phenomenon as well as oscillatory co-existence of both the populations. The stability of limit cycles has been studied and validated through numerical simulations by calculating the first Lyapunov number. It is also found that for certain parametric domain the proposed system has a unique interior equilibrium which is globally asymptotically stable.

It is shown that the system can have zero, one or two interior equilibrium points through saddle-node bifurcation as the bifurcation parameter h crosses a certain threshold value. By means of Sotomayor's theorem, the existence of saddle-node bifurcation has been shown. Ecologically speaking a maximum threshold value of h exists below which both species co-exist and above which predator species suddenly collapse to extinction. The proposed system undergoes to Bogdanov-Taken bifurcation near degenerate equilibria. The parameters h and ρ have been considered as Bogdanov-Takens bifurcation parameters and the normal form has been obtained. Ecologically speaking, a small perturbation in the bifurcation parameters is a cause of extinction, coexistence and oscillation.

The dynamical analysis of the model (2.2.3) shows complex and rich dynamics as compared to the model with no harvesting (Hsu and Hwang 1995) and with constant yield predator harvesting (Huang et al. 2013). The model without harvesting has a unique interior equilibrium point which is globally asymptotically stable (section 1.5.3), while model (2.2.3) has zero to two interior equilibrium points and the model (2.2.3) undergoes to a series of bifurcation (hopf bifurcation, saddle-node bifurcation, Bogdanov-Takens bifurcation). The model with constant yield predator harvesting has no axial equilibrium point, and the solutions once touching the $x-$ axis will leave the first quadrant (Hsu and Hwang 1995). But the model with nonlinear predator harvesting has one trivial equilibrium point $E_0 = (0, 0)$ and one axial equilibrium point $e = (1, 0)$ and the solutions touching the $x-$ axis will go to the axial equilibrium point e. Further, if no interior equilibrium point exists, then the axial equilibrium point e is globally asymptotically stable. Ecologically speaking, in the absence of predator species, the prey density approaches to the carrying capacity. Although the model with constant yield predator harvesting undergoes a series of bifurcations, like, hopf bifurcation, saddle-node bifurcation, Bogdanov-Takens bifurcation (Huang

et al. 2013) but the model with nonlinear harvesting gives more general parametric conditions for the occurrence of these bifurcations. Thus, the results of nonlinear harvesting model can explain the real life situation in a more effective and realistic manner.

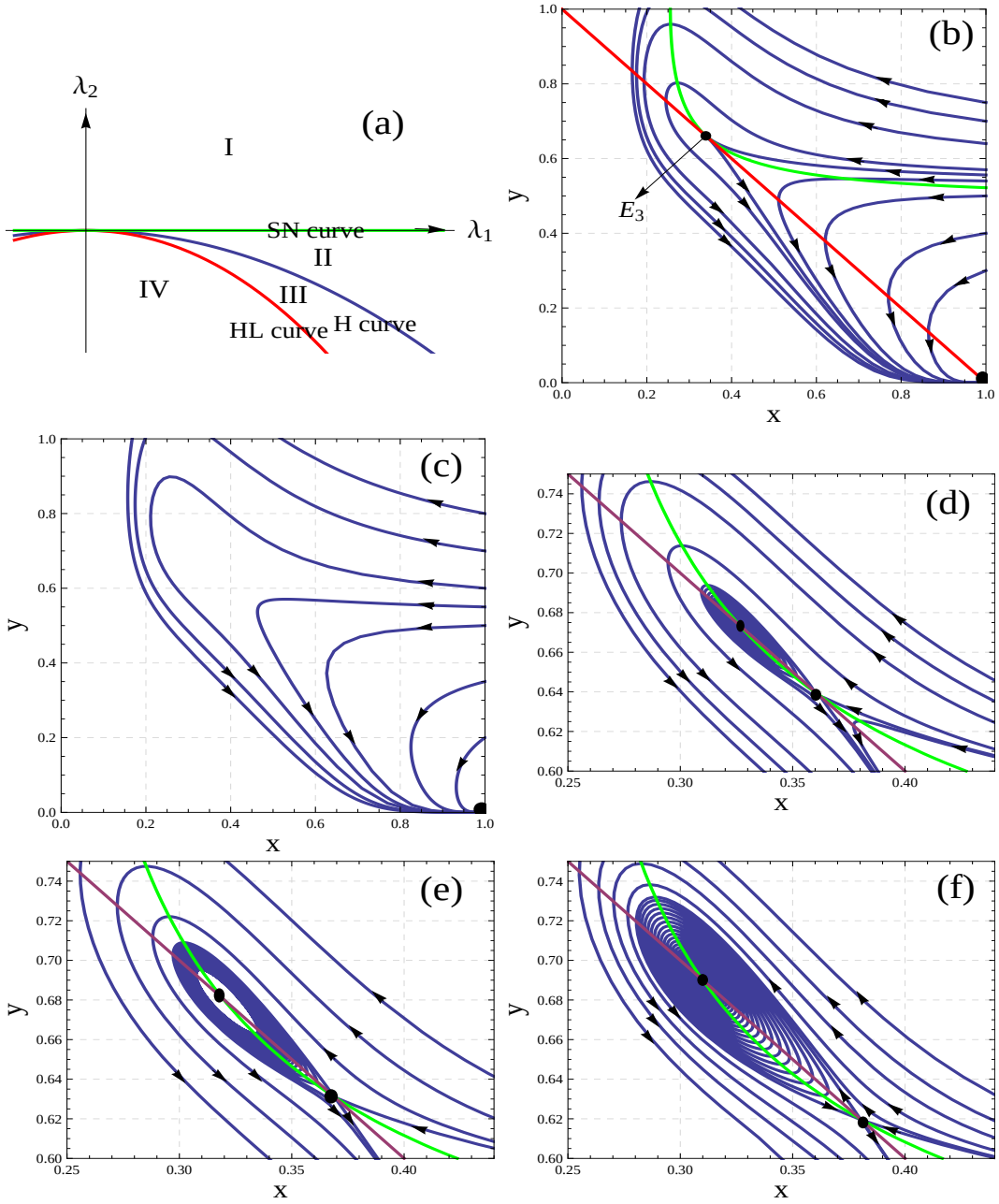

Figure 2.5: $\beta = 0.12, c = 0.1, h_0 = 0.583001, \rho_0 = 0.781849$ ***(a)*** *BT Bifurcation diagram in the* $\lambda_1\lambda_2$ *plane.* ***(b)*** *The equilibrium point* E_3 *is a cusp when* $(\lambda_1, \lambda_2) = (0, 0)$. ***(c)*** *No interior equilibrium point exist when* $(\lambda_1, \lambda_2) = (0.04, 0.001)$ *lies in the region* I. ***(d)*** *An unstable focus when* $(\lambda_1, \lambda_2) = (0.03, -0.001)$ *lies in the region* II. ***(e)*** *An unstable limit cycle when* $(\lambda_1, \lambda_2) = (0.03, -0.002)$ *lies in the region* III. ***(f)*** *A stable focus when* $(\lambda_1, \lambda_2) = (0.03, -0.004)$ *lies in the region* IV.

2.3 Model with nonlinear prey harvesting

2.3.1 Model Equations

Consider the Leslie-Gower predator-prey model with nonlinear prey harvesting (Gupta et al. 2012):

$$\begin{cases} \frac{dX}{dT} = r\Big(1-\frac{X}{K}\Big)X - \alpha XY - \frac{qEX}{m_1E+m_2X}, \\ \frac{dY}{dT} = s(1-\frac{Y}{nX})Y, \quad \text{if} \quad (X,Y) \neq (0,0) \\ \frac{dY}{dT} = 0, \quad \text{if} \ \ (X,Y) = (0,0), \end{cases} \tag{2.3.1}$$

with the initial conditions $X(0) > 0, Y(0) > 0$, where the variables and parameters are same as defined for system (2.2.1). Gupta et al. (2012) have studied the positivity, boundedness and the stability of the system (2.3.1). They have also shown that this system undergoes Hopf-bifurcation and saddle-node bifurcation. In this section, codimension 2 bifurcations (Bogdanov-Takens bifurcation of codim 2) for the system (2.3.1) has been studied in detail. The novelty obtained here is that the system (2.3.1) undergoes to two types of Bogdanov-Taken bifurcations; attracting and repelling Bogdanov-Taken bifurcations.

For nondimensionalizing the system (2.3.1), consider

$$X = Kx, \quad Y = nKy, \quad rT = t.$$

The system (2.3.1) reduces to

$$\begin{cases} \frac{dx}{dt} = \Big(1 - x - by - \frac{h}{c+x}\Big)x, \\ \frac{dy}{dt} = \rho\Big(1-\frac{y}{x}\Big)y, \quad \text{if} \quad (x,y) \neq (0,0) \\ \frac{dy}{dt} = 0, \quad \text{if} \ \ (x,y) = (0,0) \end{cases} \tag{2.3.2}$$

with the initial conditions $x(0) > 0, y(0) > 0$, where

$$b = \frac{\alpha nK}{r}, \quad c = \frac{m_1E}{m_2K}, \quad h = \frac{qE}{rm_2K}, \quad \rho = \frac{s}{r}.$$

Here, we take h and ρ as bifurcation parameters.

2.3.2 Bogdanov-Takens Bifurcation: Normal Form

The Bogdanov-Takens bifurcation (BT bifurcation) is a type of codimension 2 bifurcation that emerges, when the system (2.3.2) admits a unique degenerate equilibrium. Assuming that if $(1-c(b+1))^2-4(b+1)(h-c)=0$, then the system (2.3.2) has a unique positive equilibrium $E(x_0,y_0)$, where $x_0=y_0=\frac{1-c(b+1)}{2(b+1)}$, $c(b+1)<1$.

The Jacobian matrix of the system (2.3.2) at the point $E(x_0,y_0)$ is

$$J_E=\begin{bmatrix}\Big(-1+\frac{h}{(c+x_0)^2}\Big)x_0 & -bx_0\\ \rho & -\rho\end{bmatrix}.$$

The determinant of the above Jacobian matrix $det(J_E)=\rho x_0\Big(1+b-\frac{h}{(c+x_0)^2}\Big)=0$, which confirms that E is a degenerate singularity. The trace of the above Jacobian matrix $tr(J_E)=x_0\Big(-1+\frac{h}{(c+x_0)^2}\Big)-\rho$. As the determinant of the Jacobian matrix J_E is zero, and if in addition $bx_0=\rho$, then the Jacobian matrix J_E has a zero eigenvalue with multiplicity 2 i.e. $\lambda_1=\lambda_2=0$ but the Jacobian matrix is not a null matrix.

In Theorem (2.3.1) below, it has been proved that the unique interior equilibrium point $E(x_0,y_0)$ of the system (2.3.2) is a cusp of codimension 2.

Theorem 2.3.1. *If $bx_0=\rho$ and $b-\frac{2hx_0}{(c+x_0)^3}\neq 0$, then the unique interior equilibrium point $E(x_0,y_0)$ of the system (2.3.2) is a cusp of codimension 2.*

Proof. First, the equilibrium point $E(x_0,y_0)$ has been shifted at the origin by means of the transformation $x_1=x-x_0, y_1=y-y_0$ and then use the first condition given in the statement of the theorem. The system (2.3.2) reduces to

$$\begin{cases}\frac{dx_1}{dt}=\rho x_1-\rho x_2+\Big(b-\frac{hx_0}{(c+x_0)^3}\Big)x_1^2-bx_1x_2+P_1(x_1,x_2),\\ \frac{dx_2}{dt}=\rho x_1-\rho x_2-\frac{\rho}{x_0}x_1^2+\frac{2\rho}{x_0}x_1x_2-\frac{\rho}{x_0}x_2^2+P_2(x_1,x_2),\end{cases}\tag{2.3.3}$$

where $P_1(x_1,x_2)$ and $P_2(x_1,x_2)$ are the power series in (x_1,x_2) with powers $x_1^ix_2^j$ satisfying $i+j\geq 3$.

Now, consider the affine transformation $y_1=x_1,\ y_2=\rho x_1-\rho x_2$, to reduce the

system (2.3.3) into

$$\begin{cases} \frac{dy_1}{dt} = y_2 - \frac{hx_0}{(c+x_0)^3}y_1^2 + \frac{1}{x_0}y_1y_2 + \overline{P}_1(y_1, y_2), \\ \frac{dy_2}{dt} = -\frac{\rho hx_0}{(c+x_0)^3}y_1^2 + by_1y_2 + \frac{1}{x_0}y_2^2 + \overline{P}_2(y_1, y_2), \end{cases} \tag{2.3.4}$$

where $\overline{P}_1(y_1, y_2)$ and $\overline{P}_2(y_1, y_2)$ are the power series in (y_1, y_2) with powers $y_1^i y_2^j$ satisfying $i + j \geq 3$.

Consider the C^∞ change of coordinates in the small neighbourhood of $(0, 0)$:

$$z_1 = y_1 - \frac{1}{x_0}y_1^2, \quad z_2 = y_2 - \frac{hx_0}{(c+x_0)^3}y_1^2 - \frac{1}{x_0}y_1y_2.$$

Then, the system (2.3.4) reduces to

$$\begin{cases} \frac{dz_1}{dt} = z_2 + \widetilde{P}_1(z_1, z_2), \\ \frac{dz_2}{dt} = -\frac{\rho hx_0}{(c+x_0)^3}z_1^2 + \left(b - \frac{2hx_0}{(c+x_0)^3}\right)z_1z_2 + \widetilde{P}_2(z_1, z_2), \end{cases} \tag{2.3.5}$$

where $\widetilde{P}_1(z_1, z_2)$ and $\widetilde{P}_2(z_1, z_2)$ are the power series in (z_1, z_2) with powers $z_1^i z_2^j$ satisfying $i + j \geq 3$.

Now, let the C^∞ change of coordinates in the small neighbourhood of $(0, 0)$:

$$u_1 = z_1, \quad u_2 = z_2 + \widetilde{P}_1(z_1, z_2).$$

The system (2.3.5) reduces to

$$\begin{cases} \frac{du_1}{dt} = u_2 \\ \frac{du_2}{dt} = -\frac{\rho hx_0}{(c+x_0)^3}u_1^2 + \left(b - \frac{2hx_0}{(c+x_0)^3}\right)u_1u_2 + s(u_1, u_2), \end{cases} \tag{2.3.6}$$

where $s(u_1, u_2)$ is a power series in (u_1, u_2) with powers $u_1^i u_2^j$ satisfying $i + j \geq 3$.

Since $-\frac{\rho hx_0}{(c+x_0)^3} \neq 0$, so if $b - \frac{2hx_0}{(c+x_0)^3} \neq 0$, the system (2.3.2) has a cusp of codimension 2. ■

Now, for given suitable bifurcation parameters, it has been proved in Theorem (2.3.2) below that the system (2.3.2) will undergo the Bogdanov-Takens bifurcation. The harvesting parameter (h) has much affect on the system. The parameter h and the ratio

of intrinsic growth rate of predator and prey species (ρ) are chosen as the Bogdanov-Taken bifurcation parameters. A series of variable changes is applied to obtain the universal unfolding of system (2.3.2) near the Bogdanov-Takens (BT) point (h_0, ρ_0).

Theorem 2.3.2. *The system* (2.3.2) *undergoes a Bogdanov-Takens bifurcation with respect to the bifurcation parameters h and ρ around the cusp $E(x_0, y_0)$ if $bx_0 = \rho$ and $b - \frac{2hx_0}{(c+x_0)^3}) \neq 0$. Moreover,*

i) the system has an attracting Bogdanov-Takens bifurcation of codimension 2 if $(b - \frac{2hx_0}{(c+x_0)^3}) > 0$.

ii) the system has an repelling Bogdanov-Takens bifurcation of codimension 2 if $(b - \frac{2hx_0}{(c+x_0)^3}) < 0$.

Proof. Consider that the parameters h and ρ vary in a small neighbourhood of the BT point (h_0, ρ_0). Let $(h_0 + \lambda_1, \rho_0 + \lambda_2)$ be a point of a small neighbourhood of the BT point (h_0, ρ_0), where λ_1, λ_2 are small. Thus, the system (2.3.2) reduces to

$$\begin{cases} \frac{dx}{dt} = \Big(1 - x - by - \frac{h_0}{c+x} - \frac{\lambda_1}{c+x}\Big)x, \\ \frac{dy}{dt} = (\rho_0 + \lambda_2)\Big(1 - \frac{y}{x}\Big)y. \end{cases} \tag{2.3.7}$$

Translating the equilibrium point $E(x_0, y_0)$ into the origin by using the transformation $x_1 = x - x_0,\ x_2 = y - y_0$, and then using the Taylor's series expansion and conditions of the theorem, the system (2.3.7) reduces to

$$\begin{cases} \frac{dx_1}{dt} = -\frac{\lambda_1 x_0}{c+x_0} + \Big(\rho_0 - \frac{\lambda_1 c}{(c+x_0)^2}\Big)x_1 - \rho_0 x_2 + \\ \qquad \Big(b - \frac{h_0 x_0}{(c+x_0)^3} + \frac{\lambda_1 c}{(c+x_0)^3}\Big)x_1^2 - bx_1x_2 + R_1(x_1, x_2), \\ \frac{dx_2}{dt} = (\rho_0 + \lambda_2)x_1 - (\rho_0 + \lambda_2)x_2 - \frac{\rho_0 + \lambda_2}{x_0}x_1^2 + \frac{2(\rho_0 + \lambda_2)}{x_0}x_1x_2 - \\ \qquad \frac{(\rho_0 + \lambda_2)}{x_0}x_2^2 + R_2(x_1, x_2), \end{cases} \tag{2.3.8}$$

where $R_1(x_1, x_2)$ and $R_2(x_1, x_2)$ are the power series in (x_1, x_2) with powers $x_1^i x_2^j$ satisfying $i + j \geq 3$.

Making the affine transformation $y_1 = x_1,\ y_2 = \rho_0 x_1 - \rho_0 x_2$, the system (2.3.8) reduces to

$$\begin{cases} \frac{dy_1}{dt} = \alpha_{00} + \alpha_{10} y_1 + y_2 + \alpha_{20} y_1^2 + \alpha_{11} y_1 y_2 + \overline{R}_1(y_1, y_2), \\ \frac{dy_2}{dt} = \beta_{00} + \beta_{10} y_1 + \beta_{01} y_2 + \beta_{20} y_1^2 + \beta_{11} y_1 y_2 + \beta_{02} y_1^2 + \overline{R}_2(y_1, y_2), \end{cases} \tag{2.3.9}$$

where

$$\alpha_{00} = -\frac{\lambda_1 x_0}{c + x_0}, \quad \alpha_{10} = -\frac{\lambda_1 c}{(c + x_0)^2}, \quad \alpha_{20} = -\frac{h_0 x_0}{(c + x_0)^3} + \frac{\lambda_1 c}{(c + x_0)^3},$$

$$\alpha_{11} = \frac{b}{\rho}, \quad \beta_{00} = -\frac{\lambda_1 x_0 \rho_0}{c + x_0}, \quad \beta_{10} = -\frac{\lambda_1 c \rho_0}{(c + x_0)^2}, \quad \beta_{01} = -\lambda_2,$$

$$\beta_{20} = -\frac{h_0 x_0 \rho_0}{(c + x_0)^3} + \frac{\lambda_1 c \rho_0}{(c + x_0)^3}, \quad \beta_{11} = b, \quad \beta_{02} = \frac{\rho_0 + \lambda_2}{\rho_0 x_0},$$

$\overline{R}_1(y_1, y_2)$ and $\overline{R}_2(y_1, y_2)$ are the power series in (y_1, y_2) with powers $y_1^i y_2^j$ satisfying $i + j \geq 3$. Consider the C^∞ change of coordinates in the small neighbourhood of $(0, 0)$:

$$z_1 = y_1 - \frac{1}{2}(\alpha_{11} + \beta_{02}) y_1^2, \quad z_2 = y_2 + \alpha_{20} y_1^2 - \beta_{02} y_1 y_2,$$

the system (2.3.9) reduces to

$$\begin{cases} \frac{dz_1}{dt} = \xi_{00} + \xi_{10} z_1 + z_2 + \xi_{20} z_1^2 + \widetilde{R}_1(z_1, z_2), \\ \frac{dz_2}{dt} = \eta_{00} + \eta_{10} z_1 + \eta_{01} z_2 + \eta_{20} z_1^2 + \eta_{11} z_1 z_2 + \widetilde{R}_2(z_1, z_2), \end{cases} \tag{2.3.10}$$

where

$$\xi_{00} = \alpha_{00}, \quad \xi_{10} = \alpha_{10} - \alpha_{00}(\alpha_{11} + \beta_{02}), \quad \xi_{20} = -\frac{1}{2}(\alpha_{11} + \beta_{02})(\alpha_{00}(\alpha_{11} + \beta_{02}) + \alpha_{10}),$$

$$\eta_{00} = \beta_{00}, \quad \eta_{10} = \beta_{10} + 2\alpha_{20}\alpha_{00} - \beta_{00}\beta_{02}, \quad \eta_{01} = \beta_{01} - \alpha_{00}\beta_{02},$$

$$\eta_{20} = \frac{1}{2}(\alpha_{11} + \beta_{02})(\beta_{10} + 2\alpha_{20}\alpha_{00} - \beta_{00}\beta_{02}) - \alpha_{20}(\beta_{01} - \alpha_{00}\beta_{02}) + (\beta_{20} + 2\alpha_{20}\alpha_{10} - \beta_{02}\beta_{10}),$$

$$\eta_{11} = \beta_{11} + 2\alpha_{20} - \beta_{02}\alpha_{10} - \beta_{02}^2\alpha_{10},$$

$\widetilde{R}_1(z_1, z_2)$ and $\widetilde{R}_2(z_1, z_2)$ are the power series in (z_1, z_2) with powers $z_1^i z_2^j$ satisfying $i + j \geq 3$.

Consider the C^∞ change of coordinates in the small neighbourhood of $(0,0)$:

$$u_1 = z_1,\ u_2 = \xi_{00} + \xi_{10}z_1 + z_2 + \xi_{20}z_1^2,$$

the system (2.3.10) reduces to

$$\begin{cases} \frac{du_1}{dt} = u_2 + \widehat{R}_1(u_1,u_2), \\ \frac{du_2}{dt} = \gamma_{00} + \gamma_{10}u_1 + \gamma_{01}u_2 + \gamma_{20}u_1^2 + \gamma_{11}u_1u_2 + \widehat{R}_2(u_1,u_2), \end{cases} \tag{2.3.11}$$

where

$$\gamma_{00} = \eta_{00} - \xi_{00}\eta_{01}, \quad \gamma_{10} = \eta_{10} - \xi_{10}\eta_{01} - \xi_{00}\eta_{11}, \quad \gamma_{01} = \xi_{10} + \eta_{01},$$

$$\gamma_{20} = \eta_{20} - \xi_{20}\eta_{01} - \xi_{10}\eta_{11}, \quad \gamma_{11} = \eta_{11} + 2\xi_{20},$$

$\widehat{R}_1(u_1,u_2)$ and $\widehat{R}_2(u_1,u_2)$ are the power series in (u_1,u_2) with powers $u_1^iu_2^j$ satisfying $i+j \geq 3$.

Consider the C^∞ change of coordinates in the small neighbourhood of $(0,0)$:

$$v_1 = u_1,\ v_2 = u_2 + \widehat{R}_1(u_1,u_2),$$

the system (2.3.11) reduces to

$$\begin{cases} \dfrac{dv_1}{dt} = v_2, \\ \dfrac{dv_2}{dt} = \gamma_{00} + \gamma_{10}v_1 + \gamma_{01}v_2 + \gamma_{20}v_1^2 + \gamma_{11}v_1v_2 + F_1(v_1) \\ \qquad\qquad + v_2F_2(v_1) + v_2^2F_3(v_1,v_2), \end{cases} \tag{2.3.12}$$

where F_1, F_2 and F_3 are the power series in v_1 and (v_1,v_2) with powers $v_1^{k_1}, v_2^{k_2}$ and $v_1^iv_2^j$ satisfying $k_1 \geq 3, k_2 \geq 2$ and $i+j \geq 1$, respectively.

Applying the Malgrange Preparation theorem (Chow and Hale 1983), one gets

$$\gamma_{00} + \gamma_{10}v_1 + \gamma_{20}v_1^2 + F_1(v_1) = \Big(v_1^2 + \frac{\gamma_{10}}{\gamma_{20}}v_1 + \frac{\gamma_{00}}{\gamma_{20}}\Big)B_1(v_1,\lambda),$$

where $B_1(0,\lambda) = \gamma_{20}$ and B_1 is a power series in v_1 whose coefficients depend on parameters

(λ_1, λ_2).

Now, we have $\gamma_{20} = -\frac{h_0 x_0 \rho_0}{(c+x_0)^3} < 0$ as λ_1, λ_2 are small, so consider the transformation

$$w_1 = v_1,\ w_2 = \frac{v_2}{\sqrt{-\gamma_{20}}},\ dT = \sqrt{-\gamma_{20}}dt,$$

then the system (2.3.12) reduces to

$$\begin{cases} \frac{dw_1}{dT} = w_2, \\ \frac{dw_2}{dT} = -\frac{\gamma_{00}}{\gamma_{20}} - \frac{\gamma_{10}}{\gamma_{20}} w_1 + \frac{\gamma_{01}}{\sqrt{-\gamma_{20}}} w_2 - w_1^2 + \frac{\gamma_{11}}{\sqrt{-\gamma_{20}}} w_1 w_2 + S_1(w_1, w_2, \lambda), \end{cases} \tag{2.3.13}$$

where $S_1(w_1, w_2, 0)$ is a power series in (w_1, w_2) with powers $w_1^i w_2^j$ satisfying $i + j \geq 3$ and $j \geq 2$.

Applying the parameter dependent affine transformation $X_1 = w_1 + \frac{\gamma_{10}}{2\gamma_{20}},\ X_2 = w_2$ in the system (2.3.13), then it will become

$$\begin{cases} \frac{dX_1}{dT} = X_2, \\ \frac{dX_2}{dT} = -\frac{\gamma_{00}}{\gamma_{20}} + \frac{\gamma_{10}^2}{4\gamma_{20}^2} + \frac{1}{\sqrt{-\gamma_{20}}}\Big(\gamma_{01} - \frac{\gamma_{11}\gamma_{10}}{2\gamma_{20}}\Big) X_2 - X_1^2 \\ \qquad\qquad + \frac{\gamma_{11}}{\sqrt{-\gamma_{20}}} X_1 X_2 + S_2(X_1, X_2, \lambda), \end{cases} \tag{2.3.14}$$

where $S_2(X_1, X_2)$ is a power series in (X_1, X_2) with powers $X_1^i X_2^j$ satisfying $i + j \geq 3$ and $j \geq 2$.

Since $\gamma_{11} = b - \frac{2hx_0}{(c+x_0)^3} \neq 0$, as $\lambda_1, \lambda_2 \longrightarrow 0$, consider the final C^∞ transformation as

$$Y_1 = -\frac{\gamma_{11}^2}{\gamma_{20}} X_1,\ Y_2 = \frac{\gamma_{11}^3}{(-\gamma_{20})^{\frac{3}{2}}} X_2,\ dT = -\frac{\gamma_{11}}{\sqrt{-\gamma_{20}}} d\tau.$$

Then, the system (2.3.14) reduces to

$$\begin{cases} \frac{dY_1}{d\tau} = Y_2, \\ \frac{dY_2}{d\tau} = \frac{\gamma_{00}\gamma_{11}^4}{\gamma_{20}^3} - \frac{\gamma_{10}^2\gamma_{11}^4}{4\gamma_{20}^4} + \Big(\frac{\gamma_{01}\gamma_{11}}{\gamma_{20}} - \frac{\gamma_{11}^2\gamma_{10}}{2(\gamma_{20})^2}\Big) Y_2 + Y_1^2 \mp Y_1 Y_2 + S_3(Y_1, Y_2, \lambda), \end{cases} \tag{2.3.15}$$

where $S_3(Y_1, Y_2)$ is a power series in (Y_1, Y_2) with powers $Y_1^i Y_2^j$ satisfying $i + j \geq 3$ and

$j \geq 2$ and $\mp$ sign depends on the sign of γ_{11}. If $\gamma_{11} > 0$, then coefficient of Y_1Y_2 will be -1 and if $\gamma_{11} < 0$, then coefficient of Y_1Y_2 will be $+1$.

The above system is topologically equivalent to the normal form of the Bogdanov-Takens bifurcation which is given by

$$\begin{cases} \frac{dZ_1}{dt} = Z_2, \\ \\ \frac{dZ_2}{dt} = \mu_1(\lambda_1, \lambda_2) + \mu_2(\lambda_1, \lambda_2)Z_2 + Z_1^2 \mp Z_1Z_2. \end{cases} \tag{2.3.16}$$

Thus, the Bogdanov-Takens bifurcation will be attracting Bogdanov-Takens bifurcation, if $\gamma_{11} = (b - \frac{2hx_0}{(c+x_0)^3}) > 0$, and will be repelling Bogdanov-Takens bifurcation, if $\gamma_{11} = (b - \frac{2hx_0}{(c+x_0)^3}) < 0$.

Take

$$\mu_1(\lambda_1, \lambda_2) = \frac{\gamma_{00}\gamma_{11}^4}{\gamma_{20}^3} - \frac{\gamma_{10}^2\gamma_{11}^4}{4\gamma_{20}^4}, \quad \mu_2(\lambda_1, \lambda_2) = \frac{\gamma_{01}\gamma_{11}}{\gamma_{20}} - \frac{\gamma_{11}^2\gamma_{10}}{2(\gamma_{20})^2}.$$

Thus,

$$J\Big(\frac{\mu_1, \mu_2}{\lambda_1, \lambda_2}\Big)_{(\lambda_1=0, \lambda_2=0)} = \frac{(c+x_0)^{11}}{h^4d^4\rho^4}\Big(b - \frac{2hx_0}{(c+x_0)^3}\Big)^5\Big(\frac{1+b-x_0}{1+b} + \frac{x_0}{(c+x_0)^2}\Big) \neq 0,$$

as $b - \frac{2hx_0}{(c+x_0)^3} \neq 0$ and $x_0 < 1$. Further, the parameter transformation is a homomorphism in a small neighbourhood of the origin and μ_1, μ_2 are independent parameters. The local representation of the bifurcation curves in the small neighbourhood of the origin are given by Perko (1996)

i) The saddle-node bifurcation curve $SN = \{(\lambda_1, \lambda_2) : \mu_1(\lambda_1, \lambda_2) = 0, \mu_2(\lambda_1, \lambda_2) \neq 0\}$.

ii) The Hopf bifurcation curve

$$H = \{(\lambda_1, \lambda_2) : \mu_2(\lambda_1, \lambda_2) = \sqrt{-\mu_1(\lambda_1, \lambda_2)}, \mu_1(\lambda_1, \lambda_2) < 0\}.$$

iii) The homoclinic bifurcation curve

$$HL = \{(\lambda_1, \lambda_2) : \mu_2(\lambda_1, \lambda_2) = \tfrac{5}{7}\sqrt{-\mu_1(\lambda_1, \lambda_2)}, \mu_1(\lambda_1, \lambda_2) < 0\}.$$

■

2.3.3 Numerical Simulations

Now, numerical simulations have been performed. Considered two set of parameter values for the parameters b and c satisfying the above analytical results.

(1) Take $b = 0.6, c = 0.45$, then one can obtain $h = 0.46225, \rho = 0.0525$ and the unique interior equilibrium point is $(0.0875, 0.0875)$. Also since $b - \frac{2hx_0}{(c+x_0)^3} = 0.0791$, therefore, the system (2.3.2) undergoes attracting Bogdanov-Takens bifurcations around the unique interior equilibrium point.

The bifurcation diagram for the attracting BT bifurcation is shown in the Figure 2.6(a). The saddle-node bifurcation curve (SN) is the horizontal axis i.e. $\lambda_1 = 0$ axis and the homoclinic bifurcation curve (HL) and hopf bifurcation curve (H) are lying in the third quadrant. The SN, H and HL bifurcation curves divide the small neighbourhood of the origin in the (λ_1, λ_2)-plane into four regions. When $(\lambda_1, \lambda_2) = (0, 0)$, then the system (2.3.7) has a unique interior equilibrium point, which is a cusp of codimension 2 (Figure 2.6(b)). When $\lambda_1 = 0$, then the system (2.3.7) has a unique interior equilibrium point which is a saddle-node point. When the parameters λ_1 and λ_2 vary and lie in the region I, then the system (2.3.7) has no interior equilibrium point and all the solution trajectories go to the origin, and hence the origin is globally asymptotically stable (Figure 2.6(c)). When the parameters λ_1 and λ_2 pass the SN bifurcation curve and lie in the region II, then the system (2.3.7) has two interior equilibrium points, one is a saddle point and the other one is an unstable focus (Figure 2.6(d)). When the parameters λ_1 and λ_2 pass the region II and lie on the homoclinic bifurcation curve HL, then the system (2.3.7) has two interior equilibrium points, one is a saddle point and the other one is an unstable focus enclosed by a stable homoclinic loop (Figure 2.6(e)). When the parameters λ_1 and λ_2 pass the homoclinic bifurcation curve HL and lie in the region III, then the system (2.3.7) has two interior equilibrium points, one is a saddle point and the other is an unstable focus enclosed by a stable limit cycle (Figure 2.6(f)). Further, when the parameters λ_1 and λ_2 pass the region III and lie in the region IV, then the system (2.3.7) has two interior equilibrium points, one is a saddle point and the other is a stable focus (Figure 2.6(g)).

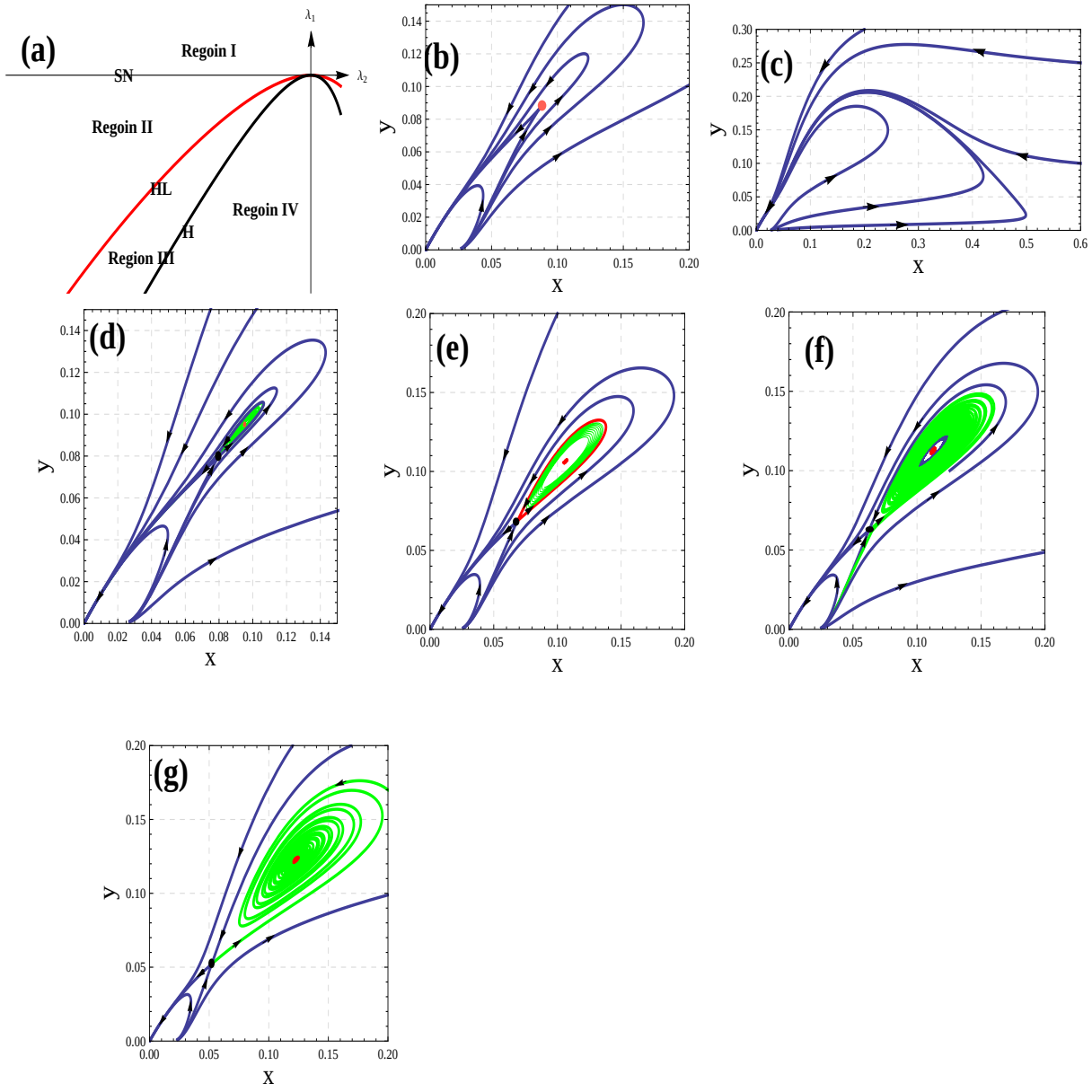

Figure 2.6: **(a)** Bifurcation diagram for attracting B-T bifurcation. The red trajectory is homoclinic bifurcation curve and black trajectory is the hopf bifurcation curve. **(b)** A cusp of codimension 2 when $(\lambda_1, \lambda_2) = (0, 0)$. **(c)** No interior equilibrium point exist when $(\lambda_1, \lambda_2) = (0.0002, -0.001)$ lies in the first region. **(d)** An unstable focus when $(\lambda_1, \lambda_2) = (-0.0001, -0.001)$ lies in the region II. **(e)** A stable homoclinic loop rises when $(\lambda_1, \lambda_2) = (-0.000568, -0.001)$ lies on the homoclinic bifurcation curve. **(f)** A stable limit cycle when $(\lambda_1, \lambda_2) = (-0.001, -0.001)$ lies in the region III. **(g)** A stable focus when $(\lambda_1, \lambda_2) = (-0.002, -0.001)$ lies in the region IV.

(2) Take $b = 0.9, c = 0.05$, then one can obtain $h = 0.1578, \rho = 0.2143$, and the unique interior equilibrium point is $(0.2382, 0.2382)$. Also since $b - \frac{2hx_0}{(c+x_0)^3} = -2.24064$, therefore, the system (2.3.2) undergoes repelling Bogdanov-Tatens bifurcation around the unique interior equilibrium point.

The bifurcation diagram for the repelling BT bifurcation is shown in Figure 2.7(a). It is clear from the figure that when the parameters λ_1 and λ_2 lie in the region I, then the system (2.3.7) has no interior equilibrium point, and the origin is globally asymptotically stable (Figure 2.7(b)). When the parameters λ_1 and λ_2 lie in the region II, then the system (2.3.7) has two interior equilibrium points one is a saddle and other is an unstable focus (Figure 2.7(c)). When the parameters λ_1 and λ_2 lie in the region III, then the system (2.3.7) has two interior equilibrium points, one is a saddle and other is a stable focus enclosed by an unstable limit cycle (Figure 2.7(d)). Also when the parameters λ_1 and λ_2 lie on the homoclinic curve, then the system (2.3.7) has two interior equilibrium points, one is a saddle and other is a stable focus enclosed by an unstable homoclinic loop (Figure 2.7(e)). Further, when the parameters λ_1 and λ_2 lie in the region IV, then the system (2.3.7) has two interior equilibrium points, one is a saddle and other is the stable focus (Figure 2.7(f)).

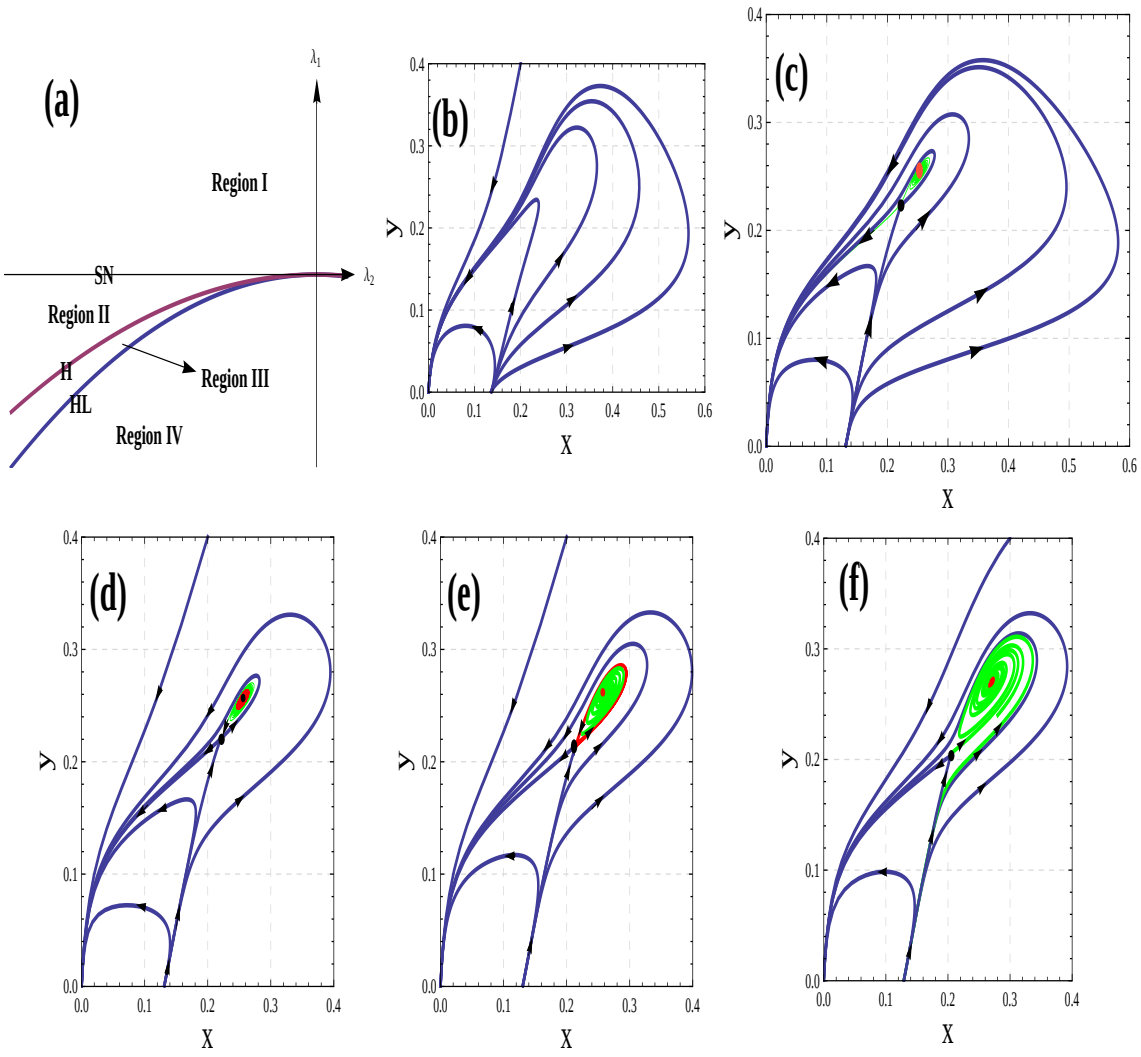

Figure 2.7: **(a)** Bifurcation diagram for repelling B-T bifurcation. The blue trajectory is homoclinic bifurcation curve and violet trajectory is the hopf bifurcation curve. **(b)** No interior equilibrium point exist when $(\lambda_1, \lambda_2) = (0.003, 0.08)$ lies in the region I. **(c)** An unstable focus when $(\lambda_1, \lambda_2) = (-0.0005, -0.04)$ lies in the region II. **(d)** An unstable limit cycle when $(\lambda_1, \lambda_2) = (-0.0006, -0.04)$ lies in the region III. **(e)** An unstable Homoclinic loop when $(\lambda_1, \lambda_2) = (-0.00106893, -0.04)$ lies on the homoclinc bifurcation curve. **(f)** A stsble focus when $(\lambda_1, \lambda_2) = (-0.002, -0.04)$ lies in the region IV.

2.3.4 Results and Discussion

In this section, bifurcations of codimension 2 have been discussed for the Leslie-Gower predator-prey model with nonlinear prey harvesting. The parameters h and ρ are taken as bifurcation parameters and by reducing the system into normal form, it is shown that for certain parametric conditions, system (2.3.2) has a cusp of co-dimension 2. Also, the parametric conditions for which the system (2.3.2) undergoes repelling BT bifurcation and attracting BT bifurcation have been obtained. From Figures 2.6(c) and 2.7(b), it is clear that if λ_1 is positive i.e. if $\mu_1(\lambda_1, \lambda_2) > 0$, then the system (2.3.7) has no interior point and all the trajectories reach to the origin. If λ_1 is negative i.e. if $\mu_1(\lambda_1, \lambda_2) < 0$, then the system (2.3.7) have two interior equilibrium points in which one is always a saddle point while other is a focus whose nature changes depending on the region in which it lies. Thus, the system (2.3.2) is very sensitive for parameters h and ρ, and the predator and prey both will coexist for some suitable values of the parameters h and ρ. Therefore, the homoclinic orbit or cusp bifurcation arises as the bifurcation parameters $h = \frac{qE}{rm_2K}$ and $\rho = \frac{s}{r}$ varied, then the biological phenomena are very complex and interesting.

Chapter 3

Ratio-dependent Holling-Tanner Predator-prey Model with Nonlinear Prey Harvesting

3.1 Introduction

In the previous chapter Leslie-Gower predator-prey model has been studied with nonlinear harvesting (in predator and prey independently). In chapter 1, it has been mentioned that Holling type II functional response is more realistic. A Leslie-Gower predator-prey model with Holling type II functional response is known as Holling-Tanner predator-prey model (Model 1.5.7) and was first proposed in May (1973). This model has been studied by many researchers, for example, Hsu and Hwang (1995); Gasull et al. (1997); Hsu and Hwang (1998); Hsu and Hwang (1999); Saez and Olvares (1999); Braza (2003), etc., which are discussed in brief in subsection (1.5.4). This model has been used by many researchers to study a number of real world problems. For example; Caughley (1976) used it to model the biological control of the prickly-pear cactus by the moth Cactoblastis cactorum, Wollkind

This chapter is based on the research article: Qualitative analysis and optimum harvesting of a ratio-dependent Holling-Tanner predator-prey model with nonlinear prey harvesting, Communicated.

and Logan (1978) and Wollkind et al. (1988) used it to model the predator-prey mite outbreak interactions on fruit trees in Washington State.

The ratio-dependent functional response is proposed by Arditi and Ginzburg (1989). Although it has been criticized many researchers, for example, Abrams (1994) and Sarnelle and Wilson (2008), but recent field and laboratory experiments (Arditi et al. 1991; Arditi and Ginzburg 1991; Berezovskaya et al. 2001; Arditi and Ginzburg 2012) shows that it is more appropriate for predator-prey interactions, when the predators involve serious hunting processes.

Xiao and Jennings (2005) studied the dynamical properties of a ratio-dependent predator-prey model with nonzero constant prey harvesting, and obtained rich dynamics compared to the model with no harvesting. Kar et al. (2006) studied a ratio-dependent predator-prey model in the presence of linear harvesting in both the prey and predator species with same effort but different catchability coefficients. Xiao and Cao (2009) studied the dynamics of ratio-dependent predator-prey model with linear harvesting rate and showed the existence of hopf bifurcation by taking the harvesting parameter as bifurcation parameter. Further, they did complete analysis of possible topological structures in a neighborhood of the origin, as well as asymptotics to orbits tending to this point. Lenzini and Rebaza (2010) studied the dynamics of a ratio-dependent predator-prey model with nonconstant harvesting in prey and predator respectively and showed the existence of several bifurcations and connecting orbits. The dynamics and bifurcations of a class of ratio-dependent predator-prey models with constant rate prey harvesting and intraspecies competition has been investigated by Chen et al. (2011). Christopher et al. (2015) studied the local stability of ratio-dependent predator-prey models with nonconstant predator harvesting in which they generalized and improved some known results.

A Holling-Tanner predator-prey model with ratio-dependent functional response was studied by Liang and Pan (2007), they also derived the sufficient condition for the global stability of the unique positive interior equilibrium point of the model by constructing Lyapunov function. Saha and Chakrabarti (2009) studied a delayed ratio-dependent Holling-Tanner predator-prey model and used blow up transformation to study the qualitative behaviour of the origin.

In this chapter, a Holling-Tanner predator-prey model with ratio-dependent functional response and nonlinear prey harvesting has been studied. The ratio-dependent model always has complex dynamics in the vicinity of the origin and its nature has been studied by using a blow up transformation technique. It is also shown that the system exhibit several bifurcations, periodic solutions and homoclinic orbits under certain parametric conditions.

3.2 Model Equations

Consider Holling-Tanner predator-prey model (1.5.7) with ratio-dependent functional response and nonlinear prey harvesting

$$\begin{cases} \frac{dX}{dT} = r\Big(1-\frac{X}{K}\Big)X - \frac{mXY}{AX+Y} - \frac{qEX}{m_1E+m_2X}, \\ \frac{dY}{dT} = s(1-\frac{Y}{bX})Y, \quad \text{if} \quad (X,Y) \neq (0,0) \\ \frac{dX}{dT} = \frac{dY}{dT} = 0, \quad \text{if} \quad (X,Y) = (0,0), \end{cases} \tag{3.2.1}$$

with the initial conditions $X(0) > 0, Y(0) > 0$, where $X(T)$ and $Y(T)$ denote the density of prey and predator at time T, respectively. The parameters r, K, m, A, s, b, q and E are positive constants and represent intrinsic growth rate of prey, carrying capacity of prey in the absence of predator, maximal predator per capita consumption rate, number of prey necessary to achieve one half of the maximum rate m, intrinsic growth rate of predator, measure of food quality that the prey provides towards the predators, catchability coefficient and effort applied to harvest individuals and m_1, m_2 are suitable positive constants.

On introducing the dimensionless variables: $x = \frac{X}{K}, \quad y = \frac{YA}{K}, \quad t = rT$, in system (3.2.1), it will become

$$\begin{cases} \frac{dx}{dt} = x(1-x) - \frac{\alpha xy}{x+y} - \frac{hx}{c+x} \equiv xf_1(x,y), \\ \frac{dy}{dt} = \rho(\beta - \frac{y}{x})y \equiv yf_2(x,y), \quad \text{if} \quad (x,y) \neq (0,0), \\ \frac{dx}{dt} = \frac{dy}{dt} = 0, \quad \text{if} \quad (x,y) = (0,0), \end{cases} \tag{3.2.2}$$

with the initial conditions: $x(0) > 0, y(0) > 0$, where $\alpha = \frac{m}{rA}$, $\beta = Ab$, $h = \frac{qE}{rKm_2}$, $C = \frac{m_1E}{m_2K}$, $\rho = \frac{s}{Abr}$. The set $\mathbb{R}^2_+ = \{(x,y) \in \mathbb{R}^2 : x, y \geq 0\}$ represents the closed first quadrant. In the

following, it is demonstrated that the system (3.2.2) is "well behaved" in $\mathbb{R}^2_+$.

Proposition 3.2.1. *a) There exists a unique continuous solution of the system* (3.2.2) *in the interior of* $\mathbb{R}^2_+$.

b) The set $\mathbb{R}^2_+$ *is invariant for the system* (3.2.2).

c) The nonnegative solutions $\Big(x(t), y(t)\Big)$ *of the system* (3.2.2) *are bounded for all* $t \geq 0$.

d) The system (3.2.2) *is permanent, whenever the condition* $\alpha + \frac{h}{c} < 1$ *holds.*

Proof.

a) Let

$$F(x,y) = \begin{cases} x\Big(1 - x - \frac{\alpha y}{x+y} - \frac{h}{c+x}\Big), & (x,y) \neq (0,0), \\ 0, & (x,y) = (0,0), \end{cases}$$

and

$$G(x,y) = \begin{cases} \rho(\beta - \frac{y}{x})y, & (x,y) \neq (0,0), \\ 0, & (x,y) = (0,0), \end{cases}$$

then, the system (3.2.2) reduces to

$$\frac{dx}{dt} = F(x,y), \qquad \frac{dy}{dt} = G(x,y).$$

It is easy to observe that the functions $F(x,y)$ and $G(x,y)$ are continuous and satisfies the Lipschitz condition in R^2_+. The existence and uniqueness theorem confirms that there exists a unique solution for the system (3.2.2) through any point $(x(0), y(0))$ of $\mathbb{R}^2_+$, which is well defined and is continuous for all $t \geq 0$.

b) The integration of the system (3.2.2) yields

$$x(t) = x(0) \exp\left(\int_0^t f_1(x(s), y(s))ds\right), \tag{3.2.3}$$

$$y(t) = y(0) \exp\left(\int_0^t f_2(x(s), y(s))ds\right), \tag{3.2.4}$$

Eq. (3.2.3) and Eq. (3.2.4) with initial conditions of system (3.2.2) confirms that $x(t) > 0, y(t) > 0$. Moreover, $x(t) = 0$ for $t > 0$, whenever $x(0) = 0$, and so, the y-axis $\{(x,y) :$

$x(t) = 0, y(t) \geq 0\}$ is positively invariant. Similarly, the x-axis $\{(x, y) : y(t) = 0, x(t) \geq 0\}$ is positively invariant. Hence the result.

c) The first equation of the system (3.2.2) with condition (*b*) implies

$$\frac{dx}{dt} \leq x(1 - x). \tag{3.2.5}$$

The inequality (3.2.5) implies

$$x(t) \leq \frac{1}{1 + C_0 e^{-t}}, \tag{3.2.6}$$

where $C_0 = \frac{1-x(0)}{x(0)}$. Now, consider the following two cases

Case *I* If $x(0) \leq 1$, then $C_0 \geq 0$. It is evident from Eq. (3.2.6) that $x(t) \leq 1$ for all $t \geq 0$.

Case *II* If $x(0) > 1$, then $C_0 < 0$, hence Eq. (3.2.6) leads to $x(t) \geq 1$. From Eq.(3.2.5), one gets $\frac{dx}{dt} \leq 0$. This implies that $x(t)$ is monotonic decreasing. Hence, $\max_{t\geq 0}\{x(t)\} = x(0)$. The above said cases yields: $x(t) \leq \max\{x(0), 1\} \equiv M_1$.

The second equation of the system (3.2.2) with the boundedness of $x(t)$ leads to

$$\frac{dy}{dt} \leq \rho y\Big(\beta - \frac{y}{M_1}\Big). \tag{3.2.7}$$

Similar computation gives

$$y(t) \leq \max\{y(0), \beta M_1\} \equiv M_2. \tag{3.2.8}$$

d) From first equation of the system (3.2.2), one gets

$$\frac{dx}{dt} \geq x\Big(1 - \alpha - \frac{h}{c} - x\Big). \tag{3.2.9}$$

If x_0 is the root of the equation $1 - \alpha - \frac{h}{c} - x = 0$, then by standard comparison argument one gets $\liminf_{t\to\infty} x(t) \geq x_0$. Hence, $x(t) \geq x_0$ for large t.

Further, from the second equation of the system (3.2.2), one gets

$$\frac{dy}{dt} \geq \rho y\Big(\beta - \frac{y}{x_0}\Big). \tag{3.2.10}$$

If y_0 is the root of the equation $\beta - \frac{y}{x_0} = 0$, one can obtain $\liminf_{t\to\infty} y(t) \geq y_0$. It is to be noticed that $x_0 > 0$ whenever $\alpha + \frac{h}{c} < 1$.

inequality (3.2.6) implies

$$\limsup_{t\to\infty} x(t) \leq 1.$$

Similarly,

$$\limsup_{t\to\infty} y(t) \leq M_1\beta.$$

Hence result. ■

3.3 Equilibria and their Stability

The equilibrium points of the system (3.2.2) are the nonnegative real solutions of zero growth isoclines of the system, that is, the nonnegative real solutions of the following system.

$$xf_1(x, y) = 0, \tag{3.3.1}$$

$$yf_2(x, y) = 0, \tag{3.3.2}$$

where Eq. (3.3.1) is the prey zero growth isocline and Eq. (3.3.2) is the predator zero growth isocline of the system. The following three types of equilibrium points for the system (3.2.2) exist.

(*a*) *Trivial equilibrium point:* The trivial equilibrium point of the system (3.2.2) is $E_0 = (0, 0)$.

(*b*) *Axial equilibrium points:* The axial equilibrium points of the system (3.2.2) are only the points of intersection of the curves $y = 0$ and $f_1(x, y) = 0$. Abscissa of these points are the roots of the quadratic equation:

$$x^2 - (1 - c)x + h - c = 0. \tag{3.3.3}$$

The quadratic equation (3.3.3) has two distinct positive roots

$x_k = \frac{1-c+(-1)^k\sqrt{(1-c)^2-4(h-c)}}{2},\ k = 1, 2.$ if $c < 1, c < h < \left(\frac{1+c}{2}\right)^2$; one positive root x_2 if $h < c$; a double positive root $x_3 = \frac{1-c}{2}$ if $c < 1, h = (\frac{1+c}{2})^2$, and a positive root $x_4 = 1 - c$, if $h = c < 1$.

(c) *Interior equilibrium points:* The interior equilibrium points of the system (3.2.2) are the intersection points of the curves $f_1(x, y) = 0$ and $f_2(x, y) = 0$ and the abscissa are given by the solution of the quadratic equation

$$(1+\beta)x^2 - (1-c+\beta-c\beta-\alpha\beta)x + h - c + h\beta - c\beta + \alpha\beta c = 0, \tag{3.3.4}$$

while the ordinance is given by $y_k^* = \beta x_k^*,\quad k = 1, 2.$

The quadratic equation (3.3.4) has two distinct positive roots

$$x_k^* = \frac{1}{2(1+\beta)}\Big(1-c+\beta-c\beta-\alpha\beta+(-1)^k \sqrt{(1-c+\beta-c\beta-\alpha\beta)^2 - 4(1+\beta)(h-c+h\beta-c\beta+\alpha\beta c)}\Big),\quad k = 1, 2$$

if $c < 1 - \frac{\alpha\beta}{1+\beta}, \frac{c(1+\beta-\alpha\beta)}{1+\beta} < h < \frac{1}{4}\left(1+c-\frac{\alpha\beta}{1+\beta}\right)^2$; one positive root x_2^*, if $h < \frac{c(1+\beta-\alpha\beta)}{1+\beta}$; a double root $\overline{x} = \frac{1-c+\beta-c\beta-\alpha\beta}{2(1+\beta)}$, if $c < 1 - \frac{\alpha\beta}{1+\beta}, h = \frac{1}{4}\left(1+c-\frac{\alpha\beta}{1+\beta}\right)^2$ and a positive root $x^* = \frac{1-c+\beta-c\beta-\alpha\beta}{1+\beta}$, if $c < 1 - \frac{\alpha\beta}{1+\beta}, h = \frac{c(1+\beta-\alpha\beta)}{1+\beta}$.

On summarizing the above discussion, the number and location of equilibrium points of system (3.2.2) can be described as

Lemma 3.3.1. *The origin $E_0 = (0, 0)$ is always an equilibrium point. If $c \geq 1$, then the system* (3.2.2) *has*

(a) *no equilibrium point, if $h > c$.*

(b) *one axial equilibrium point $E_2 = (x_2, 0)$ and one positive interior equilibrium point $E_2^* = (x_2^*, y_2^*)$, if $0 < h < \frac{c(1+\beta-\alpha\beta)}{1+\beta}$.*

Lemma 3.3.2. *Let $\frac{1+\beta-\alpha\beta}{1+\beta} < c < 1$, then the system* (3.2.2) *has*

(a) no equilibrium point, if $h > \left(\frac{1+c}{2}\right)^2$.

(b) only one equilibrium point $E_3 = (x_3, 0)$, *if* $h = \left(\frac{1+c}{2}\right)^2$.

(c) two equilibrium points $E_1 = (x_1, 0)$ *and* $E_2 = (x_2, 0)$, *if* $c < h < \left(\frac{1+c}{2}\right)^2$.

(d) only one equilibrium point $E_4 = (x_4, 0)$, *if* $h = c$.

(e) only one equilibrium point $E_2 = (x_2, 0)$, *if* $\frac{c(1+\beta-\alpha\beta)}{1+\beta} \leq h < c$.

(f) one axial equilibrium point $E_2 = (x_2, 0)$ *and one positive interior equilibrium point* $E_2^* = (x_2^*, y_2^*)$, *if* $0 < h < \frac{c(1+\beta-\alpha\beta)}{1+\beta}$.

Lemma 3.3.3. *Let* $c < \frac{1+\beta-\alpha\beta}{1+\beta}$, *then the system* (3.2.2) *has*

(a) no equilibrium point, if $h > \left(\frac{1+c}{2}\right)^2$.

(b) only one equilibrium point $E_3 = (x_3, 0)$, *if* $h = \left(\frac{1+c}{2}\right)^2$.

(c) two equilibrium point $E_1 = (x_1, 0)$ *and* $E_2 = (x_2, 0)$, *if* $c < h < \left(\frac{1+c}{2}\right)^2$.

(d) one equilibrium point $E_4 = (x_4, 0)$, *if* $h = c$

(e) one equilibrium point $E_2 = (x_2, 0)$, *if* $\frac{1}{4}\left(1 + c - \frac{\alpha\beta}{1+\beta}\right)^2 \leq h < c$.

(f) three equilibrium points $E_1 = (x_1, 0), E_2 = (x_2, 0)$ *and* $\overline{E} = (\overline{x}, \overline{y})$, *if* $h = \frac{1}{4}\left(1 + c - \frac{\alpha\beta}{1+\beta}\right)^2 > c$.

(g) four equilibrium points $E_1 = (x_1, 0), E_2 = (x_2, 0), E_1^* = (x_1^*, y_1^*)$ *and* $E_2^* = (x_2^*, y_2^*)$, *if* $c < h < \frac{1}{4}\left(1 + c - \frac{\alpha\beta}{1+\beta}\right)^2$.

(h) three equilibrium points $E_4 = (x_4, 0), E_1^* = (x_1^*, y_1^*)$ *and* $E_2^* = (x_2^*, y_2^*)$, *if* $h = c < \frac{1}{4}\left(1 + c - \frac{\alpha\beta}{1+\beta}\right)^2$.

(i) three equilibrium points $E_2 = (x_2, 0), E_1^* = (x_1^*, y_1^*)$ *and* $E_2^* = (x_2^*, y_2^*)$, *if* $\frac{c(1+\beta-\alpha\beta)}{1+\beta} < h < c$.

(j) two equilibrium points $E_2 = (x_2, 0)$ *and* $E* = (x^*, y^*)$, *if* $h = \frac{c(1+\beta-\alpha\beta)}{1+\beta}$.

(k) two equilibrium points $E_2 = (x_2, 0)$ *and* $E_2^* = (x_2^*, y_2^*)$, *if* $0 < h < \frac{c(1+\beta-\alpha\beta)}{1+\beta}$.

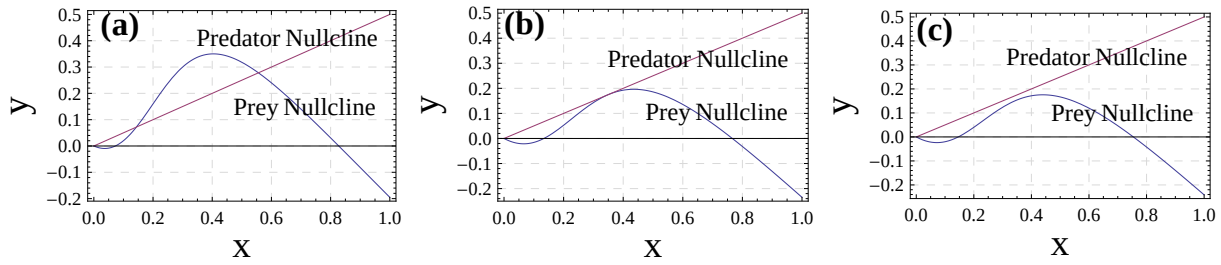

Figure 3.1: These diagrams shows the number of interior equilibrium points of the system (3.2.2), when the parameter h varies through critical value $h^{[SN]}$ and all other parameters are fixed. $\alpha = 0.6, \quad \beta = 0.5, \quad c = 0.1, \quad \rho = 0.6 \quad (a)h = 0.16 \quad (b)h = 0.2025 \quad (c)h = 0.21.$

The number of equilibrium points can be shown graphically, for each case. The possible number of equilibrium points are depicted in Figure 3.1(a) for Lemma (3.3.3)(g), Figure 3.1(b) for Lemma (3.3.3)(f) and Figure 3.1(c) for Lemma (3.3.3)(c).

Next, the dynamics of system (3.2.2) in the neighborhood of each feasible equilibria has been analyzed.

Trivial Equilibrium Point

Since functions f_1 and f_2 are not differentiable at the origin, so, the system (3.2.2) cannot be studied by using linearization technique. To study the system we use blow up transformation: $x = x, \; y = vx$ (Jost et al. 1999), which reduces the system (3.2.2) to

$$\begin{cases} \frac{dx}{dt} = x\left(1 - x - \frac{\alpha v}{1+v} - \frac{h}{c+x}\right), \\ \frac{dv}{dt} = v\left(\rho(\beta - v) - 1 + x + \frac{\alpha v}{1+v} + \frac{h}{c+x}\right). \end{cases} \tag{3.3.5}$$

The above system have either two or three equilibrium points at positive v-axis namely- $E_{00} = (0, 0)$, $E_{01} = (0, v_1)$ and $E_{02} = (0, v_2)$, where v_1 and $v_2 \;\; (0 \leq v_1 < v_2)$ are two distinct real roots of the following quadratic equation

$$c\rho v^2 + (c - h + c\rho - c\alpha - c\rho\beta)v + (c - h - c\rho\beta) = 0, \tag{3.3.6}$$

that is, $v_k = \frac{-\zeta + (-1)^k \Delta}{2c\rho}, k = 1, 2$, where $\zeta = c - h + c\rho - c\alpha - c\rho\beta, \;\; \Delta^2 = (c - h + c\rho - c\alpha - c\rho\beta)^2 - 4c\rho(c - h - c\rho\beta)$.

The Jacobian matrix of the system (3.3.5) at the equilibrium point E_{00} is

$$J_{E_{00}} = \begin{bmatrix} \frac{c-h}{c} & 0 \\ 0 & \frac{-c+h+c\rho\beta}{c} \end{bmatrix},$$

and at the equilibrium points $E_{0k} = (0, v_k), k = 1, 2$ are

$$J_{E_{0k}} = \begin{bmatrix} \rho\Big(\beta - v_k\Big) & 0 \\ v_k\Big(1 - \frac{h}{c^2}\Big) & v_k\Big(\frac{\alpha}{(1+v_k)^2} - \rho\Big) \end{bmatrix}.$$

There are only three possibilities

1) If $c - h - c\rho\beta < 0$, then the system (3.3.5) has two equilibrium points; $E_{00} = (0, 0)$ and $E_{02} = (0, v_2)$, where $v_2 = \frac{-\zeta+\Delta}{2c\rho}$ on the positive v-axis. The eigenvalues of the Jacobian matrix $J_{E_{00}}$ are $\lambda_1 = \frac{c-h}{c}$ and $\lambda_2 = \frac{-c+h+c\rho\beta}{c} > 0$. Thus, the equilibrium point E_{00} is an unstable node for $c > h$ and is a saddle point for $c < h$.

   The eigenvalues of the Jacobian matrix of the system (3.3.5) at the equilibrium point $E_{02} = (0, v_2)$ are $\lambda_1 = \rho(\beta - v_2) = \frac{2c\rho\beta+\zeta-\Delta}{2c}$ and $\lambda_2 = v_2\Big(\frac{\alpha}{(1+v_2)^2} - \rho\Big)$. From the quadratic equation (3.3.6), $\sqrt{\frac{\alpha}{\rho}} - 1 < v_2$, and so, $\lambda_2 < 0$. Thus, the equilibrium point E_{02} is a saddle point for $2c\rho\beta + \zeta - \Delta > 0$ and a stable point for $2c\rho\beta + \zeta - \Delta < 0$. Hence, by inverse blow up transformation the trivial equilibrium point E_0 of the system (3.2.2) is asymptotically stable, if $2c\rho\beta + \zeta - \Delta < 0$.

2) If $c - h - c\rho\beta > 0$, then the system (3.3.5) has three equilibrium points; $E_{00} = (0, 0)$, $E_{01} = (0, v_1)$ and $E_{02} = (0, v_2)$ on the positive v-axis provided $\zeta < 0$ and $\Delta^2 > 0$, where $v_1 = \frac{-\zeta-\Delta}{2c\rho}$ and $v_2 = \frac{-\zeta+\Delta}{2c\rho}$. The eigenvalues of the Jacobian matrix $J_{E_{00}}$ are $\lambda_1 = \frac{c-h}{c}$ and $\lambda_2 = \frac{-c+h+c\rho\beta}{c} < 0$. Thus, the equilibrium point E_{00} is a saddle point, if $c > h$.

   The eigenvalues of the Jacobian matrix of the system (3.3.5) at the equilibrium point $E_{01} = (0, v_1)$ are $\lambda_1 = \rho(\beta - v_1) = \frac{2c\rho\beta+\zeta+\Delta}{2c}$ and $\lambda_2 = v_1\Big(\frac{\alpha}{(1+v_1)^2} - \rho\Big)$. From the quadratic equation (3.3.6), $0 < v_1 < \sqrt{\frac{\alpha}{\rho}} - 1$, and so, $\lambda_2 > 0$. This shows that the equilibrium point E_{01} of the system (3.3.5) is a saddle point, if $2c\rho\beta + \zeta + \Delta < 0$ and

an unstable node, if $2c\rho\beta + \zeta + \Delta > 0$.

The eigenvalues of the Jacobian matrix of the system (3.3.5) at the equilibrium point $E_{02} = (0, v_2)$ are $\lambda_1 = \frac{2c\rho\beta+\zeta-\Delta}{2c}$ and $\lambda_2 = v_2\Big(\frac{\alpha}{(1+v_1)^2} - \rho\Big)$. From quadratic equation (3.3.6), $0 < \sqrt{\frac{\alpha}{\rho}} - 1 < v_{02}$, and so, $\lambda_2 < 0$. This shows that the equilibrium point E_{02} of the system (3.3.5) is a saddle point, if $2c\rho\beta+\zeta-\Delta > 0$ and asymptotically stable, if $2c\rho\beta + \zeta - \Delta < 0$. Hence by inverse blow up transformation the trivial equilibrium point E_0 of the system (3.2.2) is asymptotically stable, if $2c\rho\beta+\zeta-\Delta < 0$.

3) If $c-h-c\rho\beta = 0$, then the system (3.3.5) has two equilibrium points $E_{00} = (0, 0)$ and $E_{03} = (0, v_3)$ on the positive v-axis, where $v_3 = \frac{\alpha-\rho}{\rho}$. The eigenvalues of the Jacobian matrix of the system (3.3.5) at the equilibrium point E_{00} are $\lambda_1 = \rho\beta$ and $\lambda_2 = 0$. So, linearization technique fails and the technique given in Zhang et al. (1991) can be applied. Using the condition $c - h - c\rho\beta = 0$, the system (3.3.5) reduces to

$$\begin{cases} \frac{dx}{dt} = x + P_2(x, v), \\ \frac{dv}{dt} = Q_2(x, v), \end{cases} \tag{3.3.7}$$

where

$$P_2(x, v) = \frac{1}{\rho\beta}\Big(\Big(-1 + \frac{h}{c^2}x^2\Big)x^2 - \alpha v x + \cdots\Big)$$

and

$$Q_2(x, v) = \frac{1}{\rho\beta}\Big(\Big(\alpha - \rho\Big)v^2 + (1 - \frac{h}{c^2})vx\Big).$$

The equation $x + P_2(x, v) = 0$ implies

$$x(v) = 0, \qquad \psi = \frac{\alpha - \rho}{\rho\beta}v^2 + [v]_3,$$

which implies that $m = 2$ and $a_m = \frac{\alpha-\rho}{\rho\beta} > 0$ as $\alpha > \rho$. Hence, the trivial equilibrium point E_{00} is a saddle-node, and the parabolic sector is on the right half-plane.

The eigenvalues of the Jacobian matrix of the system (3.3.5) at the equilibrium point E_{03} are $\lambda_1 = \rho\beta - \alpha + \rho$ and $\lambda_2 = v_3\Big(\frac{\alpha}{(1+v_2)^2} - \rho\Big) = \frac{(\alpha-\rho)(\rho-\alpha)}{\rho}$, and so, $\lambda_2 < 0$. This shows that the equilibrium point E_{03} of the system (3.3.5) is a saddle point, if

$\rho\beta-\alpha+\rho > 0$ and is asymptotically stable, if $\rho\beta-\alpha+\rho < 0$. By using inverse blow up transformation the trivial equilibrium point E_0 of the system (3.2.2) is asymptotically stable, if $\rho\beta - \alpha + \rho < 0$.

The previous discussion can be summarized as follows.

Theorem 3.3.4. *The trivial equilibrium point $E_0 = (0, 0)$ of the system (3.2.2) is locally asymptotically stable, if any one of the following conditions is satisfied*

a) $c - h - c\rho\beta < 0$, *and* $2c\rho\beta + \zeta - \Delta < 0$. *(Figure 3.2(a))*

b) $c - h - c\rho\beta > 0, \zeta < 0, \Delta > 0$ *and* $2c\rho\beta + \zeta - \Delta < 0$. *(Figure 3.2(b))*

c) $c - h - c\rho\beta = 0$ *and* $\rho\beta - \alpha + \rho < 0$. *(Figure 3.2(c))*

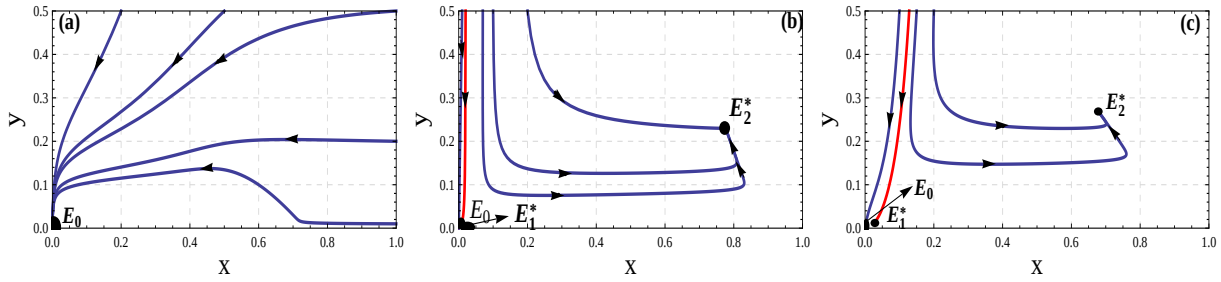

Figure 3.2: The phase portrait diagram of the system (3.2.2). (a) $\alpha = 0.6$, $\beta = 0.3$, $h = 0.2$, $c = 0.02$, $\rho = 0.2$ satisfies the conditions of the theorem 3.3.4 (a). It shows that E_0 is globally stable. (b) $\alpha = 0.4$, $\beta = 0.3$, $h = 0.12$, $\rho = 0.2$, $c = 0.13$ satisfies the conditions of the theorem 3.3.4 (b).The equilibrium points E_0 and E_2^* are locally asymptotically stable points. (c) $\alpha = 0.7$, $\beta = 0.4$, $c = 0.1$, $\rho = 0.1$, $h = 0.096$ satisfies the conditions of the theorem 3.3.4 (c). It shows that E_0 and E_2^* are locally asymptotically stable. The red trajectory is a separatrix.

Axial Equilibrium Points

The Jacobian matrix of the system (3.2.2) at the axial equilibrium point E_1 is

$$J_{E_1} = \begin{bmatrix} \frac{x_1}{c+x_1}\sqrt{(1-c)^2 - 4(h-c)} & -\alpha \\ 0 & \rho\beta \end{bmatrix},$$

which confirms that the axial equilibrium point E_1 is an unstable point.

The Jacobian matrix of the system (3.2.2) at the axial equilibrium point E_2 is

$$J_{E_2} = \begin{bmatrix} -\frac{x_2}{c+x_2}\sqrt{(1-c)^2 - 4(h-c)} & -\alpha \\ 0 & \rho\beta \end{bmatrix},$$

which confirms that the axial equilibrium point E_2 is a saddle point.

The Jacobian matrix of the system (3.2.2) at the axial equilibrium point E_3 is

$$J_{E_3} = \begin{bmatrix} 0 & -\alpha \\ 0 & \rho\beta \end{bmatrix},$$

which confirms that the axial equilibrium point E_3 is a saddle point.

The Jacobian matrix of the system (3.2.2) at the axial equilibrium point E_4 is

$$J_{E_4} = \begin{bmatrix} -(1-c) & -\alpha \\ 0 & \rho\beta \end{bmatrix},$$

which confirms that the axial equilibrium point E_4 is an unstable hyperbolic saddle.

From the above discussion, it can be concluded that

Theorem 3.3.5. *If the axial equilibrium points E_1, E_2, E_3 and E_4 exist, then E_1 is an unstable point, E_2 is a saddle point, E_3 is a saddle-node and E_4 is an unstable hyperbolic saddle.*

Interior Equilibrium Points

The Jacobian matrix of the system (3.2.2) at the equilibrium point E_1^* is $J_{E_1^*} = \begin{bmatrix} x_1^*\Big(-1+\frac{h}{(c+x_1^*)^2}\Big)+\frac{\alpha\beta}{(1+\beta)^2} & \frac{-\alpha}{(1+\beta)^2} \\ \rho\beta^2 & -\rho\beta \end{bmatrix}$.

The determinant of the Jacobian matrix $J_{E_1^*}$ is $\det(J_{E_1^*}) = \rho\beta x_1^*(1-\frac{h}{(c+x_1^*)^2}) = -\frac{\rho\beta x_1^*}{(1+\beta)(c+x_1^*)}\sqrt{(1-c+\beta-c\beta-\alpha\beta)^2-4(1+\beta)(h-c+h\beta-c\beta+c\alpha\beta)} < 0$, which confirm that the equilibrium point E_1^* is an unstable hyperbolic saddle.

The Jacobian matrix of the system (3.2.2) at the equilibrium point E_2^* is

$$J_{E_2^*} = \begin{bmatrix} x_2^*\Big(-1+\frac{h}{(c+x_2^*)^2}\Big)+\frac{\alpha\beta}{(1+\beta)^2} & \frac{-\alpha}{(1+\beta)^2} \\ \rho\beta^2 & -\rho\beta \end{bmatrix}.$$

The determinant of the Jacobian matrix $J_{E_2^*}$ is $\det(J_{E_2^*}) = \rho\beta x_2^*(1-\frac{h}{(c+x_2^*)^2}) = \frac{\rho\beta x_2^*}{(1+\beta)(c+x_2^*)}\sqrt{(1-c+\beta-c\beta-\alpha\beta)^2-4(1+\beta)(h-c+h\beta-c\beta+c\alpha\beta)} > 0$, and the trace of $J_{E_2^*}$ is $tr(J_{E_2^*}) = x_2^*\Big(-1+\frac{h}{(c+x_2^*)^2}\Big)+\frac{\alpha\beta}{(1+\beta)^2}-\rho\beta$.

The Jacobian matrix of the system (3.2.2) at the equilibrium point E^* is $J_{E^*} = \begin{bmatrix} x^*\Big(-1+\frac{h}{(c+x^*)^2}\Big)+\frac{\alpha\beta}{(1+\beta)^2} & \frac{-\alpha}{(1+\beta)^2} \\ \rho\beta^2 & -\rho\beta \end{bmatrix}$.

The determinant of the Jacobian matrix J_{E^*} is $\det(J_{E^*}) = \rho\beta x^*(1-\frac{h}{(c+x^*)^2}) = \frac{\rho\beta x^*}{(1+\beta)(c+x^*)}\sqrt{(1-c+\beta-c\beta-\alpha\beta)^2-4(1+\beta)(h-c+h\beta-c\beta+c\alpha\beta)} > 0$, and the trace

of the Jacobian matrix J_{E*} is $tr(J_{E^*}) = x^*\Big(-1+\frac{h}{(c+x^*)^2}\Big)+\frac{\alpha\beta}{(1+\beta)^2}-\rho\beta$.

On summarizing the above discussion, it can be concluded that

Theorem 3.3.6. *a) The interior equilibrium point E_1^* of the system (3.2.2), if exists, is always a saddle point. The interior equilibrium point E_2^* of the system (3.2.2), if exists, is asymptotically stable point if $x_2^*\Big(-1+\frac{h}{(c+x_2^*)^2}\Big)+\frac{\alpha\beta}{(1+\beta)^2}-\rho\beta<0$, is an unstable hyperbolic node, if $x_2^*\Big(-1+\frac{h}{(c+x_2^*)^2}\Big)+\frac{\alpha\beta}{(1+\beta)^2}-\rho\beta>0$ and is a weak focus or a center, if $x_2^*\Big(-1+\frac{h}{(c+x_2^*)^2}\Big)+\frac{\alpha\beta}{(1+\beta)^2}-\rho\beta=0$.*

b) The interior equilibrium point E^* of the system (3.2.2), if exists, is asymptotically stable point if $x^*(-1+\frac{h}{(c+x^*)^2})+\frac{\alpha\beta}{(1+\beta)^2}-\rho\beta<0$, is weak focus or center, if $x^*(-1+\frac{h}{(c+x^*)^2})+\frac{\alpha\beta}{(1+\beta)^2}-\rho\beta=0$ and is an unstable hyperbolic saddle node, if $x^*(-1+\frac{h}{(c+x^*)^2})+\frac{\alpha\beta}{(1+\beta)^2}-\rho\beta>0$.

The Jacobian matrix of the system (3.2.2) at the equilibrium point $\overline{E}$ is $J_{\overline{E}}=\begin{bmatrix}\overline{x}\Big(-1+\frac{h}{(c+\overline{x})^2}\Big)+\frac{\alpha\beta}{(1+\beta)^2} & \frac{-\alpha}{(1+\beta)^2}\\ \rho\beta^2 & -\rho\beta\end{bmatrix}$.

The determinant of $J_{\overline{E}}=0$. Thus, $\overline{E}$ is a degenerate singularity.

Theorem 3.3.7. *If $\overline{E}$ exists, it is a saddle-node, if $\rho\neq\frac{\alpha}{(1+\beta)^2}$ and is a cusp of codimension 2, if $\rho=\frac{\alpha}{(1+\beta)^2}$.*

Proof. Shift the equilibrium point $\overline{E}$ of the system (3.2.2) to the origin by using the transformation $\hat{x}=x-\overline{x},\hat{y}=y-\overline{y}$ and then by Taylor's series expansion, the system (3.2.2) can be rewritten as (denote $\hat{x}$ as x and $\hat{y}$ as y,)

$$\begin{cases}\frac{dx}{dt}=\frac{\alpha\beta}{(1+\beta)^2}x-\frac{\alpha}{(1+\beta)^2}y+\xi_1x^2+\xi_2xy+\xi_3y^2+o^3(x,y),\\ \frac{dy}{dt}=\rho\beta^2x-\rho\beta y-\frac{\rho\beta^2}{\overline{x}}x^2+\frac{2\rho\beta}{\overline{x}}xy-\frac{\rho}{\overline{x}}y^2+o^3(x,y),\end{cases}\tag{3.3.8}$$

where $\xi_1=-1+\frac{ch}{(c+\overline{x})^3}+\frac{\alpha\beta^2}{\overline{x}(1+\beta)^3},\xi_2=-\frac{2\alpha\beta}{\overline{x}(1+\beta)^3},\xi_3=\frac{\alpha}{\overline{x}(1+\beta)^3}$.

If $\rho\neq\frac{\alpha}{(1+\beta)^2}$, trace of the matrix $J_{\overline{E}}$ is nonzero while the determinant is zero. Hence $\overline{E}$ is a saddle-node.

If $\rho=\frac{\alpha}{(1+\beta)^2}$, trace and determinant both of the matrix $J_{\overline{E}}$ are zero, i.e., both

eigenvalues of the matrix $J_{\overline{E}}$ are zero. The system (3.3.8) can be written as

$$\begin{cases} \frac{dx}{dt} = \frac{\alpha\beta}{(1+\beta)^2}x - \frac{\alpha}{(1+\beta)^2}y + \xi_1 x^2 + \xi_2 xy + \xi_3 y^2 + o^3(x,y), \\ \frac{dy}{dt} = \frac{\alpha\beta^2}{(1+\beta)^2}x - \frac{\alpha\beta}{(1+\beta)^2}y - \frac{\alpha\beta^2}{\overline{x}(1+\beta)^2}x^2 + \frac{2\alpha\beta}{\overline{x}(1+\beta)^2}xy - \frac{\alpha}{\overline{x}(1+\beta)^2}y^2 + o^3(x,y). \end{cases} \tag{3.3.9}$$

Let $T = \frac{\alpha\beta}{(1+\beta)^2}t$, then the system (3.3.9) reduces to the following system (after transformation T is taken as t)

$$\begin{cases} \frac{dx}{dt} = x - \frac{1}{\beta}y + \overline{\xi_1}x^2 + \overline{\xi_2}xy + \overline{\xi_3}y^2 + o^3(x,y), \\ \frac{dy}{dt} = \beta x - y - \frac{\beta}{\overline{x}}x^2 + \frac{2}{\overline{x}}xy - \frac{1}{\overline{x}\beta}y^2 + o^3(x,y), \end{cases} \tag{3.3.10}$$

where $\overline{\xi_1} = \frac{(1+\beta)^2}{\alpha\beta}\big(-1 + \frac{ch}{(c+\overline{x})^3} + \frac{\alpha\beta^2}{\overline{x}(1+\beta)^3}\big), \overline{\xi_2} = -\frac{2}{\overline{x}(1+\beta)}, \overline{\xi_3} = \frac{1}{\beta(1+\beta)\overline{x}}$.

On using the transformation $x_0 = x, y_0 = x - \frac{1}{\beta}y$, the system (3.3.10) reduces to the following system

$$\begin{cases} \frac{dx_0}{dt} = y_0 + \hat{\xi_1}x_0^2 + \hat{\xi_3}y_0^2 + o^3(x,y), \\ \frac{dy_0}{dt} = \hat{\xi_1}x_0^2 + (\hat{\xi_3} + \frac{1}{\overline{x}})y_0^2 + o^3(x,y), \end{cases} \tag{3.3.11}$$

where $\hat{\xi_1} = -\frac{\overline{x}(1+\beta)^2}{\alpha\beta(c+\overline{x})}, \hat{\xi_3} = \frac{\beta}{(1+\beta)\overline{x}}$

On using the transformation $x_1 = x_0, y_1 = y_0 + \hat{\xi_3}y_0^2$, the system (3.3.11) reduces to

$$\begin{cases} \frac{dx_1}{dt} = y_1 + \hat{\xi_1}x_1^2 + o^3(x,y), \\ \frac{dy_1}{dt} = \hat{\xi_1}x_1^2 + (\hat{\xi_3} + \frac{1}{\overline{x}})y_1^2 + o^3(x,y). \end{cases} \tag{3.3.12}$$

On using the transformation $x_2 = x_1, y_2 = y_1 - (\hat{\xi_3} + \frac{1}{\overline{x}})x_1y_1$, the system (3.3.12) reduces to

$$\begin{cases} \frac{dx_2}{dt} = y_2 + \hat{\xi_1}x_2^2 + (\hat{\xi_3} + \frac{1}{\overline{x}})x_2y_2 + o^3(x,y), \\ \frac{dy_2}{dt} = \hat{\xi_1}x_2^2 + o^3(x,y). \end{cases} \tag{3.3.13}$$

Finally, on using the transformation $X = x_2 - \frac{1}{2}(\hat{\xi_3} + \frac{1}{\overline{x}})x_2^2, Y = y_2 + \hat{\xi_1}x_2^2 + o^3(x,y)$, the system (3.3.13) reduces to

$$\begin{cases} \frac{dX}{dt} = Y \\ \frac{dY}{dt} = \hat{\xi_1}x_2^2 + 2\hat{\xi_1}XY + o^3(X,Y). \end{cases} \tag{3.3.14}$$

Since $\hat{\xi_1} \neq 0$, therefore the system (3.3.14) confirms that origin in XY plane, that is, $\overline{E}$ in xy-plane is a cusp of codimension 2. ■

3.4 Bifurcation Analysis

In this section, bifurcations that take place in system (3.2.2) has been investigated.

3.4.1 Hopf Bifurcation

In Theorem 3.3.6(a), it is proved that if both interior equilibrium points E_1^* and E_2^* of the system (3.2.2) exist, then E_1^* is always a saddle point, while E_2^* is a weak focus or a center provided $x_2^*\Big(-1+\frac{h}{(c+x_2^*)^2}\Big)+\frac{\alpha\beta}{(1+\beta)^2}-\rho\beta=0$. Now, it is shown that system (3.2.2) undergoes to a Hopf bifurcation.

If ρ is considered as a bifurcation parameter, then the threshold magnitude is $\rho=\rho^{[hf]}=\frac{x_2^*}{\beta}\Big(-1+\frac{h}{(c+x_2^*)^2}\Big)+\frac{\alpha}{(1+\beta)^2}$. At $\rho=\rho^{[hf]}$
$a)$ $\det(J_{E_2^*})>0$; $b)$ $tr(J_{E_2^*})=0$; and $c)$ $\Big[\frac{\partial}{\partial\rho}(TrJ_{E_2^*})\Big]=-\beta\neq 0$ (transversality condition). This guaranties the existence of Hopf bifurcation, that is, a limit cycle exists around the interior equilibrium point $E_2^*(x_2^*,y_2^*)$.

Next, stability of limit cycle is discussed by computing the first Lyapunov number σ at interior equilibrium point $E_2^*(x_2^*,y_2^*)$ of the system (3.2.2) using the procedure as given in Perko (1996). Using the transformation $x=u-x_2^*,\ y=v-y_2^*$, the system (3.2.2), in the vicinity of origin, can be written as

$$\frac{du}{dt}=a_{10}u+a_{01}v+a_{20}u^2+a_{11}uv+a_{02}v^2+a_{30}u^3+a_{21}u^2v+a_{12}uv^2+a_{03}v^3+P(u,v),$$
$$\frac{dv}{dt}=b_{10}u+b_{01}v+b_{20}u^2+b_{11}uv+b_{02}v^2+b_{30}u^3+b_{21}u^2v+b_{12}uv^2+b_{03}v^3+Q(u,v),$$

where $a_{10}=x_2^*\Big(-1+\frac{h}{(c+x_2^*)^2}\Big)+\frac{\alpha\beta}{(1+\beta)^2}$, $a_{01}=-\frac{\alpha}{(1+\beta)^2}$, $a_{20}=-1+\frac{hc}{(c+x_2^*)^3}+\frac{\alpha\beta^2}{(1+\beta)^3x_2^*}$, $a_{11}=-\frac{2\alpha\beta}{(1+\beta)^3x_2^*}$, $a_{02}=\frac{\alpha}{(1+\beta)^3x_2^*}$, $a_{30}=-\frac{\alpha\beta^2}{(1+\beta)^4x_2^{*2}}-\frac{hc}{(c+x_2^*)^4}$, $a_{21}=\frac{2\alpha\beta-\alpha\beta^2}{(1+\beta)^4x_2^{*2}}$, $a_{12}=\frac{2\alpha\beta-\alpha}{(1+\beta)^4x_2^{*2}}$, $a_{03}=-\frac{\alpha}{(1+\beta)^4x_2^{*2}}$, $b_{10}=\rho\beta^2$, $b_{01}=-\rho\beta$, $b_{20}=-\frac{\rho\beta^2}{x_2^*}$, $b_{11}=\frac{2\rho\beta}{x_2^*}$, $b_{02}=-\frac{\rho}{x_2^*}$, $b_{30}=\frac{\rho\beta^2}{x_2^{*2}}$, $b_{21}=-\frac{2\rho\beta}{x_2^{*2}}$, $b_{12}=\frac{\rho}{x_2^{*2}}$, $b_{03}=0$, $P(u,v)=\sum_{i+j=4}^{\infty}a_{ij}u^iv^j$ and $Q(u,v)=\sum_{i+j=4}^{\infty}b_{ij}u^iv^j$.

Hence, first Lyapunov number σ can be computed by the formula defined in equation (1.3.7), where

$$\Delta = \frac{\rho\beta x_1^*}{(1+\beta)(c+x_1^*)}\sqrt{(1-c+\beta-c\beta-\alpha\beta)^2-4(1+\beta)(h-c+h\beta-c\beta+c\alpha\beta)}.$$

Theorem 3.4.1. *The system* (3.2.2) *undergoes a hopf bifurcation at the point* E_2^*, *whenever* $x_2^*\Big(-1+\frac{h}{(c+x_2^*)^2}\Big)+\frac{\alpha\beta}{(1+\beta)^2}-\rho\beta=0$ *and an unstable (stable) limit cycle arises around the equilibrium point* E_2^* *as* $\sigma>0(\sigma<0)$.

3.4.2 Saddle-node Bifurcation

It is clear from Lemma 3.3.2 that the system (3.2.2) has (a) two axial equilibrium points E_1 and E_2, if $\frac{1+\beta-\alpha\beta}{1+\beta}<c<1$ and $h<\Big(\frac{1+c}{2}\Big)^2$; (b) two axial equilibrium points coincide with a unique axial equilibrium point E_3, if $h=\Big(\frac{1+c}{2}\Big)^2$; (c) no axial equilibrium point, if $h>\Big(\frac{1+c}{2}\Big)^2$. Thus, the number of axial equilibrium points varies from 2 to 0 as the harvesting parameter h varies, therefore

$$SN_1=\Big\{(\alpha,\beta,c,h,\rho):\frac{1+\beta-\alpha\beta}{1+\beta}<c<1, h=\Big(\frac{1+c}{2}\Big)^2\Big\}$$

be a Saddle-node bifurcation surface. In Theorem 3.3.7, it is proved that, if $\overline{E}$ exists, it is a saddle-node, when $\rho\neq\frac{\alpha}{(1+\beta)^2}$. In Lemma 3.3.3, it has been shown that the system (3.2.2) has two interior equilibrium point E_1^* and E_2^*, whenever $c<\frac{1+\beta-\alpha\beta}{1+\beta}$ and $c\leq h<\frac{1}{4}\Big(1+c-\frac{\alpha\beta}{1+\beta}\Big)^2$ hold. These two interior equilibrium points coincide to a unique instantaneous interior equilibrium point $\overline{E}=(\overline{x},\overline{y})$ with $\overline{x}=\frac{1-c+\beta-c\beta-\alpha\beta}{2}, \overline{y}=\beta\overline{x}$, whenever $c<h=\frac{1}{4}\Big(1+c-\frac{\alpha\beta}{1+\beta}\Big)^2$ (this value of h is known as critical harvesting rate and written as $h^{[SN]}$) and no interior equilibrium point exists, whenever $h>\frac{1}{4}\Big(1+c-\frac{\alpha\beta}{1+\beta}\Big)^2$. Thus, the number of interior equilibrium points varies from 2 to 0 as the harvesting parameter h passes to the critical value $h^{[SN]}$ from left to right, therefore

$$SN_2=\Big\{(\alpha,\beta,c,h,\rho):c<\frac{1+\beta-\alpha\beta}{1+\beta}, c<h=\frac{1}{4}\Big(1+c-\frac{\alpha\beta}{1+\beta}\Big)^2, \rho\neq\frac{\alpha}{(1+\beta)^2}\Big\}$$

be another Saddle-node bifurcation surface.

Theorem 3.4.2. *The system* (3.2.2) *undergoes a Saddle-node bifurcation with respect to the bifurcation parameter h around the equilibrium point $\overline{E} = (\overline{x}, \overline{y})$, if $c < \frac{1+\beta-\alpha\beta}{1+\beta}, c < h = \frac{1}{4}\left(1 + c - \frac{\alpha\beta}{1+\beta}\right)^2, \rho > \frac{\alpha}{(1+\beta)^2}$.*

Proof. The Jacobian matrix of the system (3.2.2) at the equilibrium point $\overline{E}(\overline{x}, \overline{y})$ is $J_{\overline{E}} = DG(\overline{x}, \overline{y}) = \begin{bmatrix} \frac{\alpha\beta}{(1+\beta)^2} & -\frac{\alpha}{(1+\beta)^2} \\ \rho\beta^2 & -\rho\beta \end{bmatrix}$,
where $G(x, y, h) = (g_1, g_2)^T$, $g_1 = xf_1(x, y)$ and $g_2 = yf_2(x, y)$, and f_1, f_2 are defined in Eq. (3.2.2). The determinant of $J_{\overline{E}}$ is zero and trace is $\frac{\alpha\beta}{(1+\beta)^2} - \rho\beta < 0$ as $\rho > \frac{\alpha}{(1+\beta)^2}$, and so, one of the eigenvalues is zero and other has negative real part. Let V and W be the eigenvectors corresponding to zero eigenvalue for $J_{\overline{E}}$ and the transpose $(J_{\overline{E}})^T$, respectively. A simple computation yields $V = \begin{bmatrix} 1 \\ \beta \end{bmatrix}$ and $W = \begin{bmatrix} 1 \\ -\frac{\alpha}{\rho\beta(1+\beta)^2} \end{bmatrix}$.
Now

$$G_h(\overline{x}, \overline{y}, h^{[SN]}) = \begin{bmatrix} -\frac{\overline{x}}{c+\overline{x}} \\ 0 \end{bmatrix},$$

and

$$D^2G_h(\overline{x}, \overline{y}, h^{[SN]})(V, V) = \begin{bmatrix} -2 + \frac{2\alpha\beta}{(1+\beta)^2\overline{x}} - \frac{2\alpha\beta}{(1+\beta)^3\overline{x}} + \frac{2h}{(c+\overline{x})^2} - \frac{2h\overline{x}}{(c+\overline{x})^3} - \frac{2\alpha\beta^2}{(1+\beta)^3\overline{x}} \\ 0 \end{bmatrix}.$$

Noticed that $\frac{h}{(c+\overline{x})^2} = 1$, Therefore

$$W^T.G_h(\overline{x}, \overline{x}, h^{[SN]}) = -\frac{\overline{x}}{c+\overline{x}} \neq 0,$$

and

$$W^T.D^2G(\overline{x}, \overline{x}, h^{[SN]})(V, V) = -2(1 - \frac{hc}{(c+\overline{x})^3}) = -\frac{2\overline{x}}{c+\overline{x}} \neq 0.$$

■

3.4.3 Bogdanov-Takens bifurcation

In Theorem 3.3.7, it is shown that if $\overline{E}$ exists, then it is a cusp of codimension 2, whenever $\rho = \frac{\alpha}{(1+\beta)^2}$. Therefore, codimension 2 bifurcation (Bogdanov-Takens bifurcation of codimension 2) may occur for the system (3.2.2). Below the normal form of the Bogdanov-Takens bifurcation has been derived by using a series of nontrivial transformations Xiao and Ruan (1999).

Theorem 3.4.3. *The system* (3.2.2) *undergoes a Bogdanov-Takens bifurcation with respect to the bifurcation parameters h and ρ around the equilibrium point $\overline{E} = (\overline{x}, \overline{y})$, whenever $c < \frac{1+\beta-\alpha\beta}{1+\beta}, c < h = \frac{1}{4}\Big(1 + c - \frac{\alpha\beta}{1+\beta}\Big)^2, \rho = \frac{\alpha}{(1+\beta)^2}$. Also in the small neighbourhood of the point $\overline{E}$, the system* (3.2.2) *is topologically equivalent to the following model*

$$\begin{cases} \frac{dZ_1}{dt} = Z_2, \\ \frac{dZ_2}{dt} = \mu_1(\lambda_1, \lambda_2) + \mu_2(\lambda_1, \lambda_2)Z_2 + Z_1^2 + Z_1 Z_2. \end{cases} \tag{3.4.1}$$

Moreover, the following bifurcation curves divides the bifurcation plane into four regions.

Saddle-node curve: $SN = \{(\lambda_1, \lambda_2) : \mu_1(\lambda_1, \lambda_2) = 0\}$,

Hopf bifurcation curve:

$H = \{(\lambda_1, \lambda_2) : \mu_2(\lambda_1, \lambda_2) = \frac{\gamma_{11}}{\sqrt{\gamma_{20}}}\sqrt{-\mu_1(\lambda_1, \lambda_2)}, \mu_2(\lambda_1, \lambda_2) < 0\}$,

Homoclinic bifurcation curve:

$HL = \{(\lambda_1, \lambda_2) : \mu_2(\lambda_1, \lambda_2) = \frac{5\gamma_{11}}{7\sqrt{\gamma_{20}}}\sqrt{-\mu_1(\lambda_1, \lambda_2)}, \mu_2(\lambda_1, \lambda_2) < 0\}$.

Proof. Let the parameters h and ρ vary in a small neighbourhood of Bogdanov-Taken point (BT point) (h_0, ρ_0), where h_0 and ρ_0 are the threshold magnitude of bifurcation parameters h and ρ respectively such that $\det(J_{\overline{E}})|_{(h_0,\rho_0)} = 0$ and $tr(J_{\overline{E}})|_{(h_0,\rho_0)} = 0$. Also suppose $(h_0 + \lambda_1, \rho_0 + \lambda_2)$ be a point of a neighbourhood of the BT point (h_0, ρ_0) where λ_1, λ_2 are small. Thus, the system (3.2.2) reduces to

$$\begin{cases} \frac{dx}{dt} = x(1-x) - \frac{\alpha xy}{x+y} - \frac{h_0 x}{c+x} - \frac{\lambda_1 x}{c+x}, \\ \frac{dy}{dt} = (\rho_0 + \lambda_2)(\beta - \frac{y}{x})y. \end{cases} \tag{3.4.2}$$

Noticed that the system (3.4.2) is C^∞ smooth with respect to the variables x, y in a small

neighbourhood of (h_0, ρ_0).

By using the transformation: $x_1 = x - \overline{x}, x_2 = y - \overline{y}$, system (3.4.2) reduces to

$$\begin{cases} \dfrac{dx_1}{dt} = a_{00}(\lambda) + a_{10}(\lambda)x_1 + a(\lambda)x_1 + b(\lambda)x_2 + \dfrac{1}{2}p_{20}(\lambda)x_1^2 + p_{11}(\lambda)x_1x_2 + \\ \qquad \dfrac{1}{2}p_{02}(\lambda)x_2^2 + R_1(x_1, x_2), \\ \dfrac{dx_2}{dt} = b_{00}(\lambda) + b_{10}(\lambda)x_1 + b_{01}(\lambda)x_2 + \dfrac{1}{2}q_{20}(\lambda)x_1^2 + q_{11}(\lambda)x_1x_2 + \\ \qquad \dfrac{1}{2}q_{02}(\lambda)x_2^2 + R_2(x_1, x_2), \end{cases} \tag{3.4.3}$$

where $a_{00}(\lambda) = -\frac{\lambda_1\overline{x}}{c+\overline{x}}$, $a_{10}(\lambda) = -\frac{\lambda_1 c}{(c+\overline{x})^2}$, $a(\lambda) = \frac{\alpha\beta}{(1+\beta)^2}$, $b(\lambda) = -\frac{\alpha}{(1+\beta)^2}$, $p_{20}(\lambda) = \frac{2\alpha\beta^2}{(1+\beta)^3\overline{x}} + \frac{2\lambda_1 c}{(c+\overline{x})^3} - \frac{2\overline{x}}{c+\overline{x}}$, $p_{11}(\lambda) = -\frac{2\alpha\beta}{(1+\beta)^3\overline{x}}$, $p_{02}(\lambda) = \frac{2\alpha}{(1+\beta)^3\overline{x}}$, $b_{00}(\lambda) = 0$, $b_{10}(\lambda) = \beta^2(\rho + \lambda_2)$, $b_{01}(\lambda) = -\beta(\rho + \lambda_2)$, $q_{20}(\lambda) = -\frac{2(\rho+\lambda_2)\overline{y}^2}{\overline{x}^3}$, $q_{11}(\lambda) = \frac{2(\rho+\lambda_2)\overline{y}}{\overline{x}^2}$, $q_{02}(\lambda) = -\frac{2(\rho+\lambda_2)}{\overline{x}}$, and R_1, R_2 are the power series in (x_1, x_2) with powers $x_1^i x_2^j$ satisfying $i + j \geq 3$.

Now, on introducing the affine transformation $y_1 = x_1,\ y_2 = ax_1 + bx_2$ in the system (3.4.3), it will become

$$\begin{cases} \frac{dy_1}{dt} = \alpha_{00}(\lambda) + \alpha_{10}(\lambda)y_1 + y_2 + \frac{1}{2}\alpha_{20}(\lambda)y_1^2 + \frac{1}{2}\alpha_{02}(\lambda)y_2^2 + \overline{R}_1(y_1, y_2), \\ \frac{dy_2}{dt} = \beta_{00}(\lambda) + \beta_{10}(\lambda)y_1 + \beta_{01}(\lambda)y_2 + \frac{1}{2}\beta_{20}(\lambda)y_1^2 + \frac{1}{2}\beta_{02}(\lambda)y_2^2 + \overline{R}_2(y_1, y_2), \end{cases} \tag{3.4.4}$$

where $\alpha_{00}(\lambda) = -\frac{\lambda_1\overline{x}}{c+\overline{x}}$, $\alpha_{10}(\lambda) = \frac{\alpha\beta}{(1+\beta)^2}$, $\alpha_{20}(\lambda) = \frac{2\lambda_1 c}{(c+\overline{x})^3} - \frac{2\overline{x}}{c+\overline{x}}$, $\alpha_{02}(\lambda) = \frac{2(1+\beta)}{\alpha\overline{x}}$, $\beta_{00}(\lambda) = -\frac{a\lambda_1\overline{x}}{c+\overline{x}}$, $\beta_{10}(\lambda) = \frac{\alpha^2\beta^2}{(1+\beta)^4}$, $\beta_{01}(\lambda) = \frac{\alpha\beta}{(1+\beta)^2} - \beta(\rho + \lambda_2)$, $\beta_{20}(\lambda) = \frac{2\alpha\beta}{(1+\beta)^2(c+\overline{x})}\left(\frac{\lambda_1 c}{(c+\overline{x})^2} - \overline{x}\right)$, $\beta_{02}(\lambda) = -\frac{2}{b\overline{x}}\left(\rho + \lambda_2 + \frac{\alpha\beta}{(1+\beta)^3}\right)$, and $\overline{R_1}, \overline{R_2}$ are the power series in (y_1, y_2) with powers $y_1^i y_2^j$ satisfying $i + j \geq 3$.

Consider the C^∞ change of coordinates in the small neighbourhood of $(0, 0)$: $z_1 = y_1 - \frac{1}{2}\beta_{02}y_1^2,\ z_2 = y_2 + \frac{1}{2}\alpha_{20}y_1^2 + \frac{1}{2}\alpha_{02}y_2^2$, which transformed the system (3.4.4) into

$$\begin{cases} \dfrac{dz_1}{dt} = r_{00}(\lambda) + r_{10}(\lambda)z_1 + z_2 + r_{20}(\lambda)z_1^2 + r_{11}(\lambda)z_1z_2 + \overline{\overline{R_1}}(z_1, z_2), \\ \dfrac{dz_2}{dt} = s_{00}(\lambda) + s_{10}(\lambda)z_1 + s_{01}(\lambda)z_2 + s_{20}(\lambda)z_1^2 + s_{11}(\lambda)z_1z_2 + \\ \qquad s_{02}(\lambda)z_2^2 + \overline{\overline{R_2}}(z_1, z_2), \end{cases} \tag{3.4.5}$$

where $r_{00} = \alpha_{00}$, $r_{10} = \alpha_{10} - \alpha_{00}\beta_{02}$, $r_{20} = -\frac{1}{2}\beta_{02}(\beta_{02}\alpha_{00} + \alpha_{10})$, $r_{11} = -\beta_{02}$, $s_{00} =$

β_{00}, $s_{10} = \beta_{10} + \alpha_{00}\alpha_{20}$, $s_{01} = \beta_{01} + \alpha_{02}\beta_{00}$, $s_{20} = \frac{1}{2}(\beta_{02}\beta_{10} + \alpha_{00}\alpha_{20}\beta_{02} - \alpha_{20}\beta_{01} - \alpha_{20}\beta_{00}\alpha_{02} + \beta_{20} + 2\alpha_{10}\alpha_{20})$, $s_{11} = \alpha_{20} + \alpha_{02}\beta_{10}$, $s_{02} = \frac{1}{2}(\beta_{02} + \alpha_{02}\beta_{01} - \alpha_{02}^2\beta_{00})$ and $\overline{\overline{R_1}}$, $\overline{\overline{R_2}}$ are the power series in (z_1, z_2) with powers $z_1^i z_2^j$ satisfying $i + j \geq 3$.

Next, consider C^∞ change of coordinates in the small neighbourhood of $(0, 0)$: $u_1 = z_1 - \frac{1}{2}(r_{11} + s_{02})z_1^2$, $u_2 = z_2 + r_{20}z_1^2 - s_{02}z_1z_2$. Then, the system (3.4.5) reduces to

$$\begin{cases} \frac{du_1}{dt} = \xi_{00} + \xi_{10}u_1 + u_2 + \xi_{20}u_1^2 + \hat{R}_1(u_1, u_2), \\ \frac{du_2}{dt} = \eta_{00} + \eta_{10}u_1 + \eta_{01}u_2 + \eta_{20}u_1^2 + \eta_{11}u_1u_2 + \hat{R}_2(u_1, u_2), \end{cases} \tag{3.4.6}$$

where $\xi_{00} = r_{00}$, $\xi_{10} = r_{10} - r_{00}(r_{11} + s_{02})$, $\xi_{20} = \frac{1}{2}(r_{11} + s_{02})(r_{10} - r_{00}(r_{11} + s_{02})) - r_{10}(r_{11} + s_{02})$, $\eta_{00} = s_{00}$, $\eta_{10} = s_{10} + 2r_{20}r_{00} - s_{02}s_{00}$, $\eta_{01} = s_{01} - s_{02}r_{00}$, $\eta_{20} = \frac{1}{2}(r_{11} + s_{02})(s_{10} + 2r_{20}r_{00} - s_{02}s_{00}) - r_{20}(s_{01} - s_{02}r_{00}) + (s_{20} + 2r_{20}r_{10} - s_{02}s_{10})$, $\eta_{11} = s_{11} + 2r_{20} - s_{01}s_{02} - s_{02}r_{10} + s_{02}(s_{01} - s_{02}r_{00})$, and $\hat{R}_1$, $\hat{R}_2$ are the power series in (u_1, u_2) with powers $u_1^i u_2^j$ satisfying $i + j \geq 3$.

Again, consider C^∞ change of coordinates in the small neighbourhood of $(0, 0)$: $v_1 = u_1$, $v_2 = \xi_{00} + \xi_{10}u_1 + u_2 + \xi_{20}u_1^2$, which transformed the system (3.4.6) into

$$\begin{cases} \frac{dv_1}{dt} = v_2 + s_1(v_1, v_2), \\ \frac{dv_2}{dt} = \gamma_{00} + \gamma_{10}v_1 + \gamma_{01}v_2 + \gamma_{20}v_1^2 + \gamma_{11}v_1v_2 + s_2(v_1, v_2), \end{cases} \tag{3.4.7}$$

where $\gamma_{00} = \eta_{00} - \eta_{01}\xi_{00}$, $\gamma_{10} = \eta_{10} - \eta_{01}\xi_{10} - \xi_{00}\eta_{11}$, $\gamma_{01} = \xi_{10} + \eta_{01}$, $\gamma_{20} = \eta_{20} - \eta_{01}\xi_{20} - \xi_{10}\eta_{11}$, $\gamma_{11} = \eta_{11} + 2\xi_{20}$ and $s_1(v_1, v_2), s_2(v_1, v_2)$ are the power series in (v_1, v_2) with powers $v_1^i v_2^j$ satisfying $i + j \geq 3$.

Next, consider C^∞ change of coordinates in the small neighbourhood of $(0, 0)$: $w_1 = v_1$, $w_2 = v_2 + s_1(v_1, v_2)$, which transformed the system (3.4.7) into

$$\begin{cases} \frac{dw_1}{dt} = w_2, \\ \frac{dw_2}{dt} = \gamma_{00} + \gamma_{10}w_1 + \gamma_{01}w_2 + \gamma_{20}w_1^2 + \gamma_{11}w_1w_2 + F_1(w_1) + \\ \qquad w_2F_2(w_1) + w_2^2F_3(w_1, w_2), \end{cases} \tag{3.4.8}$$

where F_1, F_2 and F_3 are the power series in w_1 and (w_1, w_2) with powers $w_1^{k_1}, w_1^{k_2}$ and $w_1^i w_2^j$

satisfying $k_1 \geq 3, k_2 \geq 2$ and $i + j \geq 1$, respectively.

It is cumbersome to obtain the sign of $\gamma_{20}(0)$ analytically. Consider $\alpha = 0.9, \quad \beta = 0.5, \quad \rho = 0.4, \quad h = 0.16, \quad c = 0.1$. It is easy to verify that for these parameter values system (3.2.2) has a unique interior equilibrium point which is a cusp of codimension 2. Also

$\gamma_{00} = (-0.15\lambda_1 + 1.75\lambda_1^2 + 5.20833\lambda_1^3) + (-0.375\lambda_1 + 3.125\lambda_1^2)\lambda_2$, $\gamma_{10} = (0.04 - 18.0556\lambda_1^2 - 34.7222\lambda_1^3) + (0.1 + 0.833333\lambda_1 - 59.0278\lambda_1^2 - 86.8056\lambda_1^3)\lambda_2 + (2.08333\lambda_1 - 52.0833\lambda_1^2)\lambda_2^2$, $\gamma_{01} = (0.2 + 5\lambda_1 + 13.8889\lambda_1^2) + (-0.5 + 8.33333\lambda_1)\lambda_2$, $\gamma_{20} = (-0.15 - 3.4375\lambda_1 + 294.271\lambda_1^2 - 769.596\lambda_1^3 + 160.751\lambda_1^4 + -669.796\lambda_1^5) + (-0.486111 + 4.36921\lambda_1 + 1552.13\lambda_1^2 - 2780.99\lambda_1^3 + 803.755\lambda_1^4)\lambda_2 + (-0.277778 + 76.3889\lambda_1 + 2883.87\lambda_1^2 - 2652.39\lambda_1^3)\lambda_2^2 + (109.954\lambda_1 + 1880.79\lambda_1^2)\lambda_2^3$, $\gamma_{11} = (-2.83333 + 88.3102\lambda_1 - 123.457\lambda_1^2 + 128.601\lambda_1^3) + (-2.22222 + 370.37\lambda_1 - 308.642\lambda_1^2)\lambda_2 + 393.519\lambda_1\lambda_1^2$.

Therefore, $\gamma_{20}(0) = -0.15 < 0$. To make it positive, consider $Z_1 = -w_1, \ Z_2 = w_2, \ T = -t$. The system (3.4.8) reduces to

$$\begin{cases} \dfrac{dZ_1}{dT} = Z_2, \\ \dfrac{dZ_2}{dT} = -\gamma_{00} + \gamma_{10}Z_1 - \gamma_{20}Z_1^2 + R_1(Z_1) - \gamma_{01}Z_2 + \gamma_{11}Z_1Z_2 + Z_2R_2(Z_1) + \\ \qquad Z_2^2R_3(Z_1, Z_2), \end{cases} \tag{3.4.9}$$

where R_1, R_2 and R_3 are the power series in Z_1 and (Z_1, Z_2) with powers $Z_1^{k_1}, Z_1^{k_2}$ and $Z_1^iZ_2^j$ satisfying $k_1 \geq 3, k_2 \geq 2$ and $i + j \geq 1$, respectively.

Applying the Malgrange preparation theorem, one gets

$$-\gamma_{00} + \gamma_{10}Z_1 - \gamma_{20}Z_1^2 + R_1(w_1) = \Big(Z_1^2 - \frac{\gamma_{10}}{\gamma_{20}}Z_1 + \frac{\gamma_{00}}{\gamma_{20}}\Big)B_1(w_1, \lambda)$$

where $B_1(0, \lambda) = -\gamma_{20}$ and B_1 is a power series of Z_1 whose coefficients depend on parameters (λ_1, λ_2).

Let $X_1 = Z_1,\ X_2 = \frac{Z_2}{\sqrt{-\gamma_{20}}}$, and $d\tau = \sqrt{-\gamma_{20}}dT$, the system (3.4.9) reduces to

$$\begin{cases} \frac{dX_1}{d\tau} = X_2, \\ \frac{dX_2}{d\tau} = \frac{\gamma_{00}}{\gamma_{20}} - \frac{\gamma_{10}}{\gamma_{20}}X_1 - \frac{\gamma_{01}}{\sqrt{-\gamma_{20}}}X_2 + X_1^2 + \frac{\gamma_{11}}{\sqrt{-\gamma_{20}}}X_1X_2 + \overline{S}(X_1, X_2, \lambda), \end{cases} \tag{3.4.10}$$

where $\overline{S}(X_1, X_2, 0)$ is a power series in (X_1, X_2) with powers $X_1^i X_2^j$ satisfying $i+j \geq 3$ with $j \geq 2$.

Applying the parameter dependent affine transformation $Y_1 = X_1 - \frac{\gamma_{10}}{2\gamma_{20}},\ Y_2 = X_2$ in the system (3.4.10) and using Taylor series expansion, it will beome

$$\begin{cases} \frac{dY_1}{d\tau} = Y_2, \\ \frac{dY_2}{d\tau} = \mu_1(\lambda_1, \lambda_2) + \mu_2(\lambda_1, \lambda_2)Y_2 + Y_1^2 - 7.31564Y_1Y_2 + \overline{\overline{S}}(Y_1, Y_2, \mu), \end{cases} \tag{3.4.11}$$

where $\mu_1(\lambda_1, \lambda_2) = \frac{\gamma_{00}}{\gamma_{20}} - \frac{\gamma_{10}^2}{4\gamma_{20}^2}, \quad \mu_2(\lambda_1, \lambda_2) = -\frac{\gamma_{01}}{\sqrt{-\gamma_{20}}} + \frac{\gamma_{11}\gamma_{00}}{2(-\gamma_{20})^{\frac{3}{2}}}$ and $\overline{\overline{S}}(X_1, X_2, 0)$ is a power series in (Y_1, Y_2) with powers $Y_1^i Y_2^j$ satisfying $i + j \geq 3$ with $j \geq 2$.

System (3.4.11) is strongly topologically equivalent to the normal form of the Bogdanov-Takens bifurcation as given below

$$\begin{cases} \frac{dZ_1}{dt} = Z_2, \\ \frac{dZ_2}{dt} = \mu_1(\lambda_1, \lambda_2) + \mu_2(\lambda_1, \lambda_2)Z_2 + Z_1^2 + Z_1Z_2. \end{cases} \tag{3.4.12}$$

The determinant of the matrix $\begin{bmatrix} \frac{\partial \mu_1}{\partial \lambda_1} & \frac{\partial \mu_1}{\partial \lambda_2} \\ \frac{\partial \mu_2}{\partial \lambda_1} & \frac{\partial \mu_2}{\partial \lambda_2} \end{bmatrix} = 2.0757$. Thus, the system (3.2.2) undergoes to Bogdanov-Takens bifurcation. There exists bifurcation curves which divide the bifurcation plane into four regions (Perko 1996). The local representations of the bifurcation curves in the $\lambda_1\lambda_2$ plane are

$SN = \{(\lambda_1, \lambda_2) : \mu_1(\lambda_1, \lambda_2) = 0\}$,

$H = \{(\lambda_1, \lambda_2) : \mu_2(\lambda_1, \lambda_2) = -7.31564\sqrt{-\mu_1(\lambda_1, \lambda_2)}, \mu_2(\lambda_1, \lambda_2) < 0\}$

$HL = \{(\lambda_1, \lambda_2) : \mu_2(\lambda_1, \lambda_2) = -5.22546\sqrt{-\mu_1(\lambda_1, \lambda_2)}, \mu_2(\lambda_1, \lambda_2) < 0\}$. ■

These bifurcation curves has been depicted in the Figure 3.3(a) and the possible phase portrait diagrams in the small neighbourhood of the interior equilibrium point $\overline{E}$ are shown

in Figures 3.3(b),(c),(d),(e),(f).

3.5 Numerical Simulations

(1) If $\alpha = 0.9,\ \beta = 0.7,\ h = 0.1,\ c = 0.01$, the system (3.2.2) has two interior equilibrium points $E_1^*(x_1^*, y_1^*) = (0.2627, 0.1839), E_2^*(x_2^*, y_2^*) = (0.3567, 0.2497)$. The threshold value of ρ is $\rho^{[hf]} = 0.1807$ and the first Lyapunov number $\sigma = 656.371\pi > 0$. Hence, an unstable limit cycle is created around E_2^* and the other equilibrium point E_1^* is a saddle point (Figure 3.4(a)). If $\rho = 0.2 > \rho^{[hf]}$, the equilibrium point E_2^* is a stable point and the equilibrium point E_1^* is a saddle point (Figure 3.4(b)). If $\rho = 0.15 < \rho^{[hf]}$, the equilibrium point E_2^* is an unstable point and the equilibrium point E_1^* is a saddle-point (Figure 3.4(c)). If $\rho = 0.2117091$, the limit cycle collide with the saddle point E_1^*, and hence, a Homoclinic loop is created around E_2^*, this cyclic loop is unstable because of $\sigma = 480.543\pi > 0$ (Figure 3.4(d)). Thus interior equilibrium point $E_2^*(x_2^*, y_2^*)$ losses its stability as the bifurcation parameter ρ passes through the threshold value $\rho^{[hf]}$ from right to left.

(2) If $\alpha = 0.6,\ \beta = 0.5,\ \rho = 0.6,\ c = 0.1$, one can obtain $h = h^{[SN]} = 0.202499$. If $h = 0.16 < h^{[SN]}$, there exit two interior equilibrium points in which one is a saddle point, while the other is a stable (Figure 3.1(a) and 3.5(a)). If $h = 0.202499$, then these two interior equilibrium points coincide to each other and a unique instantaneous equilibrium point is obtained, which is stable from right side of the separatrix and unstable from left side of the separatix, (Figure 3.1(b) and 3.5(b)). Figures 3.5(c) and 3.5(d) are the saddle-node bifurcation diagram. When $h = 0.21$, then no interior equilibrium point exists (Figure 3.1(a)).

(3) If $\alpha = 0.7,\ \beta = 0.6,\ c = 0.5, h = 0.36875$, then the system (3.2.2) has a unique interior equilibrium point $E^*(x^*, y^*) = (0.2375, 0.1425)$, and the threshold value of ρ is $\rho^{[hf]} = 0.145966$. Thus, a stable limit cycle is created around the equilibrium point E^* (Figure 3.6(a)) as the first Lyapunov number is $\sigma = -236.907\pi < 0$. If $\rho = 0.2$, the unique equilibrium point E^* is a stable point (Figure 3.6(b)).

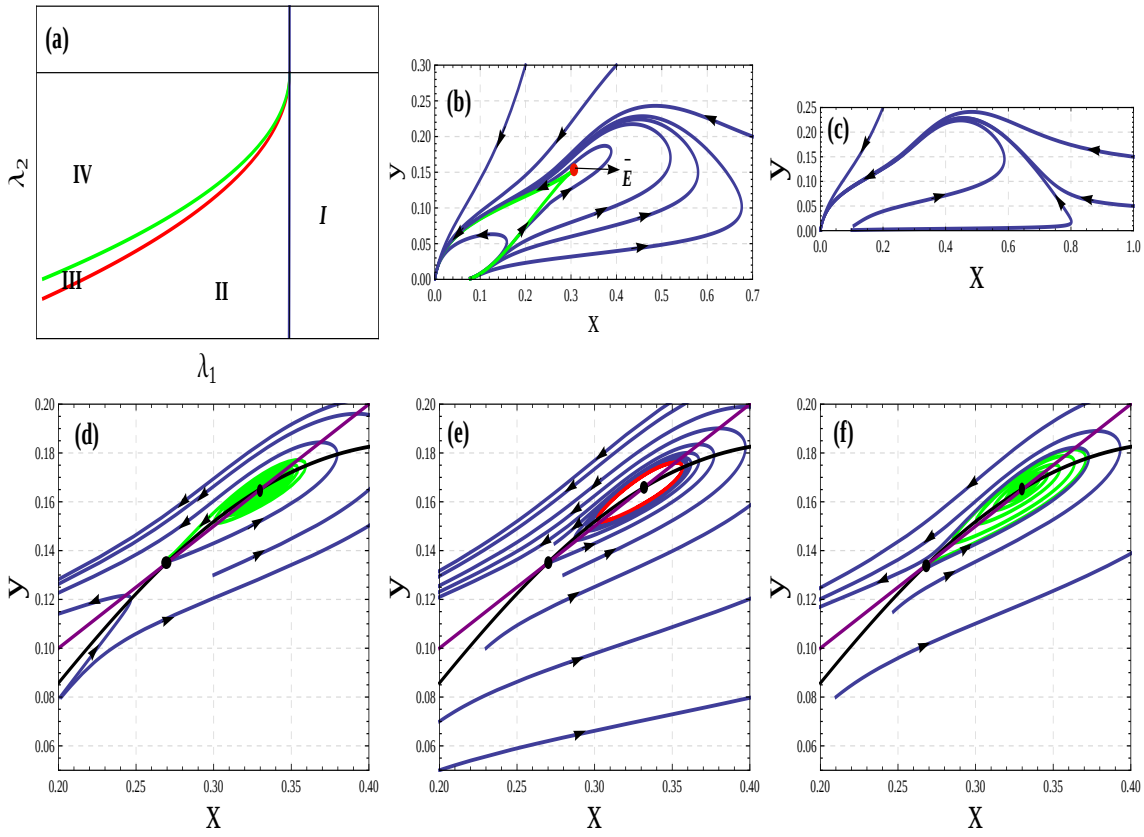

Figure 3.3: (a) The blue curve is Saddle-node bifurcation curve, red curve is Hopf bifurcation curve and green curve is Homoclinic bifurcation curve. (b) When $\lambda_1 = \lambda_2 = 0$, the unique equilibrium point $\overline{E}$ is a cusp of codimention 2. (c) When $\lambda_1 = 0.001, \lambda_2 = 0.001$ lies in the region I, then the system (3.2.2) has no interior equilibrium point and the origin is globally asymptotically stable. (d) When $\lambda_1 = -0.001, \lambda_2 = -0.1$ lies in the region II, the system (3.2.2) has two interior equilibrium point. One point is unstable and other is a saddle point. (e) When $\lambda_1 = -0.001, \lambda_2 = -0.09$ lies in the region III, the system (3.2.2) has two interior equilibrium point. One point is enclosed by an unstable limit cycle and other is a saddle point. (d) When $\lambda_1 = -0.001, \lambda_2 = -0.07$ lies in the region IV, the system (3.2.2) has two interior equilibrium point. One point is asymptotically stable and other is a saddle point. $\alpha = 0.9, \quad \beta = 0.5, \quad h = 0.16, \quad c = 0.1, \quad \rho = 0.4$.

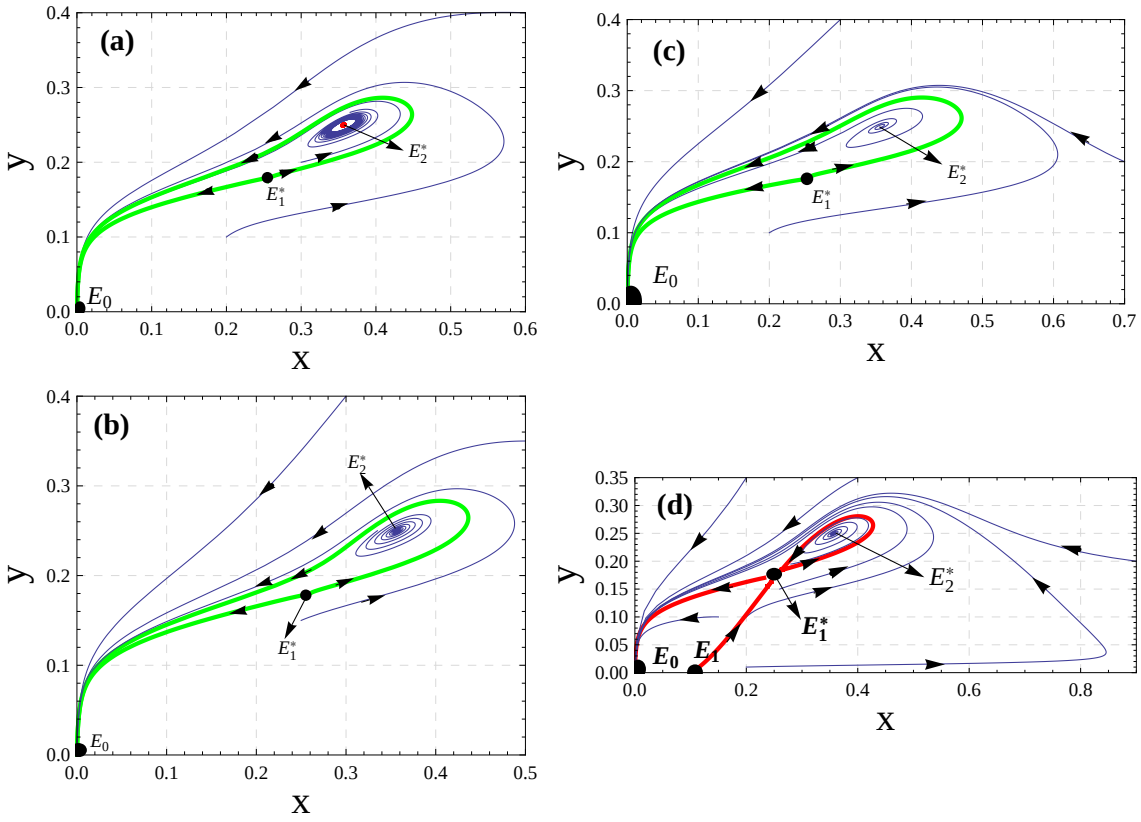

Figure 3.4: The phase portrait diagram of the system (3.2.2) E_1^* is always a saddle point. $\alpha = 0.9$, $\beta = 0.7$, $h = 0.1$, $c = 0.01$. (a) $\rho = 0.18071$, an unstable limit cycle bifurcates around the interior point E_2^* (b) $\rho = 0.2$, E_2^* is a stable point. (c) $\rho = 0.15$, E_2^* is an unstable point. (d) $\rho = 0.2117091$, Homoclinic loop is created around the interior point E_2^*.

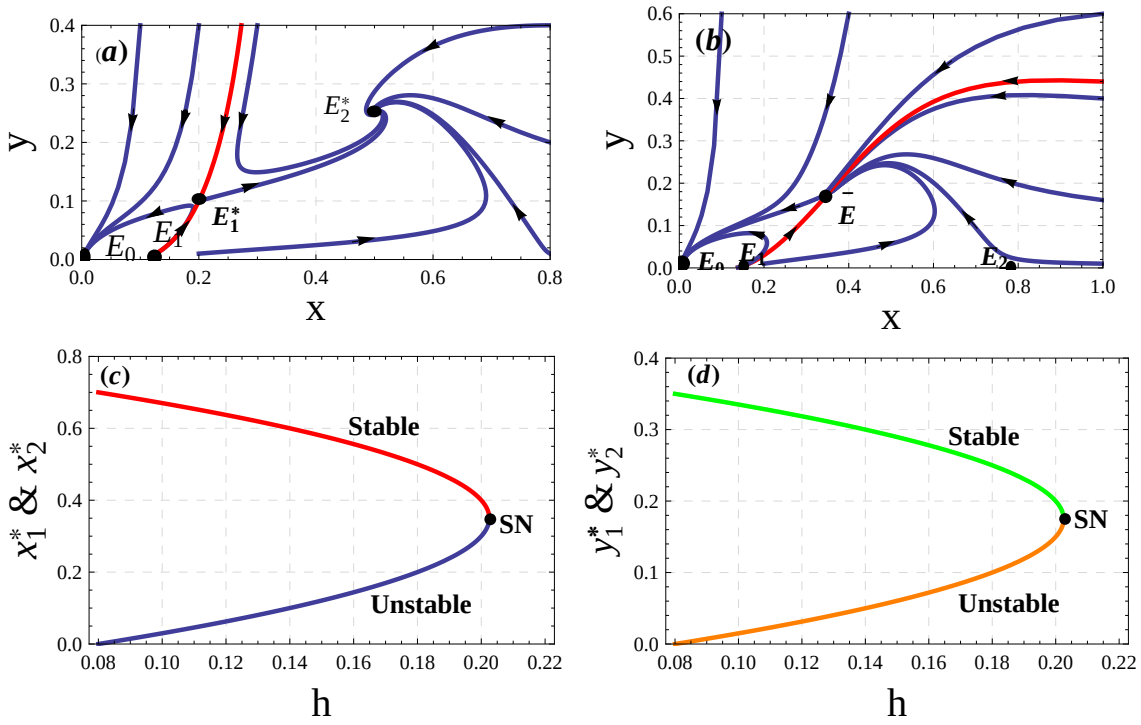

Figure 3.5: The phase portrait diagram of the system (3.2.2) for $\alpha = 0.6$, $\beta = 0.5$, $c = 0.1$, $\rho = 0.6$. The red trajectories are the separatrix. (a) $h = 0.16, E_0$ and E_2^* are two locally asymptotically stable points and E_1^* is a saddle point. (b) $h = 0.202499$, the point $\overline{E}$ is stable from right side of the separatrix and unstable from left side of the separatrix. (c) and (d) are the Saddle-node bifurcation diagrams.

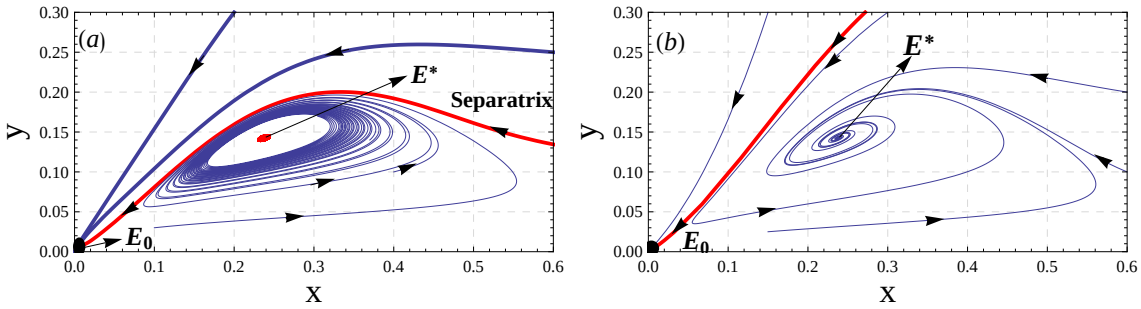

Figure 3.6: The phase portrait diagram of the system (3.2.2) for $\alpha = 0.7$, $\beta = 0.6$, $c = 0.5$, $h = 0.36875$, the red trajectory is the separatrix. (a) $\rho = 0.14597$, a stable limit cycle is created around the unique interior equilibrium point. (b) $\rho = 0.2$, the unique interior point is stable.

3.6 Results and Discussion

In this chapter, a Holling-Tanner predator-prey model with ratio-dependent functional response and Michaelis-Menten type prey harvesting has been considered. The qualitative analysis of the proposed system shows that the harvesting rate h affects much on the system. It is shown that the origin is a non-hyperbolic equilibrium point and its stability has been discussed by blow up transformation. It is clear from Figure 3.2(a) that in the absence of the interior equilibrium points, the trivial equilibrium point is globally asymptotically stable. The stability of other equilibrium points has been discussed by linearization technique. Further, it is shown that the proposed system shows bistability under certain parametric conditions, which shows that the solutions are highly sensitive for initial values.

It is shown that the proposed model undergoes Hopf bifurcation, where ρ is considered as Hopf bifurcation parameter. The stability of the limit cycle have been discussed by computing the first Lyapunov number. By using Sotomayor's theorem, it is shown that the system undergoes saddle-node bifurcation, where the harvesting parameter h is taken as the bifurcation parameter. This bifurcation gives the maximum sustainable yield (maximum harvesting compatibility with survival) (Clark 1990). The existence of the Homoclinic loop have been shown by numerical simulation and by calculating the first Lyapunov number, it is shown that it is unstable. The system (3.2.2) is reduced to the normal form of the Bogdanov-Takens bifurcation by means of a series of transformations. This ensures that the predator and prey coexists in the form of a positive equilibrium or a periodic orbit for different initial values, respectively.

Chapter 4

Modified Leslie-Gower Predator-prey Model with Weak Allee Effect II

4.1 Introduction

In chapter 3, Holling-Tanner predator-prey model with ratio-dependent functional response and nonlinear prey harvesting has been studied. One of the main demerits of the Holling-Tanner predator-prey model is that, at low prey density, predator population cannot switch to alternative prey, since its growth will be limited by the fact that its most favorite food, the prey, is absent or is in short supply. This type of predators are known as specialist predator. Aziz-Alaoui and Daher-Okiye (2003) proposed the improved model, known as modified Leslie-Gower predator-prey model, in which they considered generalist predator (at low prey population size, predator would then seek other food alternatives). Mostly predators exist in the nature are generalist, for example, the great skua Stercorarius skua in Shetland UK, little penguins at South Australia, Peruvian booby, etc. (Feng and Kang 2015).

The Allee effect (Section 1.6) affecting the prey population or predator population

This chapter is based on the research article: Qualitative analysis of modified Leslie-Gower predator-prey model with weak Allee effect type II, Communicated.

modifies the qualitative stability and quantitative aspects of the dynamics in predation models. Kent et al. (2003) and Zhou et al. (2005) discussed the stabilizing or destabilizing effects and bifurcations on the predator-prey systems subject to Allee effect. Aguirre et al. (2009a) analyzed a Leslie-type predator-prey schemes by considering a nonmonotonic functional response and additive Allee effect on prey population. They described the bifurcation diagram of limit cycles that appear only at the first quadrant and also they showed that under certain parametric conditions, the system allows the existence of a stable limit cycle surrounding an unstable limit cycle generated by Hopf bifurcation. In Aguirre et al. (2009b), it is shown that under certain parametric conditions this system allows the existence of three limit cycles: The first two cycles are infinitesimal ones generated by Hopf bifurcation; the third one arises from a Homoclinic bifurcation. Gonzalez-Olivares et al. (2011a) considered a Leslie-Gower predator-prey model incorporating the Allee effect phenomenon on prey and showed that the Allee effect significantly modifies the original system dynamics, as the model involves many non-topological equivalent behaviors. Cai et al. (2014) studied a modified Leslie-Gower predation model with additive Allee effect on prey and found that Allee effect can increase the risk of ecological extinction.

In this chapter, dynamical behavior of a modified Leslie-Gower predator-prey model with weak Allee effect II under the assumption that the extent to which the environment provides protection to both predator and prey is the same has been investigated. It has been determined how Allee effect affects the existence and the stability of the equilibria and focused on bifurcation mechanism.

4.2 Model Equations

Consider the following bidimensional predator-prey system, proposed by Aziz-Alaoui and Daher Okiye (2003)

$$\begin{cases} \frac{dX}{dT} = rX\left(1-\frac{X}{K}\right) - \frac{eXY}{a_1+X}, \\ \frac{dY}{dT} = sY\left(1-\frac{bY}{a_2+X}\right), \end{cases} \tag{4.2.1}$$

with the initial conditions $X(0) > 0, Y(0) > 0$, where $X \equiv X(T)$ and $Y \equiv Y(T)$ are prey and predator density at time T, respectively. The parameters r, K, e, s and b are positive

and represent intrinsic growth rate of prey, carrying capacity of prey in the absence of predator, maximal predator per capita consumption rate, intrinsic growth rate of predator, measure of the food quality that the prey provides for conversion into predator birth respectively, and a_1 and a_2 measures the extent to which the environment provides protection to prey and predator respectively. Many aspects of the model (4.2.1), including permanence, boundedness and global stability of solutions, have already been studied in Du et al. (2009) and Zhu and Wang (2011).

Assume that the extent to which the environment provides protection to both predator and prey is the same, that is, $a_1 = a_2 = a$. Model (4.2.1), reduces to

$$\begin{cases} \frac{dX}{dT} = rX\Big(1 - \frac{X}{K}\Big) - \frac{eXY}{a+X}, \\ \frac{dY}{dT} = sY(1 - \frac{bY}{a+X}), \end{cases} \tag{4.2.2}$$

with the initial conditions $X(0) > 0, Y(0) > 0$. Ji et al. (2009, 2011) studied the long time behavior for model (4.2.2) with stochastic perturbation. Gupta et al. (2013) studied the effect of nonlinear prey harvesting on model (4.2.2).

Consider the functional response, governed by Allee effect II, the model (4.2.2), reduces to

$$\begin{cases} \frac{dX}{dT} = rX\Big(1 - \frac{X}{K}\Big) - \frac{eXY}{a+X}\Big(1 + \frac{A}{X}\Big), \\ \frac{dY}{dT} = sY(1 - \frac{bY}{a+X}), \end{cases} \tag{4.2.3}$$

with the initial conditions $X(0) > 0, Y(0) > 0$, where $A > 0$ is the constant for Allee effect II. The bigger the A is, the stronger Allee effect II of the prey. When $A = 0$, the functional response of model (4.2.3) is the same as in model (4.2.2). When $A = X$, the functional response of model (4.2.3) is the twice as in model (4.2.2).

Let: $X = Kx, \;\; Y = \frac{Ky}{e}, \;\; T = \frac{1}{r}t$, model (4.2.3) reduces to

$$\begin{cases} \frac{dx}{dt} = x(1 - x) - \frac{(\alpha x+\beta)y}{m+x}, \\ \frac{dy}{dt} = \rho y\Big(1 - \frac{\delta y}{m+x}\Big), \end{cases} \tag{4.2.4}$$

with the initial conditions: $x(0) > 0, y(0) > 0$, where $\alpha = \frac{1}{r}, \; \beta = \frac{A}{rK}, \; m = \frac{a}{K}, \; \rho = \frac{s}{r}$, and $\delta = \frac{b}{e}$. For the biological meaning of the model variables, system (4.2.4) has been considered

in the first quadrant only, that is, in the region $\mathbb{R}^2_+ = \{(x, y) \in \mathbb{R}^2 : x \geq 0, y \geq 0\}$.

4.3 Equilibria and their Stability

The equilibrium points of the system (4.2.4) are non-negative solutions of the system

$$\frac{dx}{dt} = \frac{dy}{dt} = 0, \tag{4.3.1}$$

where $\frac{dx}{dt} = 0$ and $\frac{dy}{dt} = 0$ are prey zero growth isocline and predator zero growth isocline, respectively.

4.3.1 Model with no Allee Effect

Putting Allee effect constant $\beta = 0$, system (4.2.4) has the following equilibrium points

(*a*) $e_0 = (0, 0)$;

(*b*) $e_1 = (1, 0)$;

(*c*) $e_2 = \left(0, \frac{m}{\delta}\right)$

(*d*) $e_3 = \left(\frac{\delta-\alpha}{\delta}, \frac{\delta(1+m)-\alpha}{\delta^2}\right)$, provided $\delta > \alpha$.

So, the number and location of equilibrium points of system (4.2.4) without Allee effect can be described as:

Lemma 4.3.1. **(a)** *If $\delta \leq \alpha$, the system* (4.2.4) *has three equilibrium points e_0, e_1 and e_2.*

(b) *If $\delta > \alpha$, the system* (4.2.4) *has four equilibrium points e_0, e_1, e_2 and e_3.*

Now, the stability of each equilibria has been investigated. The Jacobian matrix of the system (4.2.4) at the equilibrium point e_0 is

$$J_{e_0} = \begin{bmatrix} 1 & 0 \\ 0 & \rho \end{bmatrix},$$

which confirms that the equilibrium point e_0 is unstable.

The Jacobian matrix of the system (4.2.4) at the equilibrium point e_1 is

$$J_{e_1} = \begin{bmatrix} -1 & -\frac{\alpha}{1+m} \\ 0 & \rho \end{bmatrix},$$

which confirms that the equilibrium point e_1 is a saddle point.

The Jacobian matrix of the system (4.2.4) at the equilibrium point e_2 is

$$J_{e_2} = \begin{bmatrix} \frac{\delta-\alpha}{\delta} & 0 \\ \frac{\rho}{\delta} & -\rho \end{bmatrix},$$

which confirms that the equilibrium point e_2 is a saddle point, whenever $\delta > \alpha$ and asymptotically stable, whenever $\delta < \alpha$.

The Jacobian matrix of the system (4.2.4) at an interior equilibrium point e_3 is

$$J_{e_3} = \begin{bmatrix} \frac{\delta-\alpha}{\delta}\left(\frac{2\alpha-\delta(1+m)}{\delta(m+1)-\alpha}\right) & \frac{\alpha(\alpha-\delta)}{\delta(m+1)-\alpha} \\ \\ \frac{\rho}{\delta} & -\rho \end{bmatrix}.$$

The determinant of Jacobian matrix J_{e_3} is $\det(J_{e_3}) = \frac{\rho(\delta-\alpha)}{\delta} > 0$, as $\delta > \alpha$ and trace is $\mathrm{tr}(J_{e_3}) = \frac{\delta-\alpha}{\delta}\left(\frac{2\alpha-\delta-\delta m}{\delta+\delta m-\alpha}\right) - \rho$. If $\frac{\delta-\alpha}{\delta}\left(\frac{2\alpha-\delta-\delta m}{\delta+\delta m-\alpha}\right) > \rho$, point e_3 is unstable and if $\frac{\delta-\alpha}{\delta}\left(\frac{2\alpha-\delta-\delta m}{\delta+\delta m-\alpha}\right) < \rho$, point e_3 is asymptotically stable.

On summarizing the above discussion, it can be concluded that:

Theorem 4.3.2. *a) The equilibrium point e_0 is always unstable.*

b) The equilibrium point e_1 is always saddle.

c) The equilibrium point e_2 is asymptotically stable, whenever $\delta < \alpha$ and unstable, whenever $\delta > \alpha$.

d) The equilibrium point e_3, if exists, it is asymptotically stable, whenever $\frac{\delta-\alpha}{\delta}\left(\frac{2\alpha-\delta-\delta m}{\delta+\delta m-\alpha}\right) < \rho$ and unstable, whenever $\frac{\delta-\alpha}{\delta}\left(\frac{2\alpha-\delta-\delta m}{\delta+\delta m-\alpha}\right) > \rho$.

In Theorem 4.3.2, it is proved that the equilibrium points e_3 and e_2 are locally asymptotically stable, whenever $\frac{\delta-\alpha}{\delta}\left(\frac{2\alpha-\delta-\delta m}{\delta+\delta m-\alpha}\right) < \rho$ and $\delta < \alpha$, respectively. Now, parametric conditions for which these points are globally asymptotically stable has been obtained.

Theorem 4.3.3. *If e_3 exists and is locally asymptotically stable, then it will be globally asymptotically stable in the region $\mathbb{R}^2_+ = \{(x, y) : x > 0, y > 0, \alpha < \rho\delta\}$.*

Proof. Define a function $H(x, y) = \frac{1}{xy}$. Clearly $H(x, y) > 0$ in the interior of positive quadrant of xy plane.

Let $f(x, y) = x(1 - x) - \frac{\alpha xy}{m+x}$ and $g(x, y) = \rho y\left(1 - \frac{\delta y}{m+x}\right)$.

Now,

$$\Delta(x, y) = \frac{\partial}{\partial x}(Hf) + \frac{\partial}{\partial y}(Hg)$$
$$= -\frac{1}{y} - \frac{(\rho\delta-\alpha)}{(m+x)^2} - \frac{\rho m\delta+2\beta}{x(m+x)^2} - \frac{\beta m}{x^2(m+x)^2} < 0, \text{provided } \alpha < \rho\delta, x > 0, y > 0.$$

Clearly $\Delta(x, y)$ does not change sign and is not identically zero in the positive quadrant of xy plane. Therefore, by Bendixson-Dulac criterion, there exists no limit cycle in the positive quadrant of xy plane. Moreover, the origin is always a repeller, axial equilibria e_1 is always a saddle and axial equilibria e_2 is saddle, whenever $\delta > \alpha$. The stable manifolds of the saddle equilibria e_1 and e_2 are x axis and y axis, respectively. So, if e_3 is locally asymptotically stable, then it will be globally asymptotically stable in the interior of positive quadrant of xy plane (Hale 1969). ■

Theorem 4.3.4. *If e_2 is locally asymptotically stable, it will be globally asymptotically stable.*

4.3.2 Model with Allee Effect

System (4.2.4) has following equilibrium points.

(*a*) $E_0 = (0, 0)$;

(*b*) $E_1 = (1, 0)$;

(*c*) If $\delta \leq \alpha$, the system (4.2.4) has no interior equilibrium point. If $\delta > \alpha$, the system (4.2.4) has two interior equilibrium points $E_2 = (x_2, y_2)$ and $E_3 = (x_3, y_3)$, whenever

$(\delta-\alpha)^2 > 4\delta\beta$; a double positive interior equilibrium point $E_4 = (x_4, y_4)$, whenever $(\delta-\alpha)^2 = 4\delta\beta$; no interior equilibrium point, whenever $(\delta-\alpha)^2 < 4\delta\beta$, where $x_2 = \frac{\delta-\alpha+\sqrt{(\delta-\alpha)^2-4\delta\beta}}{2\delta}$,

$x_3 = \frac{\delta-\alpha-\sqrt{(\delta-\alpha)^2-4\delta\beta}}{2\delta}$, $x_4 = \frac{\delta-\alpha}{2\delta}$ and $y_i = \frac{m+x_i}{\delta}, i = 2, 3, 4$.

So, the number and location of equilibrium points of system (4.2.4) can be described as:

Lemma 4.3.5. **(a)** *If $\delta \leq \alpha$, the system* (4.2.4)*, has two equilibrium points E_0 and E_1.*

(b) *If $\delta > \alpha$, the system* (4.2.4)*, has*

(i) *four equilibrium points E_0, E_1, E_2 and E_3, whenever $(\delta-\alpha)^2 > 4\delta\beta$.*

(ii) *three equilibrium points E_0, E_1 and E_4, whenever $(\delta-\alpha)^2 = 4\delta\beta$.*

(iii) *two equilibrium points E_0 and E_1, whenever $(\delta-\alpha)^2 < 4\delta\beta$.*

Now, local asymptotic stability of the boundary and interior equilibria of the system (4.2.4), obtained above have been investigated. The Jacobian matrix of the system (4.2.4) at the equilibrium point E_0 is

$$J_{E_0} = \begin{bmatrix} 1 & -\frac{\beta}{m} \\ 0 & \rho \end{bmatrix},$$

which confirms that the equilibrium point E_0 is unstable.

The Jacobian matrix of the system (4.2.4) at the equilibrium point E_1 is

$$J_{E_1} = \begin{bmatrix} -1 & -\frac{\alpha+\beta}{1+m} \\ 0 & \rho \end{bmatrix},$$

which confirms that the equilibrium point E_1 is a saddle point.

The Jacobian matrix of the system (4.2.4) at an interior equilibrium point $E(x, y)$ (say) is

$$J_E = \begin{bmatrix} 1-2x-\frac{\alpha m-\beta}{\delta(m+x)} & -\frac{\alpha x+\beta}{m+x} \\ \frac{\rho}{\delta} & -\rho \end{bmatrix}.$$

The determinant of the above Jacobian matrix is $\det(J_E) = \rho(-1 + \frac{\alpha}{\delta} + 2x)$ and trace is $tr(J_E) = 1 - 2x - \frac{\alpha m - \beta}{\delta(m+x)} - \rho$. It is observed that $det(J_{E_2}) > 0$, so the equilibrium point E_2 is stable asymptotically, whenever $1 - 2x_2 - \frac{\alpha m - \beta}{\delta(m+x_2)} - \rho < 0$ and unstable, whenever $1 - 2x_2 - \frac{\alpha m - \beta}{\delta(m+x_2)} - \rho > 0$. Also $\det(J_{E_3}) < 0$ which confirms that the equilibrium point E_3 is a saddle. Moreover, $\det(J_{E_4}) = 0$, so the equilibrium point E_4 is a degenerate singularity. Summarizing the above discussion, one gets:

Theorem 4.3.6. *a) The equilibrium points E_0 is always unstable.*

b) The equilibrium point E_1 is always saddle.

c) The equilibrium point E_2, if exists, it is an asymptotically stable point, if $1 - 2x_2 - \frac{\alpha m - \beta}{\delta(m+x_2)} < \rho$ and unstable point, if $1 - 2x_2 - \frac{\alpha m - \beta}{\delta(m+x_2)} > \rho$.

d) The equilibrium point E_3, if exists, is a saddle point.

e) The equilibrium point E_4, if exists, is a degenerate singularity.

In Theorem 4.3.6, it is shown that the interior equilibrium point E_4 is a degenerate singularity and the system (4.2.4) may have complicated properties in the neighbourhood of this point. Now, dynamics of the system (4.2.4) in the neighbourhood of the equilibrium point E_4 has been examined. First, consider transformation $\hat{x} = x - x_4, \;\; \hat{y} = y - y_4$, then expand the right-hand side of the system as a Taylor series. The system (4.2.4) can be rewritten as

$$\begin{cases} \frac{d\hat{x}}{dt} = a_{10}\hat{x} + a_{01}\hat{y} + a_{20}\hat{x}^2 + a_{11}\hat{x}\hat{y} + o|(\hat{x},\hat{y})^3|, \\ \frac{d\hat{y}}{dt} = b_{10}\hat{x} + b_{01}\hat{y} + b_{20}\hat{x}^2 + b_{11}\hat{x}\hat{y} + b_{02}y^2 + o|(\hat{x},\hat{y})^3|, \end{cases} \tag{4.3.2}$$

where $a_{10} = 1 - 2x_4 - \frac{\alpha m - \beta}{\delta(m+x_4)}, \;\; a_{01} = -\frac{\alpha x_4 + \beta}{m+x_4}, \;\; a_{20} = -1 + \frac{(\alpha m - \beta)y_4}{(m+x_4)^3}, \;\; a_{11} = -\frac{\alpha m - \beta}{(m+x_4)^2}, \;\; b_{10} = \frac{\rho}{\delta}, \;\; b_{01} = -\rho, \;\; b_{20} = -\frac{\rho}{\delta(m+x_4)}, \;\; b_{11} = \frac{2\rho}{m+x_4}, \;\; b_{02} = -\frac{\rho\delta}{m+x_4}$.

If $a_{10} + b_{01} \neq 0$, that is, $tr(J_{E_4}) \neq 0$ then one eigenvalue of the Jacobian matrix J_{E_4} is zero and other is nonzero. Hence, the equilibrium point E_4 is a saddle-node.

The condition $a_{10}+b_{01}=0$ confirms that both eigenvalues of the Jacobian matrix J_{E_4} are zero. Let $u_1=\hat{x},\ \ u_2=a_{10}\hat{x}+a_{01}\hat{y}$, then system (4.3.2) reduces to

$$\begin{cases} \frac{du_1}{dt}=u_2+\alpha_{20}u_1^2+\alpha_{11}u_1u_2+o|(u_1,u_2)^3|, \\ \frac{du_2}{dt}=\beta_{20}u_1^2+\beta_{11}u_1u_2+\beta_{02}u_2^2+o|(u_1,u_2)^3|, \end{cases} \tag{4.3.3}$$

where $\alpha_{20}=\frac{a_{20}a_{01}-a_{10}a_{11}}{a_{01}},\ \ \alpha_{11}=\frac{a_{11}}{a_{01}},\ \ \beta_{20}=a_{10}a_{20}+a_{01}b_{20}-a_{10}b_{11}+\frac{b_{02}a_{10}^2}{a_{01}}-\frac{a_{10}^2a_{11}}{a_{01}},\ \ \beta_{11}=b_{11}+\frac{a_{10}a_{11}}{a_{01}}-\frac{2b_{02}a_{10}}{a_{01}},\ \ \beta_{02}=\frac{b_{02}}{a_{01}}$.

On using the transformation $v_1=u_1,\ \ v_2=u_2-\beta_{02}u_1u_2$, the system (4.3.3) reduces to

$$\begin{cases} \frac{dv_1}{dt}=v_2+\alpha_{20}v_1^2+(\alpha_{11}+\beta_{02})v_1v_2+o|(v_1,v_2)^3|, \\ \frac{dv_2}{dt}=\beta_{20}v_1^2+\beta_{11}v_1v_2+o|(v_1,v_2)^3|. \end{cases} \tag{4.3.4}$$

Finally, using the transformation $z_1=v_1-\frac{1}{2}(\alpha_{11}+\beta_{02})v_1^2,\ \ z_2=v_2+\alpha_{20}v_1^2+o|(v_1,v_2)^3|$, the system (4.3.4) reduces to

$$\begin{cases} \frac{dz_1}{dt}=z_2, \\ \frac{dz_2}{dt}=\beta_{20}z_1^2+(2\alpha_{20}+\beta_{11})z_1z_2+o|(z_1,z_2)^3|. \end{cases} \tag{4.3.5}$$

If $\beta_{20}\neq 0$ and $2\alpha_{20}+\beta_{11}\neq 0$ (non-degeneracy condition), the origin in z_1z_2 plane is a cusp of codimension 2, that is, E_4 in xy plane is a cusp of codimension 2. The above discussion can be summarised as

Theorem 4.3.7. *The interior equilibrium point E_4, if exists, it is*

a) a saddle-node, whenever $a_{10}+b_{01}\neq 0$ holds.

b) a cusp of codimension 2, whenever $a_{10}+b_{01}=0, \beta_{20}\neq 0$ and $2\alpha_{20}+\beta_{11}\neq 0$ hold.

4.4 Bifurcation Analysis

In this section, bifurcations that occur in system (4.2.4) with and without Allee effect has been investigated.

4.4.1 Model with no Allee Effect

Hopf Bifurcation

In Theorem 4.3.2, it is shown that the unique interior equilibrium point of model (4.2.4) with no Allee effect is asymptotically stable point, whenever $\frac{\delta-\alpha}{\delta}\left(\frac{2\alpha-\delta-\delta m}{\delta+\delta m-\alpha}\right) < \rho$ and unstable point, whenever $\frac{\delta-\alpha}{\delta}\left(\frac{2\alpha-\delta-\delta m}{\delta+\delta m-\alpha}\right) > \rho$. If $\frac{\delta-\alpha}{\delta}\left(\frac{2\alpha-\delta-\delta m}{\delta+\delta m-\alpha}\right) = \rho$, the trace of the Jacobian matrix J_{e_3} is zero and determinant is positive, so, the eigenvalues of the Jacobian matrix J_{e_3} are purely imaginary, which confirms that equilibrium point e_3 is either a weak focus or a centre. Now, it has been proved that the system (4.2.4) with no Allee effect satisfies the transversality condition of Hopf bifurcation. Consider ρ be the Hopf bifurcation parameter, then the threshold magnitude $\rho = \rho^{[hf]} = \frac{\delta-\alpha}{\delta}\left(\frac{2\alpha-\delta-\delta m}{\delta+\delta m-\alpha}\right)$ exists, such that $\det(J_{e_3}) > 0$ and $tr(J_{e_3}) = 0$. Moreover, at $\rho = \rho^{[hf]}$, one gets

$$\frac{d(tr(J_{e_3}))}{d\rho} = -1 \neq 0.$$

Thus, the system (4.2.4) with no Allee effect holds transversality condition of Hopf bifurcation, which ensures that the system (4.2.4) with no Allee effect enters to Hopf bifurcation at the equilibrium point e_3.

Consider the transformation $x = u - \frac{\delta-\alpha}{\delta},\ y = v - \frac{\delta(1+m)-\alpha}{\delta^2}$. The system (4.2.4), in the vicinity of the origin, can be written as

$$\begin{aligned}
\frac{du}{dt} &= a_{10}u + a_{01}v + a_{20}u^2 + a_{11}uv + a_{02}v^2 + a_{30}u^3 + a_{21}u^2v + a_{12}uv^2 + a_{03}v^3 + P(u,v),\\
\frac{dv}{dt} &= b_{10}u + b_{01}v + b_{20}u^2 + b_{11}uv + b_{02}v^2 + b_{30}u^3 + b_{21}u^2v + b_{12}uv^2 + b_{03}v^3 + Q(u,v),
\end{aligned}$$

where $a_{10} = \frac{\delta-\alpha}{\delta}\left(\frac{\alpha}{\delta(m+1)-\alpha} - 1\right)$, $a_{01} = \frac{\alpha(\alpha-\delta)}{\delta(m+1)-\alpha}$, $a_{20} = -1 + \frac{\alpha\delta m}{(\delta(m+1)-\alpha)^2}$, $a_{11} = -\frac{\alpha\delta^2 m}{(\delta(m+1)-\alpha)^2}$, $a_{02} = 0$, $a_{30} = -\frac{\alpha\delta^2 m}{(\delta(m+1)-\alpha)^3}$, $a_{21} = \frac{\alpha\delta^3 m}{(\delta(m+1)-\alpha)^3}$, $a_{12} = 0$, $a_{03} = 0$, $b_{10} = \frac{\rho}{\delta}$, $b_{01} = -\rho$, $b_{20} = -\frac{\rho}{\delta(m+1)-\alpha}$, $b_{11} = \frac{2\rho\delta}{\delta(m+1)-\alpha}$, $b_{02} = -\frac{\rho\delta^2}{\delta(m+1)-\alpha}$, $b_{30} = \frac{\rho\delta}{(\delta(m+1)-\alpha)^2}$, $b_{21} = -\frac{2\rho\delta^2}{(\delta(m+1)-\alpha)^2}$, $b_{12} = \frac{\rho\delta^3}{(\delta(m+1)-\alpha)^2}$, $b_{03} = 0$, $P(u,v) = \sum_{i+j=4}^{\infty} a_{ij}u^iv^j$ and $Q(u,v) = \sum_{i+j=4}^{\infty} b_{ij}u^iv^j$.

Hence, first Lyapunov number σ can be computed by the formula defined in equa-

tion (1.3.7), where $\Delta = \rho^{\frac{\delta-\alpha}{\delta}}$.

If $\sigma > 0$, system (4.2.4) enters to the subcritical Hopf bifurcation, and if $\sigma < 0$ system (4.2.4) enters supercritical Hopf bifurcation.

The above discussion, can be summarised as

Theorem 4.4.1. *The system* (4.2.4) *enters to a Hopf bifurcation with respect to bifurcation parameter ρ at interior equilibrium point e_3, if exists, whenever $\rho = \rho^{[hf]}$. Moreover, an unstable (stable) limit cycle arises around the point e_3, if $\sigma > 0$ ($\sigma < 0$).*

4.4.2 Model with Allee Effect

Hopf Bifurcation

The similar discussion yield the following theorem

Theorem 4.4.2. *The system* (4.2.4) *enters to a Hopf bifurcation with respect to bifurcation parameter ρ at interior equilibrium point E_2, if exists, whenever $\rho = \rho^{[hf]}$, where $\rho^{[hf]} = 1 - 2x_2 - \frac{\alpha m-\beta}{\delta(m+x_2)}$. Moreover, an unstable (stable) limit cycle arises around the point E_2, if $\sigma > 0$ ($\sigma < 0$).*

Saddle-node Bifurcation

In Section 4.3, it is shown that if $\delta > \alpha$, the system (4.2.4) has two positive interior equilibrium points E_2 and E_3, whenever $(\delta - \alpha)^2 > 4\delta\beta$ and these two interior equilibrium points coincide with each other and a unique interior equilibrium point E^* is obtained, whenever $(\delta - \alpha)^2 = 4\delta\beta$. Also, the system (4.2.4) has no positive interior equilibrium point, whenever $(\delta - \alpha)^2 < 4\delta\beta$. Thus, the number of interior equilibrium points of the system (4.2.4) changes from two to zero. The annihilation of positive interior equilibrium points of the system (4.2.4) is may be due to the existence of Saddle-node bifurcation. In Theorem 4.3.7, it is proved that the unique interior equilibrium point E_4 is a saddle-node, whenever $a_{10} + b_{01} \neq 0$. Now, it has been shown that the system (4.2.4) enters to a Saddle-node bifurcation at the equilibrium point E_4, whenever $a_{10} + b_{01} \neq 0$.

To ensure that system (4.2.4) undergoes to a Saddle-node bifurcation Allee effect parameter β has been considered as the bifurcation parameter and Sotomayor's theorem

Perko (1996) has been applied. Since $det(J_{E_4}) = 0$ and $a_{10} + b_{01} \neq 0$, therefore, one eigenvalue of the Jacobian matrix J_{E_4} is zero. The other eigenvalue has negative (positive) real part, if $tr(J_{E_4}) < 0 (tr(J_{E_4}) > 0)$. Suppose V and W be the eigenvectors corresponding to zero eigenvalue of the matrix J_{E_4} and $J_{E_4}^T$ respectively, then

$$V = \begin{bmatrix} \delta \\ 1 \end{bmatrix}; \quad W = \begin{bmatrix} -\frac{\rho(m+x_4)}{\alpha x_4+\beta} \\ 1 \end{bmatrix}.$$

Also one gets,

$$F_\beta\Big(E_4, \beta^{[SN]}\Big) = \begin{bmatrix} -\frac{1}{\delta} \\ 0 \end{bmatrix}; \quad D^2F\Big(E_4, \beta^{[SN]}\Big) = \begin{bmatrix} -2\delta^2 \\ 0 \end{bmatrix}.$$

Now,

$W^T F_\beta\Big(E_4, \beta^{[SN]}\Big) = \frac{\rho}{\delta}\Big(\frac{x_4+m}{\alpha x_4+\beta}\Big) \neq 0,$

$W^T[D^2F\Big(E_4, \beta^{[SN]}\Big)(V, V)] = \frac{2\rho\delta^2(x_4+m)}{\alpha x_4+\beta} \neq 0.$

Thus, the transversality conditions for Saddle-node bifurcation are satisfied. Therefore, the system undergoes to a Saddle-node bifurcation of codimension 1 at E_4. The above discussion can be summarised as

Theorem 4.4.3. *The system* (4.2.4) *enters to a Saddle-node bifurcation with respect to the bifurcation parameter* β *at point* E_4*, if exists, whenever* $a_{10}+b_{01} \neq 0$ *and* $\beta = \beta^{[SN]} = \frac{(\delta-\alpha)^2}{4\delta}$.

Bogdanov-Takens Bifurcation

So far, bifurcations of codimension 1 for the model (4.2.4) have been investigated. In this subsection, Bogdanov-Takens bifurcation (codimension 2 bifurcation) for the model (4.2.4) will be investigated. In Theorem 4.3.7, it is shown that the equilibrium point E_4 is a cusp of codimension 2, whenever $a_{10} + b_{01} = 0, \beta_{20} \neq 0$ and $2\alpha_{20} + \beta_{11} \neq 0$ hold. Consider parameters β and ρ as the bifurcation parameters. The Bogdanov-Taken point (β_0, ρ_0) in the parameter space is the intersection point of the Saddle-node bifurcation curve and the Hopf-bifurcation curve. By means of the technique discussed in Xiao and Ruan (1999), normal form of the BT bifurcation for system (4.2.4) will be derived and

analytical expressions for three bifurcation curves saddle-node, Hopf and Homoclinic in a small neighborhood of BT point will be obtained.

Suppose the bifurcation parameters β and ρ vary in a small domain of BT point and $(\beta_0+\lambda_1, \rho_0+\lambda_2)$ be a point in the neighbourhood of the BT point, where λ_1, λ_2 are small. Thus, the system (4.2.4) reduces to

$$\begin{cases} \frac{dx}{dt} = x(1-x) - \frac{(\alpha x+\beta+\lambda_1)y}{m+x}, \\ \frac{dy}{dt} = (\rho+\lambda_2)y\Big(1-\frac{\delta y}{m+x}\Big). \end{cases} \tag{4.4.1}$$

The system (4.4.1) is C^∞ smooth with respect to the variables x, y in a small neighbourhood of (β_0, ρ_0).

Define $z_1 = x - x_4, \quad z_2 = y - y_4$, then the system (4.4.1) reduces to

$$\begin{cases} \frac{dz_1}{dt} = \overline{a}_{00} + \overline{a}_{10}z_1 + \overline{a}_{01}z_2 + \overline{a}_{20}z_1^2 + \overline{a}_{11}z_1z_2 + \overline{a}_{02}z_2^2 + R_1(z_1,z_2), \\ \frac{dz_2}{dt} = \overline{b}_{00} + \overline{b}_{10}z_1 + \overline{b}_{01}z_2 + \overline{b}_{20}z_1^2 + \overline{b}_{11}z_1z_2 + \overline{b}_{02}z_2^2 + R_2(z_1,z_2), \end{cases} \tag{4.4.2}$$

where $\overline{a}_{00} = -\frac{\lambda_1}{\delta}, \quad \overline{a}_{10} = 1 - 2x_4 - \frac{\alpha m-\beta_0-\lambda_1}{\delta(m+x_4)}, \quad \overline{a}_{01} = -\frac{\alpha x_4+\beta_0+\lambda_1}{m+x_4}, \quad \overline{a}_{20} = -1 + \frac{\alpha m-\beta_0-\lambda_1}{\delta(m+x_4)^2}, \quad \overline{a}_{11} = -\frac{\alpha m-\beta_0-\lambda_1}{(m+x_4)^2}, \quad \overline{a}_{02} = 0, \quad \overline{b}_{00} = 0, \quad \overline{b}_{10} = \frac{\rho_0+\lambda_2}{\delta}, \quad \overline{b}_{01} = -(\rho_0+\lambda_2), \quad \overline{b}_{20} = -\frac{\rho_0+\lambda_2}{\delta(m+x_4)}, \quad \overline{b}_{11} = \frac{2(\rho_0+\lambda_2)}{m+x_4}, \quad \overline{b}_{02} = -\frac{(\rho_0+\lambda_2)\delta}{m+x_4}$ and R_1, R_2 are the power series in (z_1, z_2) with powers $z_1^i z_2^j$ satisfying $i+j \geq 3$.

Now, on introducing the affine transformation $y_1 = z_1, \ y_2 = \overline{a}_{10}z_1 + \overline{a}_{01}z_2$ in the system (4.4.2), one gets

$$\begin{cases} \frac{dy_1}{dt} = \xi_{00}(\lambda) + y_2 + \xi_{20}(\lambda)y_1^2 + \xi_{11}(\lambda)y_1y_2 + \overline{R}_1(y_1,y_2), \\ \frac{dy_2}{dt} = \eta_{00}(\lambda) + \eta_{10}(\lambda)y_1 + \eta_{01}(\lambda)y_2 + \\ \qquad \eta_{20}(\lambda)y_1^2 + \eta_{11}(\lambda)y_1y_2 + \eta_{02}(\lambda)y_2^2 + \overline{R}_2(y_1,y_2), \end{cases} \tag{4.4.3}$$

where $\xi_{00}(\lambda) = \overline{a}_{00}(\lambda), \quad \xi_{20}(\lambda) = \frac{(\overline{a}_{01}\overline{a}_{20}-\overline{a}_{11}\overline{a}_{10})}{\overline{a}_{01}}, \quad \xi_{11}(\lambda) = \frac{\overline{a}_{11}}{\overline{a}_{01}}, \quad \eta_{00}(\lambda) = \overline{a}_{10}\overline{a}_{00}, \quad \eta_{10}(\lambda) = \overline{a}_{01}\overline{b}_{10} - \overline{a}_{10}\overline{b}_{01}, \quad \eta_{01}(\lambda) = \overline{a}_{10} + \overline{b}_{01}, \quad \eta_{20}(\lambda) = \frac{\overline{a}_{01}\overline{a}_{10}\overline{a}_{20}+\overline{a}_{01}^2\overline{b}_{20}-\overline{a}_{10}^2\overline{a}_{11}-\overline{a}_{10}\overline{a}_{01}\overline{b}_{11}+\overline{b}_{02}\overline{a}_{10}^2}{\overline{a}_{01}}, \quad \eta_{11} = \frac{\overline{a}_{10}\overline{a}_{11}+\overline{a}_{01}\overline{b}_{11}-2\overline{a}_{10}\overline{b}_{02}}{\overline{a}_{01}}, \quad \eta_{02}(\lambda) = \frac{\overline{b}_{02}}{\overline{a}_{01}}$ and $\overline{R}_1, \overline{R}_2$ are the power series in (y_1, y_2) with powers $y_1^i y_2^j$ satisfying $i+j \geq 3$.

Next, consider C^∞ change of coordinates in the small neighbourhood of $(0,0)$: $u_1 = y_1 - \frac{1}{2}(\xi_{11}+\eta_{02})y_1^2$, $u_2 = y_2 + \xi_{20}y_1^2 - \eta_{02}y_1y_2$. Then, the system (4.4.3) reduces to

$$\begin{cases} \frac{du_1}{dt} = \zeta_{00} + \zeta_{10}u_1 + u_2 + \zeta_{20}u_1^2 + \hat{R}_1(u_1,u_2), \\ \frac{du_2}{dt} = \theta_{00} + \theta_{10}u_1 + \theta_{01}u_2 + \theta_{20}u_1^2 + \theta_{11}u_1u_2 + \hat{R}_2(u_1,u_2), \end{cases} \tag{4.4.4}$$

where $\zeta_{00} = \xi_{00}$, $\zeta_{10} = -\xi_{00}(\xi_{11}+\eta_{02})$, $\zeta_{20} = -\frac{1}{2}\xi_{00}(\xi_{11}+\eta_{02})^2$, $\theta_{00} = \eta_{00}$, $\theta_{10} = \eta_{10} + 2\xi_{20}\xi_{00} - \eta_{02}\eta_{00}$, $\theta_{01} = \eta_{01} - \eta_{02}\xi_{00}$, $\theta_{20} = \frac{1}{2}(\xi_{11}+\eta_{02})(\eta_{10}+2\xi_{20}\xi_{00}-\eta_{02}\eta_{00}) - \xi_{20}(\eta_{01}-\eta_{02}\xi_{00}) + \eta_{20} - \eta_{02}\eta_{01}$, $\theta_{11} = \eta_{11} + 2\xi_{20} - \xi_{10}\eta_{02} - \xi_{00}\eta_{02}^2 + \eta_{02}(\eta_{01}-\eta_{02}\xi_{00})$, and $\hat{R}_1$, $\hat{R}_2$ are the power series in (u_1,u_2) with powers $u_1^iu_2^j$ satisfying $i+j \geq 3$.

Again consider C^∞ change of coordinates in the small neighbourhood of $(0,0)$: $v_1 = u_1$, $v_2 = \zeta_{00} + \zeta_{10}u_1 + u_2 + \zeta_{20}u_1^2$, which transforms the system (4.4.4) into

$$\begin{cases} \frac{dv_1}{dt} = v_2 + s_1(v_1,v_2), \\ \frac{dv_2}{dt} = \gamma_{00} + \gamma_{10}v_1 + \gamma_{01}v_2 + \gamma_{20}v_1^2 + \gamma_{11}v_1v_2 + s_2(v_1,v_2), \end{cases} \tag{4.4.5}$$

where $\gamma_{00} = \theta_{00} - \theta_{01}\zeta_{00}$, $\gamma_{10} = \theta_{10} - \theta_{01}\zeta_{10} - \zeta_{00}\theta_{11}$, $\gamma_{01} = \zeta_{10} + \theta_{01}$, $\gamma_{20} = \theta_{20} - \theta_{01}\zeta_{20} - \zeta_{10}\theta_{11}$, $\gamma_{11} = \theta_{11} + 2\zeta_{20}$ and $s_1(v_1,v_2), s_2(v_1,v_2)$ are the power series in (v_1,v_2) with powers $v_1^iv_2^j$ satisfying $i+j \geq 3$.

Next, consider C^∞ change of coordinates in the small neighbourhood of $(0,0)$: $w_1 = v_1$, $w_2 = v_2 + s_1(v_1,v_2)$, which transforms the system (4.4.5) into

$$\begin{cases} \frac{dw_1}{dt} = w_2, \\ \frac{dw_2}{dt} = \gamma_{00} + \gamma_{10}w_1 + \gamma_{01}w_2 + \gamma_{20}w_1^2 + \gamma_{11}w_1w_2 + F_1(w_1) + \\ \qquad w_2F_2(w_1) + w_2^2F_3(w_1,w_2), \end{cases} \tag{4.4.6}$$

where F_1, F_2 and F_3 are the power series in w_1 and (w_1,w_2) with powers $w_1^{k_1}, w_1^{k_2}$ and $w_1^iw_2^j$ satisfying $k_1 \geq 3, k_2 \geq 2$ and $i+j \geq 1$, respectively.

It is cumbersome to obtain the sign of $\gamma_{20}(0)$ analytically, therefore, consider the following two cases

Case I: $\gamma_{20}(0) < 0$**.**

To make the sign $\gamma_{20}(0)$ positive, consider the transformation $Z_1 = -w_1,\ Z_2 = w_2,\ \tau = -t$. The system (4.4.6) reduces to

$$\begin{cases} \dfrac{dZ_1}{d\tau} = Z_2, \\ \dfrac{dZ_2}{d\tau} = -\gamma_{00} + \gamma_{10}Z_1 - \gamma_{20}Z_1^2 + R_1(Z_1) - \gamma_{01}Z_2 + \gamma_{11}Z_1Z_2 + \\ \qquad Z_2R_2(Z_1) + Z_2^2R_3(Z_1, Z_2), \end{cases} \tag{4.4.7}$$

where R_1, R_2 and R_3 are the power series in Z_1 and (Z_1, Z_2) with powers $Z_1^{k_1}, Z_1^{k_2}$ and $Z_1^iZ_2^j$ satisfying $k_1 \geq 3, k_2 \geq 2$ and $i + j \geq 1$, respectively.

Applying the Malgrange preparation theorem, one gets

$$-\gamma_{00} + \gamma_{10}Z_1 - \gamma_{20}Z_1^2 + R_1(w_1) = \Big(Z_1^2 - \frac{\gamma_{10}}{\gamma_{20}}Z_1 + \frac{\gamma_{00}}{\gamma_{20}}\Big)B_1(w_1, \lambda),$$

where $B_1(0, \lambda) = -\gamma_{20}$ and B_1 is a power series of Z_1, whose coefficients depend on parameters (λ_1, λ_2).

Let $X_1 = Z_1,\ X_2 = \frac{Z_2}{\sqrt{-\gamma_{20}}}$, and $d\Gamma = \sqrt{-\gamma_{20}}d\tau$, then the system (4.4.7) reduces to

$$\begin{cases} \frac{dX_1}{d\Gamma} = X_2, \\ \frac{dX_2}{d\Gamma} = \frac{\gamma_{00}}{\gamma_{20}} - \frac{\gamma_{10}}{\gamma_{20}}X_1 - \frac{\gamma_{01}}{\sqrt{-\gamma_{20}}}X_2 + X_1^2 + \frac{\gamma_{11}}{\sqrt{-\gamma_{20}}}X_1X_2 + \overline{S}(X_1, X_2, \lambda), \end{cases} \tag{4.4.8}$$

where $\overline{S}(X_1, X_2, 0)$ is a power series in (X_1, X_2) with powers $X_1^iX_2^j$ satisfying $i + j \geq 3$ with $j \geq 2$.

Applying the parameter dependent affine transformation $Y_1 = X_1 - \frac{\gamma_{10}}{2\gamma_{20}},\ Y_2 = X_2$ in the system (4.4.8), one gets

$$\begin{cases} \frac{dY_1}{d\Gamma} = Y_2, \\ \frac{dY_2}{d\Gamma} = \mu_1(\lambda_1, \lambda_2) + \mu_2(\lambda_1, \lambda_2)Y_2 + Y_1^2 + \frac{\gamma_{11}}{\sqrt{-\gamma_{20}}}Y_1Y_2 + \overline{\overline{S}}(Y_1, Y_2, \mu), \end{cases} \tag{4.4.9}$$

where $\mu_1(\lambda_1, \lambda_2) = \frac{\gamma_{00}}{\gamma_{20}} - \frac{\gamma_{10}^2}{4\gamma_{20}^2}$, $\quad \mu_2(\lambda_1, \lambda_2) = -\frac{\gamma_{01}}{\sqrt{-\gamma_{20}}} + \frac{\gamma_{11}\gamma_{10}}{2(-\gamma_{20})^{\frac{3}{2}}}$ and $\overline{\overline{S}}(Y_1, Y_2, 0)$ is a power series in (Y_1, Y_2) with powers $Y_1^iY_2^j$ satisfying $i + j \geq 3$ with $j \geq 2$.

Case II: $\gamma_{20}(0) > 0$**.**

By Malgrange preparation theorem and by the transformation $X_1 = Z_1,\ X_2 = \frac{Z_2}{\sqrt{\gamma_{20}}},\ d\Gamma = \sqrt{\gamma_{20}}d\tau$, system (4.4.6) reduces to

$$\begin{cases} \frac{dX_1}{d\Gamma} = X_2, \\ \frac{dX_2}{d\Gamma} = \frac{\gamma_{00}}{\gamma_{20}} + \frac{\gamma_{10}}{\gamma_{20}}X_1 + \frac{\gamma_{01}}{\sqrt{\gamma_{20}}}X_2 + X_1^2 + \frac{\gamma_{11}}{\sqrt{\gamma_{20}}}X_1X_2 + \overline{S}(X_1, X_2, \lambda), \end{cases} \tag{4.4.10}$$

where $\overline{S}(X_1, X_2, 0)$ is a power series in (X_1, X_2) with powers $X_1^i X_2^j$ satisfying $i+j \geq 3$ with $j \geq 2$.

Now, applying the parameter dependent affine transformation $Y_1 = X_1 + \frac{\gamma_{10}}{2\gamma_{20}},\ Y_2 = X_2$ in the system (4.4.10), one gets

$$\begin{cases} \frac{dY_1}{d\Gamma} = Y_2, \\ \frac{dY_2}{d\Gamma} = \mu_1(\lambda_1, \lambda_2) + \mu_2(\lambda_1, \lambda_2)Y_2 + Y_1^2 + \frac{\gamma_{11}}{\sqrt{\gamma_{20}}}Y_1Y_2 + \overline{\overline{S}}(Y_1, Y_2, \mu), \end{cases} \tag{4.4.11}$$

where $\mu_1(\lambda_1, \lambda_2) = \frac{\gamma_{00}}{\gamma_{20}} - \frac{\gamma_{10}^2}{4\gamma_{20}^2}, \quad \mu_2(\lambda_1, \lambda_2) = \frac{\gamma_{01}}{\sqrt{\gamma_{20}}} - \frac{\gamma_{11}\gamma_{10}}{2(\gamma_{20})^{\frac{3}{2}}}$ and $\overline{\overline{S}}(Y_1, Y_2, 0)$ is a power series in (Y_1, Y_2) with powers $Y_1^i Y_2^j$ satisfying $i + j \geq 3$ with $j \geq 2$.

If the determinant of the matrix $\begin{bmatrix} \frac{\partial \mu_1}{\partial \lambda_1} & \frac{\partial \mu_1}{\partial \lambda_2} \\ \frac{\partial \mu_2}{\partial \lambda_1} & \frac{\partial \mu_2}{\partial \lambda_2} \end{bmatrix} \neq 0$, the parameters $\mu_1(\lambda_1, \lambda_2), \mu_2(\lambda_1, \lambda_2)$ are independent. The system (4.4.9) and (4.4.11) are topologically equivalent to the normal form of the Bogdanov-Takens bifurcation as given below

$$\begin{cases} \frac{dZ_1}{dt} = Z_2, \\ \frac{dZ_2}{dt} = \mu_1(\lambda_1, \lambda_2) + \mu_2(\lambda_1, \lambda_2)Z_2 + Z_1^2 \pm Z_1Z_2. \end{cases} \tag{4.4.12}$$

Thus, the system (4.2.4) undergoes to Bogdanov-Takens bifurcation. There exist bifurcation curves which divide the bifurcation plane into four regions (Perko 1996). The local representations of the bifurcation curves in the $\lambda_1\lambda_2$ plane are

Saddle-node curve: $SN = \{(\lambda_1, \lambda_2) : \mu_1(\lambda_1, \lambda_2) = 0\}$,

Hopf bifurcation curve:

$H = \{(\lambda_1, \lambda_2) : \mu_2(\lambda_1, \lambda_2) = \frac{\gamma_{11}}{\sqrt{\pm\gamma_{20}}}\sqrt{-\mu_1(\lambda_1, \lambda_2)}, \mu_2(\lambda_1, \lambda_2) < 0\}$

Homoclinic bifurcation curve:

$HL = \{(\lambda_1, \lambda_2) : \mu_2(\lambda_1, \lambda_2) = \frac{\gamma_{11}}{\sqrt{\pm\gamma_{20}}}\sqrt{-\mu_1(\lambda_1, \lambda_2)}, \mu_2(\lambda_1, \lambda_2) < 0\}$.

The above discussion can be summarized as

Theorem 4.4.4. *The system* (4.2.4) *undergoes a Bogdanov-Takens bifurcation with respect to the bifurcation parameter* β *and* ρ *around the equilibrium point* E_4 *whenever* $1 - 2x_4 - \frac{\alpha m - \beta}{\delta(m+x_4)} = \rho, \quad \beta_{20} \neq 0$ *and* $2\alpha_{20} + \beta_{11} \neq 0$.

4.5 Numerical Simulations

In this section numerical simulations are carried out to support the analytical results obtained above.

(1) $\alpha = 0.4, \quad m = 0.2, \quad \delta = 0.5, \quad \beta = 0.0$. The system (4.2.4) without Allee effect always has one trivial equilibrium point $e_0 = (0, 0)$ and two axial equilibrium points $e_1 = (1, 0)$ and $e_2 = (0, 0.4)$. The number of interior equilibrium points are either none or unique, depends upon the the parametric conditions. The point e_0 is always unstable, e_1 is always saddle. (a) $\rho = 0.16$, the unique interior equilibrium point is unstable (Figure 4.1(a)). (b) $\rho = 0.2$, the system undergoes to supercritical Hopf bifurcation and a stable limit cycle arises around this point (Figure 4.1(b)). The first Lyapunov number $\sigma = -14.0625\pi$ (c) $\rho = 0.22$, the point is asymptotically stable. (d) $\rho = 0.22, \quad \delta = 0.35$, the system has no interior equilibrium point and the prey free equilibrium point e_2 is asymptotically stable.

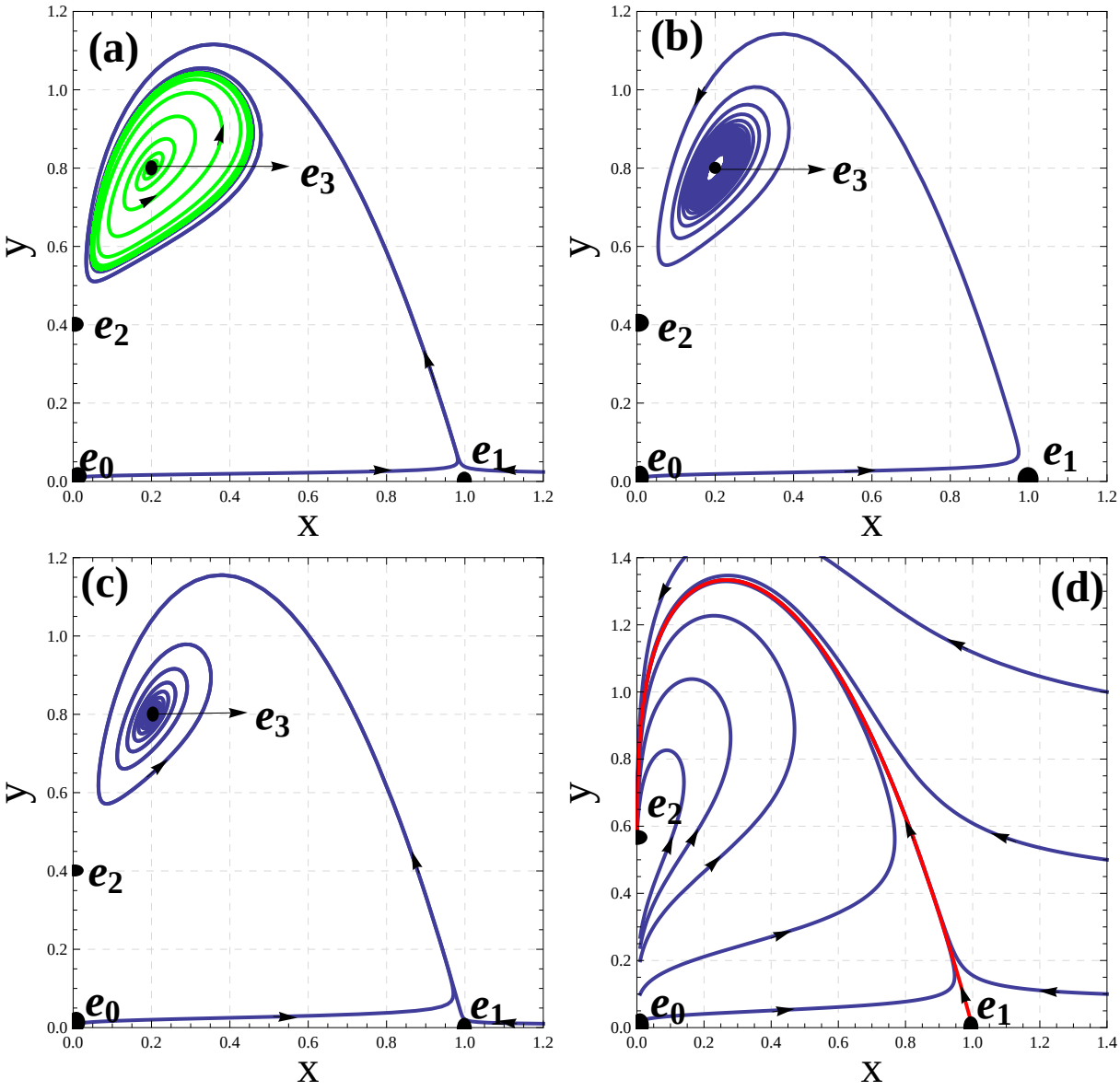

Figure 4.1: $\alpha = 0.4, \quad m = 0.2, \quad \delta = 0.5, \quad \beta = 0.0$. System (4.2.4) has a unique interior equilibrium points $e_3 = (0.2, 0.8)$, one trivial equilibrium point $e_0 = (0, 0)$ and two axial equilibrium points $e_1 = (1, 0)$ and $e_2 = (0.0.4)$. (a) $\rho = 0.16$, point e_3 is unstable (b) $\rho = 0.2$. System (4.2.4) undergoes to a supcritical hopf bifurcation at the point e_3 and an stable limit cycle arises around this point (c) $\rho = 0.22$, point e_3 is asymptotically stable (d) $\delta = 0.35, \quad \rho = 0.22$. System (4.2.4) has no interior equilibrium point and prey free equilibrium point e_2 is asymptotically stable.

(2) $\alpha = 0.3, \quad m = 0.01, \quad \delta = 0.4$. Then the threshold value of the parameter β is $\beta^{[SN]} = 0.00625$. The system (4.2.4) always has one trivial equilibrium point $E_0 = (0, 0)$ and one axial equilibrium point $E_1 = (1, 0)$. The number of interior equilibrium points changes from two to zero. The system (4.2.4) has two distinct positive interior equilibrium points, if $\beta < \beta^{[SN]}$, one positive interior equilibrium point, if $\beta = \beta^{[SN]}$ and no positive interior equilibrium point, if $\beta > \beta^{[SN]}$. The Saddle-node bifurcation diagram has been depicted in Figure 4.2(a). The phase portrait diagram for $\beta = \beta^{[SN]} = 0.00625$ is depicted in Figures 4.2(b) and 4.2(c) in which the equilibrium point E_4 is repelling saddle-node point, whenever $\rho = 0.6$ and attracting saddle-node point, whenever $\rho = 0.98$, respectively.

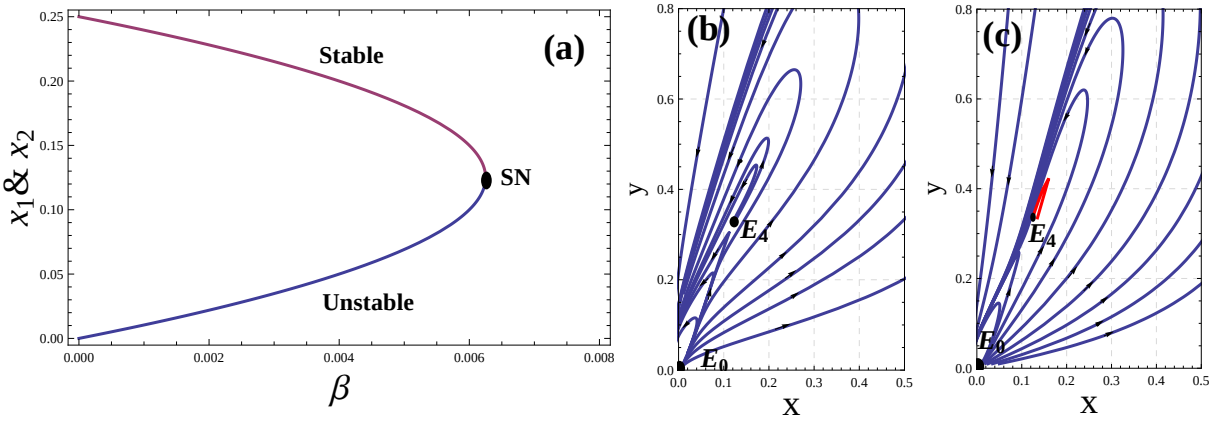

Figure 4.2: $\alpha = 0.3, \quad m = 0.01, \quad \delta = 0.4, \beta = 0.00625$. System (4.2.4) has unique interior equilibrium point $E_4 = (0.125, 0.3375)$ (a) Saddle-node bifurcation diagram (b) $\rho = 0.6$ unique interior equilibrium points E_4 of system (4.2.4) is a repelling saddle-node point (c) $\beta = 0.98$ unique interior equilibrium points E_4 of system (4.2.4) is an attracting saddle-node point

.

(3) $\alpha = 0.3, \quad m = 0.01, \quad \delta = 0.4 \quad \beta = 0.006$. The system (4.2.4) has two interior equilibrium points; $E_2 = (0.15, 0.4)$ and $E_3 = (0.1, 0.275)$. The equilibrium point E_3 is always a saddle point and the equilibrium point E_2 is unstable, whenever $\rho = 0.5$ (Figure 4.3(a)). If $\rho = \rho^{[hf]} = 0.746875$, the system (4.2.4) undergoes to a subcritical Hopf bifurcation at the point E_2, the first Lyapunov number $\sigma = 429.743\pi > 0$, an unstable limit cycle arises through the Hopf bifurcation around the point E_2 (Figure 4.3(b)). If $\rho = 0.763715$, an unstable homoclinic loop is created around E_2 and the point E_2 is stable if the solution starts in the loop (Figure 4.3(c)). If $\rho = 0.77$, the equilibrium point E_2 is asymptotically stable (Figure 4.3(d)).

(4) $\alpha = 0.3, \quad m = 0.01, \quad \delta = 0.4 \quad \beta = 0.00625, \quad \rho = 0.810185$. The system (4.2.4) has a unique interior equilibrium point $E_4 = (0.125, 0.3375)$ and $\det(J_{E_4}) = 0$ and $\mathrm{tr}(J_{E_4}) = 0$, so, both eigenvalues of the Jacobian matrix J_{E_4} are zero but the matrix J_{E_4} is not a zero matrix. For these parameters values system (4.2.4) reduces to

$$\begin{cases} \frac{dx}{dt} = x(1-x) - \frac{(3x+0.00625+\lambda_1)y}{0.01+x}, \\ \frac{dy}{dt} = (0.810185+\lambda_2)y\Big(1 - \frac{0.4y}{0.01+x}\Big). \end{cases} \tag{4.5.1}$$

Define $z_1 = x - 0.125, \quad z_2 = y - 0.3375$, then the system (4.5.1) reduces to

$$\begin{cases} \frac{dz_1}{dt} = \overline{a}_{00} + \overline{a}_{10}z_1 + \overline{a}_{01}z_2 + \overline{a}_{20}z_1^2 + \overline{a}_{11}z_1z_2 + \overline{a}_{02}z_2^2 + R_1(z_1, z_2), \\ \frac{dz_2}{dt} = \overline{b}_{00} + \overline{b}_{10}z_1 + \overline{b}_{01}z_2 + \overline{b}_{20}z_1^2 + \overline{b}_{11}z_1z_2 + \overline{b}_{02}z_2^2 + R_2(z_1, z_2), \end{cases} \tag{4.5.2}$$

where $\overline{a}_{00} = -2.5\lambda_1$, $\overline{a}_{10} = 0.810185 + 18.5185\lambda_1$, $\overline{a}_{01} = -0.324074 - 7.40741\lambda_1$, $\overline{a}_{20} = -1.44582 - 137.174\lambda_1$, $\overline{a}_{11} = 0.178326 + 54.8697\lambda_1$, $\overline{a}_{02} = 0$, $\overline{b}_{00} = 0$, $\overline{b}_{10} = 2.02546 + 2.5\lambda_2$, $\overline{b}_{01} = -0.810185 - \lambda_2$, $\overline{b}_{20} = -15.0034 - 18.5185\lambda_2$, $\overline{b}_{11} = 12.0027 + 14.8148\lambda_2$, $\overline{b}_{02} = -2.40055 - 2.96296\lambda_2$ and R_1, R_2 are the power series in (x_1, x_2) with powers $x_1^i x_2^j$ satisfying $i + j \geq 3$.

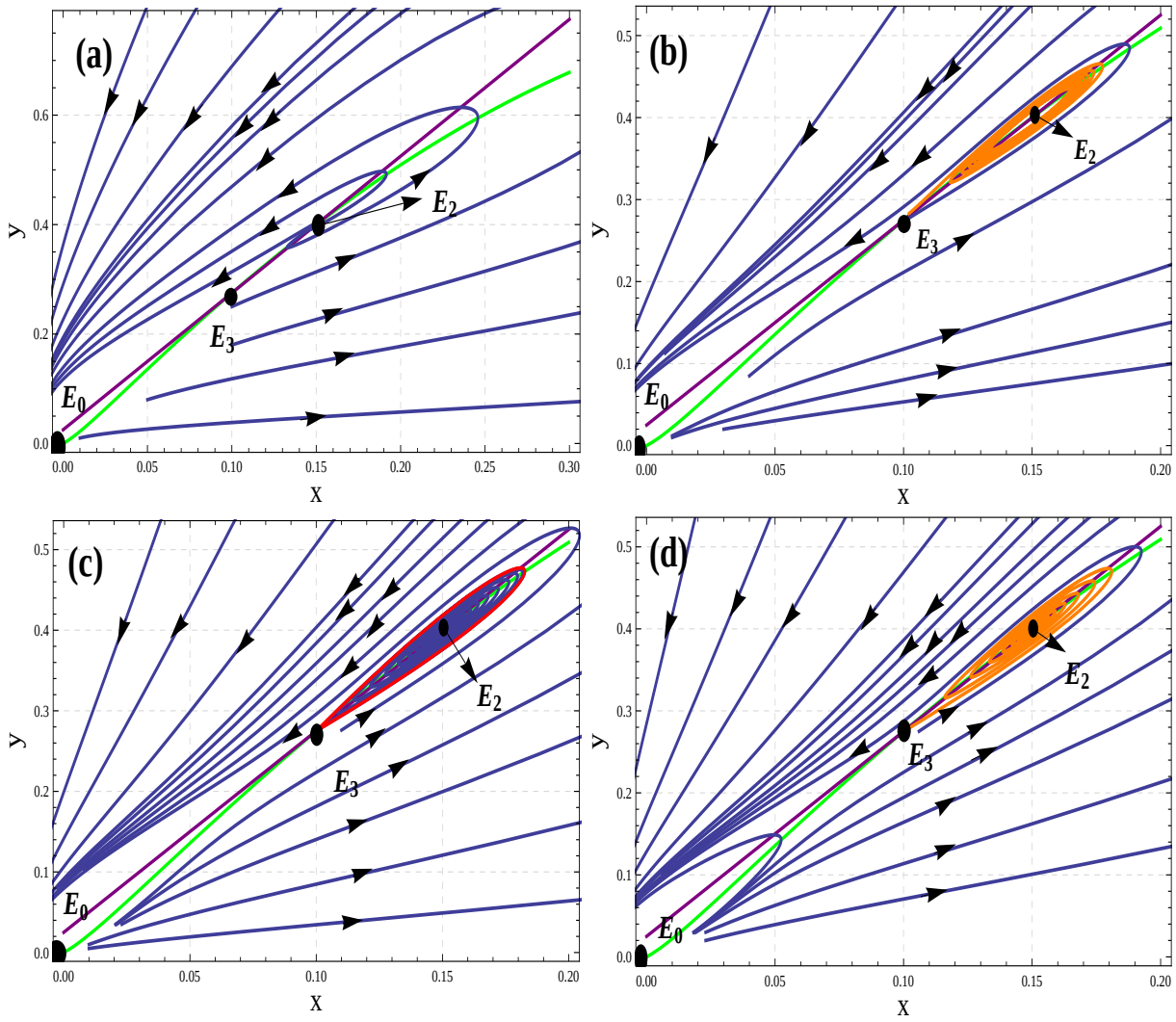

Figure 4.3: $\alpha = 0.3$, $m = 0.01$, $\delta = 0.4$, $\beta = 0.006$. System (4.2.4) has two interior equilibrium points $E_2 = (0.15, 0.4), E_3 = (0.1, 0.275)$, one unstable trivial equilibrium point $E_0 = (0, 0)$ and one saddle axial equilibrium point $E_1 = (1, 0)$. The green curve is prey isocline and the purple line is the predator isocline. (a) $\rho = 0.5$, point E_2 is unstable and point E_3 is saddle (b) $\rho = 0.746875$, System (4.2.4) undergoes to a subcritical Hopf bifurcation at the point E_2 and an unstable limit cycle arises around this point, point E_3 is saddle (c) $\rho = 0.763715$, System (4.2.4) undergoes to a Homoclinic bifurcation at the point E_2 and an unstable loop (red loop) arises around this point and point E_3 is saddle (d) $\beta = 0.77$, point E_2 is asymptotically stable and point E_3 is saddle.

Let $y_1 = x_1,\ y_2 = \overline{a}_{10}x_1 + \overline{a}_{01}x_2$, system (4.5.2) reduces to

$$\begin{cases} \dfrac{dy_1}{dt} =\xi_{00}(\lambda) + y_2 + \xi_{20}(\lambda)y_1^2 + \xi_{11}(\lambda)y_1y_2 + \overline{R}_1(y_1, y_2), \\ \dfrac{dy_2}{dt} =\eta_{00}(\lambda) + \eta_{10}(\lambda)y_1 + \eta_{01}(\lambda)y_2 + \eta_{20}(\lambda)y_1^2 + \eta_{11}(\lambda)y_1y_2 \\ \qquad + \eta_{02}(\lambda)y_2^2 + \overline{R}_2(y_1, y_2), \end{cases} \tag{4.5.3}$$

where $\xi_{00}(\lambda) = -2.5\lambda_1$, $\xi_{20}(\lambda) = -\frac{0.118767+14.7174\lambda_1+274.348\lambda_1^2}{0.04375+\lambda_1}$, $\xi_{11}(\lambda) = \frac{0.0685185+7.40741\lambda_1}{0.04375+\lambda_1}$, $\eta_{00}(\lambda) = -2.02546\lambda_1 - 46.2963\lambda_1^2$, $\eta_{10}(\lambda) = 0$, $\eta_{01}(\lambda) = 18.5185\lambda_1 - \lambda_2$, $\eta_{20}(\lambda) = -\frac{0.0962234+14.1232\lambda_1+494.818\lambda_1^2+5080.53\lambda_1^3}{0.04375+\lambda_1}$,

$\eta_{11} = \frac{0.0555127+7.27023\lambda_1+137.174\lambda_1^2}{0.04375+\lambda_1}$, $\eta_{02}(\lambda) = \frac{0.324074+0.4\lambda_2}{0.04375+\lambda_1}$ and $\overline{R}_1, \overline{R}_2$ are the power series in (y_1, y_2) with powers $y_1^i y_2^j$ satisfying $i + j \geq 3$.

Now, by means of following transformations

$$u_1 = y_1 - \frac{1}{2}(\xi_{11} + \eta_{02})z_1^2, \quad u_2 = y_2 + \xi_{20}y_1^2 - \eta_{02}y_1y_2,$$

$$v_1 = u_1, \quad v_2 = \zeta_{00} + \zeta_{10}u_1 + u_2 + \zeta_{20}u_1^2,$$

$$w_1 = v_1,\ w_2 = v_2 + s_1(v_1, v_2),$$

the system (4.5.3) reduces to

$$\begin{cases} \dfrac{dw_1}{dt} =w_2, \\ \dfrac{dw_2}{dt} =\gamma_{00} + \gamma_{10}w_1 + \gamma_{01}w_2 + \gamma_{20}w_1^2 + \gamma_{11}w_1w_2 + F_1(w_1)+ \\ \qquad w_2F_2(w_1) + w_2^2F_3(w_1, w_2), \end{cases} \tag{4.5.4}$$

where $\gamma_{00} = \frac{1}{0.04375+\lambda_1}(-0.088614\lambda_1 - 0.109375\lambda_1\lambda_2)$, $\gamma_{10} = \frac{1}{(0.04375+\lambda_1)^2}(0.0347892\lambda_1 + 1.3128\lambda_1^2 + 0.0783854\lambda_1\lambda_2 + 2.43056\lambda_1^2\lambda_2 + 0.04375\lambda_1\lambda_2^2 + \lambda_1^2\lambda_2^2)$, $\gamma_{01} = \frac{1}{0.04375+\lambda_1}(2.60185\lambda_1 + 37.037\lambda_1^2 - 0.04375\lambda_2 + \lambda_1\lambda_2)$, $\gamma_{20} = \frac{1}{(0.04375+\lambda_1)^3}(-0.000184178 - 0.0199668\lambda_1 + 0.444567\lambda_1^2 + 72.9727\lambda_1^3 + 1721.65\lambda_1^4 + 11431.2\lambda_1^5 + 0.00039297\lambda_2 + 0.0151019\lambda_1\lambda_2 - 0.0835691\lambda_1^2\lambda_2 + 31.8409\lambda_1^3\lambda_2 + 617.284\lambda_1^4\lambda_2 + 0.000765625\lambda_2^2 + 0.059265\lambda_1\lambda_2^2 - 0.316667\lambda_1^2\lambda_2^2 - 7.40741\lambda_1^3\lambda_2^2 + 0.00875\lambda_1\lambda_2^3 - 0.4\lambda_1^2\lambda_2^3)$, $\gamma_{11} =$

$\frac{1}{(0.04375+\lambda_1)^2}(-0.00796345 - 0.503841\lambda_1 - 25.6283\lambda_1^2 - 274.348\lambda_1^3 + 1.43333\lambda_1\lambda_2 + 14.8148\lambda_1^2\lambda_2 + 0.8\lambda_1\lambda_2^2)$ and F_1, F_2 and F_3 are the power series in w_1 and (w_1, w_2) with powers $w_1^{k_1}, w_1^{k_2}$ and $w_1^i w_2^j$ satisfying $k_1 \geq 3, k_2 \geq 2$ and $i + j \geq 1$, respectively.

Here $\gamma_{20}(0) = -0.810185$. Consider the transformation $Z_1 = -w_1,\ \ Z_2 = w_2,\ \ \tau = -t$. The system (4.5.4) reduces to

$$\begin{cases} \dfrac{dZ_1}{d\tau} = Z_2, \\ \dfrac{dZ_2}{d\tau} = -\gamma_{00} + \gamma_{10}Z_1 - \gamma_{20}Z_1^2 + R_1(Z_1) - \gamma_{01}Z_2 + \gamma_{11}Z_1Z_2 + \\ \qquad\qquad Z_2R_2(Z_1) + Z_2^2R_3(Z_1, Z_2), \end{cases} \tag{4.5.5}$$

where R_1, R_2 and R_3 are the power series in Z_1 and (Z_1, Z_2) with powers $Z_1^{k_1}, Z_1^{k_2}$ and $Z_1^i Z_2^j$ satisfying $k_1 \geq 3, k_2 \geq 2$ and $i + j \geq 1$, respectively.

By Malgrange preparation theorem and transformation $X_1 = Z_1,\ \ X_2 = \frac{Z_2}{\sqrt{-\gamma_{20}}}$, and $d\Gamma = \sqrt{-\gamma_{20}}d\tau$, the system (4.5.5) reduces to

$$\begin{cases} \frac{dX_1}{d\Gamma} = X_2, \\ \frac{dX_2}{d\Gamma} = \frac{\gamma_{00}}{\gamma_{20}} - \frac{\gamma_{10}}{\gamma_{20}}X_1 - \frac{\gamma_{01}}{\sqrt{-\gamma_{20}}}X_2 + X_1^2 + \frac{\gamma_{11}}{\sqrt{-\gamma_{20}}}X_1X_2 + \overline{S}(X_1, X_2, \lambda), \end{cases} \tag{4.5.6}$$

where $\overline{S}(X_1, X_2, 0)$ is a power series in (X_1, X_2) with powers $X_1^i X_2^j$ satisfying $i+j \geq 3$ with $j \geq 2$.

Finally, applying the transformation $Y_1 = X_1 - \frac{\gamma_{10}}{2\gamma_{20}},\ \ Y_2 = X_2$ in the system (4.5.6), one gets

$$\begin{cases} \frac{dY_1}{d\Gamma} = Y_2, \\ \frac{dY_2}{d\Gamma} = \mu_1(\lambda_1, \lambda_2) + \mu_2(\lambda_1, \lambda_2)Y_2 + Y_1^2 - 2.71726Y_1Y_2 + \overline{\overline{S}}(Y_1, Y_2, \mu), \end{cases} \tag{4.5.7}$$

where $\mu_1(\lambda_1, \lambda_2) = \frac{\gamma_{00}}{\gamma_{20}} - \frac{\gamma_{10}^2}{4\gamma_{20}^2}, \quad \mu_2(\lambda_1, \lambda_2) = -\frac{\gamma_{01}}{\sqrt{-\gamma_{20}}} + \frac{\gamma_{11}\gamma_{10}}{2(-\gamma_{20})^{\frac{3}{2}}}$ and $\overline{\overline{S}}(X_1, X_2, 0)$ is a power series in (Y_1, Y_2) with powers $Y_1^i Y_2^j$ satisfying $i + j \geq 3$ with $j \geq 2$.

The determinant of the matrix $\begin{bmatrix} \frac{\partial\mu_1}{\partial\lambda_1} & \frac{\partial\mu_1}{\partial\lambda_2} \\ \frac{\partial\mu_2}{\partial\lambda_1} & \frac{\partial\mu_2}{\partial\lambda_2} \end{bmatrix} = 2.77746 \neq 0$, thus parameters μ_1 and μ_2 are independent. The system (4.5.7) is topologically equivalent to the normal form

of the Bogdanov-Takens bifurcation. There exist bifurcation curves which divide the bifurcation plane into four regions. The local representations of these bifurcation curves in the $\lambda_1\lambda_2$ plane are

Saddle-node curve:

$SN = \{(\lambda_1, \lambda_2) : \mu_1(\lambda_1, \lambda_2) = 0\}$,

Hopf bifurcation curve:

$H = \{(\lambda_1, \lambda_2) : \mu_2(\lambda_1, \lambda_2) = -2.71726\sqrt{-\mu_1(\lambda_1, \lambda_2)}, \mu_2(\lambda_1, \lambda_2) < 0\}$

Homoclinic bifurcation curve:

$HL = \{(\lambda_1, \lambda_2) : \mu_2(\lambda_1, \lambda_2) = -2.71726\sqrt{-\mu_1(\lambda_1, \lambda_2)}, \mu_2(\lambda_1, \lambda_2) < 0\}$.

The above three bifurcation curves in a small neighborhood of the origin in the (λ_1, λ_2) plane has been sketched by their first approximations (Figure 4.4(a)). The bifurcation curves divide the parameter plane into four parts; I, II, III and IV. For various parameter values within regions, different phase portraits of the model are observed:

a) When the parameters $\lambda_1 = 0, \lambda_2 = 0$, the unique positive equilibrium of the model (4.2.4) is a cusp of codimension 2 (Figure 4.4(b)).

b) When the parameter values are in the region I, model (4.2.4) has no interior equilibrium point and every solution trajectories leaves the first quadrant through predator axis (Figure 4.4(c)).

c) When the parameter values are in the region II, model (4.2.4) has two interior equilibrium points in which one is a saddle point and other is unstable (Figure 4.4(d)).

d) When the parameter values are in the region III, model (4.2.4) has two interior equilibrium points in which one is a saddle point and other is enclosed by an unstable limit cycle (Figure 4.4(e)).

e) When the parameter values are in the region IV, model (4.2.4) has two interior equilibrium points in which one is a saddle point and other is asymptotically stable (Figure 4.4(f)).

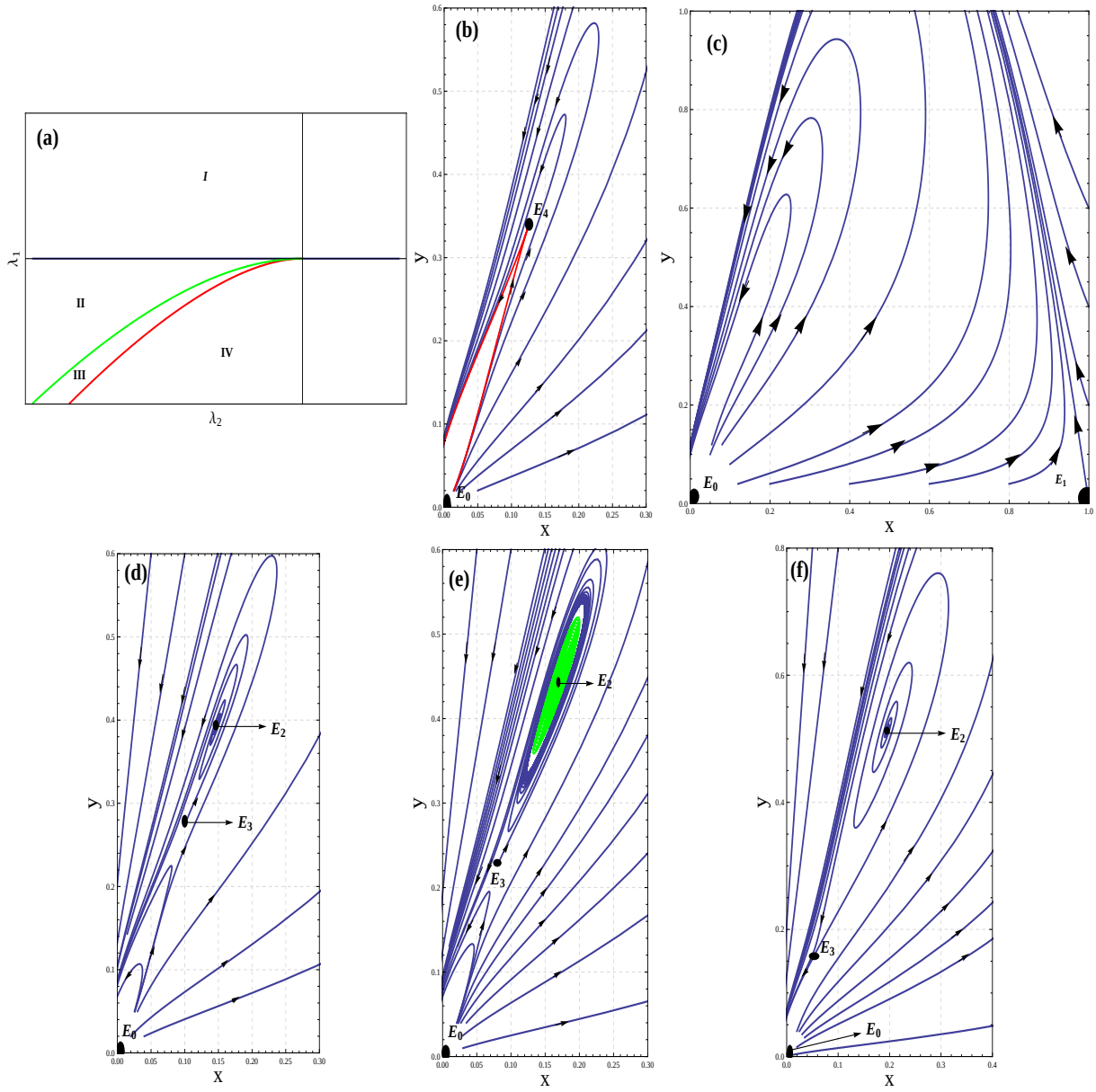

Figure 4.4: $\alpha = 0.3, \quad m = 0.01, \quad \delta = 0.4, \beta = 0.00625, \quad \rho = 0.810185$. (a) Bifurcation diagram of system (4.2.4); blue line is the Saddle-node bifrcation curve, green curve is the Hopf bifurcation curve and red curve is the Homoclinic bifurcation curve (b) $\lambda_1 = 0, \quad \lambda_2 = 0$. The unique interior equilibrium point E_4 is a cusp of of codimension 2. (c) $\lambda_2 = -0.1, \quad \lambda_1 = 0.0005$ lies in region I. No interior equilibrium point exist. (d) $\lambda_2 = -0.1, \quad \lambda_1 = -0.0002$ lies in in region II. The system (4.2.4) has two interior equilibrium points $E_2 = (0.147361, 0.393402)$ and $E_3 = (0.102639, 0.281598)$. Point E_2 is unstable and Point E_3 is saddle (e) $\lambda_2 = -0.1, \quad \lambda_1 = -0.0007$ lies in region III. The system (4.2.4) has two interior equilibrium points $E_2 = (0.166833, 0.442083)$ and $E_3 = (0.083167, 0.232917)$. Point E_2 is surrounded by an unstable limit cycle and Point E_3 is saddle. (f) $\lambda_2 = -0.1, \quad \lambda_1 = -0.002$ lies in region IV. The system (4.2.4) has two interior equilibrium points $E_2 = (0.195711, 0.514277)$ and $E_3 = (0.0542893, 0.160723)$. Point E_2 is asymptotically stable and Point E_3 is saddle.

4.6 Results and Discussion

In this chapter, a bidimensional modified Leslie-Gower predator-prey model, in which the protection provided by the environment for both the prey and predator species is the same, has been analysed in the presence of Allee effect of type II. In most predator-prey models subjected to Allee effect, it has been considered that the Allee effect has influence only on the prey growth function and this effect is independent of the functional response. In Zhou et al. (2005) authors proposed Allee effect, affecting the functional response on two classical predator-prey models; 1) Lotka-Volterra model and 2) Leslie model. In this work, they concerned only the stability of the unique interior equilibrium point. By means of analytical and numerical simulations, they have shown that the Allee effect may be a destabilizing force in the predator-prey system. From best of our knowledge, mine is the first attempt to study the qualitative analysis of a predator-prey system in the presence of Allee effect of type II.

The qualitative analysis of the model (4.2.4) reveals that the Allee effect constant β plays an important role in determining the dynamics and bifurcations of system. The model with no Allee effect always has a trivial equilibrium point, a unique predator free axial equilibrium point and a unique prey free axial equilibrium point, while it has either no or unique interior equilibrium point. The trivial equilibrium point is always an unstable point, predator free axial equilibrium point is always a saddle point and if no interior equilibrium point exists, prey free axial equilibrium point is globally asymptotically stable, otherwise it is a saddle point. The unique interior equilibrium point is globally asymptotically stable for certain parametric conditions. Moreover, the model undergoes to supercritical Hopf bifurcation, whenever bifurcation parameter ρ crosses its critical value. The local existence of limit cycles emerging through Hopf bifurcation has been shown and its stability has been examined by calculating the first Lyapunov number.

Model (4.2.4) with Allee effect type II always has two boundary equilibrium points; trivial equilibrium point and a unique predator free axial equilibrium point. The nature of trivial equilibrium point and predator free axial equilibrium point are similar to the model without Allee effect. Therefore, the extinction of both the species together or predator only

is impossible. The prey free axial equilibrium point in this case is disappeared and all solution trajectories once touching the predator-axis will leave the first quadrant. Ecologically, predator species tends to change its food habits as predator approaches for alternative foods available, but the population of predator species depends upon the initial values of prey and predators. Furthermore, it is found that model (4.2.4) can have zero, one or two positive interior equilibrium points through Saddle-node bifurcation as the bifurcation parameter β crosses a certain critical value. Therefore, a maximum threshold of β exists such that below which both the populations co-exist and above which the prey species goes extinction. Sotomayor's theorem is applied to ensure the existence of saddle-node bifurcation. It is observed that if two interior equilibrium points exist, one of them being always a saddle point and other is stable, unstable or the system undergoes to a Hopf bifurcation around this point for different choice of set of the parameters. The emergence of Homoclinic loops has been shown through numerical simulation, when the limit cycle arising through Hopf bifurcation collides with a saddle point. Further, the existence of Bogdanov-Takens bifurcation for the model has also been shown by means of reducing the model to normal form. In this situation, the system under a small perturbation may cause extinction, coexistence and oscillation. The overall analysis shows that Allee effect II can increase the risk of ecological extinction.

Chapter 5

Modified Leslie-Gower Predator-prey Model with Double Allee Effect

5.1 Introduction

In previous chapter, a bidimensional modified Leslie-Gower predator-prey model in which the protection provided by the environment for both the prey and predator species is the same, has been analysed in the presence of Allee effect of type II. Recent ecological research suggests the possibility that two or more Allee effects generate mechanisms acting simultaneously on a single population (Table 1 in Berec et al. 2007 or Table 2.1 in Courchamp et al. 2008), especially in renewable resources (Gascoigne and Lipcius, 2004). The combined influence of some of these phenomena has been named as the multiple (double) Allee effects (Berec et al. 2007; Courchamp et al. 2008; Angulo et al. 2007; Boukal and Berec 2002). The double Allee effect affecting the species has been seen in wild life ecosystem (Berec et al. 2007) and in marine ecosystem (Gascoigne and Lipcius 2004).

Gonzlez-Olivares et al. (2011b) considered that the growth of prey is affected by double Allee effect in Lotka-Volterra predator-prey model. They proved the existence

This chapter is based on the research article: Bifurcation analysis of modified Leslie-Gower predator-prey model with double Allee effect, Ain Shams Engineering Journal (Elsevier) http://dx.doi.org/10.1016/j.asej.2016.07.007 Article in press.

of two limit cycles by means of the Lyapunov quantities, whenever the Allee effect is either strong or weak. Huincahue-Arcos and Gonzlez-Olivares (2013) studied the modified Rosenzweig-MacArthur predation model (Turchin 2013) in which two Allee effects affect the prey population. They determined certain parametric conditions for which the unique interior equilibrium point is locally asymptotically stable or the existence of at least one stable limit cycle generated through Hopf bifurcation. Flores and Gonzalez-Olivares (2014) studied a ratio-dependent predator-prey model with double Allee effect on the prey, and discussed the stability and bifurcation analysis. Feng and Kang (2015) studied the stability and bifurcation of the modified Leslie-Gower predator-prey model with Allee effects in both predator and prey species. They also showed that the double Allee effects greatly alter the outcome of the survival of both species. Pal and saha (2015) studied the stability and bifurcation analysis of a ratio dependent predator-prey system with a double Allee effect in prey population growth.

In this chapter, dynamical behavior of the modified Leslie-Gower predator-prey model with double Allee effect in growth of prey population has been considered with the assumption that the extent to which the environment provides protection to both the predator and prey is the same.

5.2 Model Equations

Consider modified Leslie-Gower predator-prey model (1.5.8) incorporating the Allee effect on prey under the assumption that the extent to which the environment provides protection to predator and prey is same;

$$\begin{cases} \frac{dX}{dT} = \frac{rX}{X+n}\left(1-\frac{X}{K}\right)(X-m) - \frac{\alpha XY}{a+X}, \\ \frac{dY}{dT} = sY(1-\frac{bY}{a+X}), \end{cases} \tag{5.2.1}$$

with the initial conditions $X(0), Y(0) > 0$, where $X(T)$ and $Y(T)$ are respectively, prey and predator density at time T. The parameter $r, K, \alpha, s, b, a, m, n$ are positive constants, which represent intrinsic growth rate of prey, carrying capacity of prey in the absence of predator, maximal predator per capita consumption rate, intrinsic growth rate of predator, measure

of the food quality that the prey provides for conversion into predator birth, measures the extent to which the environment provides protection to prey and predator, Allee threshold and auxiliary parameter respectively.

On introducing the non-dimensional variables: $X = Kx, \quad Y = \frac{Ky}{b}, \quad T = \frac{1}{r}t$, in system (5.2.1), it will become

$$\begin{cases} \frac{dx}{dt} = \frac{x(1-x)(x-\beta)}{(x+\theta)} - \frac{\xi xy}{\gamma+x}, \\ \frac{dy}{dt} = \rho y\Big(1 - \frac{y}{\gamma+x}\Big), \end{cases} \tag{5.2.2}$$

with the initial conditions: $x(0) > 0, y(0) > 0$, where $\beta = \frac{m}{K}$, $\theta = \frac{n}{K}$, $\xi = \frac{\alpha}{br}$, $\rho = \frac{s}{r}$, and $\gamma = \frac{a}{K}$.

The positivity and the boundedness of the solutions of the system (5.2.2) starting from an interior point of the first quadrant are proved below.

On integrating the first equation of the system (5.2.2), one gets

$$x(t) = x(0) \exp\Big[\int_0^t \Big(\frac{(1-x(s))(x(s)-\beta)}{(x(s)+\theta)} - \frac{\xi y(s)}{\gamma + x(s)}\Big) ds\Big], \tag{5.2.3}$$

which is always non-negative as $x(0) > 0$. Similarly from second equation of the system (5.2.2), one gets

$$y(t) = y(0) \exp\Big[\rho \int_0^t \Big(1 - \frac{y(s)}{\gamma + x(s)}\Big) ds\Big], \tag{5.2.4}$$

which is always non-negative as $y(0) > 0$. Therefore, all the solutions of the system (5.2.2) starting from an interior point of the first quadrant will remain in the first quadrant for all future time. Moreover, the solution trajectories starting from a point on the positive $x(y)$- axis will remain within the positive $x(y)$- axis for all future times. Hence, the set $\mathbb{R}^2_+ = \{(x, y) : x, y \geq 0\}$ is an invariant set.

Now, boundedness of the solutions of the system (5.2.2) will be examined. Consider $(x(t), y(t))$ be any positive solution of the system (5.2.2) that satisfies the initial conditions. There arise the following two cases;

Case I. Suppose $x(0) \leq 1$, it is claimed that $x(t) \leq 1$ for all $t \geq 1$. Otherwise, there are two positive real numbers t_1 and t_2 such that $t_2 > t_1,\ x(t_1) = 1$ and $x(t) > 1,\ \forall t \in (t_1, t_2)$. Then, for all $t \in (t_1, t_2)$ the Eq. (5.2.3), can be written as

$$\begin{aligned} x(t) &= x(0) \exp\Big[\int_0^{t_1} \Big(\frac{(1-x(s))(x(s)-\beta)}{(x(s)+\theta)} - \frac{\xi y(s)}{\gamma + x(s)}\Big) ds\Big] \\ &\quad \exp\Big[\int_{t_1}^{t_2} \Big(\frac{(1-x(s))(x(s)-\beta)}{(x(s)+\theta)} - \frac{\xi y(s)}{\gamma + x(s)}\Big) ds\Big] \\ &= x(t_1) \exp\Big[\int_{t_1}^{t_2} \Big(\frac{(1-x(s))(x(s)-\beta)}{(x(s)+\theta)} - \frac{\xi y(s)}{\gamma + x(s)}\Big) ds\Big] < x(t_1), \end{aligned}$$

because $\Big(\frac{(1-x(s))(x(s)-\beta)}{(x(s)+\theta)} - \frac{\xi y(s)}{\gamma+x(s)}\Big) < 0$ for all $t \in (t_1, t_2)$, which contradicts the assumed hypothesis. Thus $x(t) \leq 1$ for all $t \geq 0$.

Case II Next, suppose $x(0) > 1$. Then as long as $x(t) \geq 1$

$$x(t) = x(0) \exp\Big[\int_0^{t} \Big(\frac{(1-x(s))(x(s)-\beta)}{(x(s)+\theta)} - \frac{\xi y(s)}{\gamma + x(s)}\Big) ds\Big] < x(0),$$

because $\Big(\frac{(1-x(s))(x(s)-\beta)}{(x(s)+\theta)} - \frac{\xi y(s)}{\gamma+x(s)}\Big) < 0$ for $x(t) \geq 1$. Hence, from the cases I and II every positive solution holds $x(t) \leq \max\{x(0), 1\} \equiv M_1$ for all $t \geq 0$.

From second Eq. of the system (5.2.2), one gets

$$\frac{dy}{dt} \leq \rho y\Big(1 - \frac{y}{\gamma + M_1}\Big),$$

Then,

$$y(t) \leq \max\{y(0), \gamma + M_1\}, \qquad \forall t \geq 0.$$

Thus, the above discussion can be conclude as:

Lemma 5.2.1. **(a)** *All the solutions of the system* (5.2.2) *with its initial conditions are defined on* $[0, \infty)$ *and remain positive for all* $t \geq 0$.

(b) *All the solutions of the system* (5.2.2) *with its initial conditions are bounded for all* $t \geq 0$.

5.3 Equilibria and their Stability

The equilibrium points of the system (5.2.2) are the points of intersection of the prey zero growth isocline ($\frac{dx}{dt} = 0$) and predator zero growth isocline ($\frac{dy}{dt} = 0$) which lie in first quadrant, that is, positive solutions of the following system

$$\frac{dx}{dt} = \frac{dy}{dt} = 0. \tag{5.3.1}$$

5.3.1 Strong Allee Effect

The equilibrium points of the system (5.2.2) in case of strong Allee effect ($\beta > 0$) are

(*a*) $E_0 = (0, 0)$;

(*b*) $E_1 = (1, 0)$;

(*c*) $E_\beta = (\beta, 0)$;

(*d*) $E_\gamma = (0, \gamma)$;

(*e*) If $1 + \beta > \xi$, the system (5.2.2), has two positive interior equilibrium points, $E_1^* = (x_1^*, y_1^*)$ and $E_2^* = (x_2^*, y_2^*)$, whenever $\left(\frac{1+\beta-\xi}{2}\right)^2 > \beta + \xi\theta$; a double multiple positive interior equilibrium point $E^* = (x^*, y^*) = \left(\frac{1+\beta-\xi}{2}, \gamma + \frac{1+\beta-\xi}{2}\right)$, whenever $\left(\frac{1+\beta-\xi}{2}\right)^2 = \beta + \xi\theta$, where $x_1^* = \frac{1+\beta-\xi+\sqrt{(1+\beta-\xi)^2-4(\beta+\xi\theta)}}{2}, x_2^* = \frac{1+\beta-\xi-\sqrt{(1+\beta-\xi)^2-4(\beta+\xi\theta)}}{2}, y_1^* = \gamma + x_1^*$ and $y_2^* = \gamma + x_2^*$.

Thus, the number and location of equilibrium points of system (5.2.2) can be described by the following lemma:

Lemma 5.3.1. *If* $1 + \beta > \xi$, *the system* (5.2.2), *has*

(a) *Four equilibrium points* E_0, E_1, E_β *and* E_γ, *whenever* $\left(\frac{1+\beta-\xi}{2}\right)^2 < \beta + \xi\theta$.

(b) *Five equilibrium points* $E_0, E_1, E_\beta, E_\gamma$ *and* E^*, *whenever* $\left(\frac{1+\beta-\xi}{2}\right)^2 = \beta + \xi\theta$.

(c) *Six equilibrium points* $E_0, E_1, E_\beta, E_\gamma, E_1^*$ *and* E_2^*, *whenever* $\left(\frac{1+\beta-\xi}{2}\right)^2 > \beta + \xi\theta$.

Next, dynamics of system (5.2.2) in the neighborhood of each feasible equilibria has been investigated.

Theorem 5.3.2. *a) The equilibrium point E_0 is always a saddle point.*

b) The equilibrium point E_1 is always a saddle point.

c) The equilibrium point E_β is always an unstable point.

d) The equilibrium point E_γ is always a stable point.

e) The equilibrium point E_1^*, if exists, it is a stable point, if $x_1^*\left(\frac{1+\beta-\xi-2x_1^*}{x_1^*+\theta}+\frac{\xi}{\gamma+x_1^*}\right)-\rho<0$.

f) The equilibrium point E_2^*, if exists, is always a saddle point.

g) The equilibrium point E^*, if exists, is a degenerate singularity.

Proof. *a)* The Jacobian matrix of the system (5.2.2) at the equilibrium point E_0 is

$$J_{E_0}=\begin{bmatrix} -\frac{\beta}{\theta} & 0 \\ 0 & \rho \end{bmatrix},$$

which confirms that the equilibrium point E_0 is a saddle point as $0<\beta<1$.

b) The Jacobian matrix of the system (5.2.2) at the equilibrium point E_1 is

$$J_{E_1}=\begin{bmatrix} -\frac{1-\beta}{1+\theta} & -\frac{\xi}{1+\gamma} \\ 0 & \rho \end{bmatrix},$$

which confirms that the equilibrium point E_1 is a saddle point.

c) The Jacobian matrix of the system (5.2.2) at the equilibrium point E_β is

$$J_{E_\beta}=\begin{bmatrix} \beta\frac{1-\beta}{\beta+\theta} & -\frac{\beta\xi}{\gamma+\beta} \\ 0 & \rho \end{bmatrix},$$

which confirms that the equilibrium point E_β is an unstable point.

d) The Jacobian matrix of the system (5.2.2) at the equilibrium point E_γ is

$$J_{E_\gamma} = \begin{bmatrix} \frac{-\beta}{\theta} - \xi & 0 \\ \rho & -\rho \end{bmatrix},$$

which confirms that the equilibrium point E_γ is a stable point.

e) The Jacobian matrix of the system (5.2.2) at an interior equilibrium point $E(x, y)$ (say) is

$$J_E = \begin{bmatrix} x\Big(\frac{1+\beta-\xi-2x}{x+\theta} + \frac{\xi}{\gamma+x}\Big) & -\frac{\xi x}{\gamma+x} \\ \rho & -\rho \end{bmatrix}. \tag{5.3.2}$$

The determinant of the above Jacobian matrix is $\det(J_E) = -\rho x\frac{1+\beta-\xi-2x}{x+\theta}$ and the trace is $tr(J_E) = x\Big(\frac{1+\beta-\xi-2x}{x+\theta} + \frac{\xi}{\gamma+x}\Big) - \rho$. A simple computation conclude that $det(J_{E_1^*}) > 0$. Thus, equilibrium point E_1^* is stable, if $x_1^*\Big(\frac{1+\beta-\xi-2x_1^*}{x_1^*+\theta} + \frac{\xi}{\gamma+x_1^*}\Big) - \rho < 0$.

f) From (5.3.2), $det(J_{E_2^*}) < 0$, which confirms that the equilibrium point E_2^* is a saddle point.

g) From (5.3.2), $det(J_{E^*}) = 0$, so the equilibrium point E^* is a degenerate singularity.

■

It is proved in Theorem 5.3.2(g) that the interior equilibrium point E^* is a degenerate singularity, and so, the system may have complicated properties in the neighbourhood of the point E^*.

In the following, the dynamics of the system (5.2.2) in the neighbourhood of the equilibrium point E^* has been discussed.

Theorem 5.3.3. *The interior equilibrium point E^*, if exists, is*

a) *a saddle-node, whenever $\frac{\xi x^*}{\gamma+x^*} \neq \rho$ holds.*

b) *a cusp of codimension* 2, *whenever $\frac{\xi x^*}{\gamma+x^*} = \rho$ and $\frac{\xi\gamma}{(x^*+\gamma)^2} - 2\frac{x^*}{x^*+\theta} \neq 0$ hold.*

Proof. (*a*) First, consider transformation $\hat{x} = x - x^*$, $\hat{y} = y - y^*$ to shift the equilibrium point E^* of the system (5.2.2) to the origin and then expand the right-hand side of the

system as a Taylor series, the system (5.2.2) can be rewritten as

$$\begin{cases} \frac{d\hat{x}}{dt} = \frac{\xi x^*}{\gamma+x^*}\hat{x} - \frac{\xi x^*}{\gamma+x^*}\hat{y} + \alpha_{20}\hat{x}^2 + \alpha_{11}\hat{x}\hat{y} + o|(x,y)^3|, \\ \frac{d\hat{y}}{dt} = \rho\hat{x} - \rho\hat{y} - \frac{\rho}{\gamma+x^*}\hat{x}^2 + \frac{2\rho}{\gamma+x^*}\hat{x}\hat{y} - \frac{\rho}{\gamma+x^*}\hat{y}^2 + o|(x,y)^3|, \end{cases} \tag{5.3.3}$$

where $\alpha_{20} = \frac{\xi\gamma}{(\gamma+x^*)^2} - \frac{x^*}{x^*+\theta}$, $\alpha_{11} = -\frac{\xi\gamma}{(x^*+\gamma)^2}$.

If $\frac{\xi x^*}{\gamma+x^*} \neq \rho$, the $tr(J_{E^*}) \neq 0$, while $\det(J_{E^*}) = 0$. Hence, the equilibrium point E^* is a saddle node.

(b) Consider $\frac{\xi x^*}{\gamma+x^*} = \rho$, then the system (5.3.3) reduces to

$$\begin{cases} \frac{d\hat{x}}{dt} = \rho\hat{x} - \rho\hat{y} + \alpha_{20}\hat{x}^2 + \alpha_{11}\hat{x}\hat{y} + o|(x,y)^3|, \\ \frac{d\hat{y}}{dt} = \rho\hat{x} - \rho\hat{y} - \frac{\rho}{\gamma+x^*}\hat{x}^2 + \frac{2\rho}{\gamma+x^*}\hat{x}\hat{y} - \frac{\rho}{\gamma+x^*}\hat{y}^2 + o|(x,y)^3|. \end{cases} \tag{5.3.4}$$

On introducing the variable $\tau = \rho t$, the system (5.3.4) reduces to the following system

$$\begin{cases} \frac{d\hat{x}}{d\tau} = \hat{x} - \hat{y} + \hat{\alpha_{20}}\hat{x}^2 + \hat{\alpha_{11}}\hat{x}\hat{y} + o|(x,y)^3|, \\ \frac{d\hat{y}}{d\tau} = \hat{x} - \hat{y} - \frac{1}{\gamma+x^*}\hat{x}^2 + \frac{2}{\gamma+x^*}\hat{x}\hat{y} - \frac{1}{\gamma+x^*}\hat{y}^2 + o|(x,y)^3|, \end{cases} \tag{5.3.5}$$

where $\hat{\alpha_{20}} = \frac{1}{\rho}\alpha_{20}$ and $\hat{\alpha_{11}} = \frac{1}{\rho}\alpha_{11}$.

Now, on using the transformation $x_1 = \hat{x}$, $x_2 = \hat{x} - \hat{y}$, the system (5.3.5) reduces to the following system

$$\begin{cases} \frac{dx_1}{d\tau} = x_2 + \overline{\alpha_{20}}x_1^2 - \hat{\alpha_{11}}x_1x_2 + o|(y_1,y_2)^3|, \\ \frac{dx_2}{d\tau} = \overline{\alpha_{20}}x_1^2 - \hat{\alpha_{11}}x_1x_2 + \frac{1}{x^*+\gamma}x_2^2 + o|(y_1,y_2)^3|, \end{cases} \tag{5.3.6}$$

where $\overline{\alpha_{20}} = \hat{\alpha_{20}} + \hat{\alpha_{11}}$.

On using the transformation $y_1 = x_1$, $y_2 = x_2 - \frac{1}{x^*+\gamma}x_1x_2$, the system (5.3.6) reduces to

$$\begin{cases} \frac{dy_1}{d\tau} = y_2 + \overline{\alpha_{20}}y_1^2 + \overline{\alpha_{11}}y_1y_2 + o|(y_1,y_2)^3|, \\ \frac{dy_2}{d\tau} = \overline{\alpha_{20}}y_1^2 - \hat{\alpha_{11}}y_1y_2 + o|(y_1,y_2)^3|, \end{cases} \tag{5.3.7}$$

where $\overline{\alpha_{11}} = \left(\frac{1}{x^*+\gamma} - \hat{\alpha_{11}}\right)$.

Finally, using the transformation $z_1 = y_1 - \frac{1}{2}\overline{\alpha_{11}}y_1^2$, $z_2 = y_2 + \overline{\alpha_{20}}y_1^2 + o|(z_1,z_2)^3|$,

the system (5.3.7) reduces to

$$\begin{cases} \frac{dz_1}{d\tau} = z_2, \\ \frac{dz_2}{d\tau} = \overline{\alpha_{20}} y_1^2 + (2\overline{\alpha_{20}} - \hat{\alpha_{11}}) y_1 y_2 + o|(z_1, z_2)^3|. \end{cases} \tag{5.3.8}$$

Since $\overline{\alpha_{20}} = -\frac{x^*}{\rho(x^*+\theta)} \neq 0$ and, if $2\overline{\alpha_{20}} - \hat{\alpha_{11}} = \frac{1}{\rho}\left(\frac{\xi\gamma}{(x^*+\gamma)^2} - 2\frac{x^*}{x^*+\theta}\right) \neq 0$, the origin in $z_1 z_2$ plane is a cusp of codimension 2, that is, E^* in xy plane is a cusp of codimension 2. ■

5.3.2 Weak Allee Effect

The equilibrium points of the system (5.2.2) in case of weak Allee effect ($\beta < 0$) are

(*a*) $e_0 = (0, 0)$;

(*b*) $e_1 = (1, 0)$;

(*c*) $e_\gamma = (0, \gamma)$;

(*d*) If $\beta + \xi < 1$, the system (5.2.2), has two positive interior equilibrium points $e_1^* = (\overline{x_1}, \overline{y_1})$ and $e_2^* = (\overline{x_2}, \overline{y_2})$, whenever $\left(\frac{1-\beta-\xi}{2}\right)^2 + \beta > \xi\theta > \beta$; a double multiple positive interior equilibrium point $e^* = (x_*, y_*) = \left(\frac{1-\beta-\xi}{2}, \gamma + \frac{1-\beta-\xi}{2}\right)$, whenever $\left(\frac{1-\beta-\xi}{2}\right)^2 + \beta = \xi\theta > \beta$, has a unique positive interior equilibrium point $e_* = (\overline{x_3}, \overline{y_3})$, whenever $\beta > \xi\theta$, has a unique positive interior equilibrium point $e = (\overline{x_4}, \overline{y_4}) = (1-\beta-\xi, 1+\gamma-\beta-\xi)$, whenever $\beta = \xi\theta$, where $\overline{x_1} = \frac{1-\beta-\xi+\sqrt{(1-\beta-\xi)^2-4(\xi\theta-\beta)}}{2}$, $\overline{x_2} = \frac{1-\beta-\xi-\sqrt{(1-\beta-\xi)^2-4(\xi\theta-\beta)}}{2}$, $\overline{x_3} = \frac{1-\beta-\xi+\sqrt{(1-\beta-\xi)^2-4(\xi\theta-\beta)}}{2}$, $\overline{y_1} = \gamma + \overline{x_1}$, $\overline{y_2} = \gamma + \overline{x_2}$ and $\overline{y_3} = \gamma + \overline{x_3}$.

Thus, the number and location of equilibrium points of system (5.2.2) can be described by the following lemma:

Lemma 5.3.4. *If $\beta + \xi < 1$, the system* (5.2.2)*, has*

(a) *Three equilibrium points, e_0, e_1 and e_γ, whenever $\left(\frac{1-\beta-\xi}{2}\right)^2 < \xi\theta - \beta$ and $\xi\theta > \beta$.*

(b) *Four equilibrium points, e_0, e_1, e_γ and e^*, whenever $\left(\frac{1-\beta-\xi}{2}\right)^2 + \beta = \xi\theta > \beta$.*

(c) *Four equilibrium points, e_0, e_1, e_γ and e_*, whenever $\beta > \xi\theta$.*

(d) *Four equilibrium points,* e_0, e_1, e_γ *and* e*, whenever* $\beta = \xi\theta$*.*

(e) *Five equilibrium points,* $e_0, e_1, e_\gamma, e_1^*$ *and* e_2^**, whenever* $\left(\frac{1-\beta-\xi}{2}\right)^2 + \beta > \xi\theta > \beta$*.*

The dynamics of system (5.2.2) in the neighborhood of each feasible equilibria are concluded in the following

Theorem 5.3.5. *a) The equilibrium point* e_0 *is always an unstable point.*

b) The equilibrium point e_1 *is always a saddle point.*

c) The equilibrium point e_γ *is asymptotically stable, whenever* $\beta < \xi\theta$ *and a saddle, whenever* $\beta > \xi\theta$*.*

d) The equilibrium point e_1^**, if exists, is a stable point if* $\overline{x_1}\left(\frac{1-\beta-\xi-2\overline{x_1}}{\overline{x_1}+\theta} + \frac{\xi}{\gamma+\overline{x_1}}\right) - \rho < 0$*.*

f) The equilibrium point e_2^**, if exists, is always a saddle point.*

g) The equilibrium point e_**, if exists, is a stable point, if* $\overline{x_3}\left(\frac{1-\beta-\xi-2\overline{x_3}}{\overline{x_3}+\theta} + \frac{\xi}{\gamma+\overline{x_3}}\right) - \rho < 0$*.*

h) The equilibrium point e*, if exist, is a stable point if* $\overline{x_4}\left(\frac{1-\beta-\xi-2\overline{x_4}}{\overline{x_4}+\theta} + \frac{\xi}{\gamma+\overline{x_4}}\right) - \rho < 0$*.*

i) The equilibrium point e^**, if exists, is a degenerate singularity. Moreover, it is*

1) *a saddle node, whenever* $\frac{\xi x_*}{\gamma+x_*} \neq \rho$ *holds.*

2) *a cusp of codimension* 2*, whenever* $\frac{\xi x_*}{\gamma+x_*} = \rho$ *and* $\frac{\xi\gamma}{(x_*+\gamma)^2} - 2\frac{x_*}{x_*+\theta} \neq 0$ *hold.*

The proof of Theorem 5.3.5 is similar to Theorem 5.3.2 and Theorem 5.3.3.

5.4 Bifurcation Analysis

This section concerns with the bifurcation analysis, occur in system (5.2.2). It has been shown that for certain parametric conditions some of the equilibrium points may be hyperbolic or degenerate singularities, and hence, system may undergo to some bifurcations.

5.4.1 Strong Allee Effect

Hopf Bifurcation

In Theorem 5.3.2, it is proved that the interior equilibrium point E_2^*, if exists, is always a saddle point while E_1^*, if exists, is stable, whenever $x_1^*\Big(\frac{1+\beta-\xi-2x_1^*}{x_1^*+\theta}+\frac{\xi}{\gamma+x_1^*}\Big) < \rho$. If $x_1^*\Big(\frac{1+\beta-\xi-2x_1^*}{x_1^*+\theta}+\frac{\xi}{\gamma+x_1^*}\Big) = \rho$, the trace of the Jacobian matrix $J_{E_1^*}$ is zero and determinant is positive, which confirms that the eigenvalues of the Jacobian matrix $J_{E_1^*}$ are purely imaginary, that is, the equilibrium point E_1^* is either a weak focus or a centre. Now, it is shown that the system (5.2.2) undergoes to a Hopf bifurcation. Consider ρ be the Hopf bifurcation parameter, then the threshold magnitude $\rho = \rho^{[hf]} = x_1^*\Big(\frac{1+\beta-\xi-2x_1^*}{x_1^*+\theta}+\frac{\xi}{\gamma+x_1^*}\Big)$ exists, which satisfies $\det(J_{E_1^*}) > 0$ and $tr(J_{E_1^*}) = 0$. Also at $\rho = \rho^{[hf]}$, one gets

$$\frac{\partial}{\partial\rho}(trE_1^*) = -1 \neq 0.$$

Thus, the transversality condition of Hopf bifurcation holds, which ensures that the system (5.2.2) undergoes to a Hopf bifurcation at the equilibrium point E_1^*.

Now, in order to discuss the stability of limit cycle, the first Lyapunov number σ at interior equilibrium point $E_1^*(x_1^*, y_1^*)$ of the system (5.2.2) is computed by using the procedure as given in Perko (1996). Let $x = u - x_1^*,\ y = v - y_1^*$, the system (5.2.2), in the vicinity of origin, can be written as

$$\begin{aligned}
\frac{du}{dt} &= a_{10}u + a_{01}v + a_{20}u^2 + a_{11}uv + a_{02}v^2 + a_{30}u^3 + a_{21}u^2v + a_{12}uv^2 + a_{03}v^3 + P(u,v),\\
\frac{dv}{dt} &= b_{10}u + b_{01}v + b_{20}u^2 + b_{11}uv + b_{02}v^2 + b_{30}u^3 + b_{21}u^2v + b_{12}uv^2 + b_{03}v^3 + Q(u,v),
\end{aligned}$$

where $a_{10} = x_1^*\Big(\frac{1+\beta-\xi-2x_1^*}{x_1^*+\theta}+\frac{\xi}{\gamma+x_1^*}\Big)$, $a_{01} = -\frac{\xi x_1^*}{\gamma+x_1^*}$, $a_{20} = \frac{\theta(1+\beta-\xi-2x_1^*)}{(\theta+x_1^*)^2} - \frac{x_1^*}{x_1^*+\theta} + \frac{\xi\gamma}{(x_1^*+\gamma)^2}$, $a_{11} = -\frac{\xi\gamma}{(x_1^*+\gamma)^2}$, $a_{02} = 0$, $a_{30} = \frac{\theta(-1-\beta+\xi+2x_1^*)}{(x_1^*+\theta)^3} - \frac{\theta}{(x_1^*+\theta)^2} - \frac{\xi\gamma}{(x_1^*+\gamma)^3}$, $a_{21} = \frac{\xi\gamma}{(x_1^*+\gamma)^3}$, $a_{12} = 0$, $a_{03} = 0$, $b_{10} = \rho$, $b_{01} = -\rho$, $b_{20} = -\frac{\rho}{\gamma+x_1^*}$, $b_{11} = \frac{2\rho}{\gamma+x_1^*}$, $b_{02} = -\frac{\rho}{\gamma+x_1^*}$, $b_{30} = \frac{\rho}{(\gamma+x_1^*)^2}$, $b_{21} = -\frac{2\rho}{(\gamma+x_1^*)^2}$, $b_{12} = \frac{\rho}{(\gamma+x_1^*)^2}$, $b_{03} = 0$, $P(u,v) = \sum_{i+j=4}^{\infty} a_{ij}u^iv^j$ and $Q(u,v) = \sum_{i+j=4}^{\infty} b_{ij}u^iv^j$.

Hence, first Lyapunov number σ can be computed by the formula defined in equation (1.3.7)

with $\Delta = \frac{\rho x_1^*}{(\theta+x_1^*)}\sqrt{(1+\beta-\xi)^2-4(\beta+\xi\theta)}$. Therefore, the subcritical Hopf bifurcation exists, if $\sigma > 0$ and supercritical Hopf bifurcation exists, if $\sigma < 0$.

From the above discussion, it can be conclude that

Theorem 5.4.1. *The system* (5.2.2) *undergoes a Hopf bifurcation with respect to bifurcation parameter* ρ *around the point* E_1^**, if exists, whenever* $x_1^*\Big(\frac{1+\beta-\xi-2x_1^*}{x_1^*+\theta}+\frac{\xi}{\gamma+x_1^*}\Big) = \rho$ *and an unstable (stable) limit cycle arises around the point* E_1^**, if* $\sigma > 0$ *(*$\sigma < 0$*).*

Saddle-node Bifurcation

It has been shown that if $1+\beta > \xi$, the system (5.2.2) has two positive interior equilibrium points E_1^* and E_2^* whenever $\Big(\frac{1+\beta-\xi}{2}\Big)^2 > \beta+\xi\theta$ and these two interior equilibrium points coincide with each other and a unique interior equilibrium point E^* is obtained, whenever $\Big(\frac{1+\beta-\xi}{2}\Big)^2 = \beta+\xi\theta$. Also the system (5.2.2) has no positive interior equilibrium point, whenever $\Big(\frac{1+\beta-\xi}{2}\Big)^2 < \beta+\xi\theta$. The annihilation of positive interior equilibrium points are may be due to the occurrence of Saddle-node bifurcation at the interior equilibrium point, whenever the parameter θ crosses the critical value $\theta = \theta^{[SN]} = \frac{1}{\xi}\Big(\Big(\frac{1+\beta-\xi}{2}\Big)^2-\beta\Big)$. In Theorem 5.3.3, it is shown that the unique interior equilibrium point E^* is a saddle-node, whenever $\frac{\xi x^*}{\gamma+x^*} \neq \rho$. To ensure that the system (5.2.2) undergoes a saddle-node bifurcation, Sotomayor's theorem has been applied (Perko 1996). The parameter θ is taken as the bifurcation parameter.

Since $det(J_{E^*}) = 0$, therefore one eigenvalue of the Jacobian matrix J_{E^*} is zero. If $tr(J_{E^*}) < 0$, the other eigenvalue has negative real part. Suppose V and W be the eigenvectors corresponding to zero eigenvalue of the matrix J_{E^*} and $J_{E^*}^T$ respectively, then

$$V = \begin{bmatrix} 1 \\ 1 \end{bmatrix}; \quad W = \begin{bmatrix} 1 \\ -\frac{\xi x^*}{x^*+\gamma} \end{bmatrix}.$$

Now,

$W^T F_\theta(E^*, \theta^{[SN]}) = -\frac{x^*(1-\beta+\xi)(1+\beta-\xi)}{2(x^*+\theta^{[SN]})^2} \neq 0$, as $1+\beta-\xi > 0, \quad 1-\beta+\xi > 0,$

$W^T[D^2F(E^*, \theta^{[SN]})(V,V)] = -\frac{2x^*}{x^*+\theta^{[SN]}} \neq 0,$

where $F_\theta(E^*, \theta^{[SN]}) = \begin{bmatrix} -\frac{x^*(1-x^*)(x^*-\beta)}{(x^*+\theta^{[SN]})^2} \\ 0 \end{bmatrix}$; $D^2F(E^*, \theta^{[SN]}) = \begin{bmatrix} -\frac{2x^*}{x^*+\theta^{[SN]}} \\ 0 \end{bmatrix}$.

Thus, the transversality conditions for Saddle-node bifurcation are satisfied. The above discussion can be summarised as

Theorem 5.4.2. *The system* (5.2.2) *undergoes a Saddle-node bifurcation with respect to the bifurcation parameter* θ *around the equilibrium point* E^*, *whenever* $1 + \beta > \xi, \theta = \frac{1}{\xi}\left(\left(\frac{1+\beta-\xi}{2}\right)^2 - \beta\right)$ *and* $\frac{\xi x^*}{\gamma+x^*} \neq \rho$.

Bogdanov-Takens Bifurcation

In Theorem 5.4.2, it is proved that the system (5.2.2) undergoes a Saddle-node bifurcation at the equilibrium point E^*, if exists, whenever $\frac{\xi x^*}{\gamma+x^*} \neq \rho$, that is, $tr(J_{E^*}) \neq 0$. Now, consider $tr(J_{E^*}) = 0$. In this case the Jacobian matrix J_{E^*} has double zero eigenvalues, but the jacobian matrix J_{E^*} is not a zero matrix. So, here is a chance of codimension 2 bifurcation (Bogdanov-Takens bifurcation). In Theorem 5.3.3, it is shown that the equilibrium point E^* is a cusp of codimension 2, whenever $\frac{\xi x^*}{\gamma+x^*} = \rho$, and $\frac{\xi\gamma}{(x^*+\gamma)^2} - 2\frac{x^*}{x^*+\theta} \neq 0$. Now, choose ξ and ρ as the bifurcation parameter as they are important from the ecological point of view. The Bogdanov-Taken point in the parameter space is the intersection point of the Saddle-Node bifurcation curve and the Hopf bifurcation curve. The algorithm given in Kuznetsov (2004) has been applied to prove the non-degeneracy conditions of Bogdanov-Takens bifurcation.

Suppose the bifurcation parameters ξ and ρ vary in a small domain of BT point (ξ_0, ρ_0), and let $(\xi_0 + \lambda_1, \rho_0 + \lambda_2)$ be a point in the neighbourhood of the BT-point (ξ_0, ρ_0) where λ_1, λ_2 are small. Thus, the system (5.2.2) reduces to

$$\begin{cases} \frac{dx}{dt} = \frac{x(1-x)(x-\beta)}{x+\theta} - \frac{(\xi+\lambda_1)xy}{x+\gamma}, \\ \frac{dy}{dt} = (\rho+\lambda_2)y\left(1 - \frac{y}{x+\gamma}\right). \end{cases} \tag{5.4.1}$$

The system (5.4.1) is C^∞ smooth with respect to the variables x, y in a small neighbourhood of (ξ_0, ρ_0).

Define $x_1 = x - x^*, x_2 = y - y^*$, then the system (5.4.1) reduces to

$$\begin{cases} \frac{dx_1}{dt} = a_{00} + a_{10}x_1 + a_{01}x_2 + a_{20}x_1^2 + a_{11}x_1x_2 + R_1(x_1, x_2), \\ \frac{dx_2}{dt} = b_{10}x_1 + b_{01}x_2 + b_{20}x_1^2 + b_{11}x_1x_2 + b_{02}x_2^2 + R_2(x_1, x_2), \end{cases} \tag{5.4.2}$$

where $a_{00} = -\lambda_1 x^*$, $a_{10} = \frac{x^*(\xi+\lambda_1)}{x^*+\gamma} - \lambda_1$, $a_{01} = -\frac{(\xi+\lambda_1)x^*}{x^*+\gamma}$, $a_{20} = -\frac{x^*}{x^*+\theta} + \frac{(\xi+\lambda_1)\gamma}{(x^*+\gamma)^2}$, $a_{11} = -\frac{(\xi+\lambda_1)\gamma}{(x^*+\gamma)^2}$, $b_{10} = \rho + \lambda_2$, $b_{01} = -(\rho+\lambda_2)$, $b_{20} = -\frac{\rho+\lambda_2}{x^*+\gamma}$, $b_{11} = \frac{2(\rho+\lambda_2)}{x^*+\gamma}$, $b_{02} = -\frac{\rho+\lambda_2}{x^*+\gamma}$ and R_1, R_2 are the power series in (x_1, x_2) with powers $x_1^i x_2^j$ satisfying $i + j \geq 3$.

Consider the affine transformation $y_1 = x_1$, $y_2 = ax_1 + bx_2 \Big(a = \frac{(\xi+\lambda_1)x^*}{x^*+\gamma}, b = -\frac{(\xi+\lambda_1)x^*}{x^*+\gamma}\Big)$ in the system (5.4.2), one gets

$$\begin{cases} \frac{dy_1}{dt} = & y_2 + \xi_{00}(\lambda) + \xi_{10}(\lambda)y_1 + \xi_{01}(\lambda)y_2 + \xi_{20}(\lambda)y_1^2 + \\ & \xi_{11}(\lambda)y_1y_2 + \overline{R}_1(y_1, y_2), \\ \frac{dy_2}{dt} = & \eta_{00}(\lambda) + \eta_{10}(\lambda)y_1 + \eta_{01}(\lambda)y_2 + \eta_{20}(\lambda)y_1^2 + \eta_{11}(\lambda)y_1y_2 + \\ & \eta_{02}y_2^2 + \overline{R}_2(y_1, y_2), \end{cases} \tag{5.4.3}$$

where $\xi_{00}(\lambda) = -\lambda_1 x^*$, $\xi_{10}(\lambda) = -\lambda_1$, $\xi_{01} = \frac{\lambda_1}{\xi}$, $\xi_{20}(\lambda) = -\frac{x^*}{x^*+\theta}$, $\xi_{11}(\lambda) = \frac{(\xi+\lambda_1)\gamma}{(x^*+\gamma)\xi x^*}$, $\eta_{00}(\lambda) = -a\lambda_1 x^*$, $\eta_{10}(\lambda) = -a\lambda_1$, $\eta_{01}(\lambda) = -\Big(\frac{\lambda_1 x^*}{x^*+\theta} + \lambda_2 + \rho\Big)$, $\eta_{20}(\lambda) = -\frac{\xi(x^*)^2}{(x^*+\gamma)(x^*+\theta)}$, $\eta_{11}(\lambda) = \frac{(\xi+\lambda_1)\gamma}{(x^*+\gamma)^2}$, $\eta_{02}(\lambda) = \frac{\rho+\lambda_2}{\xi x^*}$ and $\overline{R_1}$, $\overline{R_2}$ are the power series in (y_1, y_2) with powers $y_1^i y_2^j$ satisfying $i + j \geq 3$.

The non-degeneracy conditions of Bogodanov-Takens bifurcation (Kuznetsov 2004) are

$$\begin{bmatrix} \frac{(\xi+\lambda_1)x^*}{x^*+\gamma} & -\frac{(\xi+\lambda_1)x^*}{x^*+\gamma} \\ \rho & -\rho \end{bmatrix} \neq \theta_{2\times 2},$$

$$2\xi_{20}(0) + \eta_{11}(0) \neq 0,$$

$$\eta_{20}(0) \neq 0.$$

One gets

$$2\xi_{20}(0) + \eta_{11}(0) = \frac{\xi\gamma}{(x^*+\gamma)^2} - 2\frac{x^*}{x^*+\theta},$$

$$\eta_{20}(0) = -\frac{\xi(x^*)^2}{(x^*+\gamma)(x^*+\theta)} \neq 0.$$

Thus, the non-degeneracy condition of the Bogdanov-Takens bifurcation is satisfied whenever $\frac{\xi\gamma}{(x^*+\gamma)^2} - 2\frac{x^*}{x^*+\theta} \neq 0$.

The above discussion can be summarized as

Theorem 5.4.3. *The system* (5.2.2) *undergoes a Bogdanov-Takens bifurcation with respect to the bifurcation parameter ξ and ρ around the equilibrium point E^*, whenever $1+\beta > \xi, \theta = \frac{1}{\xi}\left(\left(\frac{1+\beta-\xi}{2}\right)^2 - \beta\right), \frac{\xi x^*}{\gamma+x^*} = \rho$ and $\frac{\xi\gamma}{(x^*+\gamma)^2} - 2\frac{x^*}{x^*+\theta} \neq 0$.*

5.4.2 Weak Allee Effect

As discussed in case of strong Allee effect, the system (5.2.2) exhibits Hopf, Saddle-node and Bogdanov-Taken bifurcations in case of weak Allee effect with respect to the corresponding parameter(s) which are concluded in the following theorem. The proof of these theorems are omitted for the shake of brevity.

Theorem 5.4.4. *The system* (5.2.2) *undergoes*

a) a hopf bifurcation with respect to bifurcation parameter ρ around the point

1) *e_1^*, if $\overline{x_1}\left(\frac{1-\beta-\xi-2\overline{x_1}}{\overline{x_1}+\theta} + \frac{\xi}{\gamma+\overline{x_1}}\right) = \rho$ and unstable (stable) limit cycle arises around the point e_1^*, if $\sigma > 0 (\sigma < 0)$*

2) *e_*, if $\overline{x_3}\left(\frac{1-\beta-\xi-2\overline{x_3}}{\overline{x_3}+\theta} + \frac{\xi}{\gamma+\overline{x_3}}\right) = \rho$ and unstable (stable) limit cycle arises around the point e_*, if $\sigma > 0 (\sigma < 0)$*

3) *e, if $\overline{x_4}\left(\frac{1-\beta-\xi-2\overline{x_4}}{\overline{x_4}+\theta} + \frac{\xi}{\gamma+\overline{x_4}}\right) = \rho$ and unstable (stable) limit cycle arises around the point e, if $\sigma > 0 (\sigma < 0)$.*

b) a Saddle-node bifurcation with respect to the bifurcation parameter θ around the equilibrium point e^*, whenever $\beta + \xi < 1, \theta = \frac{1}{\xi}\left(\left(\frac{1-\beta-\xi}{2}\right)^2 + \beta\right)$ and $\frac{\xi x_*}{\gamma+x_*} \neq \rho$.

c) a Bogdanov-Takens bifurcation with respect to the bifurcation parameter ξ and ρ around the equilibrium point e^*, whenever $\beta + \xi < 1, \theta = \frac{1}{\xi}\left(\left(\frac{1-\beta-\xi}{2}\right)^2 + \beta\right), \frac{\xi x_*}{\gamma+x_*} = \rho$ and $\frac{\xi\gamma}{(x_*+\gamma)^2} - 2\frac{x_*}{x_*+\theta} \neq 0$.

5.5 Numerical Simulations

In this section numerical simulations are carried out to support the analytical results obtained above.

(1) $\beta = 0.4$, $\gamma = 0.1$, $\xi = 0.1$, $\rho = 0.2$, $\theta = 0.05$. The system (5.2.2) has two positive interior equilibrium points; $E_1^*(x_1^*, y_1^*) = (0.782288, 0.882288)$ and $E_2^*(x_2^*, y_2^*) = (0.517712, 0.617712)$. If $\theta = \theta^{[SN]} = 0.225$, the two interior equilibrium points coincide and the system (5.2.2) has only one interior equilibrium point $E^*(x^*, y^*) = (0.65, 0.75)$. If $\theta = 0.5$, the system (5.2.2) has no interior equilibrium point (Figure 5.1(a)). The phase portrait for $\theta = \theta^{[SN]} = 0.225$ is depicted in Figure 5.1(b) in which the equilibrium point E^* is stable for the region lies right to the separatrix (dashed trajectories) while unstable for the region lies left to separatrix. The Saddle-node bifurcation diagram are depicted in figures 5.1(c)and5.1(d).

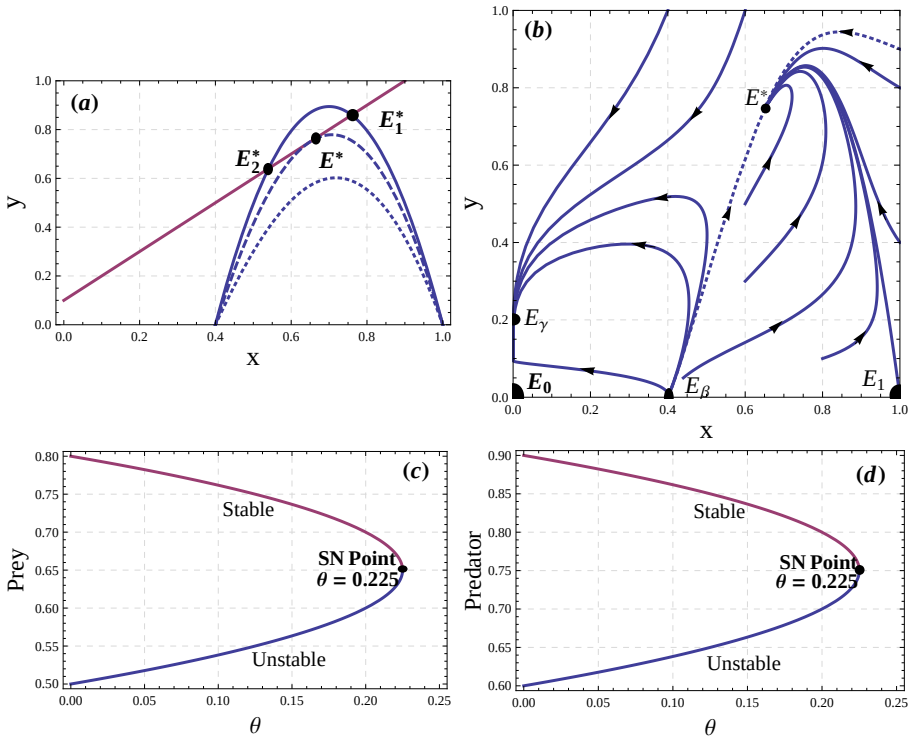

Figure 5.1: Strong Allee effect: $\beta = 0.4, \gamma = 0.1, \xi = 0.1, \rho = 0.2$. (a) This diagram shows how the number of interior equilibrium points changes with θ. All parabola are the prey nullcline for different values of θ and line is predator nullcline. For solid parabola $\theta = 0.05$ for dashed parabola $\theta = 0.225$ and for dotted parabola $\theta = 0.5$. (b) Phase portrait diagram of system (5.2.2) for $\theta = 0.225$. The dotted trajectories are the separatrix. (c) and (d) are the bifurcation diagram of the system (5.2.2). The upper curve stands for the stable equilibrium and the lower curve stands for unstable equilibrium.

(2) $\beta = 0.4,\ \gamma = 0.1,\ \xi = 0.1,\ \rho = 0.2,\ \theta = 0.2$. The system (5.2.2) has two interior equilibrium points; $E_1^*(x_1^*, y_1^*) = (0.7, 0.8)$ and $E_2^*(x_2^*, y_2^*) = (0.6, 0.7)$. The equilibrium point E_2^* is always a saddle point and the equilibrium point E_1^* is stable (Figure 5.2(a)). If $\rho = \rho^{[hf]} = 0.009722222$, the system (5.2.2) undergoes to a Hopf bifurcation at the point E_1^* and since the first Lyapunov number $\sigma = 2804.28\pi > 0$, an unstable limit cycle arises around the point E_1^* (Figure 5.2(b)). If $\rho = 0.0166067444209$, a Homoclinic loop is created around E_1^* (Figure 5.2(c)). If $\rho = 0.008$, the equilibrium point E_1^* is unstable (Figure 5.2(d))

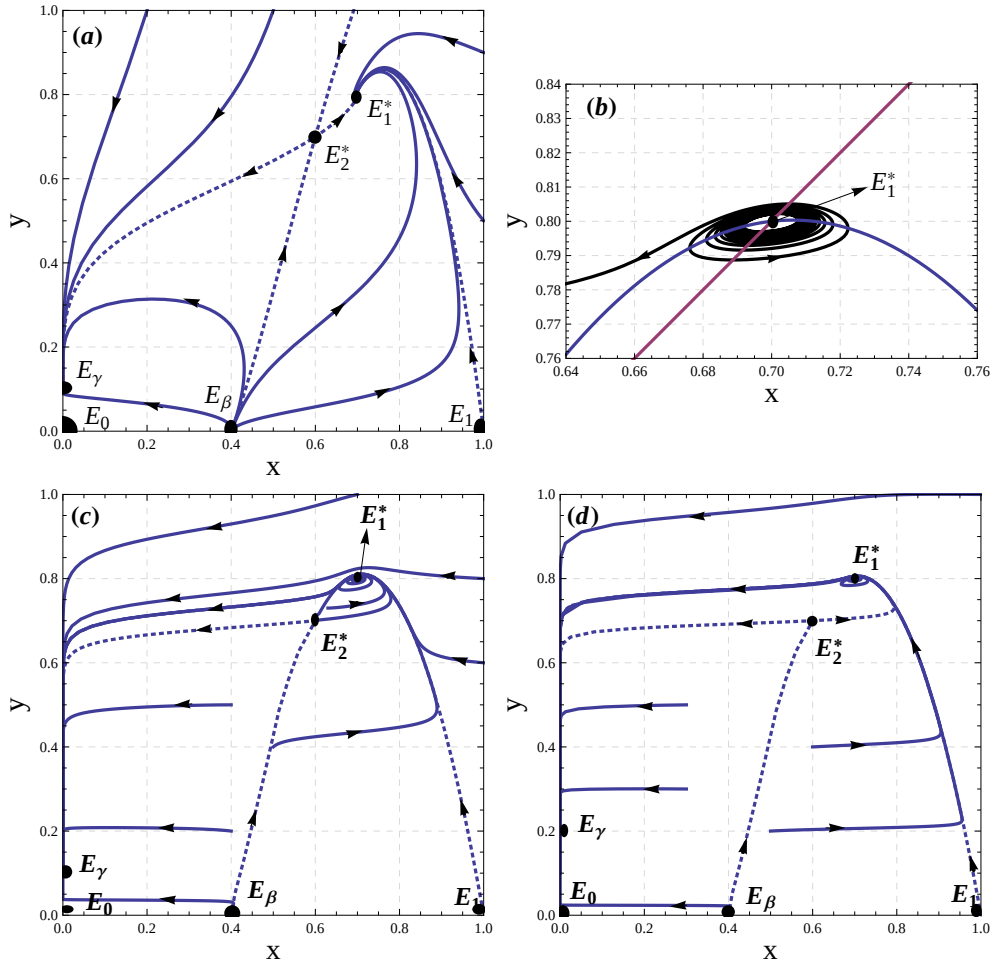

Figure 5.2: Strong Allee effect: $\beta = 0.4, \gamma = 0.1, \xi = 0.1, \theta = 0.2$. (a) $\rho = 0.2$ two interior equilibrium points exist. E_1^* is asymptotically stable and E_2^* is saddle. (b) $\rho = 0.009722$ an unstable limit cycle bifurcates through Hopf bifurcation around E_1^* (c) $\rho = 0.0166067444209415$ The diagram shows that the limit cycle collides with the saddle point E_2^* to give a Homoclinic loop. (d) $\rho = 0.008$ E_1^* is unstable point. The Dotted trajectories are the stable and unstable manifolds.

(3) $\beta = 0.3,\ \gamma = 0.2,\ \theta = 0.1$. The BT bifurcation point in the $\xi\rho$ space is $(\xi_0, \rho_0) = (0.17335, 0.12793)$, intersection point of the Saddle-node bifurcation curve and the Hopf-bifurcation curve and $E^* = (0.563325, 0.763325)$. The bifurcation diagram in the vicinity of the BT point in the parameter space is shown in Figure 5.3(a). A third curve (dotted curve) coming out from the BT point is a curve of non-local bifurcation of a formation of a separatrix loop obtained numerically. The Figure 5.3(b) shows that the unique interior equilibrium point E^* is a cusp of codimension 2. If ξ and ρ lie in first region ($(\xi_0, \rho_0) = (0.175, 0.05)$), the system (5.2.2) has no interior equilibrium point (Figure 5.3(c)). If ξ and ρ lie in second region ($(\xi_0, \rho_0) = (0.170, 0.10)$), then the system (5.2.2) has two interior equilibrium points; one is a saddle point and other is asymptotically stable. The stable manifold of the saddle equilibrium point serves as separatrix for the basin of attraction of the axial equilibrium point E_γ and the stable interior equilibrium (Figure 5.3(d)). If ξ and ρ lie in third region ($(\xi_0, \rho_0) = (0.169, 0.0634)$), the system (5.2.2) has two interior equilibrium points; one is a saddle and other is a stable point surrounded by an unstable limit cycle. The basin of attraction of the stable equilibrium point increases in this domain (Figure 5.3(e)). If ξ and ρ lie in fourth region ($(\xi_0, \rho_0) = (0.172, 0.05)$), the system (5.2.2) has two interior equilibrium points; one is a saddle and other is an unstable point (Figure 5.3(f)).

(4) $\beta = -0.05,\ \gamma = 0.3,\ \xi = 0.4,\ \rho = 0.3,\ \theta = 0.3$. The system (5.2.2) has two interior equilibrium points $e_1^* = (0.35, 0.65)$ and $e_2^* = (0.2, 0.5)$. The equilibrium point e_2^* is always a saddle point and the equilibrium point e_1^* is stable (Figure 5.4(a)). If $\rho = \rho^{[hf]} = 0.134615$, the system (5.2.2) undergoes to a Hopf bifurcation at the point e_1^*, and since the first Lyapunov number $\sigma = 318.808\pi > 0$, an unstable limit cycle arises around the point e_1^* (Figure 5.4(b)). If $\rho = 0.14681$, a homoclinic loop is created around e_1^* (Figure 5.4(c)). If $\rho = 0.12$, the equilibrium point e_1^* is unstable (Figure 5.4(d))

(5) $\beta = -0.25,\ \gamma = 0.3,\ \xi = 0.5,\ \rho = 0.3,\ \theta = 0.45$. The system (5.2.2) has only one interior equilibrium point $e_* = (0.326556, 0.626556)$, which is always a stable point

(Figure 5.5(a)). If $\rho = \rho^{[hf]} = 0.0910797$, the system (5.2.2) undergoes to a Hopf bifurcation at the point e_*, and since the first Lyapunov number $\sigma = -173.22\pi < 0$, a stable limit cycle arises around the point e_1^* (Figure 5.5(b)).

(6) $\beta = -0.225,\ \gamma = 0.3,\ \xi = 0.5,\ \rho = 0.5,\ \theta = 0.45$. The system (5.2.2) has only one interior equilibrium point $e = (0.275, 0.575)$, which is always a stable point (Figure 5.6(a)). If $\rho = \rho^{[hf]} = 0.13482$, the system (5.2.2) undergoes to a Hopf bifurcation at the point e and since the first Lyapunov number $\sigma = -274.131\pi < 0$, an stable limit cycle arises around the point e (Figure 5.6(b)).

(7) $\beta = -0.2,\ \gamma = 0.3,\ \theta = 0.6$. The BT bifurcation point in the $\xi\rho$-space is $(\xi_0, \rho_0) = (0.4, 0.16)$, also $E^* = (0.2, 0.4)$. The bifurcation diagram in the vicinity of the BT point in the parameter space is shown in Figure 5.7(a). The blue dotted curve is the Hopf bifurcation curve and the red dotted curve is the non-local bifurcation curve. The Figure 5.7(b) shows that the unique interior equilibrium point e^* is a cusp of codimension 2. If ξ and ρ lie in first region ($(\xi_0, \rho_0) = (0.45, 0.10)$), then the system (5.2.2) has no interior equilibrium point (Figure 5.7(c)). If ξ and ρ lie in second region ($(\xi_0, \rho_0) = (0.36, 0.20)$), then the system (5.2.2) has two interior equilibrium points; one is a saddle point and other is asymptotically stable (Figure 5.7(d)). If ξ and ρ lie in third region ($(\xi_0, \rho_0) = (0.30, 0.20)$), the system (5.2.2) has only one interior equilibrium point, which is globally stable (Figure 5.7(e)). If ξ and ρ lie in fourth region ($(\xi_0, \rho_0) = (0.38, 0.110355)$), the system (5.2.2) has two interior equilibrium points; one is a saddle and other is an unstable point surrounded by an unstable limit cycle (Figure 5.7(f)). If ξ and ρ lie in fifth region ($(\xi_0, \rho_0) = (0.38, 0.05)$), the system (5.2.2) has two interior equilibrium points; one is saddle and another is unstable (Figure 5.7(g)).

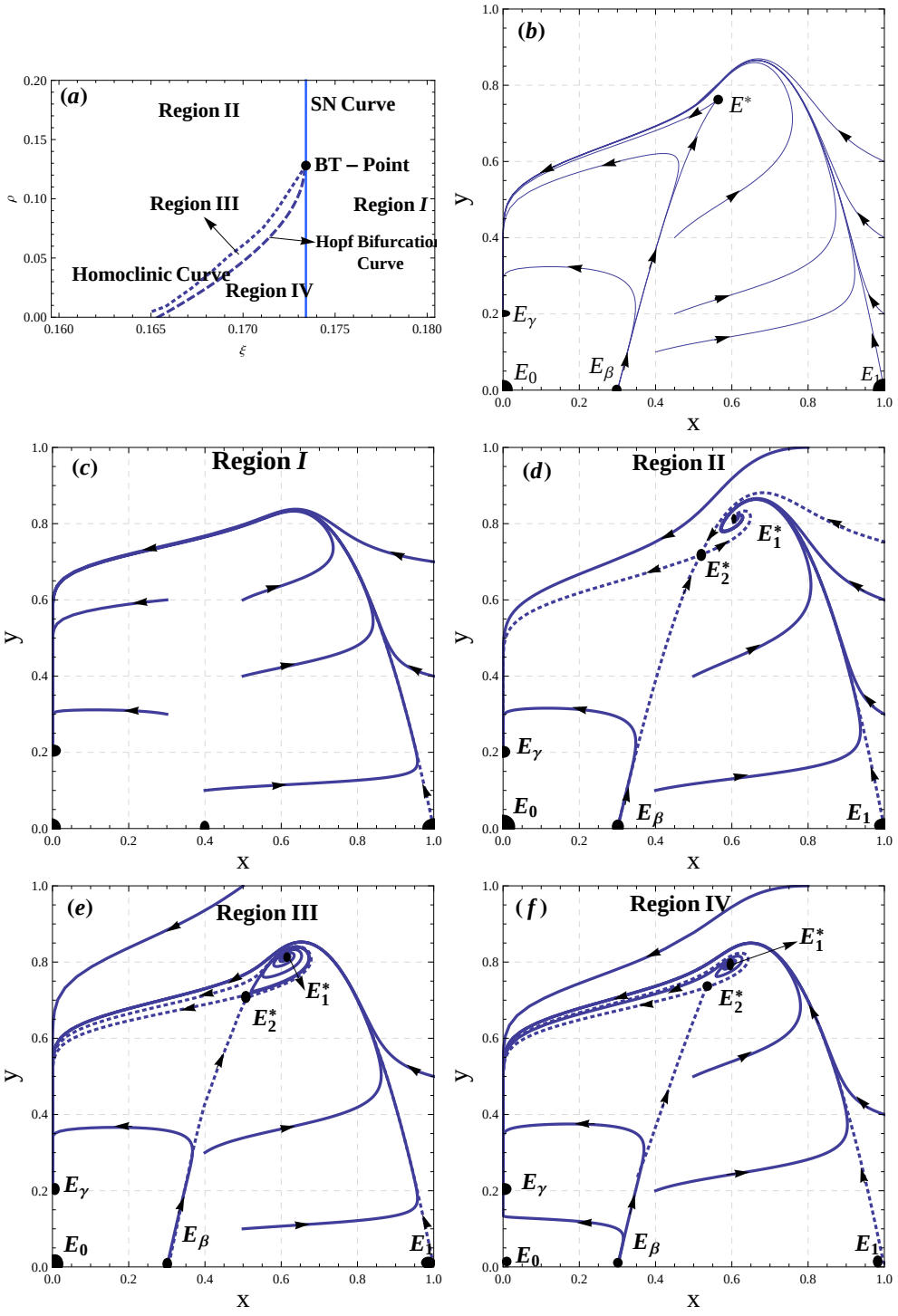

Figure 5.3: Strong Allee effect: $\beta = 0.3, \theta = 0.1, \gamma = 0.2$. (a) Bifurcation diagram of system (5.2.2) in $\xi\rho$ space (b) $\xi = 0.17335, \rho = 0.12793$ phase portrait diagram of the system (5.2.2). (c) $\xi = 0.175, \rho = 0.05$ lie in region I. No interior equilibrium point exist. The equilibrium point E_γ is globally stable. (d) $\xi = 0.170, \rho = 0.1$ lie in in region II. Two interior equilibrium points exist.(e) $\xi = 0.169, \rho = 0.0634$ lie in in region III. Two interior equilibrium points exist. (f) $\xi = 0.172, \rho = 0.05$ lie in in region IV. Two interior equilibrium points exist.

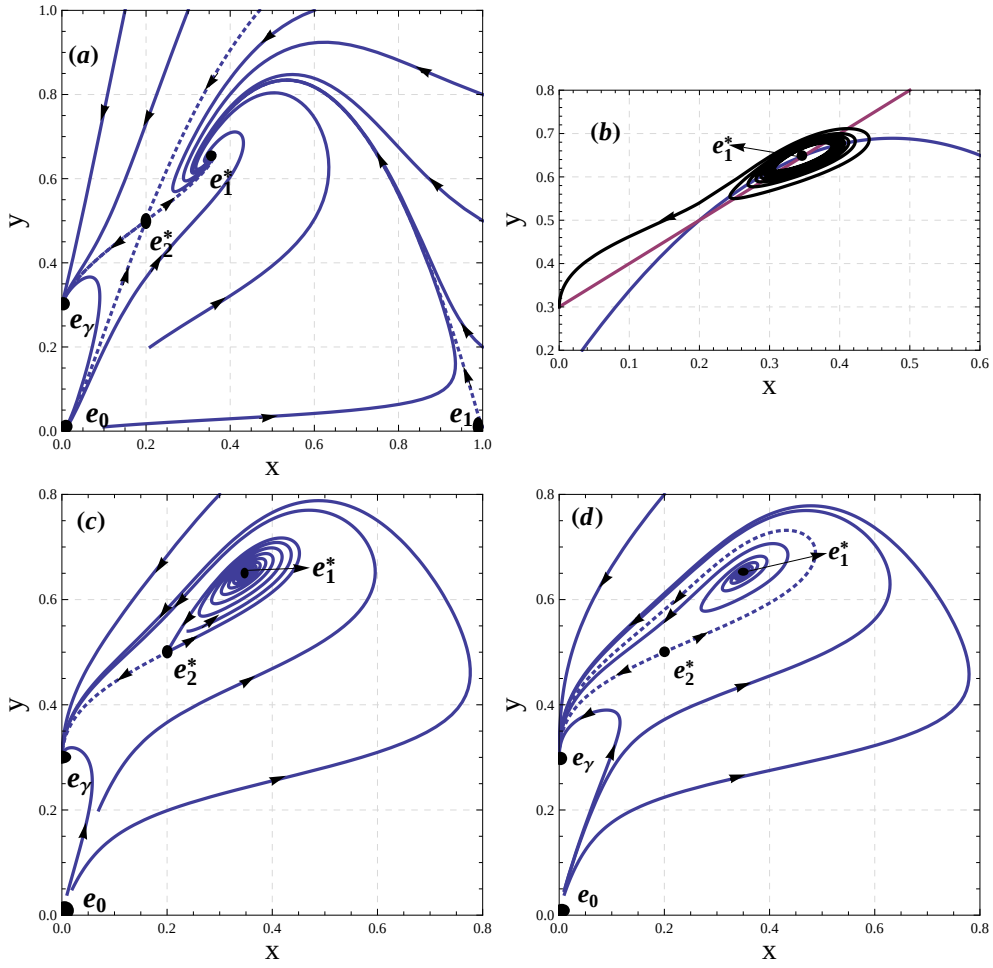

Figure 5.4: Weak Allee effect: $\beta = -0.05, \gamma = 0.3, \xi = 0.4, \theta = 0.3$. (a) $\rho = 0.3$ two interior equilibrium points exist. e_1^* is asymptotically stable and e_2^* is saddle. (b) $\rho = 0.134615$ an unstable limit cycle bifurcates through Hopf bifurcation around e_1^* (c) $\rho = 0.14681$. The diagram shows that the limit cycle collides with the saddle point e_2^* to give a Homoclinic loop.(d) $\rho = 0.12$, the point e_1^* is unstable point. The Dotted trajectories are the stable and unstable manifolds.

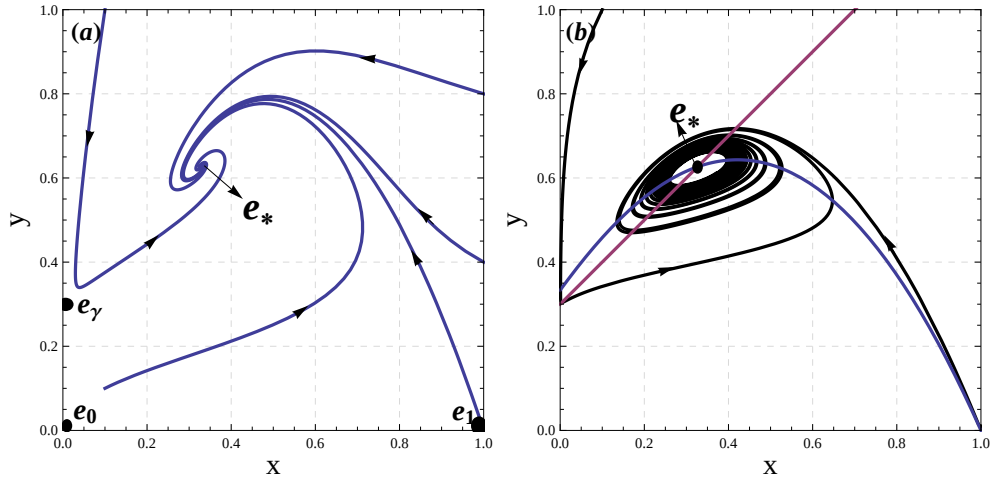

Figure 5.5: Weak Allee effect: $\beta = -0.25, \gamma = 0.3, \xi = 0.5, \theta = 0.45$. (a) $\rho = 0.3$ only one interior equilibrium point e_* exists, which is asymptotically stable. (b) $\rho = 0.0910797$ a stable limit cycle bifurcates through Hopf bifurcation around e_*

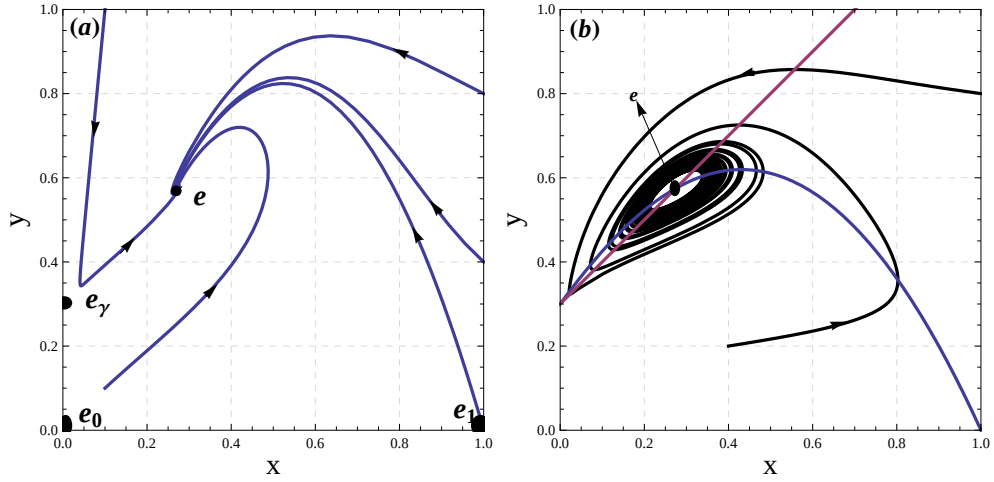

Figure 5.6: Weak Allee effect: $\beta = -0.225, \gamma = 0.3, \xi = 0.4, \theta = 0.45$. (a) $\rho = 0.5$ only one interior equilibrium point e exists, which is asymptotically stable. (b) $\rho = 0.13482$ a stable limit cycle bifurcates through Hopf bifurcation around e.

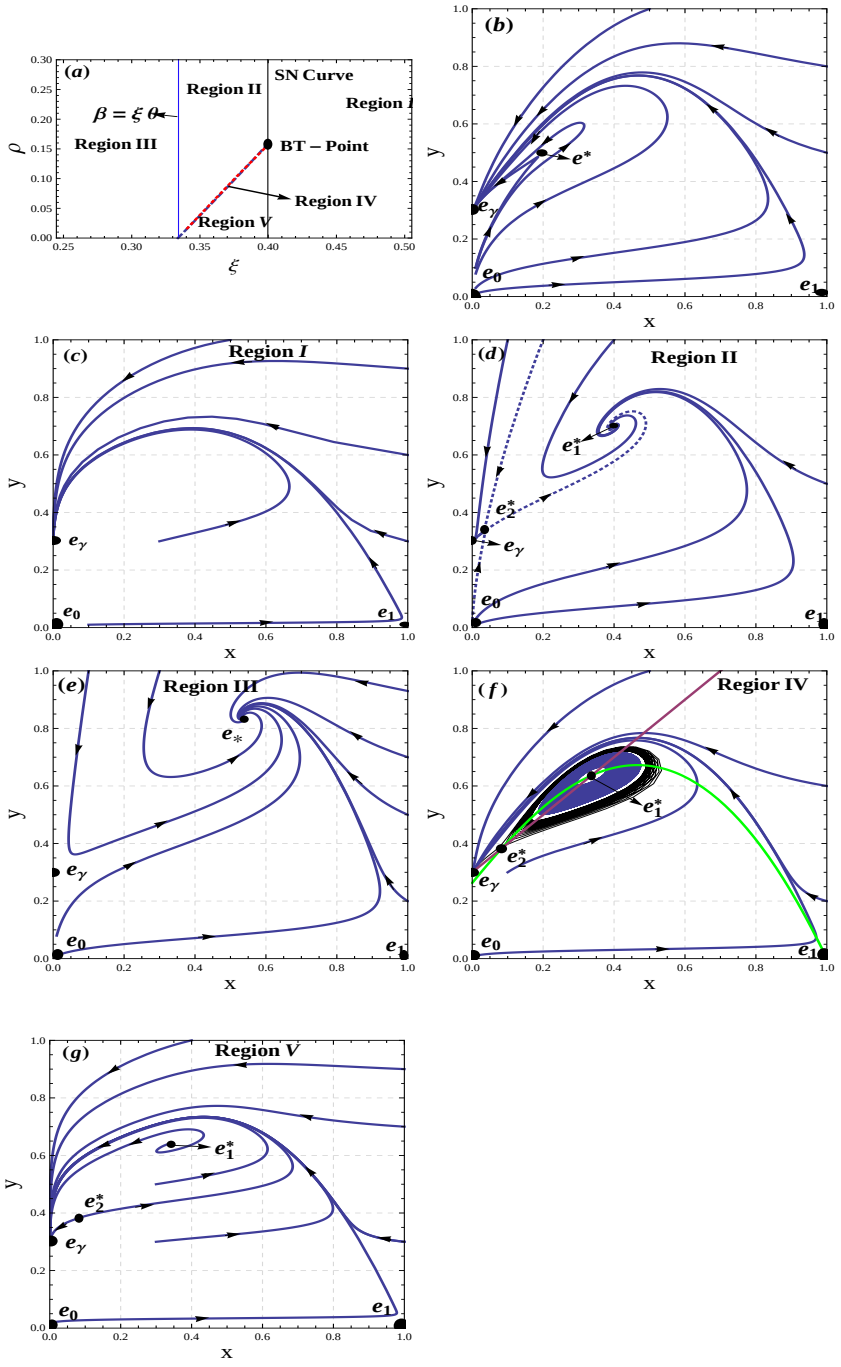

Figure 5.7: Weak Allee effect: $\beta = -0.2, \gamma = 0.3, \xi = 0.5, \theta = 0.45$. (a) Bifurcation diagram of system (5.2.2) (b) $\xi = 0.4, \rho = 0.16$ phase portrait diagram of the system (5.2.2). (c) $\xi = 0.45, \rho = 0.10$ lie in region I. No interior equilibrium point exist. The equilibrium point E_γ is globally stable. (d) $\xi = 0.36, \rho = 0.20$ lie in in region II. Two interior equilibrium points exist.(e) $\xi = 0.3, \rho = 0.2$ lies in region III. Only one interior equilibrium points exist which is globally stable. (f) $\xi = 0.38, \rho = 0.110355$ lie in region IV (region between red and blue curve). Two interior equilibrium points exist. (g) $\xi = 0.38, \rho = 0.05$ lie in region V. Two interior equilibrium points exist.

5.6 Results and Discussion

In this chapter, a bidimensional modified Leslie-Gower predator-prey model in the presence of double Allee effect in the prey population, where the protection provided by the environment for both the prey and predator species is the same, has been analyzed. From the ecological point of view, multiple (double) Allee effect has a great importance than single Allee effect, whenever managing threatened or exploited populations as combined effect accelerate population decline and extinction risk and more theoretical work are necessary to promote co-existence of such diverse communities of threatened population (Pal and Saha 2015).

The proposed model is shown biologically well-posed in the sense that any positive solution starts in the first quadrant remains both non-negative and bounded. The local stability of the system in different steady states has been discussed. Further, the system cannot collapse for any value of parameters as the origin is never stable. The existence of separatrix curves (stable manifold of the saddle interior equilibrium point), which separates the behavior of trajectories of the system, is obtained, implying that dynamics of the system is very sensitive to the variation of the initial conditions. The solutions initiating from the domain lies to the left of the separatrix curve tend to the prey free axial equilibrium, while the solutions initiating from the domain lies to the right of the separatrix curve tend to the positive interior equilibrium, which indicates coexistence of both species.

The proposed system can have zero, one or two positive interior equilibrium points through Saddle-node bifurcation as the bifurcation parameter $\theta = \frac{n}{K}$ crosses its critical value. The Sotomayor's theorem (Perko 1996) is applied to ensure the existence of Saddle-node bifurcation. Ecologically speaking, if the ratio of the non-fertile population of prey and the carrying capacity of prey is below the maximum threshold value, both the populations co-exist and above the maximum threshold, the prey species suddenly collapse to extinction, and the system suddenly experiences a transition to a qualitatively exceptionally. It is found that if two interior equilibrium points exist, one of them being always a saddle point and other is stable, unstable or the system undergoes to a Hopf bifurcation around this point, depending upon the parametric conditions. The emergence of Homoclinic loop

has been shown through numerical simulation, when the limit cycle arising through Hopf bifurcation collides with a saddle point. The non-degeneracy conditions of the Bogdanov-Takens bifurcation are also proved. In both the strong and weak Allee effects, the Bogdanov-Takens bifurcation demonstrates that there is a parametric region in which the predator and prey co-exist in the form of a positive equilibrium or prey species can be driven to extinction, depends upon the initial values. Moreover, in strong Allee effect there exists other region in which the predator and prey coexist in the form of a positive equilibrium for all initial values lying inside the unstable limit cycle, while in weak Allee effect, there exists other region in which predator and prey co-exist in form of a positive equilibrium for any initial value and also there exists another region in which the predator and prey coexist in the form of a periodic orbit for all initial values lying inside the unstable limit cycle.

Chapter 6

Predator-prey Model with Allee Effect and Additional Food for the Predators

6.1 Introduction

In chapters 5 and 6, the consequences of Allee effect type II and type I have been shown on two dimensional predator-prey models. The main feature of the Allee effect is that the population growth rate of the species experiencing Allee effect is prone to decrease under some minimum critical level and even becomes negative in some aspect, which can induce the species to extinction (Stephens et al. 1999; Wang 1999). In the predator-prey models most of the researches are focused on the Allee effect affecting prey population, which may be caused by predation or by processes inherent to the prey life history. A very few literature on the Allee effect affecting the predator population are available (Lai 2010; Wang 2013; Wu and Liu 2014; Feng and Kang 2015). Consider, a species has x adults in

This chapter is based on the research article: Qualitative analysis of an additional food provided predator-prey model in the presence of Allee effect, Communicated.

an isolated patch, then the fertility $f(x)$ increases with the population density, given by

$$f(x) = \frac{bx}{B+x}, \tag{6.1.1}$$

where $b > 0$ is the maximum per capita birth rate of the species and $B > 0$ is the Allee effect constant. This type of Allee effect, known as component Allee effect, describes a positive correlation between population size or density and any measurable component of individual fitness, such as juvenile survival or adult reproduction (Courchamp et al. 1999). The function $f(x)$ is a continuously, differentiable and increasing function such that $f(x) = 0$, whenever $x = 0$ and $f(x) \to b$, whenever $x \to \infty$. How fast $f(x)$ increases with x depends on the parameter B. The bigger B is, the stronger the Allee effect will be. It is easy to see that $f(B) = b/2$, biologically, B is the population density at which the species reaches half of its maximum fertility. When $B = 0$, the fertility is density independent and $f(x) = b$.

Most two-dimensional predator-prey models are based on one predator-one prey system, but according to Strauss (1991) many species do not feed only on a single species, but rather depend on diverse species due to many reasons. One of the most known reason is that most of predators are migratory and their spatial scale is much longer than the habitat occupied by some of their prey. For example, Spiny dogfish in the North West Atlantic and pacific hake (Kar and Ghosh 2012). Spencer and Collie in (1996) proposed a two-species predator-prey model in which growth rate of the predator depends upon predation on the modeled and alternate prey with linear predator harvesting and intraspecific competition into predator. Srinivasu et al. (2007) used nutritive value and the quantity of the additional food to model a two dimensional predator-prey system, and discussed the effect of both high and low quality of additional food in controlling the prey density. Prasad et al. (2013) proposed predator-prey dynamic model in the presence of additional food to predators and mutual interference among the predators. Sen et al. (2015) studied the global dynamics for this model in the presence of constant yield harvesting in predator.

In this chapter, it is shown that Allee effect incorporated in predator has significant effects on the dynamics of classical Lotka-Volterra predator-prey model with logistic self-

limitation, Holling type II functional response and additional food provided to predator.

6.2 Model Equations

Consider a predator-prey system in which predator is provided some additional food which is assumed to be distributed uniformly in the habitat. The species interactions are described by the following bidimensional autonomus system of ODEs

$$\begin{cases} \frac{dX}{dT} = rX\left(1-\frac{X}{K}\right) - \frac{e_1XY}{1+e_1h_1X+e_2h_2A}, \\ \frac{dY}{dT} = \frac{n_1e_1XY+n_2e_2AY}{1+e_1h_1X+e_2h_2A} - mY, \end{cases} \tag{6.2.1}$$

with the initial conditions $X(0) > 0, Y(0) > 0$, where $X(T)$ and $Y(T)$ are prey and predator density at time T. The positive parameters $r, K, A, m, e_1(e_2)$ and $h_1(h_2)$ represent intrinsic growth rate of prey, carrying capacity of prey in the absence of predator, amount of additional food, natural mortality rate of predator, ability of the predator to detect the prey (additional food) and handling time of the predator per unit quantity of prey (additional food) respectively.

Substitute $c = \frac{1}{h_1}, b = n_1c, a = \frac{1}{e_1h_1}, \eta = \frac{e_2}{e_1}$ and $\alpha = \frac{h_2}{h_1}$ (Srinivasu et al. 2007), the system (6.2.1) reduces to

$$\begin{cases} \frac{dX}{dT} = rX\left(1-\frac{X}{K}\right) - \frac{cXY}{a+\alpha\eta A+X}, \\ \frac{dY}{dT} = \frac{b(X+\eta A)Y}{a+\alpha\eta A+X} - mY, \end{cases} \tag{6.2.2}$$

with the initial conditions $X(0) > 0, Y(0) > 0$, where c stands for maximum rate of predation, a stands for half saturation value of the predator, b stands for maximum birth rate of the predator due to consumption of the food perceived by the predator, α is inversely related to the quality of the additional food and η represents effectual additional food level. Moreover, the term ηA represents quantity of additional food perceptible to the predator relative to prey. Now, by incorporating an Allee effect (form defined in Eq. (6.1.1)) into

the predator population, the system (6.2.2) can be rewritten as

$$\begin{cases} \frac{dX}{dT} = rX\left(1 - \frac{X}{K}\right) - \frac{cXY}{a+\alpha\eta A+X}, \\ \frac{dY}{dT} = \frac{b(X+\eta A)Y}{a+\alpha\eta A+X}\frac{Y}{Y+B} - mY. \end{cases} \tag{6.2.3}$$

On introducing the non-dimensional variables: $X = Kx, \quad Y = \frac{ary}{c}, \quad T = t/r$, the system (6.2.3) reduces to

$$\begin{cases} \frac{dx}{dt} = x(1 - \frac{x}{\gamma}) - \frac{xy}{1+\alpha\xi+x}, \\ \frac{dy}{dt} = \frac{\beta(x+\xi)y}{1+\alpha\xi+x}\frac{y}{y+\theta} - \delta y, \end{cases} \tag{6.2.4}$$

with the initial conditions: $x(0) > 0, y(0) > 0$, where $\gamma = \frac{K}{a}, \beta = \frac{b}{r}, \xi = \frac{\eta A}{a}, \delta = \frac{m}{r}$ and $\theta = \frac{cB}{ar}$.

6.3 Equilibria and their Stability

The equilibrium points of the system (6.2.4) are the nonnegative real solutions of the prey zero growth isocline

$$xf_1(x, y) = 0, \tag{6.3.1}$$

and predator zero growth isocline

$$yf_2(x, y) = 0, \tag{6.3.2}$$

where $f_1(x, y) = 1 - \frac{x}{\gamma} - \frac{y}{1+\alpha\xi+x}$ and $f_2(x, y) = \frac{\beta(x+\xi)}{1+\alpha\xi+x}\frac{y}{y+\theta} - \delta$.

The following are the equilibrium points of the system (6.2.4).

(*a*) *Trivial equilibrium point:* The trivial equilibrium point of the system (6.2.4) is $E_0 = (0, 0)$.

(*b*) *Axial equilibrium points:* The axial equilibrium points of the system (6.2.4) are $E_1 = (\gamma, 0)$ and $E_2 = \left(0, \frac{\delta\theta(1+\alpha\xi)}{\beta\xi-\delta(1+\alpha\xi)}\right), \beta\xi > \delta(1 + \alpha\xi)$.

(*c*) *Interior equilibrium points:* The positive interior equilibrium points of the system (6.2.4) are the intersection points of the curves $f_1(x, y) = 0$ and $f_2(x, y) = 0$, whose

abscissa are the roots of the quadratic equation

$$(\beta-\delta)x^2-(\delta+\alpha\delta\xi+\beta\gamma-\gamma\delta-\beta\xi)x+\gamma(\delta+\alpha\delta\xi+\delta\theta-\beta\xi)=0, \qquad (6.3.3)$$

while the ordinance are given by $y_k^*=\left(1-\frac{x_k}{\gamma}\right)(1+\alpha\xi+x_k), \quad k=1,2,$

The number and location of equilibrium points of system (6.2.4) can be describe as

Proposition 6.3.1. *(i)* $\beta\leq\delta$.

(a) *If* $\delta+\alpha\delta\xi-\beta\xi>0$, *the system* (6.2.4) *has no positive interior equilibrium point.*

(b) *If* $\delta+\alpha\delta\xi-\beta\xi<0$, *the system* (6.2.4) *has no positive interior equilibrium point, whenever* $\beta\xi-\delta-\alpha\delta\xi-\delta\theta<0$.

(c) *If* $\delta+\alpha\delta\xi-\beta\xi<0$, *the system* (6.2.4) *has one positive interior equilibrium point* $E_3=(x_3,y_3)$, *whenever* $\beta\xi-\delta-\alpha\delta\xi-\delta\theta>0$, *where* $x_3=\frac{\beta\xi-\delta-\alpha\delta\xi+\gamma(\delta-\beta)-\sqrt{(\beta\xi-\delta-\alpha\delta\xi+\gamma(\delta-\beta))^2-4(\beta\xi-\delta-\alpha\delta\xi-\delta\theta)(\delta-\beta))}}{2(\delta-\beta)}$ *and* $y_3=\left(1-\frac{x_3}{\gamma}\right)(1+\alpha\xi+x_3)$.

(ii) $\beta>\delta$.

(a) *If* $\delta+\alpha\delta\xi-\beta\xi>0$, *the system* (6.2.4)

(1) *for* $\beta\xi-\delta-\alpha\delta\xi+\gamma(\beta-\delta)>0$ *has two positive interior equilibrium points* $E_1^*=(x_1^*,y_1^*)$ *and* $E_2^*=(x_2^*,y_2^*)$, *whenever* $\theta<\frac{(\delta+\alpha\delta\xi-\beta\xi-\gamma(\beta-\delta))^2}{4\gamma\delta(\beta-\delta)}$, *a double positive interior equilibrium point* $E_4=(x_4,y_4)$, *whenever* $\theta=\frac{(\delta+\alpha\delta\xi-\beta\xi-\gamma(\beta-\delta))^2}{4\gamma\delta(\beta-\delta)}$ *and no positive interior equilibrium point, whenever* $\theta>\frac{(\delta+\alpha\delta\xi-\beta\xi-\gamma(\beta-\delta))^2}{4\gamma\delta(\beta-\delta)}$, *where* $x_k^*=\frac{\delta+\alpha\delta\xi-\beta\xi+\gamma(\beta-\delta)+(-1)^k\sqrt{(\delta+\alpha\delta\xi-\beta\xi-\gamma(\beta-\delta))^2-4\gamma\delta\theta(\beta-\delta)}}{2(\beta-\delta)}, y_k^*=(1-\frac{x_k^*}{\gamma})(1+\alpha\xi+x_k^*), \quad k=1,2, x_4=\frac{\delta+\alpha\delta\xi-\beta\xi+\gamma(\beta-\delta)}{2(\beta-\delta)}$ *and* $y_4=(1-\frac{x_4}{\gamma})(1+\alpha\xi+x_4)$.

(2) *for* $\beta\xi-\delta-\alpha\delta\xi+\gamma(\beta-\delta)<0$ *has no positive interior equilibrium point.*

(b) *If* $\delta+\alpha\delta\xi-\beta\xi<0$, *the system* (6.2.4)

(1) *has no positive interior equilibrium point, whenever* $\delta+\alpha\delta\xi+\beta\gamma-\gamma\delta-\beta\xi<0$ *and* $\delta+\alpha\delta\xi+\delta\theta-\beta\xi>0$.

(2) *has unique positive interior equilibrium point* $E_5 = (x_5, y_5)$, *whenever* $\delta + \alpha\delta\xi - \beta\xi + \delta\theta < 0$, *where* $x_5 = \frac{\delta+\alpha\delta\xi-\beta\xi+\gamma(\beta-\delta)+\sqrt{(\delta+\alpha\delta\xi-\beta\xi+\gamma(\beta-\delta))^2-4(\delta+\alpha\delta\xi-\beta\xi+\delta\theta)\gamma(\beta-\delta))}}{2(\beta-\delta)}$ *and* $y_5 = \big(1 - \frac{x_5}{\gamma}\big)(1 + \alpha\xi + x_5)$.

(3) *has unique positive interior equilibrium point* $E_6 = (x_6, y_6)$, *whenever* $\delta + \alpha\delta\xi - \beta\xi + \gamma(\beta - \delta) > 0$ *and* $\delta + \alpha\delta\xi - \beta\xi + \delta\theta = 0$, *where* $x_6 = \frac{\delta+\alpha\delta\xi-\beta\xi+\gamma(\beta-\delta)}{(\beta-\delta)}$ *and* $y_6 = (1 - \frac{x_6}{\gamma})(1 + \alpha\xi + x_6)$.

(4) *for* $\delta + \alpha\delta\xi - \beta\xi + \gamma(\beta - \delta) > 0$ *has two positive interior equilibrium points* E_1^* *and* E_2^*, *whenever* $\frac{\beta\xi-\delta(1+\alpha\xi)}{\delta} < \theta < \frac{(\delta+\alpha\delta\xi-\beta\xi-\gamma(\beta-\delta))^2}{4\gamma\delta(\beta-\delta)}$, *a double positive interior equilibrium point* $E_4 = (x_4, y_4)$, *whenever* $\theta = \frac{(\delta+\alpha\delta\xi-\beta\xi-\gamma(\beta-\delta))^2}{4\gamma\delta(\beta-\delta)}$ *and no positive interior equilibrium point, whenever* $\theta > \frac{(\delta+\alpha\delta\xi-\beta\xi-\gamma(\beta-\delta))^2}{4\gamma\delta(\beta-\delta)}$, *where* $x_4 = \frac{\delta+\alpha\delta\xi-\beta\xi+\gamma(\beta-\delta)}{2(\beta-\delta)}$ *and* $y_4 = (1 - \frac{x_4}{\gamma})(1 + \alpha\xi + x_4)$.

Now, the dynamics of system (6.2.4) in the neighborhood of each equilibrium point has been examined by using linearization technique.

The Jacobian matrix of the system (6.2.4) at the trial equilibrium point E_0 is

$$J_{E_0} = \begin{bmatrix} 1 & 0 \\ 0 & -\delta \end{bmatrix},$$

which confirms that the trial equilibrium point E_0 is always a saddle point.

The Jacobian matrix of the system (6.2.4) at the axial equilibrium point E_1 is

$$J_{E_1} = \begin{bmatrix} -1 & -\frac{\gamma}{1+\alpha\xi+\gamma} \\ 0 & -\delta \end{bmatrix},$$

which confirms that the axial equilibrium point E_1 is always a stable point.

The Jacobian matrix of the system (6.2.4) at the axial equilibrium point E_2 is

$$J_{E_2} = \begin{bmatrix} \frac{\beta\xi-\delta(1+\alpha\xi)-\delta\theta}{\beta\xi-\delta(1+\alpha\xi)} & 0 \\ \frac{\delta^2\theta(1+\alpha\xi-\xi)}{\xi(\beta\xi-\delta(1+\alpha\xi))} & \frac{\delta(\beta\xi-\delta(1+\alpha\xi))}{\beta\xi} \end{bmatrix},$$

which confirms that the axial equilibrium point E_2 is unstable, if $\beta\xi - \delta(1+\alpha\xi) - \delta\theta > 0$ and saddle, if $\beta\xi - \delta(1+\alpha\xi) - \delta\theta < 0$.

The Jacobian matrix of the system (6.2.4) at the positive interior equilibrium points $E_i^*, i = 1, 2$ is

$$J_{E_i^*} = \begin{bmatrix} x_i^*\Big(-\frac{1}{\gamma} + \big(1 - \frac{x_i^*}{\gamma}\big)\frac{1}{1+\alpha\xi+x_i^*}\Big) & -\frac{x_i^*}{1+\alpha\xi+x_i^*} \\ \frac{(\beta-\delta)y_i^*-\delta\theta}{y_i^*+\theta}\big(1-\frac{x_i^*}{\gamma}\big) & \frac{\delta\theta}{y_i^*+\theta} \end{bmatrix}.$$

The determinant of the Jacobian matrix $J_{E_i^*}$ is $\det J_{E_i^*} = \frac{x_i^*}{y_i^*+\theta}\Big((\beta-\delta)\big(1-\frac{x_i^*}{\gamma}\big)^2 - \frac{\delta\theta}{\gamma}\Big)$ and trace of the Jacobian matrix $J_{E_i^*}$ is $\mathrm{tr}J_{E_i^*} = x_i^*\Big(-\frac{1}{\gamma} + \big(1-\frac{x_i^*}{\gamma}\big)\frac{1}{1+\alpha\xi+x_i^*}\Big) + \frac{\delta\theta}{y_i^*+\theta}$. $\det J_{E_1^*} = \frac{\sqrt{(\delta+\alpha\delta\xi-\beta\xi-\gamma(\beta-\delta))^2-4\gamma\delta\theta(\beta-\delta)}}{2(\beta-\delta)} > 0$ and $\det J_{E_2^*} = -\frac{\sqrt{(\delta+\alpha\delta\xi-\beta\xi-\gamma(\beta-\delta))^2-4\gamma\delta\theta(\beta-\delta)}}{2(\beta-\delta)} < 0$.

The Jacobian matrix of the system (6.2.4) at the positive interior equilibrium point $E_i, i = 3, 4, 5, 6$ is

$$J_{E_i} = \begin{bmatrix} x_i\Big(-\frac{1}{\gamma} + \big(1 - \frac{x_i}{\gamma}\big)\frac{1}{1+\alpha\xi+x_i}\Big) & -\frac{x_i}{1+\alpha\xi+x_i} \\ \frac{(\beta-\delta)y_i-\delta\theta}{y_i+\theta}\big(1-\frac{x_i}{\gamma}\big) & \frac{\delta\theta}{y_i+\theta} \end{bmatrix}.$$

The determinant of the Jacobian matrix J_{E_i} is $\det J_{E_i} = \frac{x_i}{y_i+\theta}\Big((\beta-\delta)\big(1-\frac{x_i}{\gamma}\big)^2 - \frac{\delta\theta}{\gamma}\Big)$ and trace of the Jacobian matrix J_{E_i} is $\mathrm{tr}J_{E_i} = x_i\Big(-\frac{1}{\gamma} + \big(1-\frac{x_i}{\gamma}\big)\frac{1}{1+\alpha\xi+x_i}\Big) + \frac{\delta\theta}{y_i+\theta}$.
The determinant of the Jacobian matrix J_{E_3} is $\det J_{E_3} = \frac{x_3}{\gamma^2(y_3+\theta)}((\beta-\delta)(\gamma-x_3)^2 - \delta\theta\gamma) < 0$ as $\beta < \delta$.
The determinant of the Jacobian matrix J_{E_4} is $\det J_{E_4} = 0$.
The determinant of the Jacobian matrix J_{E_5} is $\det J_{E_5} = -\frac{\sqrt{(\delta+\alpha\delta\xi-\beta\xi-\gamma(\beta-\delta))^2-4\gamma\delta\theta(\beta-\delta)}}{2(\beta-\delta)} < 0$.
The determinant of the Jacobian matrix J_{E_6} is $J_{E_6} = -(\delta + \alpha\delta\xi - \beta\xi + \gamma(\beta-\delta)) < 0$.

On summarizing the above discussions, one can conclude the following theorem:

Theorem 6.3.2. *a) The trivial equilibrium point E_0 of the system (6.2.4) is always a saddle point.*

b) The axial equilibrium point E_1 of the system (6.2.4) is always a stable point.

c) The axial equilibrium point E_2 of the system (6.2.4), if exists, is unstable, if $\beta\xi - \delta(1+\alpha\xi) - \delta\theta > 0$ and saddle, if $\beta\xi - \delta(1+\alpha\xi) - \delta\theta < 0$.

d) The interior equilibrium point E_1^* of the system (6.2.4)*, if exists, is asymptotically stable point, if* $x_1^*\Big(-\frac{1}{\gamma}+\big(1-\frac{x_1^*}{\gamma}\big)\frac{1}{1+\alpha\xi+x_1^*}\Big)+\frac{\delta\theta}{y_1^*+\theta}<0$ *and unstable, if* $x_1^*\Big(-\frac{1}{\gamma}+\big(1-\frac{x_1^*}{\gamma}\big)\frac{1}{1+\alpha\xi+x_1^*}\Big)+\frac{\delta\theta}{y_1^*+\theta}>0$.

e) The interior equilibrium points E_3, E_5 and E_6 of the system (6.2.4)*, if exists, are always saddle.*

f) The interior equilibrium point E_4 of the system (6.2.4)*, if exists, is a degenerate singularity*

It is shown that interior equilibrium point E_4, if exists, is a degenerate singularity, and hence, it may has complicated properties. Define the transformation $\hat{x}=x-x_4, \hat{y}=y-y_4$ to shift equilibrium point E_4 of the system (6.2.4) to the origin and for the sake of convenience denote $\hat{x}$ as x and $\hat{y}$ as y. System (6.2.4) can be rewritten as

$$\begin{cases} \frac{dx}{dt}=\alpha_{10}x+\alpha_{01}y+\alpha_{20}x^2+\alpha_{11}xy+o|(x,y)^3|, \\ \frac{dy}{dt}=\beta_{10}x+\beta_{01}y+\beta_{20}x^2+\beta_{11}xy+\beta_{02}y^2+o|(x,y)^3|, \end{cases} \tag{6.3.4}$$

where $\alpha_{10}=x_4\big(-\frac{1}{\gamma}+\frac{y_4}{(1+\alpha\xi+x_4)^2}\big)$, $\alpha_{01}=-\frac{x_4}{1+\alpha\xi+x_4}$, $\alpha_{20}=-\frac{1}{\gamma}+\frac{y_4(1+\alpha\xi)}{(1+\alpha\xi+x_4)^3}$, $\alpha_{11}=-\frac{1+\alpha\xi}{(1+\alpha\xi+x_4)^2}$, $\beta_{10}=\frac{\beta y_4^2(1+\alpha\xi-\xi)}{(y_4+\theta)(1+\alpha\xi+x_6)^2}$, $\beta_{01}=\frac{\beta\theta y_4(x_4+\xi)}{(1+\alpha\xi+x_4)(y_4+\theta)^2}$, $\beta_{20}=-\frac{2\beta(1+\alpha\xi-\xi)y_4^2}{(1+\alpha\xi+x_4)^3(y_4+\theta)}$, $\beta_{11}=\frac{\beta(1+\alpha\xi-\xi)y_4(y_4+2\theta)}{(1+\alpha\xi+x_4)^2(y_4+\theta)^2}, \beta_{02}=\frac{\beta\theta^2(x_4+\xi)}{(1+\alpha\xi+x_4)(y_4+\theta)^3}$ and $o|(x,y)^3|$ are the terms involving order three and higher.

If $\alpha_{10}+\beta_{01}\neq 0$, the $tr(J_{E_4})\neq 0$ but $det(J_{E_4})=0$. Hence, E_4 is a saddle-node singularity. Further, whenever $\alpha_{10}+\beta_{01}=0$, the $\mathrm{tr}(J_{E_4})=0$ and $det(J_{E_4})=0$. Now, on using the transformation $y_1=x,\ \ y_2=\alpha_{10}x+\alpha_{01}y$ with the parametric conditions, the system (6.3.4) reduces to the following system

$$\begin{cases} \frac{dy_1}{dt}=y_2+\overline{\alpha}_{20}y_1^2+\overline{\alpha}_{11}y_1y_2+o|(y_1,y_2)^3|, \\ \frac{dy_2}{dt}=\overline{\beta}_{20}y_1^2+\overline{\beta}_{11}y_1y_2+o|(y_1,y_2)^3|, \end{cases} \tag{6.3.5}$$

where $\overline{\alpha}_{20}=\alpha_{20}-\frac{\alpha_{11}\alpha_{10}}{\alpha}{}_{01}$, $\overline{\alpha}_{11}=\frac{\alpha_{11}}{\alpha_{01}}$, $\overline{\beta}_{20}=\alpha_{10}\alpha_{20}+\alpha_{01}\beta_{20}-\alpha_{10}\beta_{11}+\frac{\beta_{02}\alpha_{10}^2}{\alpha_{01}}-\frac{\alpha_{10}^2\alpha_{11}}{\alpha_{01}}$, $\overline{\beta}_{11}=\beta_{11}+\frac{\alpha_{10}\alpha_{11}}{\alpha_{01}}-\frac{2\alpha_{10}\beta_{02}}{\alpha_{01}}$.

On using the transformation $z_1=y_1-\frac{1}{2}\overline{\alpha}_{11}y_1^2,\ \ z_2=y_2+\overline{\alpha}_{20}y_1^2$, the system (6.3.5)

reduces to

$$\begin{cases} \frac{dz_1}{dt} = z_2 + o|(z_1, z_2)^3|, \\ \frac{dz_2}{dt} = \omega_1 z_1^2 + \omega_2 z_1 z_2 + o|(z_1, z_2)^3|, \end{cases} \tag{6.3.6}$$

where $\omega_1 = \overline{\beta}_{20}$ and $\omega_2 = 2\overline{\alpha}_{20} + \overline{\beta}_{11}$.

Finally, using the transformation $X = z_1, \quad Y = z_2 + o|(z_1, z_2)^3|$, system (6.3.6) reduces to

$$\begin{cases} \frac{dX}{dt} = Y, \\ \frac{dY}{dt} = \omega_1 X^2 + \omega_2 XY + o|(X, Y)^3|. \end{cases} \tag{6.3.7}$$

If $\omega_1\omega_2 \neq 0$, non-degeneracy condition of a cusp of codimension 2, the origin of the system (6.3.7) is a cusp of codimension 2 in XY plane, that is, E_4 in xy plane is a cusp of codimension 2. The above discussions can be summarise as

Theorem 6.3.3. *If the unique interior equilibrium point E_4 exists, it is*

a) a saddle-node, whenever $\alpha_{10} + \beta_{01} \neq 0$.

b) a cusp of codimension 2, whenever $\alpha_{10} + \beta_{01} = 0$ and $\omega_1\omega_2 \neq 0$.

6.4 Bifurcation Analysis

In this section, the existence of Hopf bifurcation, Saddle-node bifurcation, Transcritical bifurcation and Bogdanov-Takens bifurcation for the system (6.2.4) has been discussed.

6.4.1 Hopf Bifurcation

In Theorem (6.3.2), it is proved that the interior equilibrium point E_2^* is always a saddle point, while E_1^* is asymptotically stable point, if $x_1^*\Big(-\frac{1}{\gamma} + \big(1 - \frac{x_1^*}{\gamma}\big)\frac{1}{1+\alpha\xi+x_1^*}\Big) + \frac{\delta\theta}{y_1^*+\theta} < 0$ and unstable, if $x_1^*\Big(-\frac{1}{\gamma} + \big(1 - \frac{x_1^*}{\gamma}\big)\frac{1}{1+\alpha\xi+x_1^*}\Big) + \frac{\delta\theta}{y_1^*+\theta} > 0$, respectively. A threshold magnitude $\theta = \theta^{[hf]}$ exists, which is the solution of the equation $x_1^*\Big(-\frac{1}{\gamma} + \big(1 - \frac{x_1^*}{\gamma}\big)\frac{1}{1+\alpha\xi+x_1^*}\Big) + \frac{\delta\theta}{y_{1^*}+\theta} = 0$, such that $\det(J_{E_1^*}) > 0$ and $tr(J_{E_1^*}) = 0$, and hence, both the eigenvalues of the Jacobian matrix $J_{E_1^*}$ will be purely imaginary. Thus, the equilibrium point E_1^* is a weak focus or a centre. The computation of explicit expression for θ in terms of system parameters is a very cumbersome task. The interior equilibrium E_1^* undergoes a Hopf bifurcation for the

threshold magnitude $\theta = \theta^{[hf]}$, whenever $\left[\frac{d}{d\theta}(TrJ_{E_1^*})\right]_{\theta=\theta^{[hf]}} \neq 0$, where a periodic orbit is created as the stability of the equilibrium point E_1^* loses.

Define $x = u - x_1^*,\ y = v - y_1^*$. The system (6.2.4) in the vicinity of the origin can be written as

$$\frac{du}{dt} = a_{10}u + a_{01}v + a_{20}u^2 + a_{11}uv + a_{02}v^2 + a_{30}u^3 + a_{21}u^2v + a_{12}uv^2 + a_{03}v^3 + P(u,v),$$
$$\frac{dv}{dt} = b_{10}u + b_{01}v + b_{20}u^2 + b_{11}uv + b_{02}v^2 + b_{30}u^3 + b_{21}u^2v + b_{12}uv^2 + b_{03}v^3 + Q(u,v),$$

where $a_{10} = x_1^*\big(-\frac{1}{\gamma} + \frac{y_1^*}{(1+\alpha\xi+x_1^*)^2}\big)$, $a_{01} = -\frac{x_1^*}{1+\alpha\xi+x_1^*}$, $a_{20} = -\frac{1}{\gamma} + \frac{y_1^*(1+\alpha\xi)}{(1+\alpha\xi+x_1^*)^3}$, $a_{11} = -\frac{1+\alpha\xi}{(1+\alpha\xi+x_1^*)^2}$, $a_{02} = 0$, $a_{30} = -\frac{y_1^*(1+\alpha\xi)}{(1+\alpha\xi+x_1^*)^4}$, $a_{21} = \frac{1+\alpha\xi}{(1+\alpha\xi+x_1^*)^3}$, $a_{12} = 0$, $a_{03} = 0$, $b_{10} = \frac{\beta(y_1^*)^2(1+\alpha\xi-\xi)}{(y_1^*+\theta)(1+\alpha\xi+x_1^*)^2}$, $b_{01} = \frac{\beta\theta y_1^*(x_1^*+\xi)}{(1+\alpha\xi+x_1^*)(y_1^*+\theta)^2}$, $b_{20} = -\frac{\beta(1+\alpha\xi-\xi)(y_1^*)^2}{(1+\alpha\xi+x_1^*)^3(y_1^*+\theta)}$, $b_{11} = \frac{\beta(1+\alpha\xi-\xi)y_1^*(y_1^*+2\theta)}{(1+\alpha\xi+x_1^*)^2(y_1^*+\theta)^2}$, $b_{02} = \frac{\beta\theta^2(x_1^*+\xi)}{(1+\alpha\xi+x_1^*)(y_1^*+\theta)^3}$, $b_{30} = \frac{\beta(y_1^*)^2(1+\alpha\xi-\xi)}{(1+\alpha\xi+x_1^*)^4(y_1^*+\theta)}$, $b_{21} = -\frac{\beta y_1^*(1+\alpha\xi-\xi)(y_1^*+2\theta)}{(1+\alpha\xi+x_1^*)^3(y_1^*+\theta)^2}$, $b_{12} = \frac{\beta\theta^2(1+\alpha\xi-\xi)}{(1+\alpha\xi+x_1^*)^2(y_1^*+\theta)^3}$, $b_{03} = -\frac{\beta\theta^2(x+\xi)}{(1+\alpha\xi+x_1^*)(y_1^*+\theta)^4}$, $P(u,v) = \sum_{i+j=4}^{\infty} a_{ij}u^iv^j$ and $Q(u,v) = \sum_{i+j=4}^{\infty} b_{ij}u^iv^j$.

Hence, first Lyapunov number σ can be computed by the formula defined in equation (1.3.7), where $\Delta = \frac{x_1}{y_1+\theta}\Big((\beta-\delta)\big(1-\frac{x_1}{\gamma}\big)^2 - \frac{\delta\theta}{\gamma}\Big)$.

Thus, it can be conclude that

Theorem 6.4.1. *The system* (6.2.4) *undergoes a Hopf bifurcation with respect to bifurcation parameter* θ *around the point* E_1^**, if* $x_1^*\Big(-\frac{1}{\gamma} + \big(1-\frac{x_1^*}{\gamma}\big)\frac{1}{1+\alpha\xi+x_1^*}\Big) + \frac{\delta\theta}{y_{1^*}+\theta} = 0$*. Moreover, a stable (unstable) cycle is created around the point* E_2^* *according as* $\sigma < 0 (\sigma > 0)$*.*

6.4.2 Transcritical Bifurcation

In Theorem 6.3.2, it is proved that the axial equilibrium point E_2 is unstable, if $\beta\xi - \delta(1+\alpha\xi) - \delta\theta > 0$ and saddle, if $\beta\xi - \delta(1+\alpha\xi) - \delta\theta < 0$. If $\beta\xi - \delta(1+\alpha\xi) - \delta\theta = 0$, one eigenvalue of the Jacobian matrix J_{E_2} is zero, it means that there is a chance of bifurcation. If $\beta\xi - \delta(1+\alpha\xi) - \delta\theta = 0$, the equilibrium point E_2 coincides with the equilibrium point E_1^*, whenever the condition $\delta + \alpha\delta\xi + \beta\gamma - \gamma\delta - \beta\xi > 0$ holds, that is, $E_1^* = E_2 = E^* = (0, 1+\alpha\xi)$, and coincide with the equilibrium point E_2^*, whenever the condition $\delta + \alpha\delta\xi + \beta\gamma - \gamma\delta - \beta\xi < 0$ holds, that is, $E_2^* = E_2 = E^* = (0, 1+\alpha\xi)$, and so,

Transcritical bifurcation may exist. Sotomayor's theorem has been applied to ensure the existence of the Transcritical bifurcation.

Suppose V and W are the eigenvectors corresponding to zero eigenvalue of the Jacobian matrix J_{E^*} and $J^T_{E^*}$ respectively, given by,

$$V = \begin{bmatrix} \frac{\beta\xi-\delta(1+\alpha\xi)}{\beta(\xi-1-\alpha\xi)} \\ 1 \end{bmatrix}; \quad W = \begin{bmatrix} 1 \\ 0 \end{bmatrix}.$$

Then,

$W^T F_\theta(E^*, \theta^{[tc]}) = 0,$

$W^T[DF_\theta(E^*, \theta^{[tc]})v] = \frac{\beta\xi-\delta(1+\alpha\xi}{\beta\theta(1+\alpha\xi-\xi)} \neq 0,$

$W^T[D^2F\Big(E^*, \theta^{[tc]}\Big)(v,v)] = 2\Big(\big(-\frac{1}{\gamma} + \frac{1}{1+\alpha\xi}\big)\frac{\beta\xi-\delta(1+\alpha\xi)}{\beta(\xi-1-\alpha\xi)} - \frac{1}{1+\alpha\xi}\Big)\frac{\beta\xi-\delta(1+\alpha\xi)}{\beta(\xi-1-\alpha\xi)} \neq 0$, as $\beta\xi - \delta(1+\alpha\xi) > 0$ and $\gamma(\beta-\delta) + \delta(1+\alpha\xi) - \beta\xi > 0$, where

$$F_\theta(E^*, \theta^{[tc]}) = \begin{bmatrix} 0 \\ \frac{\delta(1+\alpha\xi)}{1+\alpha\xi+\delta^{[tc]}} \end{bmatrix}; \quad DF_\theta\Big(E^*, \theta^{[tc]}\Big) = \begin{bmatrix} -\frac{\delta}{\beta\xi-\delta(1+\alpha\xi)} & 0 \\ \frac{\delta^2(1+\alpha\xi-\xi)}{\xi(\beta\xi-\delta(1+\alpha\xi))} & 0 \end{bmatrix}; \quad D^2F\Big(E^*, \theta^{[tc]}\Big)$$

$$= \begin{bmatrix} \big(-\frac{2}{\gamma} + \frac{2}{1+\alpha\xi}\big)\frac{(\beta\xi-\delta(1+\alpha\xi))^2}{\beta^2(\xi-1-\alpha\xi)^2} - \frac{2}{1+\alpha\xi}\frac{\beta\xi-\delta(1+\alpha\xi)}{\beta(\xi-1-\alpha\xi)} \\ -\frac{4\beta(1+\alpha\xi-\xi)}{(1+\alpha\xi)(1+\alpha\xi+\theta)}\frac{(\beta\xi-\delta(1+\alpha\xi))^2}{\beta^2(\xi-1-\alpha\xi)^2} + \frac{2\beta(1+\alpha\xi-\xi)(1+\alpha\xi+2\theta)}{(1+\alpha\xi)^2(1+\alpha\xi+\theta)^2}\frac{\beta\xi-\delta(1+\alpha\xi)}{\beta(\xi-1-\alpha\xi)} + \frac{2\beta\theta^{[tc]}\xi}{(1+\alpha\xi)(1+\alpha\xi+\theta)^3} \end{bmatrix}.$$

Thus, the transversality condition for transcritical bifurcation are satisfied. The above discussion can be summarised as

Theorem 6.4.2. *The system* (6.2.4) *undergoes a Transcritical bifurcation, if conditions* $\beta\xi - \delta(1+\alpha\xi) > 0, \gamma(\beta-\delta) + \delta(1+\alpha\xi) - \beta\xi \neq 0$ *and* $\beta\xi - \delta(1+\alpha\xi) - \delta\theta = 0$ *hold.*

6.4.3 Saddle-node Bifurcation

In Proposition (6.3.1), it has been shown that, if $\beta > \delta, \delta + \alpha\delta\xi - \beta\xi > 0$ and $\beta\xi - \delta - \alpha\delta\xi + \gamma(\beta-\delta) > 0$, the system (6.2.4) has two positive interior equilibrium points, E_1^* and E_2^*, whenever $\theta < \frac{(\delta+\alpha\delta\xi-\beta\xi-\gamma(\beta-\delta))^2}{4\gamma\delta(\beta-\delta)}$, and these two interior equilibrium points coincide with each other and a double interior equilibrium point E_4 is obtained, whenever $\theta = \frac{(\delta+\alpha\delta\xi-\beta\xi-\gamma(\beta-\delta))^2}{4\gamma\delta(\beta-\delta)}$. Also, the system (6.2.4) has no positive interior equilibrium point, if $\theta > \frac{(\delta+\alpha\delta\xi-\beta\xi-\gamma(\beta-\delta))^2}{4\gamma\delta(\beta-\delta)}$. The annihilation of equilibria may be due to the occurrence

of Saddle-node bifurcation for interior equilibrium points, which takes place, when the parameter θ crosses the critical value $\theta = \theta^{[SN]} = \frac{(\delta+\alpha\delta\xi-\beta\xi-\gamma(\beta-\delta))^2}{4\gamma\delta(\beta-\delta)}$. From Theorem (6.3.3), the double equilibrium point E_4 is a saddle-node, if $x_4\Big(-\frac{1}{\gamma}+\big(1-\frac{x_4}{\gamma}\big)\frac{4}{1+\alpha\xi+x_4}\Big)+\frac{\delta\theta}{y_4+\theta}\neq 0$. This confirms that there is a Saddle-node bifurcation surface which is given as

$$SN_1 = \{(\gamma,\alpha,\beta,\theta,\xi,\eta,\delta) : \beta>\delta, \delta+\alpha\delta\xi-\beta\xi>0, \beta\xi-\delta-\alpha\delta\xi+\gamma(\beta-\delta)>0,$$
$$\theta=\frac{(\delta+\alpha\delta\xi-\beta\xi-\gamma(\beta-\delta))^2}{4\gamma\delta(\beta-\delta)}, x_4\Big(-\frac{1}{\gamma}+\big(1-\frac{x_4}{\gamma}\big)\frac{1}{1+\alpha\xi+x_4}\Big)+\frac{\delta\theta}{y_4+\theta}\neq 0\Big\}.$$

Similarly, other Saddle-node bifurcation surface is

$$SN_2 = \{(\gamma,\alpha,\beta,\theta,\xi,\eta,\delta) : \beta>\delta, \delta+\alpha\delta\xi-\beta\xi<0, \beta\xi-\delta-\alpha\delta\xi+\gamma(\beta-\delta)>0,$$
$$\theta=\frac{(\delta+\alpha\delta\xi-\beta\xi-\gamma(\beta-\delta))^2}{4\gamma\delta(\beta-\delta)}, x_4\Big(-\frac{1}{\gamma}+\big(1-\frac{x_4}{\gamma}\big)\frac{1}{1+\alpha\xi+x_4}\Big)+\frac{\delta\theta}{y_4+\theta}\neq 0\Big\}.$$

The above discussion can be summarised as

Theorem 6.4.3. *The system* (6.2.4) *undergoes a Saddle-node bifurcation with respect to bifurcation parameter θ around the equilibrium point E_4, if exists, whenever $x_4\Big(-\frac{1}{\gamma}+\big(1-\frac{x_4}{\gamma}\big)\frac{1}{1+\alpha\xi+x_4}\Big)+\frac{\delta\theta}{y_4+\theta}\neq 0$.*

6.4.4 Bogdanov-Takens Bifurcation

Theorem 6.4.3 confirms that the system (6.2.4) undergoes a Saddle-node bifurcation at the equilibrium point E_4, if exists, whenever $\det(J_{E_4})=0$ and $tr(J_{E_4})\neq 0$. Now, consider the case, when $tr(J_{E_4})$ is also zero. These two parametric conditions imply that the Jacobian matrix J_{E_4} has double zero eigenvalues. Also, in Theorem 6.3.3, it is shown that the equilibrium point E_4 is a cusp of codimension 2, whenever $tr(J_{E_4})=0$ and $\omega_1\omega_2\neq 0$. Thus, here is a chance of codimension 2 bifurcation (Bogdanov-Takens bifurcation of codimension 2) near the point E_4. Consider the parameters θ and δ as the Bogdanov-Taken bifurcation parameters. The system (6.2.4) has been reduced into normal form by employing a series of nontrivial transformations.

Suppose the bifurcation parameters θ and δ vary in a small domain of Bogdanov-Taken point (θ_0,δ_0), and let $(\theta_0+\lambda_1,\delta_0+\lambda_2)$ be a point of the neighbourhood of the BT

point, where λ_1, λ_2 are small. Thus, the system (6.2.4) reduces to

$$\begin{cases} \frac{dx}{dt} = x(1-\frac{x}{\gamma}) - \frac{xy}{1+\alpha\xi+x}, \\ \frac{dy}{dt} = \frac{\beta(x+\xi)y}{1+\alpha\xi+x}\frac{y}{y+\theta_0+\lambda_2} - (\delta_0+\lambda_1)y, \end{cases} \tag{6.4.1}$$

The system (6.4.1) is C^∞ smooth with respect to the variables x, y in a small neighbourhood of (θ_0, δ_0).

Define $x_1 = x - x_4, x_2 = y - y_4$, system (6.4.1) reduces to

$$\begin{cases} \frac{dx_1}{dt} = a_{10}x_1 + a_{01}x_2 + a_{20}x_1^2 + a_{11}x_1x_2 + R_1(x_1, x_2), \\ \frac{dx_2}{dt} = b_{00} + b_{10}x_1 + b_{01}x_2 + b_{20}x_1^2 + b_{11}x_1x_2 + b_{02}x_2^2 + R_2(x_1, x_2), \end{cases} \tag{6.4.2}$$

where $a_{10} = x_4\Big(-\frac{1}{\gamma} + \frac{y_4}{(1+\alpha\xi+x_4)^2}\Big)$, $a_{01} = -\frac{x_4}{1+\alpha\xi+x_4}$, $a_{20} = -\frac{1}{\gamma} + \frac{(1+\alpha\xi)y_4}{(1+\alpha\xi+x_4)^3}$, $a_{11} = -\frac{1+\alpha\xi}{(1+\alpha\xi+x_4)^2}$, $b_{00} = y_4\Big(\frac{\beta(x_4+\xi)}{1+\alpha\xi+x_4}\frac{y_4}{y_4+\theta+\lambda_2} - \delta_0 - \lambda_1\Big)$, $b_{10} = \frac{\beta(1+\alpha\xi-\xi)y_4^2}{(1+\alpha\xi+x_4)^2(y_4+\theta+\lambda_2)}$, $b_{01} = \frac{\beta(x_4+\xi)y_4(y_4+2\theta+2\lambda_2)}{(1+\alpha\xi+x_4)(y_4+\theta+\lambda_2)^2} - \delta_0 - \lambda_1$, $b_{20} = -\frac{\beta(1+\alpha\xi-\xi)y_4^2}{(1+\alpha\xi+x_4)^3(y_4+\theta_0+\lambda_2)}$, $b_{11} = \frac{\beta(1+\alpha\xi-\xi)y_4(y_4+2\theta_0+2\lambda_2)}{(1+\alpha\xi+x_4)^2(y_4+\theta_0+\lambda_2)^2}$, $b_{02} = \frac{\beta(x_4+\xi)(\theta_0+\lambda_2)^2}{(1+\alpha\xi+x_4)(y_4+\theta_0+\lambda_2)^2}$ and R_1, R_2 are the power series in (x_1, x_2) with powers $x_1^i x_2^j$ satisfying $i + j \geq 3$.

Now, introduce the affine transformation $y_1 = x_1,\ y_2 = a_{10}x_1 + a_{01}x_2$ in the system (6.4.2), one gets

$$\begin{cases} \frac{dy_1}{dt} = & y_2 + \xi_{20}(\lambda)y_1^2 + \xi_{11}(\lambda)y_1y_2 + \overline{R}_1(y_1, y_2), \\ \frac{dy_2}{dt} = & \eta_{00}(\lambda) + \eta_{10}(\lambda)y_1 + \eta_{01}(\lambda)y_2 + \eta_{20}(\lambda)y_1^2 + \eta_{11}(\lambda)y_1y_2 + \\ & \eta_{02}(\lambda)y_2^2 + \overline{R}_2(y_1, y_2), \end{cases} \tag{6.4.3}$$

where $\xi_{20}(\lambda) = a_{20} - \frac{a_{11}a_{10}}{a_{01}}$, $\xi_{11}(\lambda) = \frac{a_{11}}{a_{01}}$, $\eta_{00}(\lambda) = b_{00}a_{01}$, $\eta_{10}(\lambda) = a_{01}b_{10} - a_{10}b_{01}$, $\eta_{01} = a_{10} + b_{01}$, $\eta_{20} = a_{10}a_{20} + a_{01}b_{20} - b_{11}a_{10} - \frac{a_{11}a_{10}^2}{a_{01}} + \frac{a_{10}^2 b_{02}}{a_{01}}$, $\eta_{11} = b_{11} + \frac{a_{10}a_{11}}{a_{01}} - \frac{2a_{10}b_{02}}{a_{01}}$, $\eta_{02} = \frac{b_{02}}{a_{01}}$ and $\overline{R_1}$, $\overline{R_2}$ are the power series in (y_1, y_2) with powers $y_1^i y_2^j$ satisfying $i + j \geq 3$.

Consider the C^∞ change of coordinates in the small neighbourhood of $(0, 0)$:

$z_1 = y_1 - \frac{1}{2}(\xi_{11}+\eta_{02})y_1^2, \quad z_2 = y_2 + \xi_{20}y_1^2 - \eta_{02}y_1y_2$, which transforms the system (6.4.3) into

$$\begin{cases} \frac{dz_1}{dt} = z_2 + \hat{R}_1(z_1, z_2), \\ \frac{dz_2}{dt} = \gamma_{00} + \gamma_{10}z_1 + \gamma_{01}z_2 + \gamma_{20}z_1^2 + \gamma_{11}z_1z_2 + \hat{R}_2(z_1, z_2), \end{cases} \tag{6.4.4}$$

where $\gamma_{00}(\lambda) = \eta_{00}, \quad \gamma_{10}(\lambda) = \eta_{10} - \eta_{00}\eta_{02}, \quad \gamma_{01} = \eta_{01}, \quad \gamma_{20} = \frac{1}{2}(\xi_{11}+\eta_{02})(\eta_{10} - \eta_{00}\eta_{02}) - \eta_{01}\xi_{20} + \eta_{20} - \eta_{02}\eta_{10}, \quad \gamma_{11} = \eta_{11} + 2\xi_{20}$ and $\hat{R}_1, \quad \hat{R}_2$ are the power series in (z_1, z_2) with powers $z_1^i z_2^j$ satisfying $i + j \geq 3$.

Next, consider C^∞ change of coordinates in the small neighbourhood of $(0, 0)$: $v_1 = z_1, \quad v_2 = z_2 + \hat{R}_1(z_1, z_2)$. Then, the system (6.4.4) reduces to

$$\begin{cases} \frac{dv_1}{dt} = v_2, \\ \frac{dv_2}{dt} = \gamma_{00} + \gamma_{10}v_1 + \gamma_{01}v_2 + \gamma_{20}v_1^2 + \gamma_{11}v_1v_2 + F_1(v_1) + v_2F_2(v_1) + v_2^2F_3(v_1, v_2), \end{cases} \tag{6.4.5}$$

where, F_1, F_2 and F_3 are the power series in v_1 and (v_1, v_2) with powers $v_1^{k_1}, v_1^{k_2}$ and $v_1^i v_2^j$ satisfying $k_1 \geq 3, k_2 \geq 2$ and $i + j \geq 1$, respectively. The sign of γ_{20}, whenever $\lambda_1 \to 0$ and $\lambda_2 \to 0$, cannot be determined through analytical computation. Thus, consider the following two cases:

Case *I*. $\gamma_{20} > 0$.

Applying the Malgrange preparation theorem, one gets

$$\gamma_{00} + \gamma_{10}v_1 + \gamma_{20}v_1^2 + F_1(v_1) = \Big(v_1^2 + \frac{\gamma_{10}}{\gamma_{20}}v_1 + \frac{\gamma_{00}}{\gamma_{20}}\Big)B_1(v_1, \lambda),$$

where $B_1(0, \lambda) = \gamma_{20}$ and B_1 is a power series of v_1 whose coefficients depend on parameters (λ_1, λ_2).

Let $X_1 = v_1, \quad X_2 = \frac{v_2}{\sqrt{\gamma_{20}}}$, and $d\tau = \sqrt{\gamma_{20}}dt$, then the system (6.4.5) reduces to

$$\begin{cases} \frac{dX_1}{d\tau} = X_2, \\ \frac{dX_2}{d\tau} = \frac{\gamma_{00}}{\gamma_{20}} + \frac{\gamma_{10}}{\gamma_{20}}X_1 + \frac{\gamma_{01}}{\sqrt{\gamma_{20}}}X_2 + X_1^2 + \frac{\gamma_{11}}{\sqrt{\gamma_{20}}}X_1X_2 + P(X_1, X_2, \lambda), \end{cases} \tag{6.4.6}$$

where $P(X_1, X_2, 0)$ is a power series in (X_1, X_2) with powers $X_1^i X_2^j$ satisfying $i + j \geq 3$ with $j \geq 2$.

Applying the parameter dependent affine transformation $Y_1 = X_1 + \frac{\gamma_{10}}{2\gamma_{20}},\ Y_2 = X_2$ in the system (6.4.6) and using Taylor series expansion, one gets

$$\begin{cases} \frac{dY_1}{d\tau} = Y_2, \\ \frac{dY_2}{d\tau} = \frac{\gamma_{00}}{\gamma_{20}} - \frac{\gamma_{10}^2}{4\gamma_{20}^2} + \Big(\frac{\gamma_{01}}{\sqrt{\gamma_{20}}} - \frac{\gamma_{11}\gamma_{00}}{2\gamma_{20}\sqrt{\gamma_{20}}}\Big)Y_2 + Y_1^2 + \frac{\gamma_{11}}{\sqrt{\gamma_{20}}}Y_1Y_2 + Q(Y_1, Y_2, \mu), \end{cases} \tag{6.4.7}$$

where $Q(X_1, X_2, 0)$ is a power series in (Y_1, Y_2) with powers $Y_1^i Y_2^j$ satisfying $i + j \geq 3$ with $j \geq 2$. Make the change of variables one more time by setting $Z_1 = \frac{\gamma_{11}^2}{\gamma_{20}}Y_1,\quad Z_2 = \frac{\gamma_{11}^3}{\gamma_{20}\sqrt{\gamma_{20}}}Y_2,\quad t = \frac{\sqrt{\gamma_{20}}}{\gamma_{11}}\tau$. Then, the system (6.4.7) reduces to

$$\begin{cases} \frac{dZ_1}{dt} = Z_2, \\ \frac{dZ_2}{dt} = \mu_1(\lambda_1, \lambda_2) + \mu_2(\lambda_1, \lambda_2)Z_2 + Y_1^2 \pm Z_1Z_2 + R(Z_1, Z_2, \mu), \end{cases} \tag{6.4.8}$$

where $\mu_1(\lambda_1, \lambda_2) = \frac{\gamma_{00}\gamma_{11}^4}{\gamma_{20}^3} - \frac{\gamma_{10}^2\gamma_{11}^4}{4\gamma_{20}^4},\quad \mu_2(\lambda_1, \lambda_2) = \frac{\gamma_{01}\gamma_{11}}{\sqrt{\gamma_{20}}} - \frac{\gamma_{00}\gamma_{11}^2}{2\gamma_{20}^2}$ and $R(X_1, X_2, 0)$ is a power series in (Z_1, Z_2) with powers $Z_1^i Z_2^j$ satisfying $i + j \geq 3$ with $j \geq 2$.

Case II $\gamma_{20} < 0$.

To make γ_{20} positive, let $V_1 = -v_1,\quad V_2 = v_2,\quad T = -t$. The system (6.4.5) reduces to

$$\begin{cases} \frac{dV_1}{dT} = V_2, \\ \frac{dV_2}{dT} = -\gamma_{00} + \gamma_{10}V_1 - \gamma_{20}V_1^2 + R_1(Z_1) - \gamma_{01}V_2 + \gamma_{11}V_1V_2 + \\ \qquad V_2R_2(V_1) + V_2^2R_3(V_1, V_2), \end{cases} \tag{6.4.9}$$

where R_1, R_2 and R_3 are the power series in V_1 and (V_1, V_2) with powers $V_1^{k_1}, V_1^{k_2}$ and $V_1^iV_2^j$ satisfying $k_1 \geq 3, k_2 \geq 2$ and $i + j \geq 1$, respectively. Applying the Malgrange preparation theorem

$$\gamma_{00} + \gamma_{10}V_1 + \gamma_{20}V_1^2 + F_1(V_1) = \Big(V_1^2 - \frac{\gamma_{10}}{\gamma_{20}}V_1 + \frac{\gamma_{00}}{\gamma_{20}}\Big)B_1(V_1, \lambda)$$

where $B_1(0, \lambda) = -\gamma_{20}$, and B_1 is a power series of v_1 whose coefficients depend on parameters (λ_1, λ_2). Let $X_1 = V_1,\quad X_2 = \frac{V_2}{\sqrt{-\gamma_{20}}}$, and $d\tau = \sqrt{-\gamma_{20}}dT$, the system (6.4.9) reduces to

$$\begin{cases} \frac{dX_1}{d\tau} = X_2, \\ \frac{dX_2}{d\tau} = \frac{\gamma_{00}}{\gamma_{20}} - \frac{\gamma_{10}}{\gamma_{20}}X_1 - \frac{\gamma_{01}}{\sqrt{\gamma_{20}}}X_2 + X_1^2 + \frac{\gamma_{11}}{\sqrt{\gamma_{20}}}X_1X_2 + P(X_1, X_2, \lambda), \end{cases} \tag{6.4.10}$$

where $P(X_1, X_2, 0)$ is a power series in (X_1, X_2) with powers $X_1^i X_2^j$ satisfying $i+j \geq 3$ with $j \geq 2$.

Applying the parameter dependent affine transformation $Y_1 = X_1 - \frac{\gamma_{10}}{2\gamma_{20}},\ Y_2 = X_2$ in the system (6.4.10) and using Taylor series expansion, one gets

$$\begin{cases} \frac{dY_1}{d\tau} = Y_2, \\ \frac{dY_2}{d\tau} = \frac{\gamma_{00}}{\gamma_{20}} - \frac{\gamma_{10}^2}{4\gamma_{20}^2} + \Big(- \frac{\gamma_{01}}{\sqrt{\gamma_{20}}} + \frac{\gamma_{11}\gamma_{00}}{2\gamma_{20}\sqrt{-\gamma_{20}}}\Big) Y_2 + Y_1^2 + \frac{\gamma_{11}}{\sqrt{-\gamma_{20}}} Y_1 Y_2 + Q(Y_1, Y_2, \mu), \end{cases} \tag{6.4.11}$$

where $Q(X_1, X_2, 0)$ is a power series in (Y_1, Y_2) with powers $Y_1^i Y_2^j$ satisfying $i + j \geq 3$ with $j \geq 2$. Make the change of variables one more time by setting $Z_1 = -\frac{\gamma_{11}^2}{\gamma_{20}} Y_1,\quad Z_2 = \frac{\gamma_{11}^3}{\gamma_{20}\sqrt{-\gamma_{20}}} Y_2,\quad t = -\frac{\sqrt{-\gamma_{20}}}{\gamma_{11}}\tau$. Then, the system (6.4.11) reduces to

$$\begin{cases} \frac{dZ_1}{dt} = Z_2, \\ \frac{dZ_2}{dt} = \mu_1(\lambda_1, \lambda_2) + \mu_2(\lambda_1, \lambda_2) Z_2 + Y_1^2 \pm Z_1 Z_2 + R(Z_1, Z_2, \mu), \end{cases} \tag{6.4.12}$$

where $\mu_1(\lambda_1, \lambda_2) = \frac{\gamma_{00}\gamma_{11}^4}{\gamma_{20}^3} - \frac{\gamma_{10}^2\gamma_{11}^4}{4\gamma_{20}^4},\ \ \mu_2(\lambda_1, \lambda_2) = -\frac{\gamma_{01}\gamma_{11}}{\sqrt{\gamma_{20}}} + \frac{\gamma_{00}\gamma_{11}^2}{2\gamma_{20}^2}$ and $R(X_1, X_2, 0)$ is a power series in (Z_1, Z_2) with powers $Z_1^i Z_2^j$ satisfying $i + j \geq 3$ with $j \geq 2$.

If matrix $\left[\frac{\partial(\mu_1, \mu_2)}{\partial(\lambda_1, \lambda_2)} \right]$ is nonsingular, systems (6.4.8) and (6.4.12) are topologically equivalent to the normal form of the Bogdanov-Takens bifurcation as given below

$$\begin{cases} \frac{du_1}{dt} = u_2, \\ \frac{du_2}{dt} = \mu_1(\lambda_1, \lambda_2) + \mu_2(\lambda_1, \lambda_2) u_2 + u_1^2 \pm u_1 u_2. \end{cases} \tag{6.4.13}$$

Moreover, the following local representations of the bifurcation curves obtain in small neighbourhood of the the origin:

1) The saddle-node bifurcation curve, $SN = \{(\mu_1, \mu_2) : \mu_1 = 0, \mu_2 \neq 0\}$.

2) The Hopf bifurcation curve, $H = \{(\mu_1, \mu_2) : \mu_2 = \sqrt{-\mu_1}, \mu_1 < 0\}$.

3) The homoclinic bifurcation curve, $HL = \{(\mu_1, \mu_2) : \mu_2 = \frac{5}{7}\sqrt{-\mu_1}, \mu_1 < 0\}$.

Theorem 6.4.4. *The system* (6.2.4) *undergoes a Bogdanov-Takens bifurcation with respect to the bifurcation parameters θ and δ around the equilibrium point E_4, if exists, whenever*

$tr(J_{E_4}) = 0$ *and* $\omega_1\omega_1 \neq 0$.

6.5 Numerical Simulations

(1) If $\gamma = 10,\ \alpha = 1,\ \beta = 0.5,\ \xi = 1.5,\ \delta = 0.4$ and $\theta = 0.3$. The parametric conditions of Proposition $(6.3.1)(ii)(a)(1)$ are satisfied. The system with these parametric values has two axial equilibrium points, $E_0 = (0,0), E_1 = (10,0)$, and two interior equilibrium points, $E_1^* = (4.81386, 3.79307)$ and $E_2^* = (7.68614, 2.35693)$. Points E_0 and E_2^* are saddle points whereas points E_1 and E_1^* are asymptotically stable. When $\theta = \theta^{[hf]} = 0.2160448$, the system (6.2.4) has two interior equilibrium points, $E_1^* = (8.57824, 1.57506)$ and $E_2^* = (3.92176, 3.9033)$. Point E_1^* is unstable and enclosed by a stable limit cycle, while the point E_2^* is saddle. The first Lyapunov number $\sigma = -2.29151 < 0$. When $\theta = \theta^{[SN]} = 0.3515625$, system (6.2.4) has a unique interior equilibrium points $E_4 = (6.25, 3.28125)$ which is a saddle-node point.

(2) If $\gamma = 10,\ \alpha = 2,\ \beta = 0.5,\ \xi = 1.5,\ \delta = 0.18$ and $\theta = 2$. The parametric conditions of Proposition $(6.3.1)(ii)(b)(4)$ are satisfied. The system with these parametric values has three axial equilibrium points, $E_0 = (0,0), E_1 = (10,0), E_2 = (0,48)$ and two interior equilibrium points, $E_1^* = (1.18206, 4.56951)$ and $E_2^* = (8.72419, 1.62336)$. The point E_0, E_2 and E_2^* are saddle points. The point E_1 is asymptotically stable and the point E_1^* is unstable. When $\theta = \theta^{[hf]} = 4.31764$, the system (6.2.4) has two interior equilibrium points, $E_1^* = (3.86489, 4.8252)$ and $E_2^* = (6.04136, 3.97502)$. Point E_1^* is unstable and enclosed by a stable limit cycle, while the point E_2^* is saddle. The first Lyapunov number $\sigma = -2.29151 < 0$. When $\theta = 4.1$, the stable limit cycle collides with the saddle point and a stable Homoclinic loop arises around the equilibrium point $E_1^* = (3.40121, 4.8839)$. The Lyapunov number $\sigma = -2.08239$. When $\theta = 4.45$, the system (6.2.4) has two interior equilibrium points, $E_1^* = (4.29003, 4.73358)$ and $E_2^* = (5.61622, 4.21554)$. The point E_1^* is stable and E_2^* is saddle. When $\theta = \theta^{[SN]} = 4.528168$, the system (6.2.4) has a unique interior equilibrium points $E_4 = (4.95313, 4.51853)$, which is a saddle-node point.

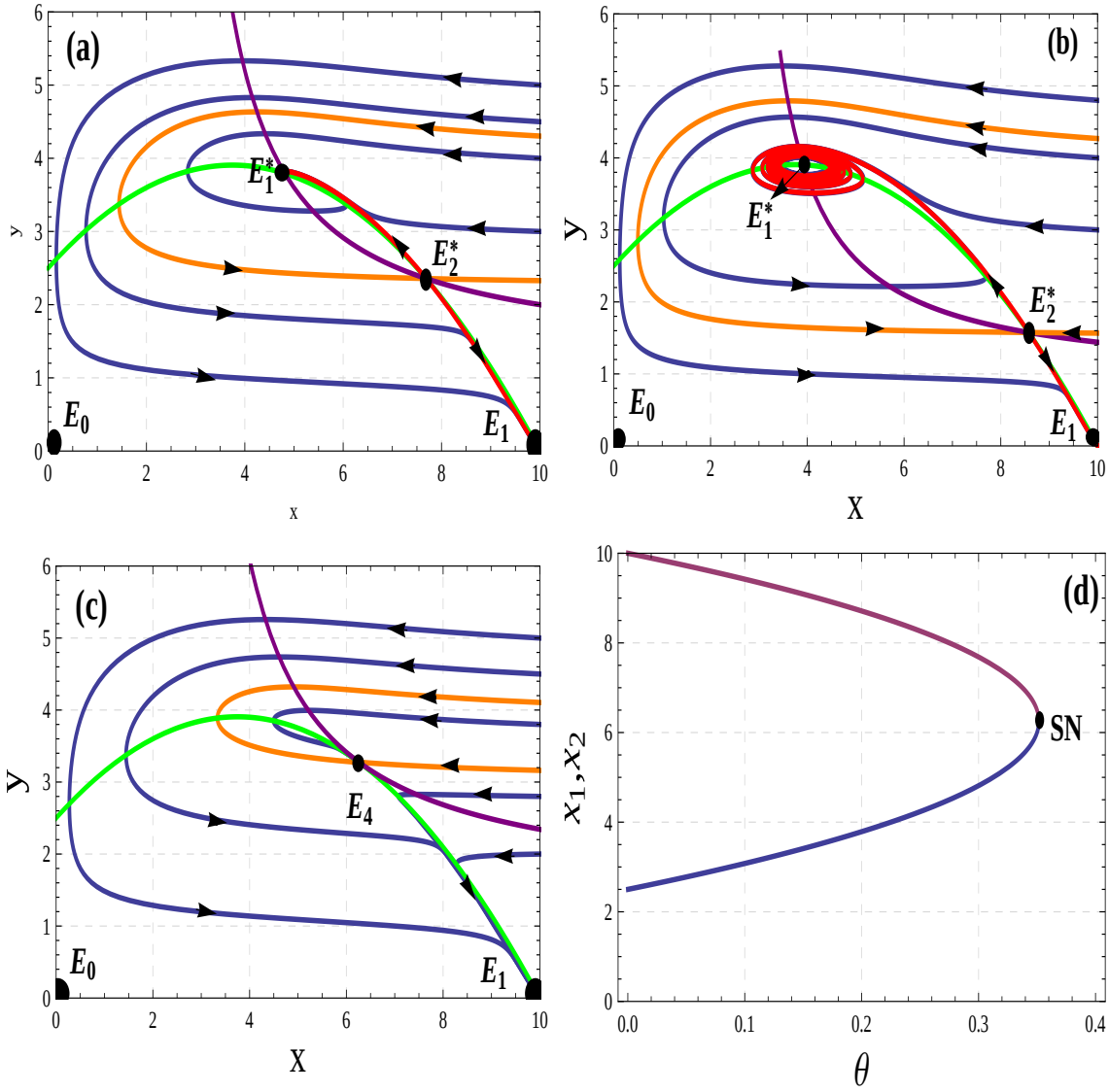

Figure 6.1: $\gamma = 10$, $\alpha = 1$, $\beta = 0.5$, $\xi = 1.5$, $\delta = 0.4$ (a) $\theta = 0.3$. System (6.2.4) has two interior equilibrium points $E_1^* = (4.81386, 3.79307), E_2^* = (7.68614, 2.35693)$. The point E_1^* is stable and E_2^* is saddle. (b) $\theta = \theta^{[hf]} = 0.2160448$. System (6.2.4) has two interior equilibrium points $E_1^* = (8.57824, 1.57506), E_2^* = (3.92176, 3.9033)$. A stable limit cycle arises through Hopf bifurcation around E_1^*, E_2^* is a saddle point. (c) $\theta = \theta^{[SN]} = 0.3515625$. System (6.2.4) has a unique interior equilibrium points $E_4 = (6.25, 3.28125)$ which is a saddle-node point. The red color trajectories are unstable manifold, the orange color trajectories are the stable manifold, the green color curve the prey nullcline and purple color curve is the predator nullcline. (d) Saddle-node bifurcation diagram. Upper curve stands for unstable equilibria and lower curve stands for stable equilibria.

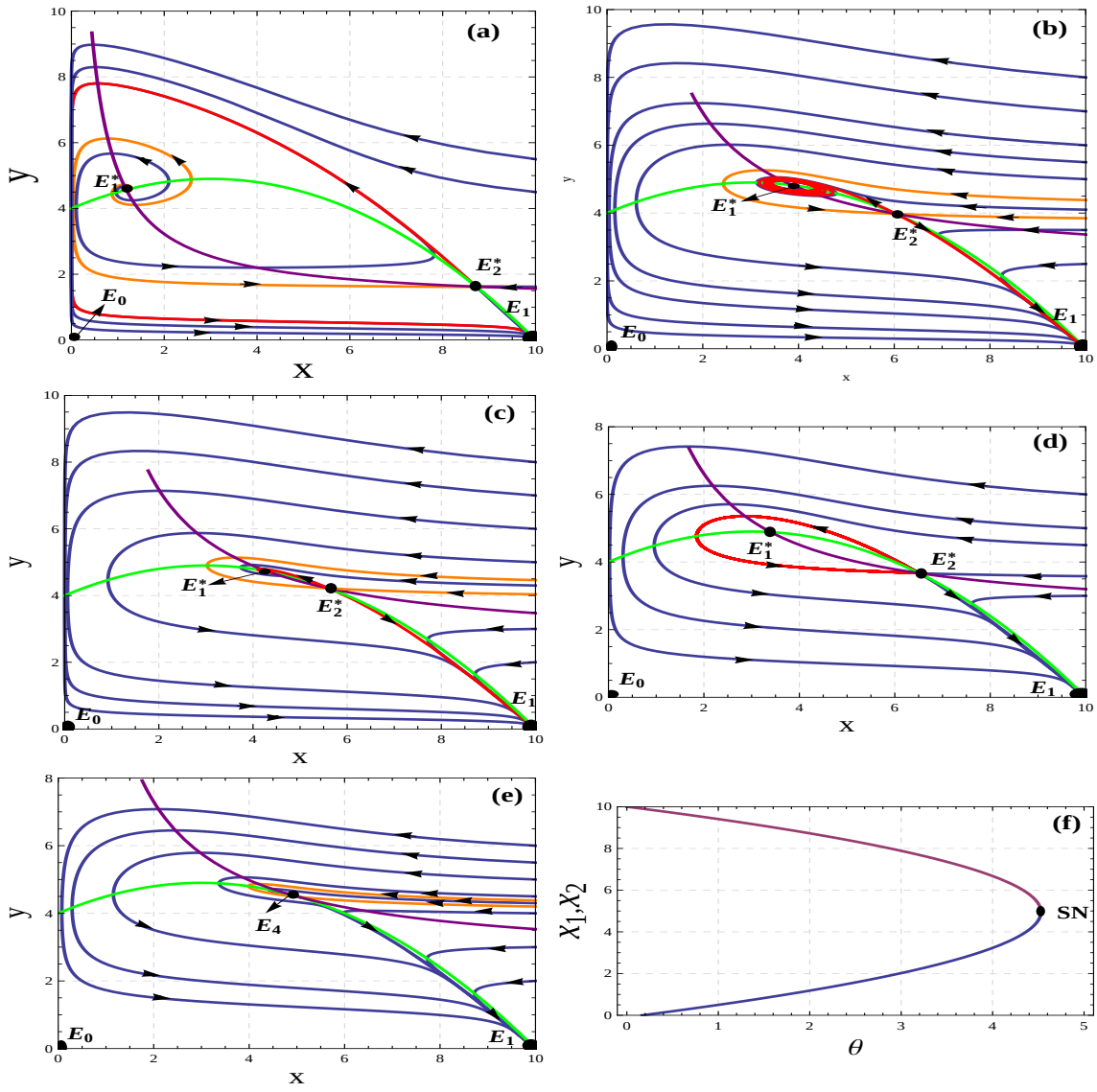

Figure 6.2: $\gamma = 10,\ \alpha = 2,\ \beta = 0.5,\ \xi = 1.5,\ \delta = 0.18$ (a) $\theta = 2$. System (6.2.4) has two interior equilibrium points $E_1^* = (1.18206, 4.56951), E_2^* = (8.72419, 1.62336)$. The point E_1^* is unstable and E_2^* is saddle. (b) $\theta = 4.31764$. System (6.2.4) has two interior equilibrium points $E_1^* = (3.86489, 4.8252), E_2^* = (6.04136, 3.97502)$. A stable limit cycle arises through Hopf bifurcation around E_1^*, point E_2^* is saddle. (c) $\theta = 4.45$. System (6.2.4) has two interior equilibrium points $E_1^* = (4.29003, 4.73358), E_2^* = (5.61622, 4.21554)$. The point E_1^* is stable and E_2^* is saddle. (d) $\theta = 4.1$. System (6.2.4) has two interior equilibrium points $E_1^* = (3.40121, 4.8839), E_2^* = (6.50504, 3.67147)$. A stable Homoclinic loop is emerging through Hopf bifurcation around E_1^*. (e) $\theta = 4.528168$. System (6.2.4) has a unique interior equilibrium points $E_4 = (4.95313, 4.51853)$ which is a saddle-node point. The red color trajectories are unstable manifold, the orange color trajectories are the stable manifold, the green color curve the prey nullcline and purple color curve is the predator nullcline. (f) Saddle-node bifurcation diagram. Upper curve stands for unstable equilibria and lower curve stands for stable equilibria.

(3) If $\gamma = 10,\ \alpha = 1.5,\ \beta = 2,\ \xi = 1$. So, $\delta_0 = 1.268389665,\ \theta_0 = 1.017347956$. Therefore, the system 6.2.4 reduces to

$$\begin{cases} \frac{dx}{dt} = x(1-\frac{x}{10}) - \frac{xy}{2.5+x}, \\ \frac{dy}{dt} = \frac{2(x+1)y}{2.5+x}\frac{y}{y+1.01735+\lambda_2} - (1.26839+\lambda_1)y, \end{cases} \tag{6.5.1}$$

The system (6.5.1) has a unique interior equilibrium point $E_4 = (5.80027, 3.48589)$. First, shift the point $E_4 = (5.80027, 3.48589)$ to the origin by means of the transformation $x_1 = x - 5.80027, x_2 = y - 3.48589$, and then introduce the affine transformation $y_1 = x_1,\ y_2 = a_{10}x_1 + a_{01}x_2$. System (6.5.1) reduces to

$$\begin{cases} \frac{dy_1}{dt} = y_2 + \xi_{20}(\lambda)y_1^2 + \xi_{11}(\lambda)y_1y_2 + \overline{R}_1(y_1, y_2), \\ \frac{dy_2}{dt} = \eta_{00}(\lambda) + \eta_{10}(\lambda)y_1 + \eta_{01}(\lambda)y_2 + \eta_{20}(\lambda)y_1^2 + \eta_{11}(\lambda)y_1y_2 + \\ \qquad \eta_{02}(\lambda)y_2^2 + \overline{R}_2(y_1, y_2), \end{cases} \tag{6.5.2}$$

where $\xi_{20}(\lambda) = -0.0698805, \quad \xi_{11}(\lambda) = 0.0519277, \quad \eta_{00}(\lambda) = -2.43596\Big(-1.26839 - \lambda_1 + \frac{5.71186}{4.50324+\lambda_2}\Big), \quad \eta_{10}(\lambda) = -0.363455 - 0.286548\lambda_1 + \frac{2.90368}{4.50324+\lambda_2} - \frac{5.70543}{(4.50324+\lambda_2)^2}, \quad \eta_{01} = -1.55494 - \lambda_1 + \frac{11.4237}{4.50324+\lambda_2} - \frac{19.9109}{(4.50324+\lambda_2)^2}, \quad \eta_{20} = 0.200241 - \frac{0.0609924}{4.50324+\lambda_2} + \frac{1.19067}{(4.50324+\lambda_2)^2} - \frac{2.33954}{(4.50324+\lambda_2)^3}, \quad \eta_{11} = -0.0148798 - \frac{1.04022}{4.50324+\lambda_2} + \frac{8.83956}{(4.50324+\lambda_2)^2} - \frac{16.3291}{(4.50324+\lambda_2)^3},, \quad \eta_{02} = -\frac{2.34481}{4.50324+\lambda_2} + \frac{16.3475}{(4.50324+\lambda_2)^2} - \frac{28.4928}{(4.50324+\lambda_2)^3}$ and $\overline{R_1}, \ \overline{R_2}$ are the power series in (y_1, y_2) with powers $y_1^i y_2^j$ satisfying $i + j \geq 3$.

Consider the C^∞ change of coordinates in the small neighbourhood of $(0, 0)$: $z_1 = y_1 - \frac{1}{2}(\xi_{11} + \eta_{02})y_1^2, \ \ z_2 = y_2 + \xi_{20}y_1^2 - \eta_{02}y_1y_2$ and $v_1 = z_1, \ \ v_2 = z_2 + \hat{R}_1(z_1, z_2)$ respectively. The system (6.5.2) reduces to

$$\begin{cases} \frac{dz_1}{dt} = z_2 + \hat{R}_1(z_1, z_2), \\ \frac{dz_2}{dt} = \gamma_{00} + \gamma_{10}z_1 + \gamma_{01}z_2 + \gamma_{20}z_1^2 + \gamma_{11}z_1z_2 + \hat{R}_2(z_1, z_2), \end{cases} \tag{6.5.3}$$

where $\gamma_{00}(\lambda) = -2.43596\Big(-1.26839 - \lambda_1 + \frac{5.71186}{4.50324+\lambda_1}\Big), \quad \gamma_{10}(\lambda) = -0.363455 - 0.286548\lambda_1 - \frac{396.444}{(4.50324+\lambda_2)^4} + \frac{315.492+69.4072\lambda_1}{(4.50324+\lambda_2)^3} - \frac{88.8403+39.8218\lambda_1}{(4.50324+\lambda_2)^2} + \frac{10.1485+5.71186\lambda_1}{4.50324+\lambda_2}, \quad \gamma_{01} = -1.55494 - \lambda_1 - \frac{19.9109}{(4.50324+\lambda_2)^2} + \frac{11.4237}{4.50324+\lambda_2}, \quad \gamma_{20} = -0.0980724 - 0.0773204\lambda_1 +$

$\frac{5647.9}{(4.50324+\lambda_2)^7} - \frac{7735.06+988.802\lambda_1}{(4.50324+\lambda_2)^6} + \frac{4146.64+1134.63\lambda_1}{(4.50324+\lambda_2)^5} - \frac{1074.91+488.24\lambda_1}{(4.50324+\lambda_2)^4} + \frac{126.936+91.0944\lambda_1}{(4.50324+\lambda_2)^3} - \frac{4.62619+5.38837\lambda_1}{(4.50324+\lambda_2)^2} + \frac{0.574682-0.187649\lambda_1}{4.50324+\lambda_2}$, $\gamma_{11} = -0.154641 - \frac{16.3291}{(4.50324+\lambda_2)^3} + \frac{8.83956}{(4.50324+\lambda_2)^2} - \frac{1.04022}{4.50324+\lambda_2}$ and $\hat{R}_1$, $\hat{R}_2$ are the power series in (z_1, z_2) with powers $z_1^i z_2^j$ satisfying $i + j \geq 3$.

Here $\gamma_{20} = 0.0395753 > 0$. By means of Malgrange preparation theorem and transformations:

$$X_1 = v_1, \quad X_2 = \frac{v_2}{\sqrt{\gamma_{20}}}, d\tau = \sqrt{\gamma_{20}}dt,$$

$$Y_1 = X_1 + \frac{\gamma_{10}}{2\gamma_{20}}, \quad Y_2 = X_2,$$

$$Z_1 = \frac{\gamma_{11}^2}{\gamma_{20}} Y_1, \quad Z_2 = \frac{\gamma_{11}^3}{\gamma_{20}\sqrt{\gamma_{20}}} Y_2, \quad t = \frac{\sqrt{\gamma_{20}}}{\gamma_{11}}\tau,$$

the system (6.5.3) reduces to

$$\begin{cases} \frac{dZ_1}{d\tau} = Z_2, \\ \frac{dZ_2}{d\tau} = \mu_1(\lambda_1, \lambda_2) + \mu_2(\lambda_1, \lambda_2)Z_2 + Z_1^2 - Z_1 Z_2 + R(Z_1, Z_2, \mu), \end{cases} \tag{6.5.4}$$

where $\mu_1(\lambda_1, \lambda_2) = \frac{\gamma_{00}\gamma_{11}^4}{\gamma_{20}^3} - \frac{\gamma_{10}^2\gamma_{11}^4}{4\gamma_{20}^4}$, $\mu_2(\lambda_1, \lambda_2) = \frac{\gamma_{01}\gamma_{11}}{\sqrt{\gamma_{20}}} - \frac{\gamma_{00}\gamma_{11}^2}{2\gamma_{20}^2}$. The determinant of matrix $\left[\frac{\partial(\mu_1,\mu_2)}{\partial(\lambda_1,\lambda_2)} \right] = 47.7723$. Thus, the system (6.5.1) undergoes to attracting Bogdanov-Takens bifurcation. The three bifurcation curves divide the small neighbourhood of the BT bifurcation point $(0, 0)$ in the $\lambda_1\lambda_2$ plane into four different regions, shown in the Figure 6.3(a). The blue curve is the Saddle-node bifurcation curve, red curve is the Hopf bifurcation curve and green curve is the Homoclinic bifurcation. When $\lambda_1 = 0 = \lambda_2$, the system (6.2.4) has a unique interior equilibrium point, which is a cusp of codimension 2 (Figure 6.3(b)). When λ_1 and λ_2 vary and satisfy $\mu_1(\lambda_1, \lambda_2) > 0$, then λ_1 and λ_2 lie in the region I. The system (6.2.4) has no interior equilibrium point, and in this region, the predator will tend to extinction (Figure 6.3(c)). When λ_1 and λ_2 keep varying and satisfy $\mu_1(\lambda_1, \lambda_2) < 0$, then system (6.2.4) has two interior equilibrium points. If λ_1 and λ_2 lie in region II, one interior equilibrium point is a saddle and other is a stable focus. The both species either can co-exist or predator species will tend to extinction depending on the initial

population (Figure 6.3(d)). If λ_1 and λ_2 lie in region III, one interior equilibrium point is a saddle and other is an unstable focus surrounded by a unique stable limit cycle (Figure 6.3(e)). Thus, in this region either both species oscillate or the predator species will tend to extinction depending on the initial population. If λ_1 and λ_2 lie in region IV, one interior equilibrium point is a saddle and other is an unstable focus (Figure 6.3(f)).

6.6 Results and Discussion

Srinivasu et al. (2007) proposed a predator-prey system incorporating some additional food to predators (System (6.2.2)). They used quality and quantity parameters of the additional food as a control variable to derive control strategies in integrated pest management. The controllability of the system (6.2.2) has also been studied by Srinivasu and Prasad (2010, 2011). These studies show the effect of providing additional food to predators and its consequences on predator-prey dynamics. In this chapter, the dynamical behaviour of the system (6.2.2) in the presence of Allee effect to predator (6.2.4) has been analysed. The qualitative analysis of the model depending on all parameters shows that the model exhibits interesting, complex and varied dynamics.

The system with Allee effect has three boundary equilibria in which the predator-prey free equilibria (origin) and prey free equilibria (E_2) are always saddle, while the predator free equilibria (E_1) is always asymptotically stable. Ecologically speaking, the prey species will never tend to extinction. The system has at most two interior equilibrium points. The stability of these interior equilibrium point for system (6.2.4) has been studied by adopting Routh-Hurwitz criterion. The system shows bi-stability in certain parametric restrictions, that is, system is very sensitive for initial values. Moreover, under certain parametric restriction the predator free equilibria (E_1) is globally asymptotically stable. Ecologically speaking, the predator species will tend to extinction and the population of prey species will tend to the carrying capacity. The model has a degenerate equilibria which is a saddle-node or a cusp of codimension 2 depending upon the parametric conditions.

The local emergence of limit cycles through Hopf bifurcation for the system has been

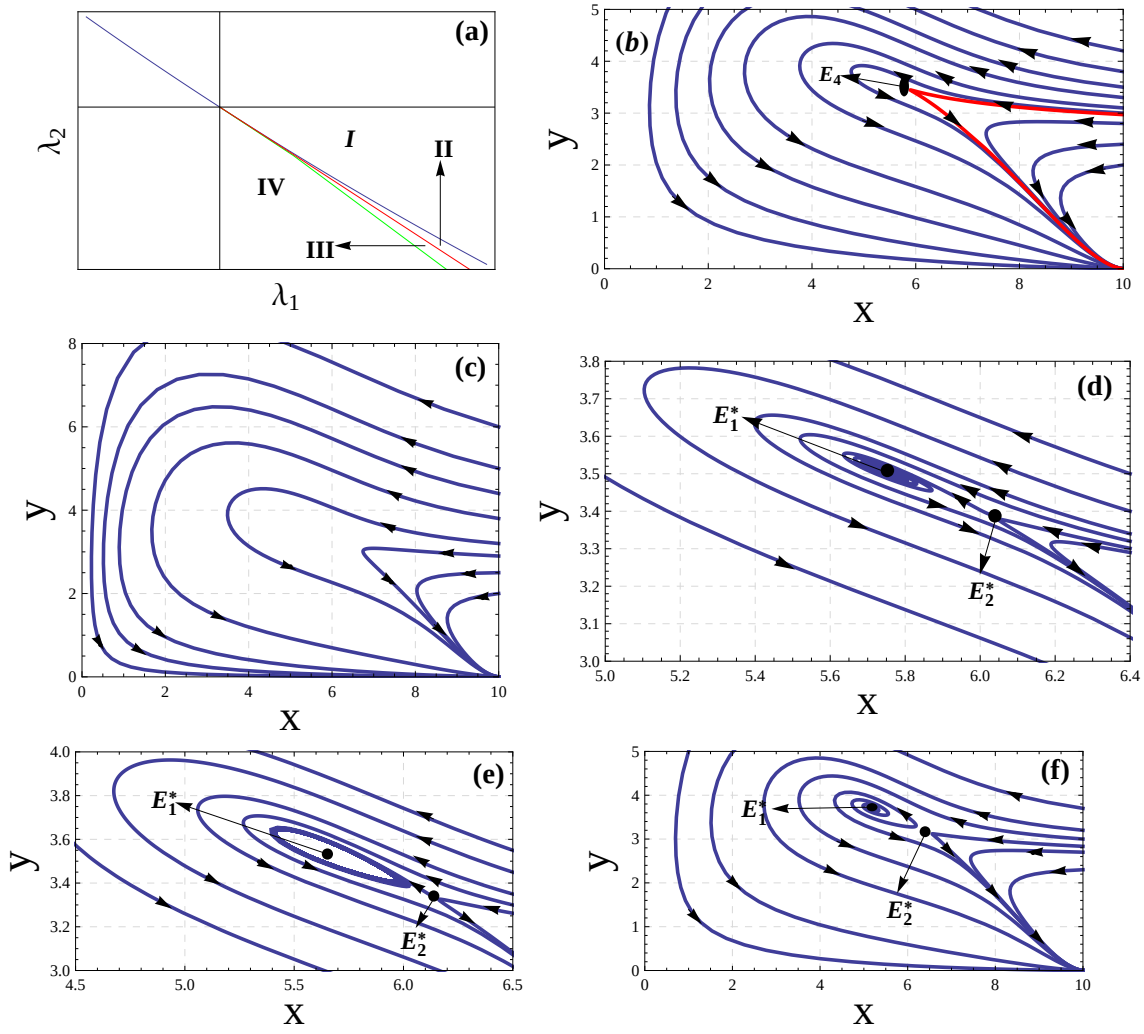

Figure 6.3: (a) Bifurcation diagram for the system (6.2.4). The blue curve is Saddle-node bifurcation curve, red curve is the Hopf bifurcation curve and green curve is the Homoclinic bifurcation curve. (b) $\lambda_1 = \lambda_2 = 0$ The unique interior equilibrium point E_4 is a cusp of codimension 2 (c) System (6.2.4) has no interior equilibrium point, whenever $(\lambda_1, \lambda_2) = (0.029, -0.1)$ lies in region I (d) System (6.2.4) has two interior equilibrium points, whenever $(\lambda_1, \lambda_2) = (0.02861, -0.1)$ lies in region II, in which one is a saddle and other is stable focus (e) System (6.2.4) has two interior equilibrium points whenever $(\lambda_1, \lambda_2) = (0.02791, -0.1)$ lies in region III, a stable limit cycle enclosing an interior point and the other interior point is a saddle. (f) System (6.2.4) has two interior equilibrium points, whenever $(\lambda_1, \lambda_2) = (0.02161, -0.1)$ lies in region IV, in which one is a saddle and other is unstable focus.

shown. It is cumbersome to determine the sign of first Lyapunov number analytically, and so, the stability of limit cycles has been studied through numerical simulations. A threshold value of the parameter θ has been obtained such that the system can have zero, one or two interior equilibria as the parameter θ crosses this value, that is, the system undergoes to a Saddle-node bifurcation. Ecologically speaking, whenever the bifurcation parameter θ is below the threshold value, then both predator and prey species co-exist and whenever it is above the threshold value, then predator species suddenly collapse to extinction. The system undergoes to Transcritical bifurcation, which has been proved analytically using Sotomayor's theorem. The system exhibits Bogdanov-Takens bifurcation, and it has been shown that, it is topologically equivalent to standard normal form of Bogdanov-Takens bifurcation. Ecologically, there exists a set of parametric values for which both the predator and prey populations co-exist in form of a positive equilibrium, oscillate or predator species tend to extinction.

The quality and quantity of the additional food also play a key role on the dynamic of the predator-prey system (6.2.4), as the parameters α and ξ are involved in all computations. Particularly, there exists a relation between these two parameters, $1 + \alpha\xi - \xi$. The system is dynamically rich, whenever $1 + \alpha\xi - \xi > 0$.

Chapter 7

Stability Analysis under Internal Heating and Gravity Modulation Effects

7.1 Introduction

The studies of thermal instability in porous media plays very significant roles in many areas such as in petroleum industry, chemical engineering and geophysics, etc. A detail account of the work on thermal instability in porous media has been given in the most excellent books due to vafai (2000); Ingham and Pop (2005) and Nield and Bejan (2013).

External regulation of convection is important either for enhancing or diminishing heat transfer in a physical system. This type of regulations (e.g. thermal, gravity, rotation and magnetic field modulation) are used effectively to control convective phenomenon. This chapter is concerned with the thermal instability under gravity modulation, first studied by Gresho and Sani (1970). In this model, they observed that the gravity modulation enables the system to get control on its instability either by suitably adjusting the values

This chapter is based on the research article: Stability analysis and internal heating effect on oscillatory convection in a viscoelastic fluid saturated porous medium under gravity modulation, Int. J. of Applied Mechanics and Engineering, 2016, vol.21, No.4, pp.785-803. (De Gruyter)

of frequency or the amplitude of modulation. The related studies of gravity modulation are given in Malashetty and Padmavathi (1997); Das and Pop (2000); Bhadauria et al. (2005, 2012a, 2012b).

The nature of non-Newtonian fluids is quite different from Newtonian fluids due to their properties like shear stress and shear strain. The basic idea for considering these fluids is due to their oscillatory nature. For example, industrial fluids are basically non-Newtonian. In particular, viscoelastic fluids have been potentially important. Proper understanding of convective motion and its behaviour is necessary for controlling many processes such as geothermal reservoirs, filtration, enhanced oil recovery. Green (1968) was the first to study the oscillatory convection in a viscoelastic fluid layer, Vest and Arpaci (1969) reported the occurrence of overstability for typical Rayleigh-Bénard convection of a horizontal homogeneous Maxwellian fluid layer heated from below. Bhatia and Steiner (1972) studied thermal instability in a rotating viscoelastic fluid layer. Some studies on thermal convection of viscoelastic fluids in porous media is available in the literature. Kim et al. (2003) investigated the critical conditions of stationary and oscillatory instabilities in a viscoelastic fluid saturated horizontal porous layer based on the modified Darcy-Oldroyd model. Malashetty and Kulkarni (2009) used a two-field model in the energy equation to investigate the thermal non-equilibrium problem of a Maxwell fluid in a porous medium, Wang and Tan (2011) performed linear and nonlinear analyses on double-diffusive convection with the Soret effect in a Maxwell fluid-saturated porous medium. Kumar and Bhadauria (2011a, 2011b) studied thermal instability in viscoelastic fluid saturated porous media under rotation and double diffusive gradients. A series of work related to oscillatory mode of convection is investigated by Bhadauria and Kiran (2014a, 2014b). These authors derived complex Ginzburg-Landau equations for obtaining finite amplitude convection under modulation, and the conditions for which the oscillatory convective flow is confirmed.

There are situations of great practical importance, where the porous material offers its own source of heat. This gives a different way in which a convective flow can be set up through the local heat generation within the porous media. Such a situation can occur through radioactive decay or through, in the present perspective, a relatively weak exothermic reaction, which can take place within the porous material.

In the present literature, no work is available related to the oscillatory convection under modulation with an internal heat source. However, there are situations of great practical importance, where the porous material offers its own source of heat, and this can modify the convective flow through local heat generation within the porous media. To be specific, internal heat is one of the main source of energy for celestial bodies caused by nuclear fusion and decaying of radioactive materials, which keeps the celestial objects warm and active. It is due to the internal heating of the earth that there exists a thermal gradient between the interior and exterior of the earth crust, saturated by multi-components fluids, which helps convective flow, thereby transferring the thermal energy towards the surface of the earth. So the role of internal heat generation becomes very important in several applications that include geophysics, reactor safety analyses, metal waste form development for spent nuclear fuel, fire and combustion studies, and in storage of radioactive materials. Some of the studies on thermal instability under internal heat generation, are due to Bhattacharya and Jena (1984); Altawallbeh et al (2013); Bhadauria et al. (2013); Srivastava (2013).

In the present chapter, the combined effect of gravity modulation and internal heating on oscillatory convection in a viscoelastic fluid saturated porous material has been studied.

7.2 Mathematical Formulation

Consider an infinitely extended horizontal viscoelastic fluid saturated porous medium, which is heated from below and cooled from above. Darcy model has been employed in the momentum equation. Further, an internal heat source term has been included in the energy equation. The physical configuration of the model is reported in Figure 7.1. The corresponding mathematical model of the problem under the Boussinesq approximation (Bhadauria and Kiran 2014) is given below:

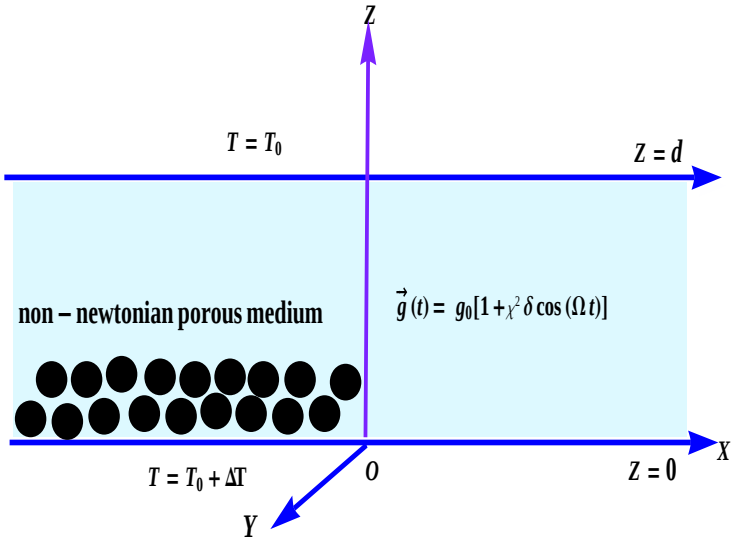

Figure 7.1: Physical configuration of the problem.

$$\begin{cases} \nabla.\vec{q} = 0, \\ \left(\overline{\lambda_1}\frac{\partial}{\partial t} + 1\right)\left(-\nabla p + \rho\vec{g}\right) - \frac{\mu}{K}\left(\overline{\lambda_2}\frac{\partial}{\partial t} + 1\right)\vec{q} = 0, \\ \frac{\partial T}{\partial t} + (\vec{q}.\nabla)T = \kappa_T\nabla^2 T + Q(T - T_0), \\ \rho = \rho_0[1 - \alpha_T(T - T_0)], \end{cases} \tag{7.2.1}$$

where the physical variables have their usual meanings as given in the nomenclature. The externally imposed gravitational field and the thermal boundary conditions are given by

$$\vec{g} = g_0[1 + \chi^2\delta\cos(\Omega t)]\hat{k}, \tag{7.2.2}$$

$$\begin{cases} T = T_0 + \Delta T, & at \quad z = 0, \\ = T_0, & at \quad z = d, \end{cases} \tag{7.2.3}$$

where g_0 is the mean gravity and $\hat{k}$ is the unit vector along the positive $z-$axis.

7.3 Basic State

At this state the velocity, pressure, temperature and density profiles are given by

$$\vec{q_b} = 0, p = p_b(z), T = T_b(z), \rho = \rho_b(z). \tag{7.3.1}$$

The following basic equations are direct from Eq. (7.3.1) and Eq. (7.2.1)

$$\frac{dp_b}{dz} = -\rho_b g, \tag{7.3.2}$$

$$\kappa_T \frac{d^2(T_b - T_0)}{dz^2} + Q(T_b - T_0) = 0, \tag{7.3.3}$$

$$\rho_b = \rho_0[1 - \alpha_T(T_b - T_0)]. \tag{7.3.4}$$

The solution of Eq. (7.3.3), subject to the boundary conditions (7.2.3), is given by

$$T_b = T_0 + \Delta T \frac{\sin((\sqrt{\frac{Q}{\kappa_T}})(1 - \frac{z}{d}))}{\sin(\sqrt{\frac{Q}{\kappa_T}})}. \tag{7.3.5}$$

Superimpose finite amplitude perturbations on the basic state in the form:

$$\vec{q} = q_b + q', T = T_b + T', p = p_b + p', \rho = \rho_b + \rho', \tag{7.3.6}$$

where the primes represents the perturbation quantities. The dimensionless governing system, as in Bhadauria and Kiran (2014), is give by

$$\Big(\lambda_1 \frac{\partial}{\partial t} + 1\Big) g_m Ra_D \frac{\partial T}{\partial x} + \Big(\lambda_2 \frac{\partial}{\partial t} + 1\Big) \nabla^2 \psi = 0, \tag{7.3.7}$$

$$-\frac{\partial\psi}{\partial x}\frac{\partial T_b}{\partial z}+\Big(\frac{\partial}{\partial t}-\nabla^2-R_i\Big)T=\frac{\partial(\psi,T)}{\partial(x,z)}, \tag{7.3.8}$$

where $g_m=(1+\chi^2\delta\cos(\Omega t))$, $Ra_D=\frac{\alpha_T g_0\Delta TKd}{\nu\kappa_T}$ is the thermal Rayleigh number, $R_i=\frac{Qd^2}{\kappa_T}$ is the internal Rayleigh number, $\nu=\frac{\mu}{\rho_0}$ is the kinematic viscosity. The above system will be solved by considering stress free and isothermal boundary conditions as given below

$$\psi=\frac{\partial^2\psi}{\partial z^2}=T=0 \;\; on \;\; z=0, z=1. \tag{7.3.9}$$

The dimensionless basic temperature field $T_b(z)$, which appears in Eq. (7.3.8), is given by

$$\frac{dT_b}{dz}=-\frac{\sqrt{R_i}\cos(\sqrt{R_i}(1-z))}{\sin\sqrt{R_i}}. \tag{7.3.10}$$

Introducing a small perturbation parameter χ which shows a deviation from the critical state of onset of convection, the variables for a weak non-linear state may be expanded in power series of χ, as Malkus and Veronis (1958) and Venezian (1969).

$$Ra_D=R_0+\chi^2R_2+\chi^4R_4+...., \tag{7.3.11}$$

$$\psi=\chi\psi_1+\chi^2\psi_2+\chi^3\psi_3+...., \tag{7.3.12}$$

$$T=\chi T_1+\chi^2T_2+\chi^3T_3+...., \tag{7.3.13}$$

where R_0 is the critical value of the Darcy-Rayleigh number at which the onset of convection takes place in the absence of gravity modulation.

7.4 Analysis of Periodic Solution

In order to study time periodic convective phenomenon according to Kim et al. (2003) and Bhadauria et al. (2014), the slow and fast time scale will be introduced as $\frac{\partial}{\partial t}=\frac{\partial}{\partial\tau}+\chi^2(\frac{\partial}{\partial s})$. The above system (7.3.7) and (7.3.8) will be solved at every order of χ.

At the first order, one can obtain the matrix operator(the reader may note that this is

similar to linear case)

$$\begin{bmatrix} (\lambda_2\frac{\partial}{\partial\tau}+1)\nabla^2 & R_0(\lambda_1\frac{\partial}{\partial\tau}+1)\frac{\partial}{\partial x} \\ -\frac{\partial}{\partial x}\frac{\partial T_b}{\partial z} & (\frac{\partial}{\partial\tau}-\nabla^2-R_i) \end{bmatrix} \begin{bmatrix} \psi_1 \\ T_1 \end{bmatrix} = \begin{bmatrix} 0 \\ 0 \end{bmatrix}. \tag{7.4.1}$$

The solution of the first order system, subject to the boundary conditions (7.3.9), is assumed as

$$\psi_1 = (A(s)e^{i\omega\tau} + \overline{A}(s)e^{-i\omega\tau})\sin ax\ \sin\pi z, \tag{7.4.2}$$

$$T_1 = (B(s)e^{i\omega\tau} + \overline{B}(s)e^{-i\omega\tau})\cos ax\ \sin\pi z. \tag{7.4.3}$$

The undetermined amplitudes are functions of slow time scale, and are related by the following expression

$$B(s) = -\frac{4\pi^2 a}{(c+i\omega-R_i)(4\pi^2-R_i)}A(s), \tag{7.4.4}$$

where $c = a^2+\pi^2$. The values of the critical Darcy-Rayleigh number and the corresponding wave number of the system for a stationary mode of convection, are as given below:

$$R_0^{st} = \frac{c(c-R_i)(4\pi^2-R_i)}{4\pi^2 a^2}, \tag{7.4.5}$$

$$a_c^2 = \sqrt{(\pi^4-\pi^2 R_i)}. \tag{7.4.6}$$

For the system without internal-heating, i.e., $R_i = 0$, one gets

$$R_0 = \frac{c^2}{a^2}, \tag{7.4.7}$$

$$a_c = \pi, \tag{7.4.8}$$

which are the classical results, as obtained in Horton and Rogers (1945). The critical Darcy-Rayleigh number and the corresponding wave number of the system for oscillatory mode of convection as

$$R_0^{osc} = \Big(\frac{c(c-R_i)-\lambda_2\omega^2}{a^2}\Big)\frac{4\pi^2-R_i}{4\pi^2}, \tag{7.4.9}$$

$$a_c^2 = \sqrt{\pi^4+\frac{\pi^2}{\lambda_2}-\pi^2 R_i}, \tag{7.4.10}$$

where ω is the oscillatory frequency which is given by

$$\omega^2 = \frac{(\lambda_1 - \lambda_2)c + R_i(\lambda_2 - \lambda_1) - 1}{\lambda_1 \lambda_2}. \tag{7.4.11}$$

Since ω is real, therefore, from the Relation (7.4.11), the necessary condition for oscillatory convection as:

$$\lambda_1 > \lambda_2 + \frac{1 - R_i(\lambda_2 - \lambda_1)}{c}. \tag{7.4.12}$$

Now, at the second order, one gets

$$\begin{bmatrix} (\lambda_2 \frac{\partial}{\partial \tau} + 1)\nabla^2 & R_0(\lambda_1 \frac{\partial}{\partial \tau} + 1)\frac{\partial}{\partial x} \\ -\frac{\partial}{\partial x}\frac{\partial T_b}{\partial z} & (\frac{\partial}{\partial \tau} - \nabla^2 - R_i) \end{bmatrix} \begin{bmatrix} \psi_2 \\ T_2 \end{bmatrix} = \begin{bmatrix} R_{21} \\ R_{22} \end{bmatrix}, \tag{7.4.13}$$

where

$$R_{21} = 0, \tag{7.4.14}$$

$$R_{22} = \frac{\partial \psi_1}{\partial x}\frac{\partial T_1}{\partial z} - \frac{\partial \psi_1}{\partial z}\frac{\partial T_1}{\partial x}. \tag{7.4.15}$$

The second order solution, subject to the boundary condition (7.3.9), is given by

$$\psi_2 = 0, \tag{7.4.16}$$

$$\Big(\frac{\partial}{\partial \tau} - \nabla^2 - R_i\Big) T_2 = (R_{22}). \tag{7.4.17}$$

Keeping Kim et al. (2003) and Bhadauria et al. (2014) in mind, the second order temperature term written as

$$T_2 = \{T_{20} + T_{22} e^{2i\omega t} + \overline{T}_{22} e^{-2i\omega t}\} \sin(2\pi z), \tag{7.4.18}$$

where T_{22} and T_{20} are temperature fields having the terms with the frequency 2ω and independent of fast time scale, respectively. The solutions of the second order problems are

$$T_{20} = \frac{\pi a}{8\pi^2 - 2R_i}\{A(s)\overline{B}(s) + \overline{A}(s)B(s)\}, \tag{7.4.19}$$

and

$$T_{22} = \frac{\pi a}{8\pi^2 + 4i\omega - 2R_i} A(s)B(s). \tag{7.4.20}$$

The horizontally averaged Nusselt number, $Nu(s)$, for the oscillatory mode of convection is given by

$$Nu(s) = 1 + \Big[\chi^2 \Big(\frac{\partial T_2}{\partial z}\Big)_{z=0} / \Big(\frac{dT_b}{dz}\Big)_{z=0}\Big]. \tag{7.4.21}$$

By using Eqs. (7.3.10), (7.4.18)-(7.4.20), one can simplify Eq. (7.4.21) as

$$\begin{aligned} Nu(s) =& 1 + \left(\frac{a^2(c - R_i)4\pi^2}{((c - R_i)^2 + \omega^2)(8\pi^2 - 2R_i)} + \frac{2\pi^2 a^2}{\sqrt{(c - R_i)^2 + \omega^2}\sqrt{(8\pi^2 - 2R_i)^2 + 16\omega^2}} \right) \\ & \Big(\frac{4\pi^2}{4\pi^2 - R_i}\Big) \frac{\tan\sqrt{R_i}}{\sqrt{R_i}} |A(s)|^2. \end{aligned} \tag{7.4.22}$$

It is clear that the gravity modulation is effective at third order, and affects $Nu(s)$ through $A(s)$, which is evaluated at third order.

At the third order, one gets

$$\begin{bmatrix} (\lambda_2 \frac{\partial}{\partial \tau} + 1)\nabla^2 & R_0(\lambda_1 \frac{\partial}{\partial \tau} + 1)\frac{\partial}{\partial x} \\ -\frac{\partial}{\partial x}\frac{\partial T_b}{\partial z} & (\frac{\partial}{\partial \tau} - \nabla^2 - R_i) \end{bmatrix} \begin{bmatrix} \psi_3 \\ T_3 \end{bmatrix} = \begin{bmatrix} R_{31} \\ R_{32} \end{bmatrix}, \tag{7.4.23}$$

where

$$R_{31} = -\lambda_2 \frac{\partial}{\partial s}(\nabla^2 \psi_1) - R_0 \lambda_1 \frac{\partial}{\partial s}\frac{\partial T_1}{\partial x} - (R_2 + R_0 \delta \cos(\Omega s))(\lambda_1 \frac{\partial}{\partial \tau} + 1)\frac{\partial T_1}{\partial x}, \tag{7.4.24}$$

$$R_{32} = \frac{\partial \psi_1}{\partial x}\frac{\partial T_2}{\partial z} - \frac{\partial T_1}{\partial s}. \tag{7.4.25}$$

Using first and second order solutions, the expressions of R_{31} and R_{32} will be determined. Now, using the solvability condition for the existence of third order solution, one can derive the complex Gingburg-Landau equation for finite amplitue convection.

$$\frac{dA(s)}{ds} - \gamma^{-1} F(s) A(s) + \gamma^{-1} k |A(s)|^2 A(s) = 0, \tag{7.4.26}$$

where

$$\gamma = \Big[\lambda_2 c - \frac{R_2\lambda_1 a^2}{(c+i\omega-R_i)}\frac{4\pi^2}{(4\pi^2-R_i)} + \frac{a^2R_2(1+\lambda_1 i\omega)}{(c+i\omega-R_i)^2}\frac{4\pi^2}{(4\pi^2-R_i)}\Big],$$

$$F(s) = \Big[\frac{a^2R_2(1+i\omega\lambda_1)(1+\delta\cos(\Omega s))}{(c+i\omega-R_i)}\frac{4\pi^2}{(4\pi^2-R_i)}\Big] and$$

$$k = -\Big[\frac{R_2a^4(1+\lambda_1 i\omega)(c-R_i)}{(c+i\omega-R_i)[(c-R_i)^2+\omega^2]}\frac{4\pi^2}{(8\pi^2-2R_i)} + \frac{R_2a^4[(c-R_i)^2+\omega^2\lambda_1]}{(c+i\omega-R_i)[(c-R_i)^2+\omega^2]}\frac{4\pi^2}{(8\pi^2-2R_i+4i\omega)}\Big]\Big(\frac{4\pi^2}{(4\pi^2-R_i)}\Big).$$

Writing $A(s)$ in the phase-amplitude form, one gets

$$A(s) = |A(s)|e^{i\phi}. \tag{7.4.27}$$

Now, substituting Eq. (7.4.27) in Eq. (7.4.26), one gets the following expression for the amplitude $|A(s)|$ as

$$\frac{d|A(s)|^2}{ds} - 2p_r|A(s)|^2 + 2l_r|A(s)|^4 = 0, \tag{7.4.28}$$

$$\frac{d(ph(A(s)))}{ds} = p_i - l_i|A(s)|^2, \tag{7.4.29}$$

where $\gamma^{-1}F(s) = p_r + ip_i$, $\gamma^{-1}k = l_r + il_i$ and ph(.) represents the phase shift. The Eq. (7.4.28) solved numerically using the function ND Solve of Mathematica, subject to the suitable initial condition $A(0) = a_0$, where a_0 is the chosen initial amplitude of convection. In our calculation, it is assumed that $R_2 = R_0$, to keep the parameters to the minimum.

7.5 Bifurcation Analysis

The qualitative study of dynamical system is very important, thus attracted attentions of the researchers during the last few decades. Bifurcations are important scientifically, which provide models of transitions and instabilities as some control parameter is varied (Strogatz 2007). In this section, two types of bifurcation (1) Pitchfork bifurcation (this bifurcation is common in physical problems that have a symmetry); (2) Hopf bifurcation (bifurcation corresponding to the presence of $\lambda_{1,2} = \pm i\omega_0, \omega_0 > 0$) are discussed, for details, refer Kuznetsov (2004).

7.5.1 Hopf Bifurcation

The complex Ginzburg−Landau equation (7.4.26) can be written as

$$\frac{dA(s)}{ds} = (\alpha + i\beta)A(s) - (\xi + i\zeta)|A(s)|^2 A(s), \tag{7.5.1}$$

where $\alpha = Re\big[\frac{F(s)}{\gamma}\big], \beta = Im\big[\frac{F(s)}{\gamma}\big], \xi = Re\big[\frac{k}{\gamma}\big]$, and $\zeta = Im\big[\frac{k}{\gamma}\big]$.
Putting $A(s) = \rho_1 e^{i\phi}$ in Eq. (7.5.1), and equating the real and imaginary parts, one gets

$$\dot{\rho_1} = \rho_1(\alpha - \xi\rho_1^2) \tag{7.5.2}$$

$$\dot{\phi} = \beta - \zeta\rho_1^2. \tag{7.5.3}$$

Clearly, the Eq. (7.5.2) has an equilibrium point $\rho_1 = 0$, for all values of α. Further, the Eq. (7.5.3) describes the rotation. Hence, Eq. (7.5.1) has an equilibrium at the point $A(s) = 0$ i.e. origin. This equilibrium is a stable focus for $\alpha < 0$ and an unstable focus for $\alpha > 0$ and at $\alpha = 0$ (critical value) the equilibrium is non-linearly stable and topologically equivalent to the focus. This equilibrium is surrounded, for $\alpha > 0$, by an isolated limit cycle that is unique and stable. All orbits starting outside or inside the cycle except at the origin tend to the cycle as $s \to +\infty$ (Figure 7.2(a)). This is an Andronov-Hopf bifurcation. Consider λ_1 as the bifurcation parameter, the critical value of the Hopf-bifurcation is $\lambda_1 = 0.14336936$. The phase portrait diagram for the critical value shows that the System (7.5.1) undergoes Hopf bifurcation around the origin (Figure 7.2(b)). This bifurcation can also be represented in (x, y, α) coordinate system (Figures 7.2(c)). Figure 7.2(d) shows that these $\alpha-$ family of limit cycles forms a paraboloid surface.

7.5.2 Pitchfork bifurcation

The Eq. (7.4.28) can be written as

$$\frac{d|A(s)|}{ds} - p_r|A(s)| + l_r|A(s)|^3 = 0. \tag{7.5.4}$$

The steady state solution (equilibrium point) of the equation (7.5.4) is $|A(s)| = 0$ for all value of p_r and l_r, and $|A(s)| = \pm\sqrt{\frac{p_r}{l_r}}$ for $p_r > 0, l_r > 0$.
The unsteady state solution of equation (7.5.4) is given by

$$|A(s)|^2 = \frac{A_0^2}{\frac{l_r}{p_r}A_0^2 + (1 - \frac{l_r}{p_r}A_0^2)e^{-2p_r s}}, p_r > 0, l_r > 0 \tag{7.5.5}$$

where A_0 is the initial value of the amplitude. From Eq. (7.5.5), it is clear that as $s \to -\infty, |A(s)| \to 0$ and if $s \to \infty$, then $|A(s)|$ grows towards $\sqrt{p_r/l_r}$, when $0 < A_0 < \sqrt{p_r/l_r}$ and decreases towards $\sqrt{p_r/l_r}$, when $A_0 > \sqrt{p_r/l_r}$. Thus, the equilibrium point $A(s) = 0$ is the only equilibrium point, when $p_r < 0$ and it is stable. When $p_r = 0$, then in this case, the origin is again the only equilibrium point, which is still stable but much more weakly so. When $p_r > 0, l_r > 0$, then $|A(s)| = 0$ is still an equilibrium point, but becomes unstable and two new stable equilibrium points appear on either side of $|A(s)| = 0$, symmetrically located at $|A(s)| = \pm\sqrt{p_r/l_r}$ (Figure 7.3). This is known as supercritical pitchfork bifurcation, shown in Figure 7.4.

7.6 Results and Discussion

This chapter investigates the combined effect of internal heating and gravity modulation on oscillatory convection in a viscoelastic fluid saturated porous medium. A weakly nonlinear stability analysis is performed to investigate the effect of gravity modulation on heat transport in the presence of internal heat generation. This analysis helps us to derive an amplitude equation in terms of complex coefficients which gives finite amplitude of convection. The present model is valued for oscillatory mode of convection, when the relation (7.4.12) holds for viscoelastic parameters. The new contribution to the recent study by Bhadauria and Kiran (2014) is the effect of heat generation and bifurcation analysis. The results of the corresponding problem is presented in the Figures 7.5-7.10, where the graphs are drawn for Nu versus slow time s. Relation (7.4.22), confirms that the value of Nu starts with 1, thus showing the conduction state initially. The value of Nu increases as time varies, thus showing the modulation effect. The numerical values of Nu have been

obtained from the expression (7.4.22) while solving the amplitude equation (7.4.28).

The effect of internal Rayleigh number R_i on heat transport is to increase the heat transport in the system as depicted in Figure 7.5. It is to be noted that, when the value of R_i increases, the internal energy of the system increases. The moderate values of R_i are considered to avoid its domination in the system. This confirms the results obtained recently in the studies Bhadauria (2012). The effects of relaxation parameter λ_1 (Figure 7.6) and retardation parameter λ_2 (Figure 7.7) are found to destabilize or stabilize the system respectively, and consequently increase or decrease the heat transfer in the system. The effects of the amplitude δ and frequency Ω of modulation on heat transport are given in Figure 7.8 and Figure 7.9 respectively. Figure 7.8 confirms that an increment in amplitude of modulation increases the magnitude of Nu, thus enhances the heat transfer and advances the onset of convection. An opposite effect is obtained in the case of frequency of modulation Ω (Figure 7.9). Moreover, the effect of gravity modulation decreases as the frequency of modulation increases. The effect disappears altogether, when the frequency of modulation becomes very large. The proposed results of internal heating have been compared with the results of non-internal heating system, reported in Figure 7.10. It is observed that in the presence of internal heat source, the magnitude of Nu is larger than that in the absence of internal-heating, i.e. the heat transport in the system is due to internal-heating. Thus, internal-heating advances the onset of convection, confirming the results obtained by Bhadauria et al. (2013).

In Figures 7.11 and 7.12, the streamlines and corresponding isotherms are depicted respectively, at $s = 0.0, 0.13, 0.16, 0.2, 0.3, 0.43$ for $\lambda_1 = 0.5, \lambda_2 = 0.1, \delta = 0.2, \chi = 0.5$ and $R_i = 0.1$. From the figures, it is observed that initially, when time is small, the magnitude of streamlines is also small (Figures 7.11(a) and (b)) and isotherms are straight (Figures 7.12(a) and (b)), that is, the system is in conduction state. However, as time increases, the magnitude of streamlines increase (Figures 7.11(c) and (d)) and the isotherms lose their evenness (Figures 7.12(c) and (d)). This shows that convection is taking place in the system. The system achieves the steady state beyond $s = 0.2$ as there is no change in the streamlines and isotherms, (Figures 7.11 (e) and (f); Figures 7.12(e) and (f)).

Also, by taking λ_1 as bifurcation parameter, it has been shown that the system

represented by Landau Eq. (7.4.26) undergoes a Hopf bifurcation. Further, the limit cycles are found to be stable circles. A sketch of this bifurcation in (x, y, α) coordinate plane, results in a paraboloid surface. Apart from the Hopf bifurcation, it is also shown that the system represented by amplitude equation (7.4.28) undergoes a supercritical pichfork bifurcation. The Figure 7.13 shows that as s increases, the amplitude $|A(s)|$ becomes stable and remains stable for all future of time.

7.7 Conclusions

A combined effect of internal heating and gravity modulation on oscillatory convection have been investigated by performing a weak nonlinear stability analysis using the Gingburg-Landau equation. Following conclusions are drawn:

a) The nature and the effect of viscoelastic fluid is in agreement with the studies of Kim et al. (2003) and Bhadauria and Kiran (2014).

b) The effects of amplitude and frequency of modulation are, respectively to increase and decreases the heat transfer.

c) The effect of internal Rayleigh number is to increase the heat transport in the system.

d) The equilibrium point of the Ginzburg-Landau equation losses its stability as λ_1 increases .

e) If $p_r > 0$ and $l_r > 0$, then the amplitude equation gives two more equilibrium points, which are stable, while the origin losses its stability.

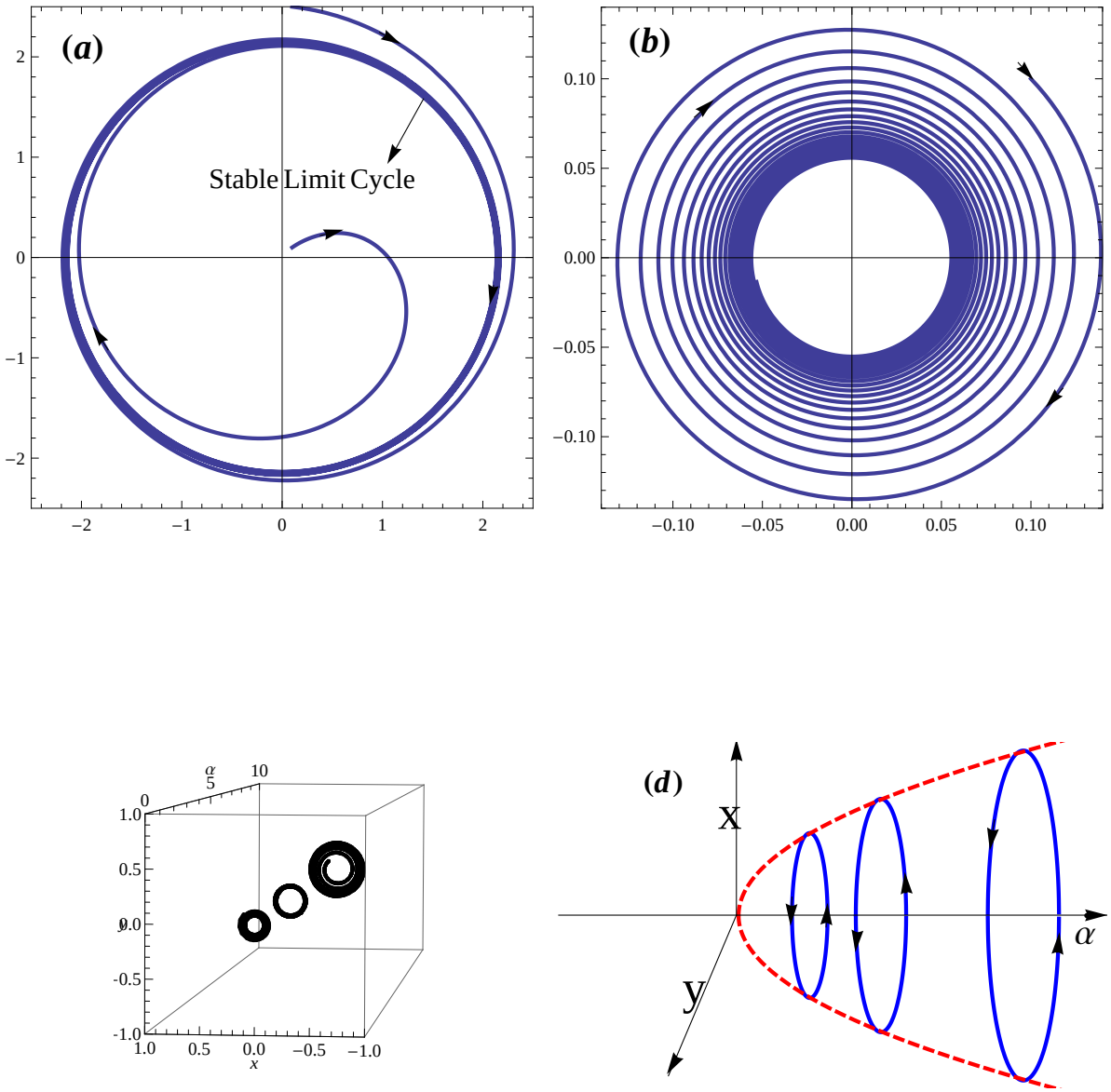

Figure 7.2: Hopf bifurcation diagram for parameter values $\lambda_2 = 0.1, \Omega = 1, \delta = 0.02, R_i = 0.4$ (a) $\lambda_1 = 0.5$ (b) $\lambda_1 = 0.14336936$ (c) Supercritical Hopf bifurcation in the phase parameter (x, y, α) space (d) Paraboloid surface formed by α family of limit cycles.

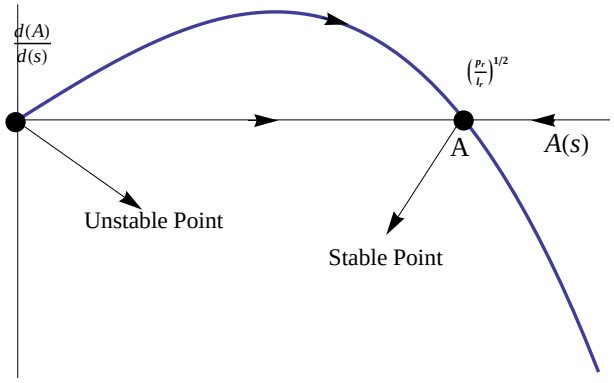

Figure 7.3: The point A is stable while the origin is unstable. $\lambda_1 = 0.5, \lambda_2 = 0.1, \Omega = 2, \delta = 0.02, R_i = 1$

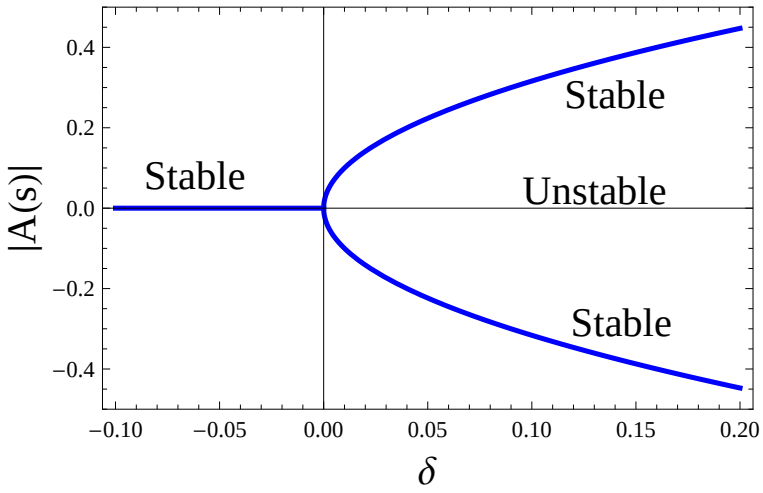

Figure 7.4: Supercritical Pitchfork Bifurcation. $\lambda_1 = 0.5, \lambda_2 = 0.1, \Omega = 2, \delta = 0.02, R_i = 1, s = \pi/3$

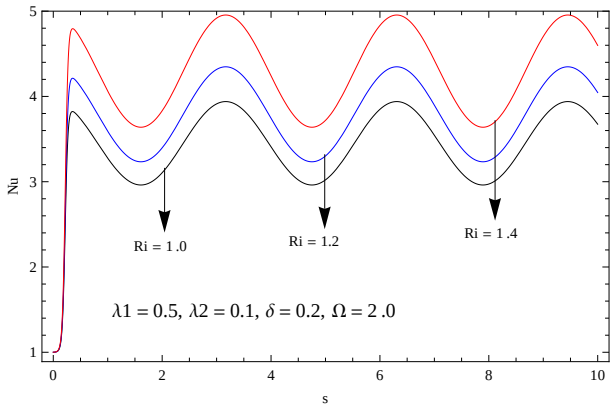

Figure 7.5: Effect of Ri on Nu For fixed values of the other parameters.

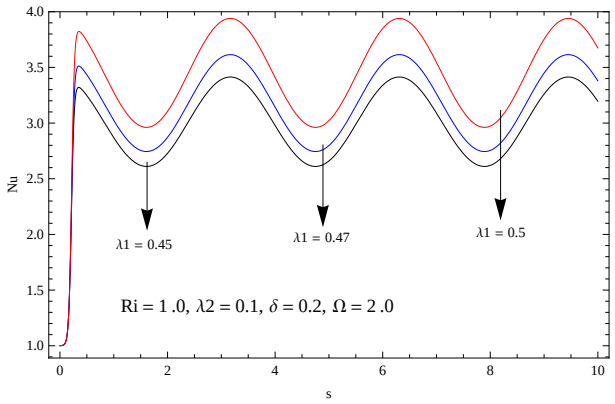

Figure 7.6: Effect of λ_1 on Nu For fixed values of the other parameters.

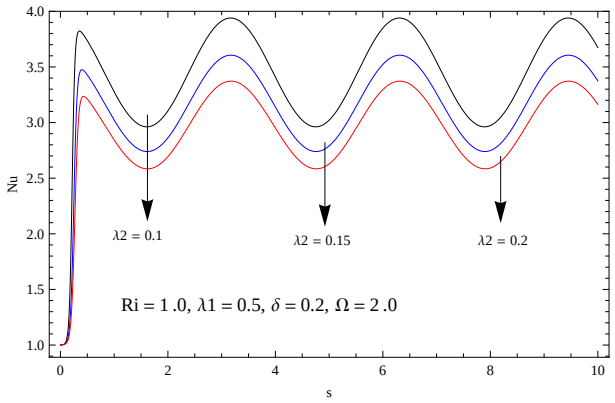

Figure 7.7: Effect of λ_2 on Nu For fixed values of the other parameters.

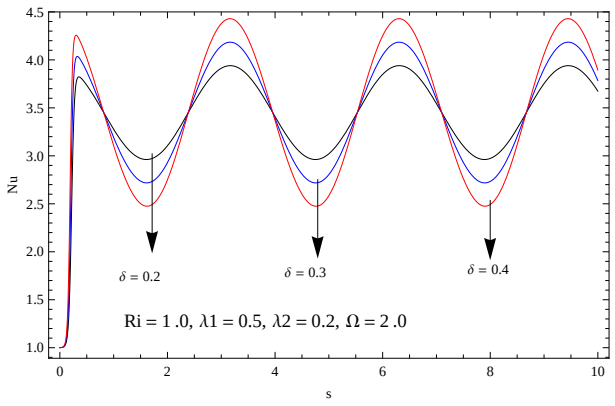

Figure 7.8: Effect of δ on Nu For fixed values of the other parameters.

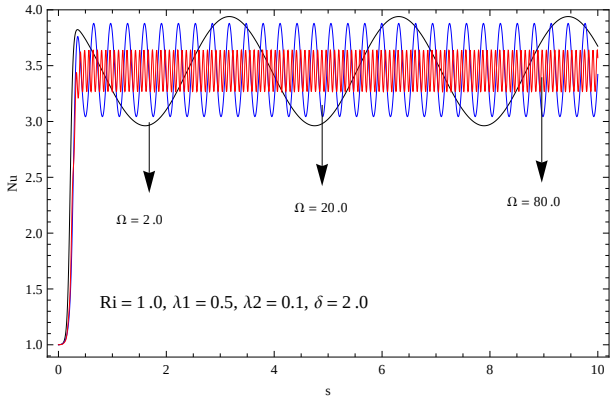

Figure 7.9: Effect of Ω on Nu For fixed values of the other parameters.

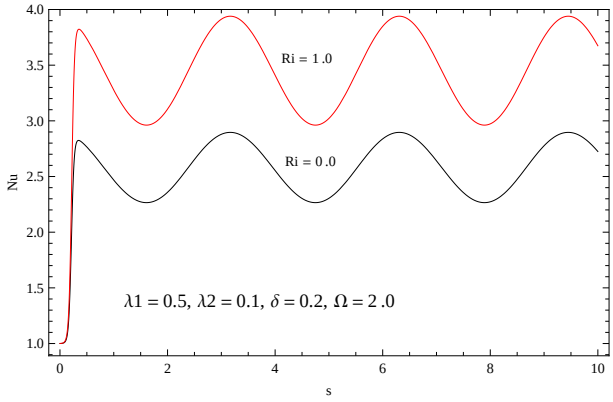

Figure 7.10: Comparison between internal and non-internal heating system.

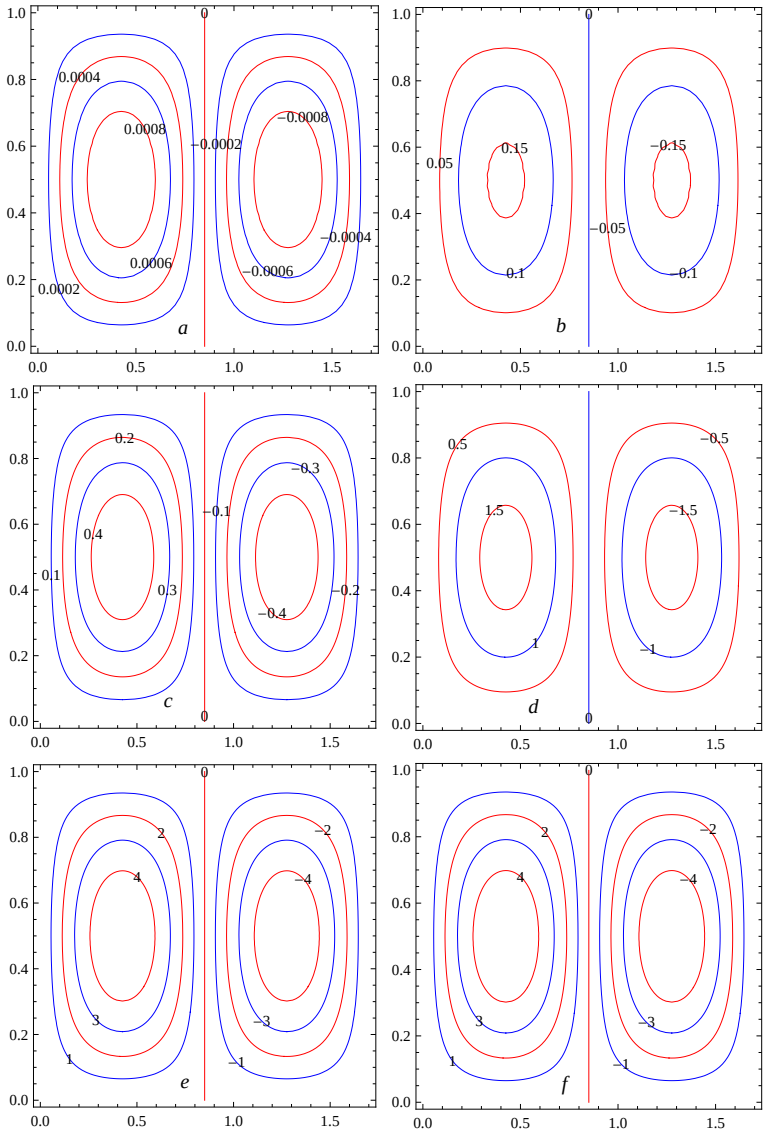

Figure 7.11: Stremlines at (a) $s = 0.0$, (b) $s = 0.13$, (c) $s = 0.16$, (d) $s = 0.2$, (e) $s = 0.3$, (f) $s = 0.43$.

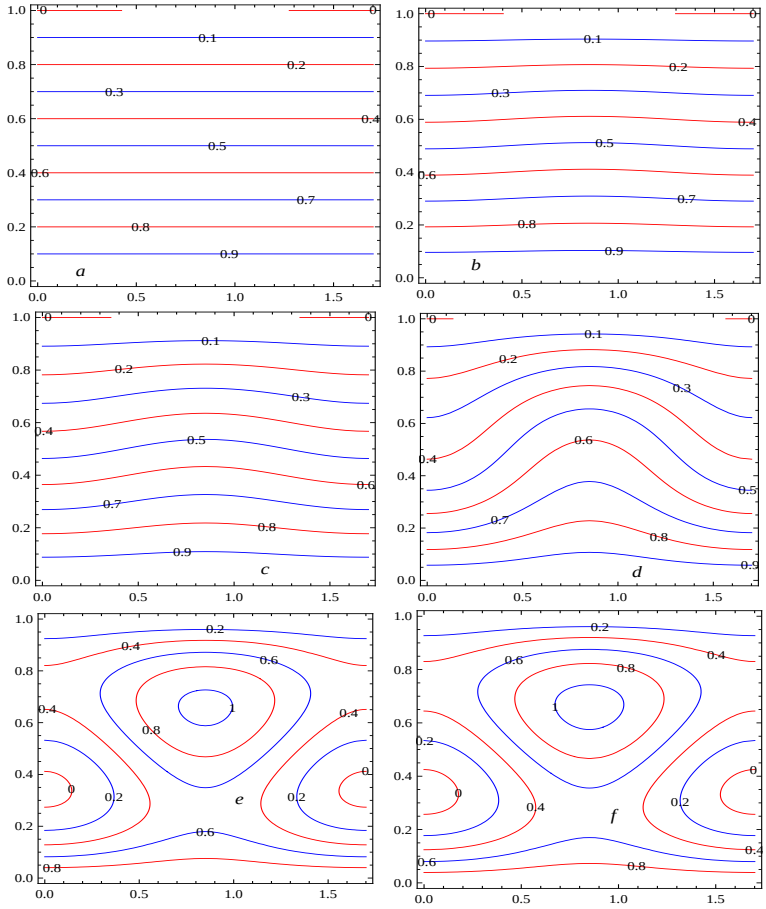

Figure 7.12: Isotherms at (a) $s = 0.0$, (b) $s = 0.13$, (c) $s = 0.16$, (d) $s = 0.2$, (e) $s = 0.3$, (f) $s = 0.43$.

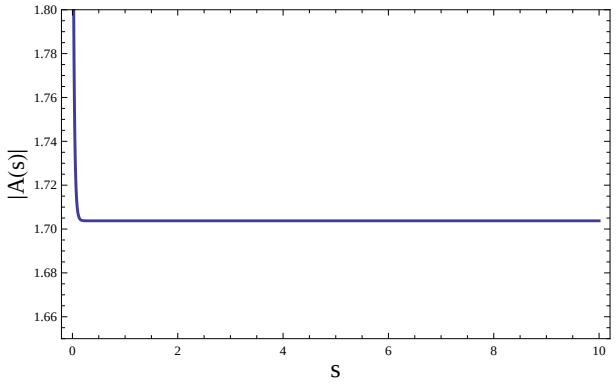

Figure 7.13: Phase portrait diagram for $A(s)$ and s, shows that $A(s)$ is stable when s increases.

Bibliography

[1] Abrams PA (1994); The fallacies of ratio-dependent predation. Ecology 75: 1842-1850.

[2] Aguirre P, Alez-Olivares EG, Saez E (2009a); Two limit cycles in a Leslie-Gower predator-prey model with additive Allee effect. Nonlinear Ana.: Real World Appl. 10: 1401-1416.

[3] Aguirre P, Alez-Olivares EG, Saez E (2009b); Three limit cycles in a Leslie-Gower predator-prey model with additive Allee effect. Siam J. Appl. Math. 69(5): 1244-1262.

[4] Allee WC (1931); Animal Aggregations: A study in General Sociology. University of Chicago Press, USA.

[5] Altawallbeh AA, Bhadauria BS, Hashim I (2013); Linear and nonlinear double-diffusive convection in a saturated anisotropic porous layer with Soret effect and internal heat source. Int. J. Heat Mass Transf. 59: 103-111.

[6] Andrews JF (1968); A mathematical model for the continuous culture of microorganisms utilizing inhibitory substrates. Biotech. Bioeng. 10: 707-723.

[7] Angulo E, Roemer GW, Berec L, Gascoigne J, Courchamp F (2007); Double Allee effects and extinction in the island fox. Conser. Biol. 21: 1082-1091

[8] Arditi R, Ginzburg L, Akcakaya H (1991); Variation in plankton densities among lakes: a case for ratio-dependent predation models. The Am. Nat. 138: 1287-1296.

[9] Arditi R, Perrin N, Saah H (1991); Functional responses and heterogeneities: an experimental test with cladocerans. Oikos 60(1): 69-75.

[10] Arditi R, Ginzburg L (2012); How species interact: altering the standard view on trophic ecology. USA: OUP.

[11] Arino O, Mikram J, Chattopadhyay J (2004); Infection on prey population may act as a biological control in ratio-dependent predator-prey model. Nonlinearity 17: 1101-1116.

[12] Ayala FJ, Gilpin ME, Ehrenfeld JG (1973); Competition between species: Theorical models and experimental tests. Theo. Pop. Biol. 4: 331-356.

[13] Aziz-Alaoui MA, Daher Okiye M (2003); Boundedness and global stability for a predator-prey model with modified Leslie-Gower and Holling-type II schemes. Appl. Math. Lett. 16(7): 1069-1075.

[14] Bazykin AD (1998); Nonlinear Dynamics of Interacting Populations. World Sci. Ser. Nonlinear Sci. Ser. A. World Scientific. Singapore vol.11.

[15] Beddington JR (1975); Mutual interference between parasites or predators and its effect on searching efficiency. J. Anim. Ecol. 44: 331-340.

[16] Beddington JR, Cooke JG (1982); Harvesting from a prey-predator complex. Ecol. Model. 14: 155-177.

[17] Beddington JR and May RM (1982); Maximum sustainable yields in systems subject to harvesting at more than one trophic level. Math. Biosci. 51: 261-281.

[18] Berec L, Angulo E, Courchamp F (2007); Multiple Allee effects and population management. Trends Ecol. Evol. 22: 185-191.

[19] Bhadauria BS (2012); Double diffusive convection in a saturated anisotropic porous layer with internal heat source. Transp. Porous Med. 92: 299-320.

[20] Bhadauria BS, Bhatia PK, Lokenath D (2005); Convection in Hele-Shaw cell with parametric excitation. Int. J. Non-Linear Mech. 40(4): 475-484.

[21] Bhadauria BS, Hashim I, Siddheshwar PG (2013); Effects of time-periodic thermal boundary conditions and internal heating on heat transport in a porous medium. Transp. Porous Med. 97: 185-200.

[22] Bhadauria BS, Kiran P (2014a); Weak non-linear oscillatory convection in a viscoelastic fluid saturated porous medium under gravity modulation. Transp. Porous Med. 104: 451-467.

[23] Bhadauria BS, Kiran P (2014b); Weak non-linear oscillatory convection in a viscoelastic fluid layer under gravity modulation. Int. J. Nonlinear Mech. 65: 133-140.

[24] Bhadauria BS, Srivastava AK, Sacheti NC, Chandran P (2012); Gravity modulation of thermal instability in a viscoelastic fluid-saturated-anisotropic porous medium. Z Naturf. 67a: 1-9.

[25] Bhadauria BS, Siddheshwar PG, Kumar Jogendra, Suthar Om P (2012); Non-linear stability analysis of temperature / gravity modulated Rayleigh-Benard convection in a porous medium. Transp. Porous Med. 92: 633-647.

[26] Bhatia PK, Steiner JM (1972); Convective instability in a rotating viscoelastic fluid layer. ZAMM, 52: 321-327.

[27] Bhattacharya SP, Jena SK (1984); Thermal instability of a horizontal layer of micropolar fluid with heat source. Proc. Indian Acad. Sci. (Math Sci) 93(1): 13-26.

[28] Boukal DS, Berec L (2002); Single-species models and the Allee effect: extinction boundaries, sex ratios and mate encounters. J. Theor. Biol. 218: 375-394.

[29] Boukal DS, Sabelis MW, Berec L (2007); How predator functional responses and Allee effects in prey affect the paradox of enrichment and population collapses. Theor. Popul. Biol. 72: 136-147.

[30] Brauer F, Soudack AC (1979); Stability regions and transition phenomena for harvested predator-prey system. J. Math. Biol. 7: 319-337.

[31] Braza PA (2003); The bifurcation structure of the Holling-Tanner model for predator-prey interactions using two-timing. SIAM J. Appl. Math. 63: 889-904.

[32] Cai Y, Zhao C, Wang W, Wang J (2014); Dynamics of a Leslie-Gower predator-prey model with additive Allee effect. Appl. Math. Model. 39(7): 2092-2106.

[33] Caughley G (1976); Plant-herbivoresystems. In: May RM, editor. Theoretical ecology: principles and applications. Philadelphia, PA: W. B. Saunders Co. 1976: 94-113.

[34] Chen L, Li Y, Xiao D (2011); Bifurcations in a ratio-dependent predator-prey model with prey harvesting. Can. Appl. Math. 19(4): 293-318.

[35] Chow SN, Hale JK (1983); Methods of Bifurcation Theory, Tim Clutton-Brock Grundlehren Mathematischen Wissenschaften. Springer-Verlag, New York, Berlin.

[36] Christopher M, Heggerud CM, Lan K (2005); Local stability analysis of ratio-dependent predator-prey models with predator harvesting rates. Appl. Math. Comp. 270: 349-357.

[37] Clark CW (1976); Mathematical Bioeconomics: The Optimal Management of Renewable Resources, Wiley, New York.

[38] Clark CW (1990); Mathematical Bioeconomics, in: The Optimal Management of Renewable Resources. 2nd ed., John Wiley New York.

[39] Cote IM, Gross MR (1993); Reduced disease in offspring: a benefit of coloniality in sunfish. Behav. Ecol. Sociobiol. 33: 269-274.

[40] Courchamp F, Clutton-Brock T, Grenfell B (1999); Inverse density dependence and the Allee effect. Trends Ecol. Evol. 14(10): 405-410.

[41] Courchamp F, Berec L, Gascoigne J (2008); Allee Effects in Ecology and Conservation. Oxford University Press.

[42] Das T, Mukherjee RN, Chaudhuri KS (2009a); Harvesting of a prey-predator fishery in the presence of toxicity. Appl. Math. Model. 33(5): 2282-2292.

[43] Das T, Mukherjee RN, Chaudhuri KS (2009b); Bioeconomic harvesting of a prey-predator fishery. J. Biol. Dyn. 3(5): 447-462.

[44] Das R, Pop I (2000); The effect of G-jitter on vertical free convection boundary-layer flow in porous media. Int. Comm. Heat Mass Transf. 27(3): 415-424.

[45] DeAngelis D (1992); Dynamics of Nutrient Cycling and Food Webs. Chapman and Hall, London. vol. 9.

[46] DeAngelis DL, Goldstein RA, ONeill RV (1975); A model for tropic interaction. Ecology 56: 881-892.

[47] Dennis B (1989); Allee effects: population growth, critical density, and the chance of extinction. Nat. Res. Model. 3: 481-538.

[48] Deredec A, Courchmp F (2003); Extinction thresholds in host parasite dynamics. Ann. Zool. Fenn. 40: 115-130.

[49] Du Y, Peng R, Wang M (2009); Effect of a protection zone in the diffusive Leslie predator-prey model. J. Diff. Eq. 246(10): 3932-3956.

[50] Edelstein-Keshet L (1988); Mathematical Models in Biology. SIAM, New York.

[51] Edwards VH (1970); Influence of high substrate concentrations on microbial kinetics. Biotech. Bioeng. 12: 679-712.

[52] Feng P, Kang Y (2015); Dynamics of a modified Leslie-Gower model with double Allee effects. Nonlinear Dyn. 80(1): 1051-1062.

[53] Flores JD, Gonzalez-Olivares E (2014); Dynamics of a predator-prey model with Allee effect on prey and ratio-dependent functional response, Ecol. Comp. 18: 59-66.

[54] Freedman HI (1980); Deterministic Mathematical Models in Population Ecology. Marcel Dekker, New York.

[55] Freedman HI, Waltman P(1984); Persistence in models of three interacting predator-prey populations. Math. Biosci. 68(2): 213-231, 1984.

[56] Gao Y, Li B (2013); Dynamics of a ratio-dependent predator-prey system with a strong Allee effect. Dis. Cont. Dyn. Syst-Ser B 18(9): 2283-2313.

[57] Gascoigne JC, Lipcius RN (2004); Allee effects driven by predation. J. Appl. Ecol. 41: 801-810.

[58] Gasull A, Kooij RE, Torregrosa J (1997); Limit cycles in the Holling-Tanner model. Publ. Mat. 41: 149-167

[59] Gause GF (1935); La Theorie mathematique de la lutte pour la vie. Hermann Paris.

[60] Gilpin ME (1973); Do hares eat lynx?, Amer. Nat. 107: 727-730.

[61] Gompertz B (1825); On the nature of the function expressing the law of human mortality. Phil. Trans. 115: 513-585.

[62] Gong Y, Huang J (2014); Bogdanov-Takens bifurcation in a Leslie-Gower predator-prey model with prey harvesting. Acta Math. Appl. Sin. Engl. ser. 30(1): 239-244.

[63] Gonzlez-Olivares E, Rojas-Palma A (2011a); Multiple limit cycles in a Gause type predatorprey model with Holling type III functional response and Allee effect on prey. Bull. Math. Biol. 73(6): 1378-1397.

[64] Gonzlez-Olivares E, Mena-Lorca J, Rojas-Palma A, Flores JD (2011b) Dynamical complexities in the Leslie-Gower predator-prey model as consequences of the Allee effect on prey. Appl. Math. Model. 35: 366-381.

[65] Green T. III. (1968); Oscillating convection in an elasticoviscous liquid. Phys. Fluids, 11: 1410.

[66] Gresho PM, Sani R (1970); The effects of gravity modulation on the stability of a heated fluid layer. J. Fluid Mech. 40: 783-806.

[67] Groom M(1998); Allee effects limit population viability of an annual plant. Am. Nat. 151: 487-496.

[68] Guckenheimer J, Holmes P (1983); Nonlinear Oscillators, Dynamical Systems, and Bifucations of Vector Fields. Appl. Math. Sci. Springer vol. 42.

[69] Gupta RP, Banarjee M, Chandra P (2012); Bifurcation analysis and control of Leslie-Gower predator-prey model with Michaelies-Menten type prey harvesting. Diff. Eq. Dyn. Sys. 20: 339-366.

[70] Gupta RP, Banarjee M, Chandra P (2015); Dynamical complexity of a prey-predator model with nonlinear predator harvesting. Dis. Cont. Dyn. Syst. Ser. B 20(2): 423-443.

[71] Gupta RP, Chandra P (2013); Bifurcation analysis of modified Leslie-Gower predator-prey model with Michaelis-Menten type prey harvesting, J. Math. Anal. Appl. 398: 278-295.

[72] Gutierrez A (1992); Physiological basis of ratio-dependent predator-prey theory: the metabolic pool model as a paradigm. Ecology 73: 1552-1563.

[73] Hale JK (1969); Ordinary Differential Equations. Johan Wiley and Sons, New York.

[74] Hale JK, Somolinos AS (1983); Competition for fluctuating nutrient. J. Math. Biol. 18: 255-280.

[75] Hassell MP, May RM, (1973); Stability in insect host-parasite models. J. Anim. Ecol. 42: 693-726.

[76] Holling CS (1965); The functional response of invertebrate predators to prey density. Mem. Entomol. Soc. Can. 45: 3-60.

[77] Holt RD (1977); Predation, apparent competition, and the structure of prey communities. Theo. Popul. Biol. 12: 197-229.

[78] Holt RD, Lawton JH (1994); The ecological consequences of shared natural enemies. Ann. Rev. Ecol. Syst. 25: 495-520.

[79] Horton CW and Rogers FT (1945); Convection currents in a porous medium. J. Appl. Phys. 16: 367-370.

[80] Hsu SB, Hwang TW (1995); Global stability for a class of predator-prey systems. SIAM J. Appl. Math. 55: 763-783.

[81] Hsu SB, Hwang TW (1998); Uniqueness of limit cycles for a predator-prey system of Holling and Lesile type. Can. Appl. Math. 6: 91-117.

[82] Hsu SB, Hwang TW (1999); Hopf bifurcation analysis for a predator-prey system of Holling and Leslie type. Taiw. J. Math. 3: 35-53.

[83] Huang J, Gong y, Ruan S, Lou Y (2013); Bifurcation analysis in a predator-prey model with constant yield predator harvesting. Dis. Con. Dyn. Sys. Ser. B. 18(8): 2101-2121.

[84] Huang J, Ruan S, Song J (2014); Bifurcations in a predator-prey system of Leslie type with generalized Holling type III functional response. J. Diff. Eq. 257: 1721-1752.

[85] Huang J, Xiao D (2004); Analyses of bifurcations and stability in a predator-prey system with Holling type IV functional response, Acta Math. Appl. Sin. Eng. Ser. 20: 167-178.

[86] Huincahue-Arcos J, Gonzlez-Olivares E (2013); The Rosenzweig-MacArthur predation model with double Allee effects on prey. In: Proceedings of the 2013 international conference on applied mathematics and computational methods in engineering.

[87] Hwang TW (2003); Global analysis of the predatorprey system with Beddington-DeAngelis functional response, J. Math. Anal. Appl. 281: 395-401.

[88] Hwang TW (2004); Uniqueness of limit cycles of the predator-prey system with Beddington-DeAngelis functional response. J. Math. Anal. Appl. 290: 113-122.

[89] Ingham DB, Pop I (2005); Transport Phenomena in Porous Media, vol. III, 1st edn. Elsevier, Oxford .

[90] Ji Y, Jiang D, Shi N (2009); Analysis of a predator-prey model with modified Leslie-Gower and Holling type II schemes with stochastic perturbation. J. Math. Anal. Appl. 359: 482-498.

[91] Ji C, Jiang D, Shi N (2011); A note on a predator-prey model with modified Leslie-Gower and Holling type II schemes with stochastic perturbation. J. Math. Anal. Appl. 377(1): 435-440.

[92] Jost C, Arino O, Arditi R (1999); About deterministic extinction in ratio-dependent predator-prey models. Bull. Math. Biol. 61: 1932.

[93] Kang Y, Yakubu A (2011); Weak Allee effects and species coexistence. Nonlinear Anal: Real World Appl. 12(6): 3329-3345.

[94] Kar TK, Ghosh B (2012); Sustainability and optimal control of an exploited prey predator system through provision of alternative food to predator. BioSystems. 109: 220 232.

[95] Kar TK, Mishra S, Mukhopadhyay B (2006); A bionomic model of a ratio-dependent predator-prey system and optimal harvesting, J. Appl. Math. Com. 22(1-2): 387-401.

[96] Kent A, Doncaster CP, Sluckin T (2003); Consequences for predators of rescue and Allee effects on prey. Ecol. Model. 162: 233-245.

[97] Kim MC, Lee SB, Kim S, Chung BJ (2003); Thermal instability of viscoelastic fluids in porous media. Int. J. Heat Mass Transfer 46: 5065-5072

[98] Korobeinikov A (2001); A Lyapunov function for Leslie-Gower predator-prey models. Appl. Math. Lett. 14: 697-699.

[99] Kuang Y, Beretta E (1998); Global qualitative analysis of a ratio-dependent predator-prey system. J. Math. Biol. 36: 389-406.

[100] Kuang Y, Freedman HI (1988); Uniqueness of limit cycles in Gause type models of predatorprey systems. Math. Biosci. 88: 67-84.

[101] Kumar A, Bhadauria BS (2011a); Non-linear two dimensional double diffusive convection in a rotating porous layer saturated by a viscoelastic fluid. Transp. Porous Med. 87: 229-250.

[102] Kumar A, Bhadauria BS (2011b); Thermal instability in a rotating anisotropic porous medium saturated with viscoelastic fluid. Int. J. Nonlinear Mech. 46: 47-56.

[103] Kuznetsov YA (2004); Elements of Applied Bifurcation Theory, Appl. Math. Sci. Springer-Verlag, New York.

[104] Lai X, Liu S, Lin R (2010); Rich dynamical behaviours for predator-prey model with weak Allee effect. Appl. Anal.: An International Journal, 89(8): 1271-1292.

[105] Lamontagne Y, Coutu C, Rousseau C (2008); Bifurcation analysis of a predator-prey system with generalized Holling type III functional response. J. Dyn. Diff. Eq. 20: 535-571.

[106] Lande R (1987); Extinction thresholds in demographic models of territorial populations. Am. Nat. 130: 624-635.

[107] Lenzini P, Rebaza J (2010); Non-constant predator harvesting on ratio-dependent predator-prey models, Appl. Math. Sci. 4(16): 791-803.

[108] Leslie PH (1948); Some further notes on the use of matrices in population mathematics. Biometrica 35: 213-244.

[109] Leslie PH, Gower JC (1960); The properties of a stochastic model for the predator-prey type of interaction between two species. Biometrica 47: 219-223.

[110] Lewis MA, Kareiva P (1993); Allee dynamics and the spread of invading organisms. Theor. Popul. Biol. 43: 141-158.

[111] Liang Z, Pan H (2007); Qualitative analysis of a ratio-dependent Holling-Tanner model. J. Math. Anal. Appl. 334: 954-964.

[112] Liermann M, Hilborn R (2001); Depensation: evidence, models and implications. Fish and Fishe. 2: 33-58.

[113] Lotka A (1925); Elements of Physical Biology. Williams and Williams, Baltimore.

[114] Malashetty MS, Kulkarni S (2009); The convective instability of Maxwell fluid-saturated porous layer using a thermal non-equilibrium model. J. Non-Newton Fluid Mech. 162(3): 29-37.

[115] Malashetty MS, Padmavathi V (1997); Effect of gravity modulation on the onset of convection in a fluid and porous layer. Int. J. Engg. Sci. 35: 829-839.

[116] Malkus WVR, Veronis G (1958); Finite amplitude cellular convection. J. Fluid Mech. 4: 225-260.

[117] May RM (2001); Stability and Complexity in Model Ecosystems. Princeton University Press. Princeton

[118] May R, Beddington JR, Clark CW, Holt SJ, Laws RM (1979); Management of multispecies fisheries. Science 205: 267-277.

[119] Mena-Lorca J, Gonzalez-Olivares E, Gonzlez-Yaez B (2007); The LeslieGower predator-prey model with Allee effect on prey: a simple model with a rich and interesting dynamics. In: Mondaini, R. (ed.) Proceedings of the International Symposium on Mathematical and Computational Biology BIOMAT 2006, E-papers Servios Editoriais Ltda., R'io de Janeiro. 105-132.

[120] Murdoch WW, Chesson J, Chesson PL (1985); Biological control in theory and practice. Am. Nat. 125(3): 344-366.

[121] Nield DA, Bejan A (2013); Convection in Porous Media. 3rd edn. Springer, New York 2013.

[122] Owen MR, Lewis MA (2001); How predation can slow, stop or reverse a prey invasion. Bull. Math. Biol. 63: 655-684.

[123] Pal PJ, Saha T (2015); Qualitative analysis of a predator-prey system with double Allee effect in prey. Cha. Sol. Fra. 73: 36-63.

[124] Perko L (1996); Differential Equations and Dynamical Systems. Springer, New York.

[125] Petrovskii SV, Morozov A, Venturino E (2002); Allee effect makes possible patchy invasion in a predator-prey system. Ecol. Lett. 5: 345-352.

[126] Pielou EC (1969); An Introduction to Mathematical Ecology. Wiley-Interscience, New York.

[127] Prasad BSRV, Banerjee M, Srinivasu PDN (2013); Dynamics of additional food provided predatorprey system with mutually interfering predators. Math. Biosc. 246: 176-190.

[128] Reeve J (1997); Predation and bark beetle dynamics. Oecologia 112(1): 48-54.

[129] Reinhardt K, Kohler G (2002); Conservation of the red-winged grasshopper, Oedipoda germanica (Latr.): the influence of reproductive behaviour. Biol. Cons. 107: 221-228.

[130] Rosenzweig ML, MacArthur RH (1963); Graphical representation and stability conditions of predator-prey interactions. Am. Nat. 209-223.

[131] Saez E, Gonzalez-Olivares E (1999); Dynamics of predator-prey model. SIAM J. Appl. Math. 59: 1867-1878.

[132] Saha T, Chakrabarti C (2009); Dyanamical analysis of a delayed ratio-dependent Holling-Tanner predator-prey model. J. Math. Anal. Appl. 358: 389-402.

[133] Sarnelle O, Wilson AE (2008); Type III functional response in Daphnia. Ecology 89: 1723-1732.

[134] Sen M, Banerjee M, Morozov A (2012); Bifurcation analysis of a ratio-dependent prey-predator model with the Allee effect. Ecol. Comp. 11: 12-27.

[135] Sen M, Srinivasu PDN, Banerjee M (2015); Global dynamics of an additional food provided predatorprey system with constant harvest in predators. Appl. Math. Comp. 250: 193-211.

[136] Seo G, DeAngelis DL (2011); A predator-prey model with a Holling type I functional response including a predator mutual interference. J. Nonlinear Sci. 21: 811-833.

[137] Shi J, Shivaji R (2006); Persistence in reaction diffusion models with weak Allee effect. J. Math. Biol. 52: 807-829.

[138] Smith FE (1963); Population dynamics in Daphnia magna and a new model for population growth. Ecology. 44: 651-663.

[139] Sokol W, Howell JA (1980); Kinetics of phenol exidation by washed cells. Biotec. Bioeng. 23: 2039-2049.

[140] Solomon ME (1949); The natural control of animal populations. J. Anim. Ecol. 18: 1-35.

[141] Spataro T, Bacher S, Bersier L, Arditi R (2012); Ratio-dependent predation in a field experiment with wasps. Ecosphere 3(12): art124.

[142] Spencer PD, Collie JS (1996); A simple predator-prey model of exploited marine fish populations incorporating alternative prey. ICES J. Marine Sci. 53: 615-628.

[143] Srinivasu PDN (2001); Bioeconomics of a renewable resource in presence of a predator. Nonlinear Anal. Real World Appl. 2: 497-506.

[144] Srinivasu PDN, Prasad BSRV, Venkatesulu M (2007); Biological control through provision of additional food to predators: a theoretical study, Theo. Popul. Biol. 72: 111-120.

[145] Srinivasu PDN, Prasad BSRV (2010); Time optimal control of an additional food provided predator-prey system with applications to pest management and biological conservation. J. Math. Biol. 60: 591-613.

[146] Srinivasu PDN, Prasad BSRV (2011); Role of quantity of additional food to predators as a control in predator-prey systems with relevance to pest management and biological conservation. Bull. Math. Biol. 73: 2249-2276.

[147] Srivastava A, Bhadauria BS, Siddheshwar PG, Hashim I (2013); Heat transport in an anisotropic porous medium saturated with variable viscosity liquid under g-jitter and internal heating effects. Transp. Porous Med. 99: 359-376.

[148] Stephens PA, Sutherland WJ, Freckleton RP (1999); What is the Allee effect? Oikos, 87: 185190.

[149] Stephens PA, Sutherland WJ (1999); Consequences of the Allee effect for behaviour, ecology and conservation. Trends Ecol. Evol. 14(10): 401-405.

[150] Stiefs D, Van Voorn GAK, Kooi BW, Feudel U, Gross T (2010); Food quality in producer-grazer models: a generalized analysis, Am. Nat. 176: 367-380.

[151] Strauss SY (1991); Indirect effects in community ecology: their definition, study and importance, Trends Ecol. Evol. 6: 206210.

[152] Strogatz SH (2007); Non-linear Dynamics and Chaos. Levant Books, Edition-I Kolkata India.

[153] Tanner JT (1975); The stability and the intrinsic growth rates of prey and predator populations. Ecology 56: 855-867.

[154] Turchin P (2003); Complex Population Dynamics: A Theoretical/Empirical Synthesis, in: Monographs in Population Biology. Princeton University Press.

[155] Upadhyay RK, Roy P, Datta J (2015); Complex dynamics of ecological systems under nonlinear harvesting: Hopf bifurcation and Turing instability. Nonlinear Dyn. 79(4): 2251-2270.

[156] Vafai K (2000); Handbook of Porous Media. Marcel Dekker, New York 2000.

[157] Van Baalen M, Krivan V, Van Rijn PCJ, Sabelis MW Sabelis (2001); Alternative food, switching predators, and the persistence of predator-prey systems, Am. Nat. 157(5): 512-524.

[158] Van Rijn PCJ, van Houten, Sabelis MW (2002); How plants benefit from providing food to predators even when it is also edible to herbivores. Ecology 83: 2664-2679.

[159] Venezian G (1969); Effect of modulation on the onset of thermal convection. J. Fluid Mech. 35: 243-254.

[160] Vest CM, Arpaci VS (1969); Overstability of a viscoelastic fluid layer heated from below. J. Fluid Mech. 36: 13-623.

[161] Volterra V (1926); Fluctuations in the abundance of species considered Mathematically. Nature CXVIII 558-560.

[162] Wang X, Cai Y, Ma H (2013); Dynamics of a Diffusive Predator-Prey Model with Allee Effect on Predator. Dis. Dyn. Nat. Soc. Article ID 984960, 10 pages.

[163] Wang ME, Kot M (2001); Speeds of invasion in a model with strong or weak Allee effects. Math. Biosci. 171: 83-97.

[164] Wang G, Liang XG, Wang FZ (1999); The competitive dynamics of populations subject to an Allee effect. Ecol. Model. 124: 183-192.

[165] Wang S, Tan W (2011); Stability analysis of Soret-driven double-diffusive convection of Maxwell fluid in a porous medium. Int. J. Heat Fluid Flow 32(1): 88-94.

[166] Wollkind DJ, Collings JB, Logan JA (1988); Metastability in a temperature-dependent model system for predator-prey mite outbreak interactions on fruit trees. J. Math. Biol. 50: 379-409.

[167] Wollkind DJ, Logan JA (1978); Temperature-dependent predator-prey mite ecosystem on apple tree foliage. J. Math. Biol. 6: 265-283.

[168] Wootton JT (1994); The nature and consequences of indirect effects in ecological communities. Am. Rev. Ecol. Syst. 25: 443-466.

[169] Wu R, Liu X (2014); Dynamics of a Predator-Prey System with a Mate-Finding Allee Effect. Abs. Appl. Ana. Article ID 673424, 14 pages.

[170] Xiao M, Cao J (2009); Hopf bifurcation and non-hyperbolic equilibrium in a ratio-dependent predator-prey model with linear harvesting rate: Analysis and computation. Math. Comp. Model. 50: 360-379.

[171] Xiao D, Jennings LS (2005); Bifurcation of a ratio-dependent ratio-dependent predator-prey system with constant rate harvesting. SIAM J. Appl. Math. 65(3): 737-753.

[172] Xiao D, Ruan S (1999); Bogdanov-Takens bifurcations in predator-prey systems with constant rate harvesting. Fields Inst. Commun. 21: 493-506.

[173] Xiao M, Wenxia L, Maoan H (2006); Dynamics in a ratio-dependent predator-prey model with predator harvesting. J. Math. Anal. Appl. 324: 14-29.

[174] Yilong L, Dongmei X (2007); Bifurcations of a predator-prey system of Holling and Leslie types. Cha. Sol. Fra. 34: 606-620.

[175] Zhang Z, Ding T, Huang W, Dong Z (1991); Qualitative Theory of Differential Equations. Amer. Math. Soc. Peking Univ. Press.

[176] Zhou SR, Liu YF, Wang G (2005); The stability of predator-prey systems subject to the Allee effects. Theo. Popul. Biol. 67: 23-31.

[177] Zhu CR, Lan KQ (2010); Phase portraits, Hopf bifurcation and limit cycles of Leslie-Gower predator-prey systems with harvesting rates. Dis. Con. Dyn. Sys. ser. B, 14(1): 389-306.

[178] Zhu Y, Wang K (2011); Existence and global attractivity of positive periodic solutions for a predator-prey model with modified Leslie-Gower Holling-type II schemes, J. Math. Anal. Appl. 384: 400-408.

List of Publications

1. Manoj Kumar Singh, B.S. Bhadauria, B. K. Singh, Qualitative analysis of a Leslie-Gower predator-prey system with nonlinear harvesting in predator. Ain Shams Engineering Journal (Elsevier), http://dx.doi.org/10.1016/j.asej.2016.07.007. (In press)

2. Manoj Kumar Singh, B.S. Bhadauria, B. K. Singh, Qualitative analysis of a Leslie-Gower predator-prey system with nonlinear harvesting in predator. International Journal of Engineering Mathematics (Hindawi), Volume 2016, Article ID 2741891, 15 pages, http://dx.doi.org/10.1155/2016/2741891.

3. B.S. Bhadauria, Manoj Kumar Singh, Ajay Singh, Palle Kiran, B.K. Singh, Stability analysis and internal heating effect on oscillatory convection in a viscoelastic fluid saturated porous medium under gravity modulation. International Journal of Applied Mechanics and Engineering (De Gruyter), 21(4), 785-803 (2016).

4. Manoj Kumar Singh, B.S. Bhadauria, Qualitative analysis of an additional food provided predator-prey model in the presence of Allee effect. (Communicated)

5. Manoj Kumar Singh, B.S. Bhadauria, Qualitative analysis of modified Leslie-Gower predator-prey model with weak Allee effect type II. (Communicated)

6. Manoj Kumar Singh, B.S. Bhadauria, Bogdanov-Takens bifurcations for a predator-prey system with nonlinear harvesting in prey. (Communicated)

7. Manoj Kumar Singh, B.S. Bhadauria,Qualitative analysis and optimum harvesting of a ratio-dependent Holling-Tanner predator-prey model with nonlinear prey harvesting. (Communicated)